POSTURAL CONTROL: LEARNING TO BALANCE AND RESPONSES TO MECHANICAL AND SENSORY PERTURBATIONS

by

Glen Martin Blenkinsop

A Doctoral Thesis

Submitted in partial fulfilment of the requirements for the award of Doctor of Philosophy of Loughborough University

October 2014

ABSTRACT

The purpose of the current research was to examine how a novel balance task is learnt by individuals with a mature neurological system, and to investigate the responses of experienced hand balancers to mechanical and sensory perturbations. Balance in each posture was assessed by various techniques, including: traditional measures of centre of pressure, nonlinear time series analysis of centre of pressure, estimates of feedback time delay from cross correlations and delayed regression models, and calculation of small, medium, and large movement corrections. Data from this study suggests that the best balance metric for distinguishing between each of the balance conditions was the traditional balance measure of sway velocity. However, sway velocity cannot provide any further information on the underlying process of balance. Nonlinear measures of balance offer insight into the underlying deterministic processes that control balance, offering measures of system determinism, complexity, and predictability. Assessments of feedback time delay and movement corrections provide both an insight into the control of posture and help distinguish one condition from another. Both feedback time delay and movement corrections and magnitudes may be used simultaneously to delve further into the control of posture. Delayed regression models seem to be an appropriate and useful tool for estimating feedback time delays during balance. Findings support the use of the third term in the adapted regression model as a means of estimating the effect of passive stiffness on feedback time delay. Generally, with increased duration in handstand subjects displayed reduced sway as measured by traditional measures of balance. A more marked change in nonlinear measures of balance can be seen, with quicker reductions in variance for some nonlinear measures of balance than in the traditional measures. It may be that more pronounced changes in nonlinear measures represent changes in the subjects' underlying process of postural control, whereas less pronounced changes in traditional measures relate more to their general ability or performance in the balance task.

PUBLICATIONS

Conference Proceedings

Blenkinsop, G.M., Hiley, M.J., and Pain, M.T.G. (2012). A stationary vs non-stationary analysis of inverted stance, *Proceedings of the Biomechanics Interest Group of the British Association of Sport and Exercise Sciences*, University of Ulster, 2012, pp 20.

Blenkinsop, G.M., Pain, M.T.G., and Hiley, M.J. (2012). Using stationary and non-stationary measures of balance to assess handstand performance, *Proceedings of the 36th Annual Meeting of the American Society of Biomechanics*, University of Florida, 2012, 124.

Blenkinsop, G.M., Hiley, M.J., and Pain, M.T.G. (2013). A comparison of methods for calculating neurological delays in perturbed stance, *Proceedings of the Biomechanics Interest Group of the British Association of Sport and Exercise Sciences*, University of Wolverhampton, 2013.

Blenkinsop, G.M., Hiley, M.J., and Pain, M.T.G. (2013). A comparison of methods for calculating neurological delays in perturbed stance, *Proceedings of the XXIV Congress of the International Society of Biomechanics*, Natal, Brazil, 2013, 110.

Blenkinsop, G.M., Pain, M.T.G., and Hiley, M.J. (2013). Integrating postural control and neurocognitive tasks to test for concussion and assess recovery in sporting populations, *CAREN User Group Meeting, University of Strathclyde,* 2013.

Blenkinsop, G.M., Pain, M.T.G., and Hiley, M.J. (2014). Assessing learning to balance in inverted stance: Traditional and Non-linear methods, *Proceedings of the 7th World Congress of Biomechanics*, Boston, USA, 2014, M249.

ACKNOWLEDGEMENTS

To my family and friends, even if it does bore you

(not that you'll read it)

TABLE OF CONTENTS

LIST OF FIGURES

LIST OF TABLES

CHAPTER 1

INTRODUCTION

In this chapter, an introduction to balance and postural control is provided, a brief overview of previous literature is presented, and the rationale for the research is offered. Research questions pertaining to the purpose are posed and described with reference to the literature, before an outline of the thesis is presented with a brief description of each chapter.

1.1. Area of Study

Balance and postural control is essential to the efficient execution of a vast array of skills, and poor balance has been linked to an increased risk of injuries in sport. Balance in a relatively static position, such as quiet stance, can be viewed as a dynamic process, with the execution of multiple postural adjustments to maintain a vertical orientation. There may be no separate mechanisms for posture and movement, where movement in its most elementary form can be seen as a modification of posture (Hayes, 1982). Thus, postural control is dependent to a large degree on the goal of any voluntary movement and on the contextual setting or environment in which it takes place (Wade and Jones, 1997). Historically, research literature has focused primarily on factors relating to balance during relatively static related activities, such as static standing (Lin et al., 2008; Wilson et al., 2008) with very little consideration to the nature of balance and postural control during other postural orientations.

The term posturography refers to the description of posture, and is commonly related to a relatively static position of different body parts with respect to each other and the body as a whole (Visser et al., 2008). The numerous investigative techniques that are grouped under this term actually have a much wider perspective, as many of these techniques aim to describe not only posture, but also the active and passive regulation of balance (Bloem et al., 2003). Furthermore, several of these techniques move beyond a simple descriptive

capacity and actively manipulate the subject's posture and balance to delve further into the control mechanisms of balance, such as during sensory or mechanical perturbations (Bloem et al., 2003; Visser et al., 2008). Static posturography involves the assessment of spontaneous sway during quiet stance on a fixed support surface with no external perturbations; whereas dynamic posturography exposes subjects to experimentally controlled perturbations during quiet stance (Bloem et al., 2003; Visser et al., 2008). Many studies in this area employ a combination of both static and dynamic posturography to address a particular aspect of postural control, such as the importance of different sensory systems (Nashner et al., 1982; Peterka and Benolken, 1995; McCollum et al., 1996; Peterka, 2002; Mergner et al., 2005; Maurer et al., 2006; Parietti-Winkler et al., 2006).

Posturography employs a variety of biomechanical techniques to assess the changes to the underlying physiological control of posture and the subsequent mechanical manifestations of these changes. The most appropriate techniques to be selected will depend on the testing protocol chosen. Using electromyography (EMG) may be an appropriate measure for assessing the neuromuscular delays in response to an external perturbation, but may not offer a significant insight into the absence of vision on unperturbed stance.

During the first decade of life the human body undergoes the most significant transitions in motor development, making this an excellent time to study the emergence and development of postural control (Roncesvalles et al., 2001). There appears to be a relationship between the development of postural control and increased motor competence in activities such as walking, jumping, and hopping (Woollacott and Sveistrup, 1992; Roncesvalles et al., 2001; Sundermier et al., 2001). It may be that the association between postural control and general motor development can be viewed as a cycle or positive spiral, whereby development of one leads to the opportunity for further development in the other, and that the development of both postural control and general motor skills should be examined together to further our understanding in either one. However, we must also consider the possible

2

effects of physical development and maturation of key physiological systems, such as myelination of neurological pathways, enhanced muscular strength, and development of visual and vestibular acuity. Future studies into the development of balance and postural control may wish to examine how individuals with a mature neurological system learn to balance. This would require assessing neurologically sound adults in a balance task that is unfamiliar to them, and therefore could not be assessed in normal upright stance. One possible approach for this would be to assess how individuals learn to balance in inverted stance.

Past literature on balance in inverted stance suggests that a wrist strategy is the preferred strategy to correct for small perturbations, but as balance becomes more precarious the performer may begin to rely on more distal corrections from the shoulder and hip (Kerwin and Trewartha, 2001; Yeadon and Trewartha, 2003); similar to the role of the ankle and hip strategies used in normal stance (Horak and Nashner, 1986). Since previous research investigated expert handstanders, further study into the corrective responses to internal and external perturbations may be required to discover the full array of corrective strategies employed by individuals in inverted stance. Future research into this area may find worth in the procedures employed in previous studies into postural responses during normal stance, such as using a combination of EMG and dynamic posturography to measure muscle latencies and muscle activity patterns in response to controlled perturbations.

1.2. Statement of Purpose

The focus of the current research was to examine how a novel balance task is learnt by individuals with a mature neurological system, and what factors differentiate an expert performer from a novice in this task. As any adult with a sound neurological system will have many years of practice with performing a variety of balance tasks in standing, the primary focus was to assess how individuals learnt to balance in inverted stance over a period of eight months. In addition, the ability of expert hand balancers to maintain inverted stance whilst experiencing a variety of sensory and mechanical perturbations was assessed,

following similar procedures to those used by Nashner et al. (1982) on upright stance.

1.3. Research Questions

Q1. How are balance metrics expressed differently when balancing in different postures; including handstand, single leg stance and normal standing?

Some balance variables would be expected to be sensitive to the nature of the balance task. However, such changes in a balance metric may not truly represent an increase or decrease in balance performance, but instead might be related to the mechanical limitations of the task. It is important to understand the underlying principles and assumptions of each variable used to measure balance, and to be clear about how the mechanics and control of posture is thought to be expressed by these variables. A comprehensive review of each balance metric will be presented prior to application of each metric to experimental data in the various balance tasks.

Q2. Which balance metrics best characterise improvements in balance performance when a novice first learns to balance in handstand?

A number of variables have been proposed to assess the balance of an individual. Several of these variables have been used to distinguish between clinical and healthy populations with little insight into the sensitivity of such measures for assessing improvements in balance over time. If balance is considered as a continuous task, then we may assume that as an individual first learns this task they will only be able to maintain balance for a short period of time. Therefore, the amount of time subjects can maintain balance in handstand will be used as the main determinant for assessing improvements in balance performance, and all other measures will be compared with reference to this.

4

Q3. How are the responses to mechanical perturbations different when balancing in handstand and normal stance postures?

Alterations in balance strategies may be difficult to find in static balance conditions where experienced balancers may exhibit small amounts of sway. Employing perturbations to delve further into the mechanisms of postural control is common in normal stance. This method may provide further insight into strategies experienced balancers use to maintain balance during demanding conditions. Furthermore, perturbations may highlight important differences in the demands of balance in handstand, compared to normal standing.

Q4. In what way is balance affected by altered sensory inputs, and does this result in a change to the corrective strategies used to maintain balance?

To further understand the roles of the three main sensory systems available during balance tasks, somatosensory proprioception and vision can be restricted during balance. Past literature has focused on either examining simple measures of balance, such as range of sway (Nashner, 1972; Peterka, 2002), or only examining the effect of vision (Riley et al., 1999). The current research will expand these principles to include the examination of the nonlinear dynamics of COP trajectories, feedback time delay, and the number and size of joint movement corrections during balance with and without visual inputs and with normal and altered somatosensory feedback.

1.4. Thesis Organisation

The outline of the remainder of the thesis is as follows:

Chapter 2 provides a critical review of the literature pertaining to postural control and balance. The review is divided into several sections addressing issues related to both inverted and normal stance, including: mechanical considerations, neurological control, developmental factors, and external factors that can influence balance.

Chapter 3 describes the methods used for the collection and treatment of data to assess balance. A detailed description of the experimental protocol used within the current research is given, and the procedure for the collection and processing of experimental data is provided.

Chapter 4 follows on from the previous chapter, and examines the assumptions used by various methods to assess balance, with specific reference to the calculation and implementation of different balance metrics used within the literature. This chapter relates specifically to question one, and aims to determine which balance metrics best express the underlying postural control strategies for each posture.

Chapter 5 addresses experimental question two and examines which balance metrics best characterise improvements in balance performance when a novice learns to balance in handstand.

Chapter 6 examines responses to external mechanical perturbations when balancing in normal and inverted stance. The chapter assesses previous methods for estimating feedback time delays and examines how these may differ in normal and inverted stance. Balance strategies during perturbations, and how they may differ in normal and inverted stance are presented and applied to answer question three.

Chapter 7 assesses how balance in handstand may be affected by altered sensory feedback. Question four is addressed, and the importance of sensory information is assessed via the various balance metrics described in Chapter 4.

Chapter 8 provides a summary of the thesis, discussing the findings in relation to each experimental question and considerations for future research.

CHAPTER 2

REVIEW OF LITERATURE

This chapter gives a critical appraisal of past literature concerning balance and postural control. Firstly, issues relating to the description of balance and postural control are revised, followed by specific reference to the neurological and mechanical considerations for the control of static balance. The implications for the assessment of balance are reviewed, and research examining the development of postural control is examined. Finally, research literature pertaining to postural control in handstand is discussed.

2.1. Description of Balance and Postural Control

The word posture comes from the Latin verb ponere, which means to put or place, and in general posture can refer to the carriage of the body as a whole, the attitude of the body, or the position of the limbs. Alternatively, Winter (1995) describes posture as 'the orientation of any body segment relative to the gravitational vector, and is an angular measure from the vertical'. Both descriptions relate to the position or orientation of the body, however, Winter's description places increased emphasis on this orientation relative to gravity as it is described with relevance to standing upright, which may not always be applicable. Measuring posture as a simple angular measure to the vertical is sometimes referred to as postural sway, based on the motion of an individual's centre of mass (COM). However, this is a somewhat simple measure, simplifying the body into a single segment or point, making it difficult to gain understanding of the many small postural adjustments that may be made in order to gain or maintain balance. Consequently, postural control may be defined as the act of maintaining, achieving or restoring a state of balance during any posture or activity (Pollock et al., 2000). Postural control will therefore relate to the mechanical and neurological control of the orientation of individual body parts and the body as a whole. In this sense, posture can be

considered as task specific, where the orientation of the body parts is determined by the constraints of the balance task.

Balance, from a mechanical perspective, is equivalent to equilibrium, which is the state of an object when the resultant force acting upon it is zero (Pollock et al., 2000). Over time, and with a static base of support, this assumes a static position, which may be stable or unstable, and is related to some of the inherent characteristics of the object; such as the distance of the COM from the edge of the base of support, the weight of the object, and the height of the centre of gravity above the base. These inherent characteristics determine the stability of the object, which relates to the ability of the object to remain in, or return to, a state of balance after experiencing a perturbation. However, this may not be the best description of human balance, where a static equilibrium cannot be maintained as a result of passive insufficiencies due to these characteristics, and balance can only be achieved through numerous postural adjustments.

In general, human balance may be described as 'the state of postural equilibrium, whereby the vertical projection of the COM is maintained over the body's base of support' (Alderton, 2003; Hryomallis, 2007). However, the requirement for the COM to remain within the base of support comes from the generic definition of static equilibrium, and may not apply to human balance. This has led some authors to suggest that it may be possible to maintain balance even if the COM moves outside of the base of support (Yeadon and Trewartha, 2003). In fact, the opposite can also be true, whereby the COM may remain within the base of support but the 'system' can find itself in a state where balance cannot be maintained unless the base of support is moved, such as due to limited strength or poor control (Popovic et al., 2000). The definition of human balance can be confused further when considering the wider implications of balance in more dynamic conditions, such as locomotion or sporting activities. It is not surprising therefore, that, when considering the wider implications for balance and posture, some researchers feel that there are no universal definitions for postural control or balance (Massion and

Woolacott, 2004; Shumway-Cook and Woolacott, 2007). In fact, one could argue that, from a static stability perspective, bipedal locomotion is invariably unstable, and falling is only prevented by the ability of the neuromuscular system to constantly change the base of support and therefore control the COM (Patla, 2004). However, some researchers believe that the problem lies with applying a single definition to all balance tasks, and the process of postural control should be considered to be on a continuum between static stance and more dynamic movements (Wade and Jones, 1997; Moe-Nilssen and Helbostad, 2002).

According to Wade and Jones (1997) postural stability is modulated by postural control, which is exhibited in the form of postural adjustments, and may be measured by the small postural oscillations known as postural sway. These adjustments can occur prior to or during voluntary movements and are thought to minimise the displacement of the COM caused by voluntary movements and also to affect these movements directly. Similarly, Hayes (1982) believes that there are no separate mechanisms for posture and movement, postural reactions are fundamental in neural organisation, and movement in its most elementary form can be seen as a modification of posture. Thus, postural control is dependent, to a large degree, on the goal of the voluntary movement and on the contextual setting or environment in which it takes place (Wade and Jones, 1997). Balance and postural control is therefore an inseparable part of almost any movement, and adequate balance and postural control during the execution of one task in a specific environment may not be readily generalised to other tasks and situations (Moe-Nilssen and Helbostad, 2002). These views are shared by Winter (1995), who explains that the term dynamic balance should be more appropriately related to activities such as gait initiation, gait termination or walking and running, where the swing limb has a trajectory that will achieve balance conditions during the next stance phase. In fact, Winter (1995) goes on to explain that the demands on balance and postural control differ significantly from one activity to another, and that the simple task of walking from point A to point B along a linear path would involve dramatic changes to the system as you move from quiet stance, to gait initiation, to

steady state walking, to gait termination and finally back to quiet stance. Therefore any assessment of balance may lead to a different conclusion depending on the task being demonstrated and the chosen setting in which they are performed, and performances on one balance task may or may not relate to performances on another balance task (Winter, 1995; Wade and Jones, 1997; Moe-Nilssen and Helbostad, 2002; Hrysomallis et al., 2006).

In view of these factors, this review will consider human balance as the task of attempting to remain upright, or in some other predefined posture, without falling. Specifically, static balance will refer to any balance task in which the individual attempts to maintain a static base of support with minimal displacement of their COM, which may also be viewed as quiet stance. Correspondingly, postural control will refer to the numerous postural adjustments made throughout the body in an attempt to maintain balance, and human stability will refer to the inherent ability of a person to maintain, achieve or restore a specific state of balance and not fall. This ability refers specifically to the physical properties of the person and the numerous sensory and motor processes through which the mechanisms of postural control are executed.

2.2. Control of Balance and Posture

The postural control of human upright balance is commonly viewed as a complex continuous process of the stabilisation of a multi-segment inverted pendulum (Winter, 1995; Gage et al, 2004; Blaszczyk, 2008). In this model, the main controlled parameter is the COM position; where postural sway is the consequence or side effect of the motor control process (Bottaro et al, 2005; Blaszczyk, 2008). During quiet stance, stabilising torques generated at different levels of the body's kinetic chain are transmitted down to the base of support (BOS) in response to the neurological feedback from multiple sensorimotor processes (Horak, 2006). Therefore, when assessing the implications of balance and postural control it is essential that researchers consider the importance of both the mechanical and the neurological aspects of postural control.

2.2.1. Neurological Control of Balance and Posture

The control of posture involves a continuous feedback system of processing visual, vestibular and somatosensory inputs and executing neuromuscular actions to maintain equilibrium (Winter, 1995; Wade and Jones, 1997; Horak, 2006; Casslebrant, 2007; Hryromallis, 2007; Cappa et al, 2008; Visser et al, 2008). According to Winter (1995), the visual system is involved in planning our locomotion and avoiding obstacles, the vestibular system acts as our 'gyro', which senses linear and angular accelerations, and the somatosensory system is a multitude of sensors that sense the position and velocity of all body segments, their contacts with external objects and the orientation of gravity. However, Wade and Jones (1997) believe that it is the nature of the integration between of these three systems, labelled as the 'triad of posture and locomotion', that holds the key to how the postural system works. Furthermore, some believe that it is the ability to readjust how these systems integrate during different tasks and environmental conditions that is crucial to all-round balance and independent mobilisation (Peterka, 2002; Horak, 2006).

Neurological control of posture tends to rely heavily on the somatosensory system during normal stance conditions, however, as environmental conditions or the balance task change, the system will re-weight its relative dependence on each of the three senses depending on the reliability of the information received (Peterka, 2002). For example, when in a well-lit environment with a firm base of support the neurological system will rely on the somatosensory system for approximately 70% of its information, and on the visual and vestibular systems for 10% and 20% respectively (Horak, 2006). However, when standing on an unstable surface, the neurological system will increase sensory weighting to the vestibular and visual systems as it decreases its dependence on the less accurate surface somatosensory inputs (Peterka, 2002; Horak, 2006). However, it is unclear whether this represents a simple percentage change due to reduced inputs in one area, or whether the central nervous system (CNS) actually attenuates some aspects of postural control. Nevertheless, this may explain why virtually all neuromusculoskeletal disorders result in some degeneration in the postural control system (Winter, 1995);

which may be due to an impairment to one of the sub-systems employed, or due to an inability of the central nervous system (CNS) to effectively re-weight the sensorimotor system (Peterka, 2002; Horak, 2006).

Balance and postural control requires a great deal of cognitive resources, which can be observed by the increased reaction times in persons when standing compared to those when sitting (Teasdale and Simoneau, 2001; Tucker et al, 2008). In addition, an individual's postural control will become impaired if required to simultaneously perform a cognitive task; with a further decline in postural control with an increased complexity of the cognitive task (Camicioli et al, 1997). Therefore, neurologically impaired patients with cognitive dysfunction, such as those with Alzheimer's disease or dementia, are at an increased risk of falling, especially if simultaneously performing a cognitively demanding task (Prince et al, 1997; Horak, 2006; Marchetti and Whitney, 2006). This may be due to a difficulty interpreting a complex and sometimes conflicting array of sensory signals or may be due to an inability to rapidly change focus to the appropriate sensory inputs for that given environment (Horak, 2006; Marchetti and Whitney, 2006). However, we must not neglect the possibility that some balance issues in the elderly and neurologically impaired populations are due to other factors, as some neurological conditions, such as stroke or unilateral vestibular loss, may result in a misinterpretation of what is gravitationally vertical, causing the individual to be unstable during certain conditions.

Spatial orientation is vital to postural control and healthy nervous systems will automatically alter how the body is orientated depending on the context and the task (Wade and Jones, 1997; Horak, 2006). Research has shown that healthy individuals are able to identify the gravitational vertical without visual input to within 0.5º; as during dark conditions a person will orientate themselves perpendicular to the support surface until the support surface tilts, at which they will orientate their posture to gravity (Karnath et al, 2000; Horak, 2006). In addition, the perception of what is gravitationally vertical, either via visual or vestibular inputs, is independent of the perception of postural verticality and the ability to align the body in space (Bisdorff et al, 1996; Karnath et al, 1998).

Therefore, an inaccurate internal representation of gravitational vertical will result in an automatic postural alignment that is not aligned with gravity, resulting in an unstable posture (Horak, 2006). However, the importance of visual cues for spatial orientation should not be underplayed, as small changes to our visual inputs can result in some striking changes to postural control (Wade et al., 1995; Wade and Jones, 1997).

Firstly, there is a wealth of evidence within the research that has shown a decreased performance on a variety of balance tasks when removing all visual inputs, such as by closing the eyes. These include an increased postural sway during eyes closed conditions for sitting balance (McInnes et al, 2000) and standing balance (Blaszczyk, 2008; Cappa, 2008). Past research has shown there is a decrease in postural control during human movement for participants with decreased visual input, such as; walking into a darkened room (Moe-Nilssen et al, 2006), blurred vision during sit to stand (Buckley et al, 2005) and changes in gait following cataract surgery (Helbostad et al, 2005). Furthermore, postural control may be influenced by the nature of the visual inputs received, even in relation to changes in the peripheral vision (Wade and Jones, 1997), such as an increase in postural sway with lamellar flow verses radial flow, with a larger effect in older adults compared to younger adults (Wade et al., 1995).

During human movement an optical field is generated that contains a variable geometric structure, with an optic flow field that radiates outwards from a point that corresponds with the direction of motion and is projected to the centre of the retina (Stoffregen, 1985; Wade and Jones, 1997). The flow structure at the peripheral edges of this field of view is nearly parallel to the line of motion, which is called 'lamellar flow', and contains important geometric information required for postural control (Wade and Jones, 1997). Research has shown that the visual system, and consequently postural control, is sensitive to changes in this flow, with a decrease in postural stability when: walking from a wide to a narrow walkway (Schrager et al, 2008; Shkuratova and Taylor, 2008), experiencing optic flow oscillations in the anterioposterior (AP) direction during standing (Casselbrant et al, 2007), and experiencing optic flow oscillations in

13

the AP and mediolateral (ML) direction during standing and walking (O'Connor and Kuo, 2009). Furthermore, O'Connor and Kuo (2009) found that AP optical perturbations resulted in a greater decrease in postural stability during normal quiet stance, but ML optical perturbations resulted in a greater decrease in postural stability during walking and tandem standing. O'Connor and Kuo (2009) concluded that there may be an interaction between an individual's base of support and how the CNS processes optic flow information for maintaining balance. Alternatively, this may relate to an inability to interpret the reduced somatosensory information from a change in the base of support, leading to an increased reliance on visual information. Nevertheless, this does bring to mind the importance of considering not only the neurological processes involved with postural control, but also the mechanical constraints to a standing posture.

2.2.2. Mechanical Control of Balance and Posture

During quiet stance, postural control has been modelled as an inverted pendulum, which predicts that the difference between the centre of pressure (COP) and the COM is proportional to the horizontal acceleration of the COM (Winter, 1995; Gage et al, 2004; Winter et al, 2003). In the inverted pendulum model, changes in COP represent the stabilising torques generated at different levels of the body's kinetic chain, which control the motion of the COM and are transmitted down to the BOS (Blaszczyk, 2008). Although the human body is a multi-segmental structure, capable of moving all joints involved, modelling postural control as a single segment inverted pendulum generally assumes a simple rigid structure above the ankles (Winter, 1995; Winter *et al.*, 2003; Gage *et al.*, 2004). Here the human body is modelled as a simple rigid segment with mass m and a mass centre at a distance h from the fixed supporting ankle/wrist joint *J* (Figure 2.1).
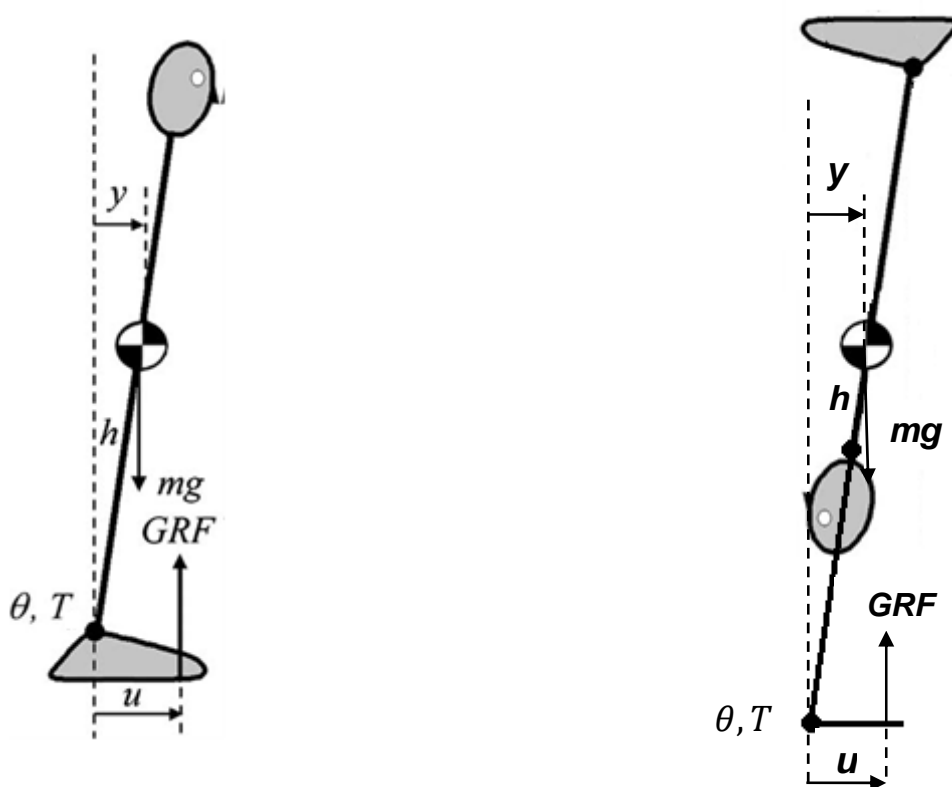
Figure 2.1: The inverted pendulum model of postural control in normal stance and inverted stance (adapted from Bottaro *et al.*, 2005).

The horizontal position of the COM y, (relative to *J)* is related to the joint torque T, the moment of inertia I and the angular acceleration $\ddot{\theta}$ to give:

$$T - mgy = I\ddot{\theta} \qquad (2.1)$$

Replacing $T = vGRF \cdot u$ gives:

$$vGRF \cdot u - mgy = I\ddot{\theta} \qquad (2.2)$$

Where $vGRF$ is the vertical ground reaction force of the body, and u is the position of the COP relative to *J*.

If θ is close to $\pi/2$ then $vGRF \approx mg$ and $\ddot{y} \approx -h\ddot{\theta}$, to give:

$$mg(u - y) = -\frac{I\ddot{y}}{h} \hspace{3cm} (2.3)$$

$$u - y = -\frac{I}{mgh}\ddot{y} \hspace{3cm} (2.4)$$

During quiet stance with small oscillations about the ankle joint, $\frac{I}{mgh}$ can be considered as a biomechanical constant, to give:

$$u - y \propto \ddot{y} \hspace{3cm} (2.5)$$

This simplified view is useful for describing the importance of the ankle or wrist joints for controlling anteroposterior motion during quiet stance or inverted stance (Winter, 1995; Bottaro et al., 2005). However, viewing the system in this simplified way may not be appropriate for assessing more global postural control mechanisms and a double or triple segment inverted pendulum model may be required, with control at the ankles and the hips for normal stance (Winter, 1995; Horak, 2006; Colobert et al., 2006) and at the wrists, shoulders and hips for inverted stance (Kerwin and Trewartha, 2001; Yeadon and Trewartha, 2003). In addition, it should be noted that the relationship between COP and COM may change as more joints are involved in the control of posture, especially if these strategies include large changes to the vertical position of the COM, leading to vertical forces which are no longer approximately equal to body weight, and the quantity $\frac{I}{mgh}$ to change significantly.

According to Winter (1995), the difference between the COP and the COM can be considered as the error signal that the postural control system is sensing, and the magnitude and frequency of this error signal is of importance in the interpretation of the postural control system. The 'gain' of the feedback control system would alter both the magnitude and the frequency of the error signal,

and classical feedback control theory would describe the inverted pendulum model as being an underdamped system; thus an increased gain would not only increase the amplitude of the error signal but also the frequency of the oscillations. However, it is important to note, that this description relates to a large extent to the control of posture through a passive stiffness control mechanism, which as yet has not been validated. This reveals the importance of examining postural control from neither a single mechanical or neurological perspective; but rather researchers should join the two strands together to further our understanding of postural control strategies.

2.2.3. Unified Control of Balance and Posture

The process through which balance is maintained has been considered from several view points, including a passive stiffness control mechanism (Winter et al,. 1998; Winter et al., 2003), a reactive mechanism (Yeadon and Trewartha, 2003; Masani et al., 2006) or as an anticipatory mechanism (Gatev et al., 1999; Morasso and Sanguineti, 2002; Jacono et al., 2004). Each hypothesis attempts to assess different aspects of the postural control system, such as using regressions or cross-correlations to detect any delays between EMG, joint torques, COP and COM. However, authors often come to different conclusions when describing the same characteristics, leaving the results of such studies to open interpretation by the reader.

It has been argued that the active control of posture should result in a delay of approximately 100-150 ms between the COM and COP trajectories, caused by neurological latencies in the control system, however, research has shown that this delay is approximately zero (Winter et al., 1998; Winter et al., 2003). Subsequently, Winter et al. (1998) concluded that balance was maintained by a passive process by means of intrinsic stiffness in the ankle joint, which may be tuned by muscular activity over time, accounting for any drift in COM position. However, this approach only considers the relationship between COM and COP, and does not account for the detection of motion from other sources, such as velocities and accelerations. Furthermore, the authors fail to realise

that such a delay between COM and COP trajectories would result in amplified motion that was inherently unstable.

The single segment inverted pendulum model of postural control explains that the position of the COM is controlled by the ankle joint torque, expressed in the COP trajectory. Therefore, joint torques must be larger than gravitational torque for the COM motion to be reversed. If the peak torque was not reached until 100-150 ms after peak COM displacement, then the large difference between joint torque and gravitational torque would result in large angular accelerations. This would lead to harmonic motion that is amplified over time, and stable control would not be possible. Nevertheless, the concept of passive stiffness control has been advocated by direct assessments of ankle stiffness during standing.

Winter et al. (2001) reasoned that by plotting ankle joint torques against sway angles, a simple inverted pendulum would predict the passive ankle torque required to maintain stable balance. In addition, the gravitational torque (mgy) could also be plotted against sway angle to discover the critical torque required by such a passive torque, and by comparing the two, determine if control by passive stiffness was occurring. This showed that for all subjects the slope for the gravitational torque was less than that from the regression of joint torque against sway angle, with the authors concluding that control was achieved by passive stiffness. However, this method calculated the total torque about the joint via inverse dynamics, which represents all active and passive components. In addition, the authors failed to comprehend that the slope for the gravitational torque represents the minimum torque needed to maintain balance, and if the slope from the regression of joint torque against sway angle was less than this line then, on average, too little torque is produced and stable control would not be possible. However, the estimation of ankle joint stiffness is still of importance, as this stiffness may still play a role in postural control.

Intrinsic stiffness of the ankle has been estimated as approximately 91% of that necessary to provide minimal stabilisation in standing, suggesting that intrinsic

stiffness plays little part in postural stabilisation (Loram and Lakie, 2002a; Lakie et al., 2003). Similarly, Casadio et al. (2005) showed that intrinsic ankle stiffness accounted for approximately 64% of the critical stiffness required for stabilisation during disturbances of 1°. Furthermore, it has been suggested that the minimisation of sway size is caused by improvements in the anticipatory torque impulses, and that balance is achieved by the constant repetition of ballistic biphasic throw and catch patterns of torque and not by an elastic mechanism (Loram and Lakie, 2002). This view is supported Gatev et al. (1999) who used cross-correlation to show there was a zero time lag between COP and COM trajectories, but a 250 – 300 ms time lag between EMG activity of the lateral gastrocnemius muscle and COM or COP trajectories. Once again, such approaches only consider the relationship between the displacement and the variable under investigation, and does not account for the detection of motion from other sources, such as velocities and accelerations.

A proportional and derivative (PD) control model uses the position and its derivative, with position and derivative gains for each, to control another variable. It may be the case that such a process is used to control posture, where the position and velocity of the COM is used to determine the magnitude of the response to maintain balance. Yeadon and Trewartha (2003) used this principle to examine postural control in handstand by regressing joint torques against COM displacements and velocities with increasing time delays, finding feedback latencies of approximately 160-240 ms. Similarly, Masani et al. (2006) applied this method to examine the magnitude of EMG responses as an input into a PD controlled computer simulation model of postural control. Using this approach within a computer simulation model, Masani et al. (2006) found that the PD controller is robust and has a large space for the proportional and derivative gains for which the system is stable. Although this is only for time delays up to 135 ms, the authors argue even longer delays are possible if the passive elements are added. In support, it is believed that the intrinsic joint stiffness may scale the time axis, allowing larger delays to be used, by reducing the effective value of the acceleration caused by gravity, and thus reducing the rate of sway (Bottaro et al., 2005). In comparison, it may be that instead of

19

using a continuous PD controller to control posture, the CNS may use an intermittent PD control system, explaining the ballistic biphasic throw and catch patterns of torque described by Loram and Lakie (2002). In fact, Bottaro et al. (2008) have shown that a computer simulation model of postural control that employs an intermittent PD control system is able to maintain balance even if the delay is increased from 180 ms to 240 ms, which is difficult with continuous time PD controllers. Such a control system is likely to use both feedback and feedforward to determine the magnitude of the intermittent burst of muscle activity.

2.3. Assessment of Balance and Posture

The aim of any test of balance in quite stance is to remain standing, either on one leg or two, with as little motion as possible from the standardised starting position; where small changes in postural sway represents good postural control (Winter, 1995). A common method of assessing this type of postural control is to use a force platform, where changes in the COP through the feet are used to infer alterations in postural sway, and therefore assess postural control. This is very similar to the concept of postural sway, measured via the displacement of the COM, and has resulted in a great deal of confusion between the two measures when used with static balance tasks (Means et al., 1998; Lin et al., 2008), however, both the COM and the COP are separate measures, linked together via the inverted pendulum model of postural control (Winter, 1995; Winter et al., 2003; Gage et al., 2004). Although some researchers question the validity of only using COP measurements to assess postural control (Winter, 1995; Winter et al, 2003), there is little doubt that a force platform can be used to infer the ability to retain static balance (Bottaro et al., 2005; Colobert et al., 2006; Blaszczyk, 2008); though caution should be taken when trying to make elaborate mechanical interpretations into the nature of postural control based on this data alone (Alderton et al., 2003; Gage et al., 2004). These concepts have led to two branches of postural control research, one that aims to achieve greater understanding through more complex analyses of the COP signal, and the other which aims to understand balance by examining multiple aspects of the postural control process. Consequently, other

methods to the collection of COP in static stance have been introduced to try to examine the complex interactions involved in the underlying neurological process of postural control; these can be described collectively under the umbrella term of 'posturography'.

2.3.1. Posturography

The term posturography refers to the description of posture, and is commonly related to a relatively static position of different body parts with respect to each other and the body as a whole (Visser et al., 2008). However, the numerous techniques that are grouped under this term actually have a much wider perspective, as many of these techniques aim to describe not only posture but also the active and passive regulation of postural control (Bloem et al., 2003). Furthermore, several of these techniques move beyond a simple descriptive capacity, and may actively manipulate the subject's posture to delve further into the control mechanisms, such as during sensory or mechanical perturbations (Bloem et al., 2003; Visser et al., 2008). The techniques within posturography can be divided into two main groups of 'static' or 'dynamic posturography'.

2.3.1.1. Static Posturography

Static posturography involves the assessment of spontaneous sway during quiet stance on a fixed support surface and with no external perturbations. Whilst in dynamic posturography subjects are exposed to experimentally controlled perturbations during quiet stance, either via carefully controlled platform movements or perturbations applied directly to the subject via pushes or pulls to selected body areas (Bloem et al., 2003; Visser et al., 2008). However, there is some confusion as to the most appropriate term to use during balance tasks that do not fit directly into these descriptions, such as during voluntary sway (Ruder et al., 1989; Caron et al., 1997; Lafond et al., 2004; Slobounov et al, 2005a), internal perturbations caused by the swinging of the arms (Yamada, 1995; Horak, 2006) or reaching (Row and Cavanagh, 2007), and standing on inclined static surfaces (Sasagawa et al., 2009). Furthermore, this confusion is enhanced when combined with the uncertainty previously mentioned with regards static and dynamic balance, leaving researchers

unsure as how to best classify the study of postural control during activities such as gait with the presence or absence of external perturbations. Therefore this review will follow the advice of Bloem et al. (2003) and consider static and dynamic posturography from the view point of static stance only, in which case the previous descriptions will be sufficient.

The absence of external perturbations in static posturography results in a relatively low demand on the underlying postural control process, allowing for large trial lengths ranging from 30 seconds to 30 minutes (Duarte and Zatsiorsky, 1999; Bloem et al., 2003; Visser et al., 2008); with trial lengths of 20-30 seconds being reported as having the best test-retest reliability (LeClaire and Riach, 1996). Common approaches within static posturography includes asking subjects to stand quietly with eyes closed or eyes open whilst looking straight ahead, or focusing on a wall several meters away. Within this area research has assessed the role of feet position on ML and AP sway (Kirby et al., 1987). In addition, several studies have examined the importance of sensory inputs by assessing the effects from altered sensory feedback, such as: fingertip contact on the leg (Nagano et al., 2006) or an adjacent support surface (Jeka and Lackner, 1994; Jeka and Lackner, 1995; Jeka et al., 1998); via an anchoring system connected to the hands (Mauerberg-deCastro, 2004); reduced gravity related load due to part-immersion in water; decreased peripheral sensation in supporting limbs due to cryotherapy (Magnusson et al., 1990a; Magnusson et al., 1990b) or ischemic hypoxia of nerve fibres via ligatures (Horak et al., 1990); vibrations applied to supporting muscles or tendon to confuse postural reflexes (Nakagawa et al., 1993); and from standing on compliant surfaces (Blackburn et al., 2003). Although localised vibrations or standing on compliant surfaces may be considered as a form of dynamic posturography; in these examples the intention was to assess the effect of altering sensory accuracy and not to assess the effect of specific perturbations to the postural control process.

2.3.1.2. Dynamic Posturography

The most common method used in dynamic posturography is the moving support surface, where participants are asked to attempt to remain standing in as static a position as possible during controlled platform translations and/or rotations. Such studies may assess the participant's responses to a variety of support surfaces movements, including: slow vs. fast translations (Diener et al., 1988); small vs. large amplitude perturbations (Diener et al., 1988; Horak et al., 1989); pseudorandom vs. predictable or sinusoidal movements; or unidirectional vs. multidirectional perturbations (Nashner et al., 1979; Moore et al., 1988; Allum and Honegger, 1998). Additionally, mechanical perturbations may also be applied directly to the individual via an external push or a pull applied to the hip, trunk, or shoulder, such as a subject with weight connected to the waist via a pulley, which is released at an unpredictable time or via direct contact of a weight on a swinging pendulum (Rietdyk et al., 1999; Hasson et al., 2009). In addition, both support surface motions and external forces may be used together to exhibit specific responses, such as lateral pelvic tilt in standing without lateral translation of the pelvis (Goodworth and Peterka, 2009).

It is important to note that researchers must be aware of the mechanical implications of the specific perturbations used and the consequent effects this may have on the neuromuscular control of posture. For example, Bothner and Jensen (2001) showed that the deceleration phase of a platform perturbation played an important part in helping to re-stabilise stance during platform movements. Similarly, the predictable nature of rhythmical perturbations can be used by individuals to help maintain stance and reduce neuromuscular demand. In fact, the neuromuscular response to a specific perturbation can change with several repetitions of the same perturbation, indicating an adaptation of the neurological system to specific environmental demands, and is an integral part of the adaptation test (Nashner, 1976). Therefore, researchers wishing to understand the nature of neurological responses to unexpected perturbations may need to use platform movements with relatively larger amplitudes to ensure a response is present before the platform begins to decelerate. However, this may result in the individual attempting to regain balance on a

platform that is moving. Consequently, researchers must be clear with the purpose of any external perturbations that are applied to an individual when assessing postural control in this way. Furthermore, a variety of platform movement directions and amplitudes that are ordered in a random fashion may be needed to reduce the chance that subjects are able to predict the required response before the perturbation is applied.

Traditionally, dynamic posturography involves the application of external or internal mechanical perturbations, however, within the field of posturography other perturbations can be applied to postural control which does not strictly fit into this classification, such as sensory perturbations through disturbances to the visual inputs. Furthermore, many studies in this area employ a combination of approaches to address a particular aspect of postural control, such as the importance of the visual, vestibular, and somatosensory systems during perturbed and unperturbed stance (Nashner et al., 1982; Peterka and Benolken, 1995; McCollum et al., 1996; Peterka, 2002; Mergner et al., 2005; Maurer et al., 2006; Parietti-Winkler et al., 2006). One of the most recognised assessments of postural control is computerised posturography, which involves three separate tests of balance to examine the importance of the various underlying neurological processes; these are the sensory organisation test, the motor control test and the adaptation test, which was first introduced by Nashner et al. (1982).

2.3.1.3. Computerised Posturography

During computerised posturography the patient stands on a movable dual force plate support surface within a moveable surround, which under control of a computer, can either translate along the sagittal plane or rotate around the mediolateral axis level with the ankle joint. Standardized test protocols expose the patient to support surface and visual surround motions, during which the patient's postural control and motor reactions are recorded. The sensory organization test (SOT) objectively identifies problems with postural control by assessing the patient's ability to make effective use of, or suppress inappropriate, visual, vestibular, and somatosensory information. The motor

control test (MCT) assesses the patient's ability to quickly and automatically recover from unexpected external provocations. Finally, the adaptation test (AT) assesses the patient's ability to modify motor reactions and minimize sway when the support surface moves unpredictably in the toes-up or toes-down direction. Measurements include postural sway via COM displacement for the sensory organisation test, and muscle onset timing, strength, and lateral symmetry of responses for the motor control and adaptation tests.

All forms of posturography typically employ a variety of biomechanical techniques to assess the changes to the underlying neurophysiological control of posture and the subsequent mechanical manifestations of these changes. However, the most appropriate biomechanical techniques to be selected will depend of the chosen testing protocol. Using EMG may be an appropriate measure for assessing the neuromuscular delays in response to an external perturbation, but may not offer a significant insight into the absence of vision on unperturbed stance. Nevertheless, the most common measure of postural control in quiet stance is still postural sway, measured via the displacement of either the COM or the COP. However, the trajectory of the COP is far from simple, with many studies moving away from a simple analysis of this signal, such as sway range, and attempting to gain further insight into the postural control process through more sophisticated analysis techniques, such as using nonlinear time series analysis.

2.3.2. Advanced Analysis of Balance

The analysis of postural control in quiet stance often employs techniques that assume that the COP signal to be stationary, and will therefore have a constant mean and standard deviation throughout the time of the trial. However, several studies have shown that this is not true (Carroll and Freedman, 1993; Schumann et al., 1995; Newell et al., 1997); leading to a growing number of studies that have employed sophisticated non-stationary data analysis techniques to examine the nature of postural control.

Power spectral analysis has been employed as a useful technique to determine the frequency composition of time series data, such as COP or ground reaction forces during standing (McClenaghan et al., 1995). Schumann et al. (1995) and Newell et al. (1997) expanded on the common use of these stationary spectral density techniques by employing a time-frequency analysis to examine the changes in the spectral characteristics of the COP signal over time. Newell et al. (1997) discovered that 100% of experimental trials were non-stationary in the time domain for 3- and 5-year-old children and young and elderly adults during quiet stance with and without vision. However, time-frequency analysis of postural control has been mainly descriptive in nature, making it difficult to test research hypotheses and compare populations via statistical methods (Schumann et al., 1995). This highlights the important of any non-stationary analysis tool to be able to yield meaningful and sensitive statistical measures that can be used in further statistical tests to determine if there are any significant differences between experimental groups. That being said, researchers should choose the approach that they believe best describes the underlying process of postural control. It may be that, due to the complex interactions involved within postural control, no single quantity can appropriately describe balance in all its nuances, and whichever analyses that are used must be interpreted with great care and with reference to multiple theoretical concepts.

The Lyapunov exponent is a measure of the rate at which nearby trajectories diverge, and can be an important means for the quantification of unstable systems (Collins and DeLuca, 1994; Stergiou et al., 2004; Pascolo et al., 2006). Periodic signals will result in Lyapunov exponents that are negative or zero, and positive values suggest the presence of chaos within the signal (Yamada, 1995). Studies using the Lyapunov exponent as a means of determining the extent of chaotic motion within postural control have shown that the chaotic swaying of the COP during quiet standing plays an important role in the adjustment of posture during standing with voluntary swinging arms (Yamada, 1995). However, although a positive Lyapunov exponent indicates that postural control in standing is chaotic, it is not sensitive enough to discriminate between

adults with Parkinson's disease and healthy subjects (Pascolo et al., 2005; Pascolo et al., 2006). Furthermore, a positive Lyapunov exponent may indicate the presence of chaos within a signal, however, random signals will also result in positive Lyapunov exponents, making it difficult to determine whether the underlying process of the signal is of a stochastic or deterministic nature, unless results are validated against surrogate data sets (Stergiou et al., 2004). Surrogation is a technique that can be used to help determine if a signal is deterministic or stochastic in nature by comparing actual data against a random data set with the same mean, variance and power spectra as the original (Stergiou et al., 2004). Collins and DeLuca (1994) found that there was no significant difference between the Lyapunov exponents of surrogate data and the original COP signal during quiet stance, concluding that postural control should not be modelled as a chaotic process and consequently modelled postural control as a correlated random walk.

Collins and DeLuca (1993) examined the COP trajectory during quiet standing as one- and two-dimensional random walks. This involved calculating a stabilogram-diffusion plot from the mean square displacements of the COP over an increasing time interval, and dividing the resulting plot into a short- and long-term region based on the intersection of two lines fitted to the trace. Collins and DeLuca (1993) attributed the short- and long-term regions to different mechanisms of postural control. Over short periods of time an open-loop mechanism is employed, and over longer time intervals a closed-loop mechanism is dominant. Within this analysis, diffusion coefficients are calculated for both the short- and the long-term phases, which represent the stochastic activity of the COP. In addition Hurst exponents are generated from the log-log plot of the stabilogram-diffusion plot, which are the scaling exponents and quantify the positive and negative correlations between the step increments, termed as persistence and anti-persistence respectively. So far, random walk analysis of postural control has shown that when standing with eyes open subjects showed decreased diffusion coefficients and Hurst exponents during the short term phase, suggesting that vision helps to reduce the stochastic activity of the open-loop control of posture (Collins and DeLuca,

1995; Riley et al., 1997). However, this research does not offer an explanation as to how the absence of vision can affect the stochastic activity of postural control during open-loop control, which by definition should be control with the absence of feedback. Consequently, Newell et al., (1997) have questioned the assumption that the trajectory of the COP is best modelled as a correlated random walk with two distinct phases, and have shown that a simple linear random walk can account for as much as 92% of the variance of the COP, with the Collins and DeLuca (1993) model accounting for 96% of the variance. According to Yamada (1995), in chaotic dynamics randomness emerges out of deterministic dynamics whereas in random walk dynamics, noise is not directly linked to deterministic dynamics. Therefore future analyses of balance may need to consider both the stochastic and the deterministic components of the COP signal, such as using stochastic differential equations (Bonnet et al., 2010). However, the underlying difficulty with obtaining an understanding of the underlying process of postural control from such methods may be that force plate data represents the sum of the corrective forces from all segments of the body to remain upright, suggesting that a more thorough analysis of the mechanisms of postural control is required.

2.3.3. Muscle Activity and Joint Torques

Muscle coordination can be described as the distribution and timing of muscular activity or force among individual muscles to produce the overall joint moments, and thus can be studied from EMG and force patterns of individual muscles or joints (Hug, 2011). To date the majority of studies that have used EMG to examine the coordination of muscle activity during balance tasks have focused mainly on examining postural control during external perturbations.

During anterior postural sway caused by an external perturbation a coordinated muscular response can be seen in the muscles of the posterior aspect of the lower limbs and trunk, namely the ankle, hip and trunk extensors (Horak and Nashner, 1986; Diener et al., 1988; Horak et al., 1989). During posterior postural sway caused by an external perturbation a coordinated muscular response can be seen in the muscles of the anterior aspect of the lower limbs

and trunk, the ankle, hip and knee flexors. However, young infants present less coordinated muscular responses to imposed postural sway, with more organised muscular patterns developing with increased age and experience (Woollacott and Sveistrup, 1992; Sveistrup and Woollacott, 1997; Sundermier et al., 2001).

Nashner (1976) examined responses to anteroposterior platform translations and/or rotations, designed to elicit a functional stretch reflex of the ankle musculature, with EMG electrodes placed on the tibialis anterior and medial gastrocnemius muscles. This study revealed that healthy adults displayed a long latency stretch reflex of approximately 120 ms, exhibited to reduce postural sway as a result of a sudden external perturbation. Furthermore, when exposed to successive perturbations of a similar nature, subject's functional stretch reflexes adapted to reduce sway further, with increased EMG activity during platform translations and decreased EMG activity during platform rotations. On the other hand, Gottlieb and Agarwal (1979) discovered that under sudden dorsiflexion and plantar-flexion of the foot a myotatic reflex of approximately 45 ms can be seen in the tibialis anterior and gastrocnemius muscles respectively. The functional roles for the myotatic reflex in the leg extensors may be limited to conditions of postural maintenance or slow precise movements. During rapid movements the myotatic reflex will be ineffective and load compensating reactions are mediated by longer latency loops of approximately 120 ms or more. Furthermore, the gain of the myotatic reflex was proportional to the rate of voluntary movements of the ankle, with increased muscle activity associated with increased plantar-flexion torque (Gottlieb and Agarwal, 1979). These findings may highlight the importance of examining muscular activity of postural muscles in quiet stance as well as during external perturbations.

The synchronicity of muscle firing patterns of the lower extremities show an increased regularity during stance with random voluntary sway compared to stance with regular voluntary sway (Morrison et al., 2007). There was a high degree of regularity in the COP trajectory during quiet stance and regular

voluntary sway. However, the presence of a significant amount of irregularity during random sway suggests a complex relationship between muscle activity patterns and COP trajectories. Saffer et al. (2008) examined the EMG activity of leg and trunk muscles during quiet stance, and used coherence analysis to assess the patterns of coordination between muscles and body segments. Although these results indicated that ankle and hip patterns during quiet stance involve mainly lower leg muscles, and there was an anti-phase movement of the trunk relative to the legs, there was surprisingly little coherence between individual muscles. This may be a consequence of assessing muscle activity during quiet stance, resulting in decreased muscle activity compared to those of perturbation studies, however, this may also be due to the limitations of using surface EMG, with a poor signal-to-noise ratio, to assess muscular coordination (Hug, 2011).

Past research has examined the coordination of multiple joint torques when experiencing external perturbations in upright stance in adults (Runge et al., 1999; Seo and Choi, 2005) and children (Roncesvalles et al., 2001). To counter a perturbation resulting in anterior postural sway adults generated positive extensor torques at the ankles and hips, with a counterbalancing negative flexor torque at the knees (Runge et al., 1999; Roncesvalles et al., 2001). Similar to previous EMG studies, infants displayed less coordinated joint torques, which gradually became more organised with increasing age and experience (Roncesvalles et al., 2001). Furthermore, response latencies for ankle, knee and hip torques to external perturbations occurred at approximately 150 ms, with EMG responses occurring up to 60 ms prior to joint torque responses (Runge et al., 1999). In addition, the magnitude of hip torques was significantly higher during perturbations that also elicited a significant EMG response in the rectus abdominis muscle, indicating the importance of the activity of neighbouring muscle groups in the generation of appropriate joint torque responses (Runge et al., 1999). However, to date the coordination between multiple joint torques during static balance activities has only been assessed in inverted stance (Kerwin and Trewartha, 2001; Yeadon and Trewartha, 2003).

Similar to upright quiet stance, both Kerwin and Trewartha (2001) and Yeadon and Trewartha (2003) found that, although all joints contributed to the control of the COM, the main control strategy comes from the most distal supporting joint, which in inverted stance is the wrist joint. Furthermore, the joint torques were regressed against the COM position and velocity at progressively earlier times, revealing time delays of 160 to 240 ms for this wrist strategy (Yeadon and Trewartha, 2001). These torque delays are somewhat longer than those observed by Runge et al. (1999) regarding perturbations in upright stance, however, an increase in the torque delays induced by platform perturbations with small velocities were observed, suggesting a possible relationship between response delays and sway velocity. It can be assumed that neuromuscular responses to postural sway are related to the sensitivity of the involved sensory receptors, which would mean that important sensory thresholds are invariably linked to the control of posture and could explain differences in response timings to different velocities of sway.

Fitzpatrick and McCloskey (1994) assessed sensory thresholds on simulated standing conditions, and the results suggested that only visual and somatosensory proprioception was sensitive enough to detect sway in quiet stance. At low sway velocities, ankle proprioceptors were more sensitive than vision in detecting a change in sway, but at higher sway velocities there was little difference between the two sensory systems. These thresholds were 0.17° when sway was at a velocity of $0.06°s^{-1}$, with even smaller movements perceived as the mean velocity of sway increased up to $0.17°s^{-1}$. Similarly, Clark et al. (1985) also found a relationship between speed and position thresholds when examining the ankle joint and metacarpophalangeal (MCP) joint of the hand. However, Clark et al. (1985) reported higher position thresholds of ± 3.5° for the ankle joint and ± 2.5° for the MCP joint. This difference may be explained by the experimental protocol used in each case, as Fitzpatrick and McCloskey (1994) assessed subjects in restricted standing positions, with the legs weight bearing. Clark et al. (1985) isolated each joint in turn and used neural blocks in an attempt to isolate the detection of movement and position separately. Furthermore, Clark et al. (1985) showed that the

position threshold remained relatively constant throughout movement speeds, even with extremely slow movements in the order of ± 0.25º/min. Ultimately, both studies show that movement thresholds depend on both the speed and amplitude of the movement, and with higher speeds a change in position can be detected within a fraction of a degree.

2.4. Development of Postural Control

During the first decade of life the human body undergoes the most significant transitions in motor development, making this time an excellent time to study the emergence and development of postural control (Roncesvalles et al., 2001). Furthermore, general postural control can be viewed as the foundation for which the development of more advanced movement skills can arise, leading some to examine postural control in relation to motor development and motor competency in addition to chronological age (Woollacott and Sveistrup, 1992; Roncesvalles et al., 2001; Sundermier et al., 2001). Within the field of motor control it is generally believed that with more practice at a given task there is less reliance on exteroceptive information from visual and auditory receptors and more use of interoceptive information from the proprioceptive systems (Gurfinkel et al., 1965; Lee and Lishman, 1975; Nashner and McCollum, 1985). Although some researchers claim that there is not an overwhelming amount of support for this view in postural control studies (Slobounov and Newell, 1994), there is some research suggesting developmental changes to the utilisation of visual and vestibular information during balance tasks.

Infants as young as 5 months of age are able to detect and interpret the change in visual flow produced by the movement of the room as body sway, and the motor system is able to produce the directionally appropriate postural responses that serve to correct the perceived loss of stability (Foster et al., 1996). In addition, new walkers are most influenced by a change in visual flow created by the motion of a moving room, which may indicate an enhanced reliance on visual perception of children at this developmental stage (Foster et al., 1996). Furthermore, anteroposterior optic flow has a significant effect on children aged 4 to 8 years above that of adults, with a significant decrease in

visual flow induced sway from 5 to 6 years of age (Casselbrant et al., 2007). This period seems to coincide with a period of sensory exploration between the ages of 4 to 6 years, were children begin a transition from reliance on visual and vestibular cues during stance to a better utilisation of somatosensory cues, and with the emergence of the integration of these sensory systems during balance tasks (Shumway-Cook and Woollacott, 1985; Woollacott et al., 1987). Although children at this stage are capable of re-weighting the integration of visual, vestibular and somatosensory cues during times of sensory conflict, they are not proficient until all three systems are mature, which may not occur until age 10 (Shumway-Cook and Woollacott, 1985; Woollacott et al., 1987), or perhaps age 12 (Peterson et al., 2006; Rinaldi et al., 2009). Although the integration of sensory cues is essential to the maintenance of upright stance, the generation of appropriate motor responses to the perceived orientation of the body is also of importance.

The patterns of muscle activation following a perturbation to the visual system are not stereotypical at different ages, and task experience has been demonstrated to affect the muscle activation patterns observed in other balance tasks (Woollacott et al., 1987). While directionally specific response synergies are present in children of a very young age, structured organisation of these synergies is not yet fully developed since variability in timing and amplitude relationships between proximal and distal muscles is high (Shumway-Cook and Woollacott, 1985; Roncesvalles et al., 2001). During the early development towards independent stance, such as in the appearance of pull to stand behaviour, an infant will display disorganised muscular activity in the supporting limbs, including high variability with the magnitude, burst duration, activation patterns and onset latencies of muscular responses to external perturbations (Woollacott and Sveistrup, 1992; Roncesvalles et al., 2001; Sundermier et al., 2001). With increased motor competence through experience of more advanced motor skills, such as walking, running, jumping, hopping and skipping, muscular responses to an external perturbation evolve to exhibit faster recovery times and reduced onset latencies, shorter and more direct COP trajectories, greater peak torque magnitudes with reduced burst duration, and a coordinated

unimodal torque pattern between joints and muscle groups (Woollacott and Sveistrup, 1992; Roncesvalles et al., 2001; Sundermier et al., 2001). In addition, older children are more likely to exhibit a systematic strategy to accommodate the increased demands from a change to a balance task, such as standing on one leg; with these children showing an increased number and variety of corrective responses to maintain upright (Slobounov and Newell, 1994). Therefore, these older or more experienced children were more successful at re-introducing additional biomechanical degrees of freedom into the coordination of muscular activity patterns to enhance postural stability during the increased demands of the task.

The previously mentioned literature seem to support the view held by Woollacott and Sveistrup (1992), who believe that the development of postural control during childhood can be compared to the three specific phases in the development of behaviour suggested by Bernstein (1967). Woollacott and Sveistrup (1992) explain that before the emergence of independent stance a child will not show a clear behavioural strategy or a coordinated muscle response pattern as they struggle to deal with the excessive 'degrees of freedom' available to them from control of the hips, knees and ankles. With increased experience, the emergence of independent stance will result from the infant reducing the degrees of freedom available to them by freezing the motion at proximal joints in order to simplify the task and control posture within a small boundary of stability via control of the ankle joint. Further experience of independent stance will allow mastery of this ankle strategy, eventually allowing the infant to experiment with expanding the degrees of freedom by allowing motion of the other joints in the legs and body, to explore and develop other control strategies and eventually increase the boundaries of stability (Woollacott and Sveistrup, 1992).

An interesting question that is yet to be answered is 'does the development of postural control abilities allow the expression of behaviours that have been designated as developmental milestones, or do the motor experiences during the attempts at these behaviours help to develop and refine postural control

abilities?' (Sundermier et al., 2001). It may be that the association between postural control and general motor development can be viewed as a cycle or positive spiral, whereby development of one leads to the opportunity for further development in the other, and that the development of both postural control and general motor skills should be examined together to further our understanding in either one. However, we must also consider the possible effects of physical development and maturation of key physiological systems, such as mylination of neurological pathways, enhanced muscular strength and development of visual and vestibular acuity. Therefore, future studies into the development of postural control may wish to examine how individuals with a mature neurological system learn to balance. However, this would require assessing neurologically sound adults in a balance task that is unfamiliar to them, and therefore could not be assessed in normal upright stance. One possible approach for this would be to assess how individuals learn to balance in inverted stance.

2.5. Handstand Balance

Several studies examining postural control in inverted stance have continued to employ COP as the main determinate of balance ability (Clement and Rezette, 1985; Clement et al., 1988; Slobounov and Newell, 1996; Asseman et al., 2004; Asseman et al., 2005; Asseman and Gahery, 2005; Gautier et al., 2007; Sobera et al., 2007; Gautier et al., 2009; Croix et al., 2010; Croix et al., 2010a). Such studies have examined postural control in inverted stance by calculating mean sway velocity, sway area, sway radius, and sway range and standard deviation. In addition, some studies have measured the duration of inverted stance trials as a measure of balance performance, however, it is unclear how these studies have accounted for the differences in trial lengths when calculating particular measures of balance, such as sway area and sway length (Asseman and Gahery, 2005). Similar to normal stance, these studies have shown that sway in the anteroposterior direction is larger than in the mediolateral direction (Slobounov and Newell, 1996; Sobera et al., 2007), and balance performance in inverted stance decreases during eyes closed conditions (Asseman et al., 2004; Asseman et al., 2005; Asseman and Gahery, 2005; Gautier et al., 2007;

Croix et al., 2010), with restricted central or peripheral vision (Gautier et al., 2007), during altered visual gaze (Clement et al., 1988) and when balancing on a compliant surface (Croix et al., 2010). Furthermore, balance performance can be significantly affected by the alignment of the head in different positions, such as standard, dorsiflexion, aligned with the trunk, and ventroflexion (Clement and Rezette, 1985; Asseman and Gahery, 2005). However, vision only has a significant effect on postural control in handstand when the head is in the standard position or when in dorsiflexion, suggesting that the effect of the head position on postural control in handstand may be due to more than vision alone.

Research examining the kinematics of inverted stance suggests that an individual's trunk and head will remain relatively static throughout the balance task, with increasing magnitudes of motion in the more distal segments, such as hips and ankles (Slobounov and Newell, 1996; Kerwin and Trewartha, 2001). In addition, Kerwin and Trewartha (2001) discovered that, although the combined joint torques from wrist, shoulder and ankle contributed to the COM movements, wrist torques played the most dominant role in controlling sway for skilled hand balancers. However, less skilled hand balancers employed increased hip torques to control the COM and maintain balance. Unfortunately, this supposition is based on the relationship between joint torques and COM displacement only, and does not take into account any possible neurological delays as was highlighted previously in section 2.2.3. Nevertheless, this has been considered by Yeadon and Trewartha (2003), who discovered that gymnasts in inverted stance used a compensatory wrist torque, with time delays ranging from 160 to 240 ms, and accompanied by synergistic shoulder and hip torques acting in the same direction to control for COM displacement and velocity. These results seem to suggest that the preferred corrective strategy employed by hand balancers is a wrist strategy to correct for small perturbations, but as balance becomes more precarious the performer will begin to rely on more distal corrections from the shoulder and hip. However, further study into the corrective responses to internal and external perturbations may be required to discover the full array of corrective strategies employed by individuals in inverted stance, such as the relevance of an elbow mechanism

(Slobounov and Newell, 1996). Future research into this area may find worth in the procedures employed in previous studies into postural control during normal stance, such as using a combination of EMG and dynamic posturography to measure muscle latencies and muscle activity patterns in response to controlled perturbations. In addition, previous research has only assessed COP trajectories with traditional analysis methods, therefore, further insight into inverted stance through more sophisticated analysis techniques is needed.

2.6. Chapter Summary

The literature surrounding balance has been reviewed and the description of static balance and postural control has been clarified. The relevance of both the neurological and the mechanical implications for postural control have been highlighted, and a means through which these may be assessed have been provided. In addition, the development of postural control as a child ages has been discussed, with some reference to the problem of how the degrees of freedom in the system may change during this process. Lastly, the above was discussed with relevance to balance in the handstand position, which was suggested as a possible alternative to assessing how the postural control is learnt.

CHAPTER 3

METHODS

This chapter reviews the literature concerning the collection and treatment of data used to assess balance, and justifies the data collection and data processing methods used in the current research. A detailed description of the experimental protocol is given, and the procedure for the collection and processing of experimental data is provided.

3.1. Subjects

All subjects involved in the current research were recruited from the Loughborough University gymnastics club or from the Loughborough University Sport and Exercise Science undergraduate programme. All subjects gave informed consent for the procedures in accordance with protocols approved by the Loughborough University Ethical Advisory Committee (Appendix 1 and 2). All subjects were required to be free from injury at the time of testing, and have no history of upper limb injuries up to six months prior to the commencement of testing.

3.1.1. Subjects: Study One

Study one recruited 22 subjects who were interested in learning to handstand for eight months during the 2011-2012 academic year. To be included in this study each subject was required to be available to practice handstands for at least three times a week for 10-15 minutes each session and attend a testing session every four weeks. An additional inclusion criterion was that individuals must be able to safely get into the handstand position against a wall, but when they moved into independent support they would only be able to maintain balance for a maximum of five seconds. Before the end of the eight month period of handstand practice and testing, nine subjects dropped out of the study for a variety of reasons, resulting in 13 subjects that completed all required parts of the study, including five males (age: 20.4 ± 1.14 years; mass:

76.6 ± 4.7 Kg; height: 1.81 ± 0.06 m) and eight females (age: 19.4 ± 1.7 years; mass: 61.6 ± 3.9 Kg; height: 1.67 ± 0.09 m).

3.1.2. Subjects: Study Two

Study two recruited 12 subjects who were experienced at balancing in handstand and could maintain independent balance for at least 30 seconds, including nine males (age: 23.1 ± 3.6 years; mass: 69.9 ± 2.2 Kg; height: 1.73 ± 0.05 m) and three females (age: 20.5 ± 0.7 years; mass: 57.9 ± 1.9 Kg; height: 1.64 ± 0.02 m). These subjects were all experienced artistic or acrobatic gymnasts with many years of experience in performing tasks in hand support and were comfortable with the challenging nature of the tasks involved during platform perturbations and altered sensory inputs.

3.2. Data Collection

Data for all balance trials were collected on the Computer Assisted Rehabilitation Environment (CAREN) system developed by Motek Medical. This system consists of a Stewart platform with six hydraulic rams allowing the platform to move with six degrees of freedom, which allows up to ± 0.15 m of translation and ± 15º of rotation. The CAREN system incorporates a Vicon motion analysis system to collect kinematic data, and has two Bertec strain gauge force plates imbedded into the Stewart platform to allow reaction forces, moments, and centres of pressure to be determined. In addition, a Delsys Trigno wireless EMG system was linked to the system so that surface electromyographic (EMG) activity could be measured. All data from the force plates and EMG unit were passed through the same analog-to-digital converter (ADC) via the Vicon MX Giganet control box to synchronise EMG and kinetic data with the kinematic data. During all data collection sessions, kinematic data were sampled at 200 Hz and force plate and EMG data at 2000 Hz, with data synchronised to within ± 0.5 ms.

3.2.1. Platform Movements

Movements of the Stewart platform allowed for specific perturbations to be applied to an individual attempting to balance on the platform surface; motion

was controlled by the Motek Medical D-Flow software designed for this purpose. Within the D-Flow software an application was created that would allow the amplitude and velocity of the platform translations and rotations to be controlled. The range of motion allowed within this application was restricted to ± 0.1 m for horizontal translations and ± 10° for rotations about the x-axis; and the velocities were restricted to a range of ± 0.2 m·s^{-1} for translations and ± 100°·s^{-1} for rotations. Furthermore, rotation of the platform can be combined with horizontal and vertical translations so that the axis, or point, of rotation of the platform can be moved (Barton et al., 2006). Using the algorithms of Barton et al. (2006), an application was created using the script module within the D-Flow software to allow the system to track the motion of an individual in standing and rotate the platform about the ankle joint so as to track the body sway and reduce ankle motion. This employed the principles of the sway referenced condition from the sensory organisation test (Nashner, 1972); whereby this sway referenced platform motion would reduce the feedback from the proprioceptive sensors around the ankle and help assess the role of this feedback during standing balance. In addition, the application allowed for the sway referenced test to be performed in handstand, where the platform would rotate about the subjects' wrist joint to reduce the associated proprioceptive feedback.

3.2.2. Kinematic Data

The optoelectronic motion capture system (Vicon, Oxford Metrics Group), situated within the CAREN system consisted of nine T20 vicon cameras. The cameras have a sensor size of 1600 by 1280 pixels, with maximum resolution up to a frame rate of 500 Hz, allowing the sample frequency used in the current research to utilize the full resolution of 2 megapixels. The T20 cameras emit near inferred light which is reflected back to the cameras from the retroreflective markers placed on the individual under investigation. The 2D images from each camera are combined to provide the reconstructed 3D coordinates for each reflected marker within the capture volume. However, the accuracy of the reconstruction is dependent upon the camera positions, settings, and the camera parameters determined during the calibration

procedure which was completed before each data collection session. The nine T20 cameras were positioned around the 2 metre diameter Stewart platform on a rigid metal frame measuring 5 m by 5 m across and 4 m in height (Figure 3.1).
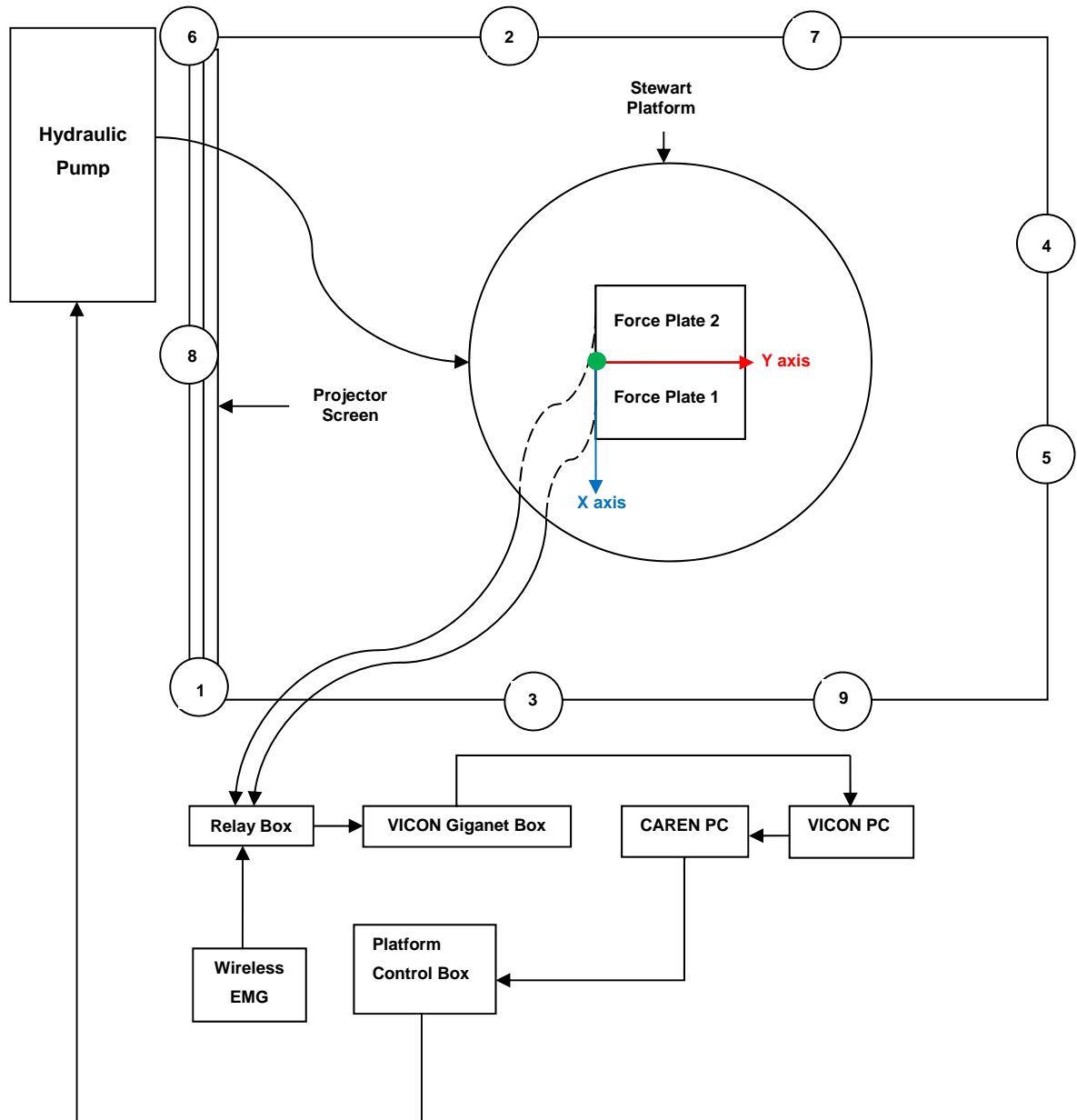
Figure 3.1: The CAREN system setup and connecting equipment, including the nine T20 vicon cameras (circles numbered 1-9), with the origin (green dot) and orientation of the global coordinate system.

The dynamic calibration involved waving a 5-marker L-frame wand around the full capture volume, which was a cube of 3 m by 3 m wide and 3 m in height above the surface of the platform, centred on the centre of the Stewart platform. The static calibration required the same 5-marker L-frame to be positioned

41

within the capture volume so that the origin and orientation of the global coordinate system (GCS) could be set. The origin was set to the front edge of the join between the two force plates, with the positive x-axis to the left, positive y-axis to the rear, and the positive z-axis vertically up, as seen from an individual standing in the centre of the platform facing the projector screen (Figure 3.1). The calibration procedure provides the user with an estimate of the camera errors, given as the camera residuals measured in pixels, which represents the RMS difference between each camera view of a marker and its reconstructed 3D coordinate. The locations of the nine cameras relative to the centre of the Stewart platform can be seen in Figure 3.1; with the position and mean residual error for each camera also shown in Table 3.1.

Table 3.1: The position of each camera relative to the centre of the platform, and the mean and SD of the camera residual errors for all data collection trials.

	Position (m)			Distance to Centre (m)	Residual Error in Pixels (mean ± SD)
Camera	X	Y	Z		
1	2.27	-2.58	2.45	4.22	0.166 ± 0.012
2	2.49	-0.16	3.32	4.15	0.163 ± 0.012
3	-2.30	-0.37	3.31	4.05	0.201 ± 0.013
4	-0.74	2.53	1.40	2.99	0.251 ± 0.018
5	0.95	2.47	2.20	3.44	0.153 ± 0.013
6	-2.48	-2.19	2.48	4.14	0.189 ± 0.017
7	-2.30	1.23	3.29	4.20	0.208 ± 0.019
8	0.26	-2.43	3.31	4.11	0.174 ± 0.011
9	2.52	1.23	3.35	4.37	0.172 ± 0.016
Mean residual for all cameras					**0.186 ± 0.014**

3.2.2.1. Marker Placement

A marker set consisting of 53 spherical markers of 14 mm diameter was used to divide the body into 19 segments (Figure 3.2 and Appendix 3). Marker pairs positioned at medial and lateral projections of the joint centre were used to calculate the metacarpophalangeal, wrist, elbow, metatarsophalangeal, ankle and knee joint centres. In normal and single leg stance the shoulder joint centre was calculated as ⅓ of the distance from the anterior shoulder (AS) marker to the posterior shoulder (PS) marker. In handstand the shoulder joint centre was calculated as ½ the distance from the lateral shoulder (LS) marker to the AS marker.
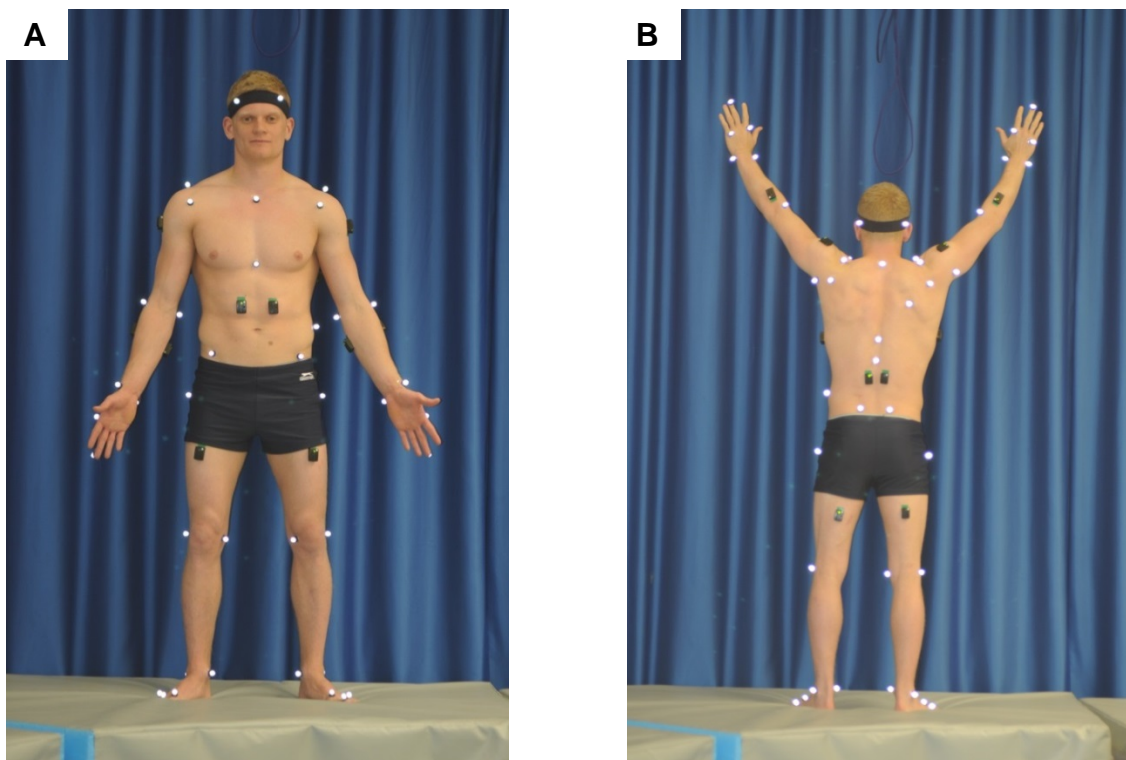
Figure 3.2: Position of markers and EMG sensors (full details in Appendix 3)

The hip joints were predicted using the method of Davis et al. (1991), where the three dimensional location of the right and left hip joint centres are estimated via:

$$C = 0.115 L_{leg} - 0.0153 \qquad (3.1)$$

$$X_h = S \left[C \sin \theta - \frac{d_{ASIS}}{2} \right] \qquad (3.2)$$

$$Y_h = [-y_{dis} - r_{marker}] \cos \beta + C \cos \theta \sin \beta \qquad (3.3)$$

$$Z_h = [-y_{dis} - r_{marker}] \sin \beta - C \cos \theta \cos \beta \qquad (3.4)$$

Where d_{ASIS} is the distance between the right and left ASIS (anterior-superior-iliac-spine), y_{dis} is the anterior/posterior component of the ASIS-to-hip centre distance, L_{leg} is the mean leg length, $\theta = 28.4°$ (representing the angle from the hip joint centre to the ASIS in the frontal plane), and $\beta = 18°$ (representing the angle of pelvic tilt in the sagittal plane). The exact motion of the Stewart platform was determined by placing four extra markers on the platform, aligned with the four corners of the forces plates. These markers were used to track the translation and rotation of the platform and were required so that the origin of the force plates could be reconstructed to make adjustments to the position of the centre of pressure (COP) and the orientation of the force vector during platform motions.

3.2.3. Force Data

The two Bertec FP4060-07 strain gauge force plates are embedded side-by-side into the centre of the Stewart platform, each measuring 0.4 m in width and 0.6 m in length, giving a total area of 0.8 m by 0.6 m. Each force plate measures horizontal and vertical forces in four locations to calculate the resultant force applied to the surface of the plate, with a maximum load of 10 kN in the vertical direction and 5 kN in the horizontal directions. The three orthogonal components of the applied force, and the three components of the resultant moment, are calculated within the force plate before being amplified and converted to a digital signal using a 16-bit ADC. The three force and three moment channels are transmitted from the force plate to an AM6501 digital-to-analog converter with a gain of unity before being passed via a relay box into the Vicon Giganet control box. Each channel has a voltage range of ± 5 V resulting in the signal scaling factors shown in Table 3.2 required to convert these voltages into the appropriate units.

Table 3.2: The maximum loads, signal scaling factors and mean errors for the six channels outputted from each force plate.

	Fx	Fy	Fz	Mx	My	Mz
Maximum Load (N, Nm)	5,000	5,000	10,000	3,000	2,000	1,500
Signal Scaling Factor (N/V, Nm/V)	1,000	1,000	2,000	600	400	300
Mean Error (± N, ± Nm)	0.136	0.162	0.470	0.126	0.098	0.062

The six channels from each force plate were used to calculate the COP and the free moment about the COP via:

$$A_x = \frac{M_y - F_x h}{F_z} = \frac{M'_y}{F_z} \tag{3.5}$$

$$A_y = \frac{M_x + F_y h}{F_z} = \frac{M'_x}{F_z} \tag{3.6}$$

$$T_z = M_z - F_y A_x + F_x A_y = M_z - \frac{F_y M'_y}{F_z} + \frac{F_x M'_x}{F_z} \tag{3.7}$$

However, both the moment and force signals have their own errors associated with them, resulting in corresponding errors in the COP and free moment, given by:

$$A_x \pm \delta_{Ax} = \frac{M'_y \pm \delta_{My}}{F_z \pm \delta_{Fz}} \tag{3.8}$$

$$A_y \pm \delta_{Ay} = \frac{M'_x \pm \delta_{Mx}}{F_z \pm \delta_{Fz}} \tag{3.9}$$

$$T_z \pm \delta_{Tz} = M_z \pm \delta_{Mz} - \frac{\left(F_y \pm \delta_{Fy}\right)\left(M'_y \pm \delta_{My}\right)}{F_z \pm \delta_{Fz}} + \frac{(F_x \pm \delta_{Fx})(M'_x \pm \delta_{Mx})}{F_z \pm \delta_{Fz}} \tag{3.10}$$

Error propagation relates to the effects that the uncertainties in a variable have on the uncertainties in a function based on that variable. When summing multiple variables which contain uncertainties the variance in the variable is

additive, which means the uncertainties add in quadrature; and when multiplying or dividing variables that have uncertainties, the fractional uncertainties add in quadrature. Therefore the uncertainties for COP and free moment can be calculated via:

$$\frac{\delta_{Ax}}{A_x} = \sqrt{\left(\frac{\delta_{My}}{M'_y}\right)^2 + \left(\frac{\delta_{Fz}}{F_z}\right)^2} \tag{3.11}$$

$$\frac{\delta_{Ay}}{A_y} = \sqrt{\left(\frac{\delta_{Mx}}{M'_x}\right)^2 + \left(\frac{\delta_{Fz}}{F_z}\right)^2} \tag{3.12}$$

$$\frac{\delta_{Tz}}{T_z} = \sqrt{\delta_{Mz}^2 + \left(\frac{\delta_{Fx}}{F_x}\right)^2 + \left(\frac{\delta_{Fy}}{F_y}\right)^2 + \left(\frac{2\delta_{Fz}}{F_z}\right)^2 + \left(\frac{\delta_{Mx}}{M'_x}\right)^2 + \left(\frac{\delta_{My}}{M'_y}\right)^2} \tag{3.13}$$

Equations 3.11 – 3.13 show that even when the errors in the measured forces and moments remain relatively constant, the errors in both COP and free moment can increase significantly if the vertical force is small. It is for this reason that researchers often employ a force threshold below which the errors are considered too high and COP and free moment are not calculated. The estimated errors in a measured variable, such as the forces and moments of a force plate, can be obtained by calculating the standard deviation (SD) of the signal to give the average uncertainty of the measurement. This requires knowledge of the true value being measured, which is not always possible, however, if the same value is recorded multiple times, then the mean value provides a reasonable estimate of the true value, assuming there are enough samples.

A weight lifting disc with a mass of 10 kg was placed on each force plate and the force and moment data were recorded at 200 Hz for a period of 10 seconds, so that the mean and SD could be determined, shown in Table 3.2. These values were used with equations 3.11 and 3.12 to estimate a force threshold so that the uncertainties within the COP measurements would remain below ± 1 mm. Calculations show that a vertical force threshold of 99 – 136 N and 126 – 189 N is required to maintain the error within the mediolateral (ML) and

anteroposterior (AP) components of the COP below 1 mm, with the upper ranges required for COP locations towards the limits of the platforms' dimensions. Consequently, in all cases where the trial was stopped due to the subject moving their base of support, a force threshold of 200 N was used to determine the end of the trial.

Additionally, the values in Table 3.2 and equations 3.11 – 3.13 can also be used with the actual forces and moments from an experimental trial to give the estimated error in COP and free moment during that trial. For a subject with a mass of 72.5 kg, the error in COP during single leg stance will be < 0.2 mm, and for normal standing or handstand, with the mass distributed across both force plates, it will be < 0.5 mm (Figure 3.3). Nevertheless, it should be stressed that this is just an estimate of the actual error in the COP measurements, as equations 3.11 – 3.12 assume that the errors within the variables are independently random, with either normal or uniform distribution. These assumptions are not strictly true, as force plates may also have errors relating to hysteresis and possibly some vibrations, however, these errors will be minimised during static balance.
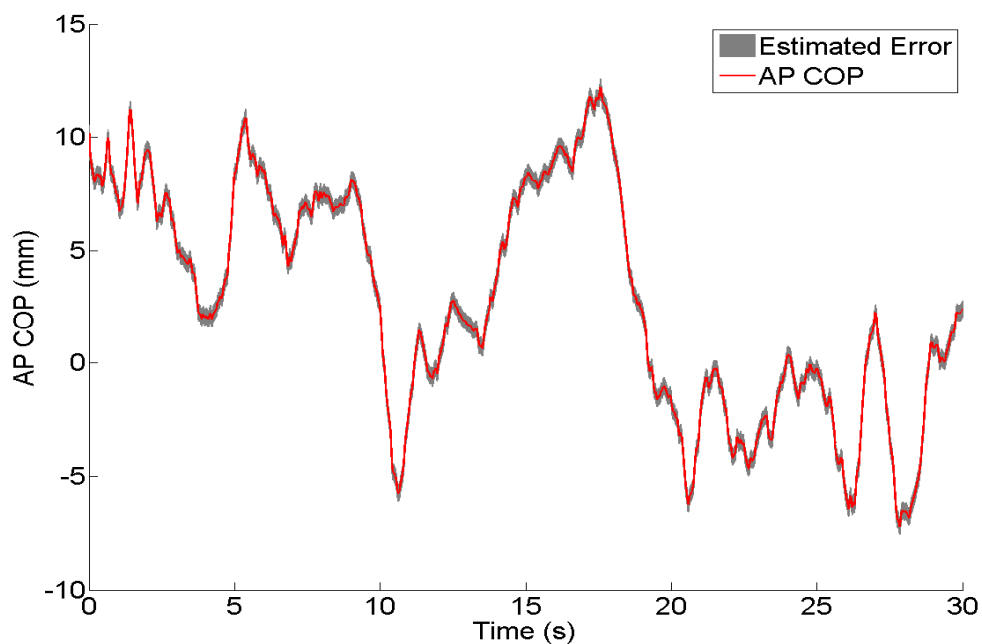
Figure 3.3: Example of the AP COP and the estimated error of the COP for a standing trial of a subject with a mass of 72.5 kg

3.2.4. EMG Data

The Delsys Trigno™ wireless EMG system (Delsys Inc.) incorporates 16 wireless EMG sensors, each with four separate 5 mm by 1 mm silver electrodes positioned in parallel pairs with an interelectrode distance of 10 mm. The four separate electrodes record the electrical potential that is generated by the underlying muscles and propagates to the surface of the skin; where two EMG signals are measured as the difference between each electrode in a lengthwise pair. The sensors use the two EMG inputs with proprietary stabilizing references to calculate the EMG activity of the area under the sensor without the need for a reference contact to remove, or reduce, the electrical signal from electrostatic, garment, and motion artefacts (Delsys, 2009). Each sensor has a signal range of ± 5 mV with a signal resolution of 153 nV/bit when sampled through a 16 bit ADC.

All trials required the full array of 16 EMG sensors to be positioned on the subject to obtain the activity of eight muscle groups on both the right and left side of the body. All sensors were fixed following the advice from the Delsys Trigno manual for the preparation of the skin and the use of the specially designed adhesive interfaces intended to simplify sensor attachment and reduce the electrical resistance of the site (Delsys, 2009).

The skin was shaved with a dry razor and cleaned with an alcohol wipe before EMG sensors were placed on the skin, aligned with the expected line of muscle fibres, and over the muscle bellies of the wrist flexors (WF), wrist extensors (WE), medial deltoid (MD), latissimus dorsi (LD), rectus abdominus (RA), erector spinae (ES), rectus femoris (RF) and biceps femoris (BF) muscles (Figure 3.2 and Appendix 4). In each data collection session, three maximum voluntary contraction (MVC) trials were collected to be used as a reference for the maximum activity possible for each muscle in that particular session, to be later used to scale all EMG measures to a percentage of maximum muscle activity. The MVC's included resisted isometric wrist flexion and extension (WF and WE muscles), resisted shoulder flexion and extension with arms fully

elevated in a seated position (MD, LD and RA muscles), and a resisted deadlift (ES, RF and BF muscles).

During standing trials with platform translations it was necessary to obtain EMG data for the tibialis anterior (TA) and medial gastrocnemius (MG) muscles as these are the muscle which control body sway about the ankle joint in standing. Therefore, for these trials, the four EMG sensors from the forearm muscles were repositioned to the lower leg and two MVC trials were recorded specifically for these muscles. The MVC trials included a resisted isometric deadlift with the feet in a heel raised position (MG), and a resisted isometric toe raise in a seated position (TA). All EMG placements are in accordance with the SENIAM guidelines or from Konrad (2005).

3.2.5. Anthropometric Data

Forty-five anthropometric measurements were taken for each subject as input into the geometric inertia model of Yeadon (1990), utilising the segmental density values from Chandler et al. (1975). This model sections the body into 40 solids by planes perpendicular to the longitudinal axes of the body segments; these are typically joined together via the parallel axis theorem to reconstruct the required number of segments for the model employed. In addition, the model uses the subject's known body mass, and compares it to the one estimated by the model, to subsequently correct the estimated segmental densities before recalculating all values. For each segment the mass, location of mass centre, principle moments of inertia about the mass centre, and distance between joint centres are calculated.

The pelvis, trunk and chest may be combined to model the torso as a single rigid segment from the hip joint centre to the shoulder joint centre, which may be a reasonable simplification for activities with minimal torso motion. In activities where there is more motion of the torso these segments are usually modelled separately, however, the boundaries between each segment are based on the anthropometric measurements in the geometric model and may not adequately correspond to the points used to construct the kinematic model

used to track the motion. Therefore, the solids and sub-segments within the geometric model were adjusted so that boundaries between the segments that make up the torso aligned with the retro-reflective markers used to track torso motion. This was achieved by calculating the heights of PSIS, L1, T10, and C7 markers above the hip joint centres during a static trial, and adjusting the measurements input to the geometric model accordingly.

The inertia model of Yeadon (1990) uses the sub-segment lengths, perimeters and widths from the anthropometric measurements of the torso to calculate the volume of stadium solids, each bounded by two parallel stadia. Where markers lay within one of the stadium solids that make up the torso segment, the solid was divided by finding intermediate lengths, perimeters and widths based on the height of the marker above the base of the solid as a percentage of the total height of the solid. The stadium solids were recalculated and, where required, adjacent solids were combined via the parallel axis theorem, resulting in a total of 18 segments to represent the body (Table 3.3 and Figure 3.4). In addition to the above adjustments, separate subject body masses were measured for each session and used to reconstruct a separate set of subject segmental inertial data for each session from the single set of anthropometric measurements.
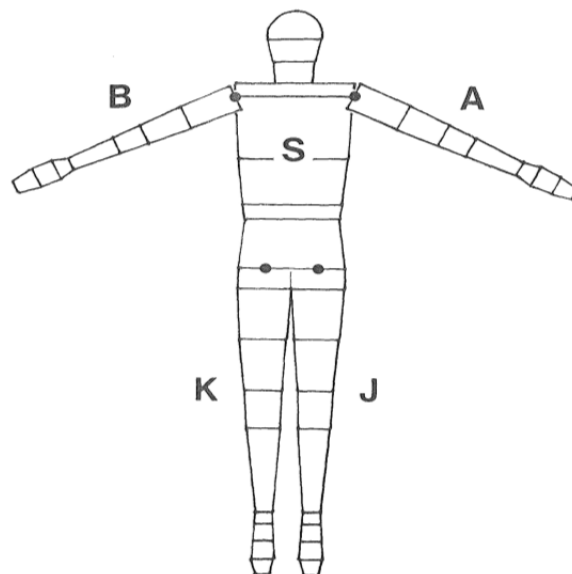
Figure 3.4: The 40 segments from the Yeadon geometric inertia model, showing the segmentation of the body into 40 solids (taken from Yeadon, 1990).

50

Table 3.3: The 40 solids from the geometric inertia model of Yeadon (1990), with the original 11 segments, and the new arrangement of 18 segments used in the current research.

Original Segment	Solids	New Segment
	s6, s7, s8	Head & Neck
	s5R	Right Shoulder Girdle
Chest-head	s5L	Left Shoulder Girdle
	s4	Thorax
Thorax	s3B	
	s3A	Abdomen
Pelvis	s1B, s2	
	s1A	Pelvis
Left upper arm	a1, a2	Left upper arm
	a3, a4	Left forearm
Left forearm-hand	a5, a6, a7	Left hand
Right upper arm	b1, b2	Right upper arm
	b3, b4	Right forearm
Right forearm-hand	b5, b6, b7	Right hand
Left thigh	j1, j2, j3	Left thigh
	j4, j5	Left shank
Left shank-foot	j6, j7, j8, j9	Left foot
Right thigh	k1, k2, k3	Right thigh
	k4, k5	Right shank
Right shank-foot	k6, k7, k8, k9	Right foot

(Note: segments s1A, s1B, s3A, s3B, s5R, and s5L are new solids that have been recalculated from the original arrangement)

3.2.5.1. Anthropometrics: Study One

The novice balancers from study one were tested over an eight month period, which might result in some changes to the anthropometric measurements collected. To ensure any changes would not adversely affect the integrity of the inertial data the subjects' body mass was monitored at each data collection session so that the anthropometric data could be re-measured if the body mass varied by more than 5%.

Table 3.4: The estimated masses, densities and volumes of a single subject with all measurements adjusted by ± 1 mm, ± 5 mm, and ± 10 mm.

Measurements	Mass	Density	Volume	Mass Difference
+ 10 mm error	65.83	0.956	68.15	5.28%
+ 5 mm error	64.17	0.955	67.19	2.62%
+ 1 mm error	62.86	0.954	65.86	0.53%
Original	62.53	0.954	65.54	0.00%
- 1 mm error	62.15	0.954	65.15	-0.61%
- 5 mm error	60.91	0.953	63.89	-2.59%
- 10 mm error	59.30	0.952	62.26	-5.17%

All anthropometric measurements will contain a certain amount of measurement error, which will be related to the expertise of the investigator taking the measurements. Yeadon (1990) showed that the estimated body mass of the current model may have an error of up to 2.3% when compared to the measured body mass. Although the 5% limit used in the current research may appear to be somewhat large compared to the previously reported error, the correction of body mass used within the inertia program allows for some leniency. In addition, when measuring segmental lengths, widths and perimeters, the estimated measurement error expected from an experienced investigator is approximately 5 – 10 mm (Yeadon, personal communication), which corresponds to an error in the estimated body mass of 2.6 – 5.2% (Table 3.4), justifying the 5% threshold used here. The largest change in body mass

for any subject, from that measured during the anthropometric measurements, was 4.1%; therefore no subject was required to have their anthropometric measurements retaken.

3.3. Procedure

During all experimental sessions subjects were allowed several minutes warm up, including several practice handstands, before the details of that session were reiterated to them. With the subject in a prone position, two markers were first placed on the spinous processes of the T10 and L1 vertebra; this was to allow accurate placement of these markers and aid in the placement of the EMG sensors on the erector spinal muscle group. The EMG sensors were placed on the subject using the procedure mentioned previously in section 3.2.4 before the three MVC trials were collected. Following the MVC trials the remaining 51 markers were placed on the subject before the subject was instructed to stand in the middle of the calibrated volume on the force plates so that two static trials could be recorded and body mass could be determined.

The first static trial required the subject to stand in the anatomical position facing the projection screen, with arms by their sides and the palms of their hands facing forward, similar to Figure 3.2a. The second trial required the subject to stand facing the projection screen with their arms fully extended above the head, similar to Figure 3.2b. These provided trials where all markers were easily viewed to be used as a standardised position to help create and run the marker file for automatic labelling, help replace markers that may become occluded during the experimental trial, and give a standard alignment for body segments to refer to. The subject was allowed a final practice to ensure they could perform the tasks with all markers and EMG sensors in place before they completed the required tasks for that session.

Past research has often placed stringent restrictions on starting positions, orientation, and movements allowed by the subjects involved. These included: dictating the position and angle of the feet, the height and angles of the free leg or arms, and even on insisting that no free limb motion is allowed to assist

53

postural control. The purpose of the current research was to assess the strategies used by novice and experienced balancers, and to assess how these strategies may change over time or during perturbations. Therefore, all subjects were instructed to maintain balance by whichever strategy they preferred, and no restriction was placed on the movements of the supporting limbs or free limbs during the balance trials. During all trials subjects were instructed to maintain a static base of support, where a change to the base of support would be considered as a failure to maintain balance, such as a step, a shuffle, or a free limb contacting the ground or support.

It is possible that a lenient approach to the positioning and control of the supporting and free limbs such as used here may result in a less controlled environment, which might result in greater variability within or between the subjects' performance. However, it was felt that this approach was necessary to firstly allow novice balancers to experiment and adjust whilst learning to balance, and secondly to gain a fuller understanding of the various ways in which an individual attempts to maintain balance in various challenging scenarios.

3.3.1. Static Trials

During all static trials, subjects were instructed to maintain a static base of support, and attempt to remain in, or return to the standard starting position for each condition. The standard positions were: fully extended arms, trunk, and legs with feet together for handstand; standing on the preferred leg, with free leg off the ground and not touching the support leg, and the arms in a comfortable position by the side for single leg stance; and feet at a comfortable distance apart and the arms in a comfortable position by the side for normal stance (Figure 3.5).
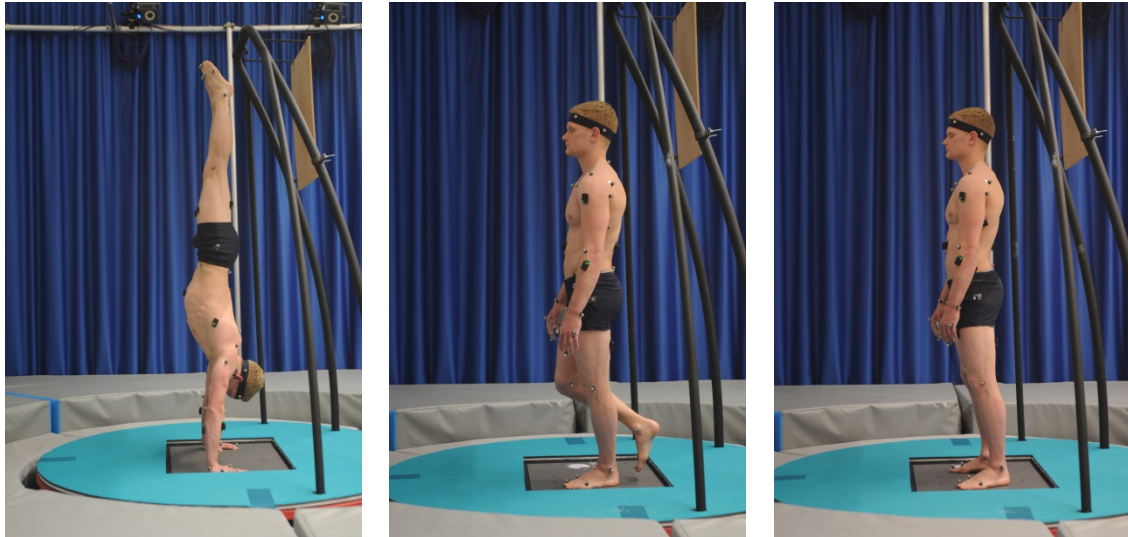
Figure 3.5: The standard starting position for the three conditions of handstand, single leg stance, and normal standing respectively.

3.3.1.1. Novice Handstanders

Study one involved the assessment of novice handstanders every month over an eight month period. During the first four assessment sessions, subjects were asked to perform five trials in handstand with eyes open for maximal duration, with a minimum one minute rest between trials. From the fifth assessment session onwards, once subjects became accustomed to performing handstands, they were asked to perform two blocks of five handstand trials, one block with eyes open and one with eyes closed. In addition, subjects were asked to perform trials in standing between the blocks of five trials in handstand; this was to increase the time between handstand blocks and reduce the chance that fatigue may occur. A random number generator was used to assign each subject to one of two groups to perform the trials in one of the orders shown in Table 3.5.

The experimental order was alternated for each subsequent session so that a subject assigned to order one in session five would follow order two the following session. The standing trials used between the blocks of handstand trials included blocks of five trials in normal standing for sessions five and six, and blocks of five trials in single leg stance during the subsequent sessions. Standing trials were completed for a maximum of 30 seconds duration for both

single leg stance and double leg stance, and all single leg stance trials were performed on the individuals' preferred leg.

Table 3.5: Two orders of blocks of trials used for assessing static stance.

Order One	Order Two
Handstand – Eyes Open	Handstand – Eyes Closed
Standing – Eyes Open	Standing – Eyes Closed
Standing – Eyes Closed	Standing – Eyes Open
Handstand – Eyes Closed	Handstand – Eyes Open

3.3.1.2. Experienced Handstanders

All experienced handstanders completed static trials in handstand, normal stance, and single leg stance; with eyes open and eyes closed conditions. Each condition was completed in a block of five trials with a minimum one minute rest between trials. Each trial lasted for a maximum of 30 seconds for all conditions, and subjects were allowed to retry any trial that lasted less than five seconds, with a maximum of 5 retries for each block of trials. To increase the time between blocks of trials in handstand, and reduce the chance that fatigue may occur, a random number generator was used to assign each subject to a group to perform the trials in one of the orders shown in Table 3.6.

Table 3.6: Two orders of blocks of trials used for assessing static stance

Order One	Order Two
Handstand – Eyes Open	Handstand – Eyes Closed
Single Leg Stance – Eyes Open	Single Leg Stance – Eyes Closed
Normal Stance – Eyes Open	Normal Stance – Eyes Closed
Normal Stance – Eyes Closed	Normal Stance – Eyes Open
Single Leg Stance – Eyes Closed	Single Leg Stance – Eyes Open
Handstand – Eyes Closed	Handstand – Eyes Open

3.3.2. Platform Perturbations

Experienced handstanders were asked to perform handstand and standing trials while receiving a discrete platform perturbation controlled by the application previously described in section 3.2.1. A total of 12 discrete platform translations were administered to the experienced handstanders in each posture, with three trials for each perturbation, consisting of a forwards or backwards translation, with a large or small perturbation. The large perturbations had an amplitude of 0.1 m and a velocity of $\pm$ 0.2 ms^{-1}, and the small perturbations had an amplitude of 0.05 m and a velocity of $\pm$ 0.1 ms^{-1}. The order of the 12 perturbations was randomly assigned to each subject via a random number generator using a simple Matlab script. This was firstly to reduce the chance that a subject would be able to anticipate the direction and size of each perturbation, and secondly to ensure that each subject received a different order of perturbations to reduce any order effects, such as fatigue or practice.

All experience handstanders completed the above procedure firstly while in the handstand position, followed by the same procedure while in the standing position. This was to allow the replacement of EMG sensors 1 – 4 from the wrist muscles to the lower leg muscles as described in section 3.2.4. In addition, it was felt that there was unlikely to be any crossover practice effect from experiencing the perturbations while in the handstand position to the perturbations while in the standing position.

All trials in handstand and standing lasted for approximately 4 – 6 seconds; with a perturbation administered at a random time within the first 1 – 3 seconds of balancing. The trial was stopped when either the subject failed to maintain balance with a static base of support or when the experimenter believed the subject had returned to a stable balanced position.

3.3.3. Sensory Organisation Test

Experienced handstanders were asked to perform trials with eyes open and eyes closed in both handstand and standing postures while experiencing the

sway referenced platform condition previously described in section 3.2.1. A total of 12 trials were administered in each posture; with 3 trials in each of the four conditions of eyes open or eyes closed, with a static or sway referenced platform. The handstand posture was completed in four blocks of three trials interspaced with three blocks of four trials in the standing posture (Table 3.7); where the order of trials were once again determined via a random number generator.

Table 3.7: An example of the order of trials for the sensory organisation test

Posture	Vision	Platform Motion
Handstand	Eyes Closed	Static Platform
Handstand	Eyes Open	Sway Referenced Platform
Handstand	Eyes Closed	Sway Referenced Platform
Standing	Eyes Open	Sway Referenced Platform
Standing	Eyes Closed	Sway Referenced Platform
Standing	Eyes Open	Static Platform
Standing	Eyes Open	Sway Referenced Platform
Handstand	Eyes Closed	Sway Referenced Platform
Handstand	Eyes Open	Static Platform
Handstand	Eyes Open	Sway Referenced Platform
Standing	Eyes Open	Static Platform
Standing	Eyes Open	Static Platform
Standing	Eyes Closed	Static Platform
Standing	Eyes Closed	Sway Referenced Platform
Handstand	Eyes Closed	Sway Referenced Platform
Handstand	Eyes Closed	Static Platform
Handstand	Eyes Open	Static Platform
Standing	Eyes Open	Sway Referenced Platform
Standing	Eyes Closed	Sway Referenced Platform
Standing	Eyes Closed	Static Platform
Standing	Eyes Closed	Static Platform
Handstand	Eyes Open	Sway Referenced Platform
Handstand	Eyes Closed	Static Platform
Handstand	Eyes Open	Static Platform

All trials lasted for a maximum of 30 seconds, until the subject lost balance by moving the base of support, or until the application stopped the trial due to an exceeded safety limit. Two safety limits were used, including a limit for the maximum amount of platform sway allowed, which was set to ± 5° to the

vertical, and one based on the minimum amount of vertical force, set to 100 N, to indicate that a foot or hand is about to lift off the surface of the force plate.

3.4. Data Processing

Throughout the current research every attempt was made to remove systematic errors, and reduce the random errors within the measurements, however, measurements will still contain some error, even if this is simply the added errors from the electrical noise within the equipment. Because of this, various steps may need to be taken in an attempt to reduce errors further. It should be noted that such measures cannot completely remove these errors from the data. Furthermore, several of the data analysis methods that have been used within the current research required that the signals are not excessively processed, and researchers often advise that these processing methods are not undertaken at all. These circumstances will be discussed further in Chapter 4, but unless it is stated otherwise it should be assumed that the following processing methods have been implemented.

3.4.1. Signal Filtering

A normally distributed random signal, such as can be seen in the error added to a signal due to electrical noise, will contain frequencies that are constant across the power spectrum, and is usually referred to as white noise. The higher frequency components of this signal may be removed, or attenuated, by using a low pass filter, however, the lower frequency components will remain. A low pass filter is often used to reduce the high frequency components of noise, and consequently reduce the errors within a signal, however, the low pass filter will also attenuate any frequencies of the true signal under investigation that are higher than the cutoff frequency (Winter, 2009). Therefore the choice of cutoff frequency can be crucial to ensure the maximum amount of noise is removed whilst also minimising the distortion to the true underlying signal (Derrick, 2004). The optimum cutoff frequency may be found by either examining the power spectrum of the signal or performing a residual analysis. Although there are some authors with preferences for one method over the other, if used appropriately these two methods should provide a similar cutoff frequency.

3.4.1.1. Residual Analysis

Residual analysis attempts to discover the optimum cutoff frequency by filtering the data at several different frequencies and calculating the residual between the raw and filtered signals (Winter, 2009); given by:

$$R(f_c) = \sqrt{\frac{1}{N}\sum_{i=1}^{N}(x_i - \hat{x}_i)^2}$$

(3.14)

Where f_c is the cutoff frequency, x_i is the raw signal, and $\hat{x}_i$ is the filtered signal. The residuals of the raw and filter signals represent the change in the signal due to the filtering process. This assumes that the residuals of any noise would fluctuate about zero and would increase gradually as the cutoff frequency is reduced, leading to a relatively linear line when plotted. Winter (2009) describes how this principle can be used to choose the appropriate cutoff frequency, by selecting the point at which the slope begins to deviate from the expected linear line of a random signal. However, this should be approached with caution, as this method may result in an underestimation of the cutoff frequency if a signal contains large amounts of noise, leading to attenuation of the true signal.

3.4.1.2. Power Spectrum

The power spectrum describes how the power of a signal is distributed over the different frequencies within the signal; and the cutoff frequency can be determined as the point below which 95% or 99% of the total power occurs. If the high frequency noise within a lower frequency signal represents only a small component of the whole signal, then the power spectrum can be used as an appropriate method to determine the cutoff frequency. If the noise within a signal is excessive, this method will overestimate the cutoff frequency, leading to a filtered signal that still contains significant amounts of noise, making it difficult to calculate accurate velocities and accelerations.

Force, COP displacements, and marker displacements resulted in low pass cutoff frequency estimates of 4 to 9 Hz based on residual analysis and 6 to 10 Hz based on power spectral analysis. To provide consistency across trials, and

to reduce the possibility of attenuating the true signal by over filtering data, all data were filtered using a fourth order, zero lag, low-pass Butterworth filter with a cut-off frequency of 10 Hz.

Raw EMG data were filtered with a fourth order, zero lag, band-pass Butterworth filter with cut-off frequencies of 20 Hz and 450 Hz (De Luca et al., 2010), before being rectified. Subsequently, EMG data were analysed unfiltered for perturbation trials and filtered using a fourth order, zero lag, low-pass Butterworth filter with a cut-off frequency of 10 Hz for static balance trials.

3.4.2. Data Resampling

Force plate data were collected at a high sample frequency due to both the force and EMG data being passed through the same ADC. In order to use the force data with the kinematic data it was necessary to resample the force data at the lower sample frequency of 200 Hz. This was achieved using the Matlab decimate function, where the signal was first filtered with a low pass anti-aliasing filter before being resampled at the lower rate.

3.4.3. Centre of Mass Calculation

The motion of the centre of mass (COM) is of great importance in postural control research, however, the COM is an imaginary quantity and is not easily measured during human movement. The COM is the unique point at the centre of a distribution of mass in space; essentially, it is the point at which the weighted positions of all masses within the body sum to zero. Furthermore, if all forces applied to a body of known mass can be determined, then the motion of the COM can be calculated from Newton's second law of motion. These two principles lead to the two main methods by which COM is calculated during postural control studies.

The position of the COM of a person can be determined as the weighted average of the positions of the COM of each body segment. The COM of each segment may be calculated from anthropometric data such as is described in section 3.2.5. This method relies on the accurate tracking of segment and joint

centre locations, along with accurate estimates of segment masses. This method will result in a reasonable estimate of the displacement of the COM, however, errors in kinematic data will result in increased errors in any time derivatives calculated from this displacement. Alternatively, COM motion calculated as the double integral of force divided by mass will not have this limitation.

In standing the motion of the COM can be determined by the ground reaction force (GRF) measured from a force plate and the known mass of the person, via:

$$\ddot{x} = \frac{F}{m} \tag{3.15}$$

$$\dot{x} = \int \frac{F}{m} dt + \dot{x}_0 \tag{3.16}$$

$$x = \iint \frac{F}{m} dt + \dot{x}_0 t + x_0 \tag{3.17}$$

Equations 3.15 to 3.17 are sensitive to the initial velocity and displacement of the COM, which may be estimated from zero crossings of horizontal force (King and Zatsiorsky, 1997; Zatsiorsky and King, 1998). However, errors with estimating these values will result in systematic errors in the COM displacement. Errors within the measured force or subject mass can result in further systematic errors; leading some authors to combine both force data and kinematic data to calculate COM motion (Yeadon and Trewartha, 2003).

Yeadon and Trewartha (2003) estimated the initial velocity and displacement of the COM, along with an estimated error in acceleration due to errors in force or measured body mass, based on regressions of the COM calculated from the two previous methods. The COM displacement and velocity was then recalculated via:

$$\dot{x} = \int \frac{F}{m} dt + \dot{x}_0 + 2et \tag{3.18}$$

$$x = \iint \frac{F}{m} dt + \dot{x}_0 t + x_0 + et^2 \tag{3.19}$$

The above method results in reasonable estimates of COM displacement when compared to those obtained from force plate data alone, and in smooth COM velocities when compared to those obtained from unfiltered kinematic data. The above method will result in a mean COM position which is equivalent to that obtained from the kinematic method. Unfortunately, estimates of COM displacements from kinematic data often have a systematic offset due to poor estimates of segment COM locations.

3.4.3.1. Systematic Offset of Centre of Mass

A significant source of error in the determination of body COM position is the estimation of the masses and COM of each body segment, with the determination of trunk COM especially prone to error (Kingma et al., 1995). Yeadon and Trewatha (2003) addressed this issue by making a systematic correction via minimising the RMS difference between the COM and the COP positions, so that mean values would be identical. This is a fair assumption in static stance trials of sufficient duration, were the mean position of the COM and COP must be approximately equal for stable balance to be maintained. However, this correction only results in a change to the position of the whole body COM, and not the segmental COM positions which determine its location, resulting in increased errors when using these positions in inverse dynamics calculations. An alternative is to follow a similar method to that used by Kingma et al. (1995), which repositions the COM locations of the segments that make up the trunk by a proportional amount so as to achieve the required change in whole body COM position. In the current research COM positions were adjusted by calculating the difference between the mean positions of the COM and COP in the horizontal directions, and based on the percentage of the torso mass to whole body mass, adjusting the COM locations of the pelvis, abdomen, thorax, and head segments.

3.5. Inverse Dynamics

The kinematic data collected was used to calculate segment positions and orientations, and combined with the kinetic data from the force plates and the segmental inertial data to calculate joint forces and moments. There are a number of factors which must be considered for the various ways through which this may be accomplished; therefore a brief review of these methods is warranted.

3.5.1. Euler angles and Rotation Matrices

The attitude of an object describes its orientation in space, and requires the construction of the object's local coordinate system (LCS) expressed relative to the global coordinate system (GCS). The most common way to represent the attitude of a rigid body is via a set of three Euler angles (Diebel, 2006); where

'any two independent orthonormal coordinate frames can be related by a sequence of rotations (not more than three) about the coordinate axes, where no two successive rotations may be about the same axis'

(Leonhard Euler, 1707-1783; in Kuipers, 1999).

There are a total of 12 possible sequences of coordinate rotations which satisfy the above theorem, where the sequence can be represented either by the axis sequence, such as 'ZXZ', or by the number of the rotation, such as '313'. Both of these examples describe the first rotation about the z-axis, followed by the second rotation about the new orientation of the x-axis and the final rotation about the new orientation of the z-axis. The sequence used is dependent upon the nature of the task, and the sequence mentioned above is considered to be the original sequence used by Leonard Euler; however, the 'XYZ' sequence is possibly the most often used in biomechanics, and is sometimes referred to as a Cardan rotation sequence (Winter, 2009).

The 'XYZ' rotation sequence can be represented by the first rotation about the x-axis by the angle ψ resulting in new orientations of the y- and z-axes, described by:

$$x_1 = x_0$$

$$y_1 = y_0 cos_\psi + z_0 sin_\psi$$

$$z_1 = -y_0 sin_\psi + z_0 cos_\psi \tag{3.20}$$

This can be represented in matrix form by the rotation matrix R_ψ^x:

$$\begin{bmatrix} x_1 \\ y_1 \\ z_1 \end{bmatrix} = \begin{bmatrix} 1 & 0 & 0 \\ 0 & cos_\psi & sin_\psi \\ 0 & -sin_\psi & cos_\psi \end{bmatrix} \begin{bmatrix} x_0 \\ y_0 \\ z_0 \end{bmatrix} = [R_\psi^x] \begin{bmatrix} x_0 \\ y_0 \\ z_0 \end{bmatrix} \tag{3.21}$$

The second rotation about the y-axis by the angle θ results in the new orientations of the x- and y-axes is described by:

$$\begin{bmatrix} x_2 \\ y_2 \\ z_2 \end{bmatrix} = \begin{bmatrix} cos_\theta & 0 & -sin_\theta \\ 0 & 1 & 0 \\ sin_\theta & 0 & cos_\theta \end{bmatrix} \begin{bmatrix} x_1 \\ y_1 \\ z_1 \end{bmatrix} = [R_\theta^y] \begin{bmatrix} x_1 \\ y_1 \\ z_1 \end{bmatrix} \tag{3.22}$$

The third rotation about the z-axis by the angle ϕ results in the new orientations of the x- and y-axes is described by:

$$\begin{bmatrix} x_3 \\ y_3 \\ z_3 \end{bmatrix} = \begin{bmatrix} cos_\phi & sin_\phi & 0 \\ -sin_\phi & cos_\phi & 0 \\ 0 & 0 & 1 \end{bmatrix} \begin{bmatrix} x_2 \\ y_2 \\ z_2 \end{bmatrix} = [R_\phi^z] \begin{bmatrix} x_2 \\ y_2 \\ z_2 \end{bmatrix} \tag{3.23}$$

The product of these rotation matrices is itself a rotation matrix, which represents the combination of each of these rotations in sequence:

$$\begin{bmatrix} x_3 \\ y_3 \\ z_3 \end{bmatrix} = [R_\phi^z][R_\theta^y][R_\psi^x] \begin{bmatrix} x_0 \\ y_0 \\ z_0 \end{bmatrix}$$

$$\begin{bmatrix} x_3 \\ y_3 \\ z_3 \end{bmatrix} = \begin{bmatrix} cos_\theta cos_\phi & sin_\phi cos_\psi + sin_\psi sin_\theta cos_\phi & sin_\psi sin_\phi - cos_\psi sin_\theta cos_\phi \\ -cos_\theta sin_\phi & cos_\phi cos_\psi - sin_\psi sin_\theta sin_\phi & sin_\psi cos_\phi + cos_\psi sin_\theta sin_\phi \\ sin_\theta & -sin_\psi cos_\theta & cos_\psi cos_\theta \end{bmatrix} \begin{bmatrix} x_0 \\ y_0 \\ z_0 \end{bmatrix}$$

$$\begin{bmatrix} x_3 \\ y_3 \\ z_3 \end{bmatrix} = \begin{bmatrix} R_{xyz} \end{bmatrix} \begin{bmatrix} x_0 \\ y_0 \\ z_0 \end{bmatrix}$$

(3.24)

Finally, the inverse mapping of this function, which gives the Euler angles as a function of the rotation matrix to describe the rotations about the x-, y- and z-axes is:

$$\begin{bmatrix} \psi_{xyz}(R) \\ \theta_{xyz}(R) \\ \phi_{xyz}(R) \end{bmatrix} = \begin{bmatrix} atan2(-r_{32}, r_{33}) \\ asin(r_{31}) \\ atan2(-r_{21}, r_{11}) \end{bmatrix}$$

(3.25)

The three successive coordinate rotations described above results in the 3×3 rotation matrix R, which describes the rotations required to align one coordinate system with another. In addition, this rotation matrix can be multiplied by a vector to rotate that vector from one coordinate system into another whilst also preserving its length. The rotation matrix may also be thought of as the matrix of basis vectors that define the two coordinate systems (Diebel, 2006). The rows of the rotation matrix are the basis vectors of the LCS expressed in the GCS and the columns are the basis vectors of the GCS expressed in the LCS. At least three points are required to define the axes of each body segment, which define the three linearly independent vectors required to form an orthonormal basis for the construction of the LCS of that segment. In the current research all segments were defined with their LCS aligned approximately with the GCS when the subject was in the anatomical standing position, using the following convention:

$$\hat{\imath} = x \; axis = mediolateral \; axis$$

$$\hat{\jmath} = y \; axis = anteroposterior \; axis$$

$$\hat{k} = z \; axis = longitudinal/vertical \; axis$$

Each segment is defined by the normalised vectors created by pairs of points and the cross product between these vectors to ensure an orthonormal coordinate system. Therefore, a limb segment can be defined by the normalised vector $\hat{k}$ from the distal to proximal joint centres, representing the z-

66

axis of the segment, and the normalised vector $\hat{\imath}$ from the distal joint centre to lateral aspect of the distal joint representing the x-axis, designated as points P_1 to P_3:

$$\hat{\imath} = x\ axis = \frac{\overrightarrow{P_1P_3}}{\left\|\overrightarrow{P_1P_3}\right\|} = \frac{P_3 - P_1}{\|P_3 - P_1\|} \tag{3.26}$$

$$\hat{k} = z\ axis = \frac{\overrightarrow{P_1P_2}}{\left\|\overrightarrow{P_1P_2}\right\|} = \frac{P_2 - P_1}{\|P_2 - P_1\|} \tag{3.27}$$

The y-axis is defined as the vector $\hat{\jmath}$, which is perpendicular to the plane formed between the x- and z-axes, via their cross product:

$$\hat{\jmath} = y\ axis = \frac{z\ axis \times xaxis}{\|z\ axis \times xaxis\|} \tag{3.28}$$

Additionally, as the x- and z-axes may not be strictly orthogonal to one another, the cross product of the z- and y-axes is calculated as the new x-axis to ensure three orthogonal vectors of unit length:

$$\hat{\imath} = x\ axis = y\ axis \times z\ axis \tag{3.29}$$

Collectively these three vectors describe the attitude of the segment and can be combined in matrix form to represent the GCS to LCS rotation matrix:

$$R_{G \to L} = \begin{bmatrix} x\ axis_x & x\ axis_y & x\ axis_z \\ y\ axis_x & y\ axis_y & y\ axis_z \\ z\ axis_x & z\ axis_y & z\ axis_z \end{bmatrix} = \begin{bmatrix} i_x & i_y & i_z \\ j_x & j_y & j_z \\ k_x & k_y & k_z \end{bmatrix} \tag{3.30}$$

The GCS to LCS rotation matrix is required to transform global vectors into the local coordinate system, such as transferring the global force vector into the local force vector so that local joint moments may be calculated:

$$[\boldsymbol{f}_{LCS}] = [R_{G \to L}][\boldsymbol{F}_{GCS}]$$

$$\begin{bmatrix} f_x \\ f_y \\ f_z \end{bmatrix} = \begin{bmatrix} i_x & i_y & i_z \\ j_x & j_y & j_z \\ k_x & k_y & k_z \end{bmatrix} \begin{bmatrix} F_x \\ F_y \\ F_z \end{bmatrix} \tag{3.31}$$

In addition, the transpose of the GCS to LCS rotation matrix is the equivalent to the LCS to GCS rotation matrix, required to transform local vectors back into the global coordinate system:

$$R_{L \to G} = R_{G \to L}^T = \begin{bmatrix} x\,axis_x & y\,axis_x & z\,axis_x \\ x\,axis_y & y\,axis_y & z\,axis_y \\ x\,axis_z & y\,axis_z & z\,axis_z \end{bmatrix} = \begin{bmatrix} i_x & j_x & k_x \\ i_y & j_y & k_y \\ i_z & j_z & k_z \end{bmatrix}$$

$$[\boldsymbol{F}_{GCS}] = [R_{L \to G}][\boldsymbol{f}_{LCS}]$$

$$\begin{bmatrix} F_x \\ F_y \\ F_z \end{bmatrix} = \begin{bmatrix} i_x & j_x & k_x \\ i_y & j_y & k_y \\ i_z & j_z & k_z \end{bmatrix} \begin{bmatrix} f_x \\ f_y \\ f_z \end{bmatrix} \tag{3.32}$$

An advantage to the use of Euler angles to describe the orientation of a body segment is that it is widely used within biomechanics and provides a well understood anatomical representation of motion (Hamill and Selbie, 2004). However, Euler angles suffer from discontinuities and singularities caused by gimbal lock, especially when computing angular velocities and accelerations (Dumas et al., 2004; Dumas and Cheze, 2007). Quaternions offer an alternative to using Euler angles to describe the attitude of a rigid body and have been employed in biomechanics (Dumas et al., 2004; Dumas et al., 2007) and aerospace engineering (Altmann, 2005; Kuipers, 1999).

3.5.2. Quaternion Algebra

A quaternion may be represented in several ways, such as a 4-tuple of real numbers:

$$q = (q_0, q_1, q_2, q_3) \tag{3.33}$$

A hyper-complex number:

$$q = q_0 + iq_1 + jq_2 + kq_3$$

$$i^2 = j^2 = k^2 = ijk = -1 \tag{3.34}$$

Or as the sum of a scalar and a vector:

$$q = (q_0, q_1, q_2, q_3) = q_0 + \boldsymbol{q} = \begin{bmatrix} q_0 \\ \boldsymbol{q} \end{bmatrix}$$

$$\boldsymbol{q} = \hat{\boldsymbol{\imath}}q_1 + \hat{\boldsymbol{\jmath}}q_2 + \widehat{\boldsymbol{k}}q_3 \tag{3.35}$$

(where $\hat{\boldsymbol{\imath}}$, $\hat{\boldsymbol{\jmath}}$ and $\widehat{\boldsymbol{k}}$ are the standard orthonormal basis vectors)

Defined as the sum of a scalar and a vector a quaternion is a mathematically strange object that is not well defined in ordinary linear algebra (Kuipers, 1999), requiring specific mention of quaternion operations. Firstly, two quaternions are equal if they have exactly the same components, so that if:

$$p = q$$

then:

$$p_0 = q_0$$

$$p_1 = q_1$$

$$p_2 = q_2$$

$$p_3 = q_3 \tag{3.36}$$

The sum of the two quaternions p and q is defined by adding the corresponding components, so that:

$$p + q = (p_0 + q_0) + i(p_1 + q_1) + j(p_2 + q_2) + k(p_3 + q_3) \tag{3.37}$$

The *quaternion product*, the product of two or more quaternions, becomes a little more complicated as it must satisfy the fundamental special products of a hyper-complex number, so that:

$$i^2 = j^2 = k^2 = ijk = -1$$

$$ij = k = -ji$$

$$jk = i = -kj$$

$$ki = j = -ik \tag{3.38}$$

Therefore the product of the two quaternions p and q is defined by:

$$r = pq = (p_0 + ip_1 + jp_2 + kp_3)(q_0 + iq_1 + jq_2 + kq_3)$$

$$\begin{aligned} = \; & p_0q_0 - (p_1q_1 + p_2q_2 + p_3q_3) + p_0(iq_1 + jq_2 + kq_3) \\ & + q_0(ip_1 + jp_2 + kp_3) + i(p_2q_3 - p_3q_2) \\ & + j(p_3q_1 - p_1q_3) + k(p_1q_2 - p_2q_1) \end{aligned} \tag{3.39}$$

In matrix form this becomes:

$$\begin{bmatrix} r_0 \\ r_1 \\ r_2 \\ r_3 \end{bmatrix} = \begin{bmatrix} p_0 & -p_1 & -p_2 & -p_3 \\ p_1 & p_0 & -p_3 & p_2 \\ p_2 & p_3 & p_0 & -p_1 \\ p_3 & -p_2 & p_1 & p_0 \end{bmatrix} \begin{bmatrix} q_0 \\ q_1 \\ q_2 \\ q_3 \end{bmatrix} \tag{3.40}$$

When the quaternion is represented as a scalar and a vector, the product of two quaternions may be written in the more concise form:

$$r = pq = (p_0 + \boldsymbol{p})(q_0 + \boldsymbol{q})$$

$$= p_0q_0 - \boldsymbol{p} \cdot \boldsymbol{q} + p_0\boldsymbol{q} + q_0\boldsymbol{p} + \boldsymbol{p} \times \boldsymbol{q} \tag{3.41}$$

The complex conjugate of a quaternion is denoted by:

$$q^* = q_0 - \boldsymbol{q} = q_0 - iq_1 - jq_2 - kq_3 \tag{3.42}$$

The norm of a quaternion is denoted by:

$$N(q) = \sqrt{q^*q} = \sqrt{q_0^2 + q_1^2 + q_2^2 + q_3^2} = \|q\|$$

(3.43)

The inverse of a quaternion is denoted by:

$$q^{-1} = \frac{q^*}{N^2(q)} = \frac{q^*}{\|q\|^2}$$

(3.44)

Therefore, if the quaternion q is a normalised quaternion of unit length, denoted by $\boldsymbol{U}q$, the inverse of q is simply the complex conjugate:

$$\boldsymbol{U}q = \frac{q}{\|q\|}$$

(3.45)

$$\boldsymbol{U}q^{-1} = \frac{q^*}{\|q\|^2} = \frac{q^*}{1} = q^*$$

(3.46)

A quaternion with a vector component equal to zero is known as a *real quaternion* as it multiplies like a real number and can also be identified as a real number, so that:

$$pq = \begin{bmatrix} p_0 \\ \boldsymbol{0} \end{bmatrix} \begin{bmatrix} q_0 \\ \boldsymbol{0} \end{bmatrix} = \begin{bmatrix} p_0 q_0 \\ \boldsymbol{0} \end{bmatrix}$$

(3.47)

$$\begin{bmatrix} x \\ \boldsymbol{0} \end{bmatrix} \equiv x$$

(3.48)

A quaternion with a scalar component equal to zero is known as an *imaginary* or *pure quaternion*, and the product of the two pure quaternions p and q is equal to the quaternion product of the two vectors $\boldsymbol{p}$ and $\boldsymbol{q}$:

$$pq = \begin{bmatrix} 0 \\ \boldsymbol{p} \end{bmatrix} \begin{bmatrix} 0 \\ \boldsymbol{q} \end{bmatrix} = \begin{bmatrix} \boldsymbol{p} \cdot \boldsymbol{q} \\ \boldsymbol{p} \times \boldsymbol{q} \end{bmatrix}$$

(3.49)

Therefore, the vector $\boldsymbol{v}$ in R^3 space can be treated as though it were a quaternion in R^4 space by creating a pure quaternion, with a zero scalar component and a vector component equal to $\boldsymbol{v}$. In this way, quaternions can transform a vector expressed in one coordinate system into another coordinate system via a triple quaternion product of an attitude quaternion and the vector expressed as a pure quaternion, such as:

$$\begin{bmatrix} 0 \\ \boldsymbol{f}_{LCS} \end{bmatrix} = q^* \begin{bmatrix} 0 \\ \boldsymbol{F}_{GCS} \end{bmatrix} q \tag{3.50}$$

$$\begin{bmatrix} 0 \\ \boldsymbol{F}_{GCS} \end{bmatrix} = q \begin{bmatrix} 0 \\ \boldsymbol{f}_{LCS} \end{bmatrix} q^* \tag{3.51}$$

3.5.3. Attitude Quaternions

Similar to Euler angles and a rotation matrix, a unit quaternion can be used to represent the attitude of a rigid body. Euler angles align one coordinate system with another through a sequence of three axis rotations, related to Euler's rotation theorem, however, a second part to this theorem states that

'any two independent orthonormal coordinate frames can be related by a single rotation about some axis

(Leonhard Euler, 1707-1783; in Kuipers, 1999).

Therefore, the attitude of a body may also be described by the rotation angle β and the axis of rotation, represented by the unit vector $\boldsymbol{u}$, required to align one coordinate system with another. Using the rotation matrix R this may be calculated via:

$$\boldsymbol{u} = \begin{bmatrix} (r_{33} - 1)r_{12} - r_{13}r_{32} \\ r_{31}r_{13} - (r_{33} - 1)(r_{11} - 1) \\ (r_{11} - 1)r_{32} - r_{12}r_{31} \end{bmatrix}$$

$$\boldsymbol{u} = \hat{\boldsymbol{\imath}}(r_{23} - r_{32}) + \hat{\boldsymbol{\jmath}}(r_{31} - r_{13}) + \hat{\boldsymbol{k}}(r_{12} - r_{21}) \tag{3.52}$$

$$Tr(R) = r_{11} + r_{22} + r_{33} = 1 + 2cos\beta$$

$$\beta = acos\frac{Tr(R) - 1}{2} = acos\frac{r_{11} + r_{22} + r_{33} - 1}{2} \qquad (3.53)$$

Likewise the quaternion that arises from the rotation β about the axis $\boldsymbol{u}$ can be calculated by the axis-angle quaternion function:

$$q = \begin{bmatrix} q_0 \\ \boldsymbol{q} \end{bmatrix} = \begin{bmatrix} cos\left(\dfrac{\beta}{2}\right) \\ \boldsymbol{u}\, sin\left(\dfrac{\beta}{2}\right) \end{bmatrix} \qquad (3.54)$$

And the inverse function, from a unit quaternion to the corresponding axis and angle of rotation is:

$$\beta = 2acos(q_0) \qquad (3.55)$$

$$\boldsymbol{u} = \frac{\boldsymbol{q}}{\|\boldsymbol{q}\|} = \frac{\boldsymbol{q}}{\sqrt{1 - q_0^2}} \qquad (3.56)$$

Similarly, the conversion of a quaternion into a rotation matrix can be described as:

$$R = \begin{bmatrix} r_{11} & r_{12} & r_{13} \\ r_{21} & r_{22} & r_{23} \\ r_{31} & r_{32} & r_{33} \end{bmatrix}$$

$$R = \begin{bmatrix} q_0^2 + q_1^2 - q_2^2 - q_3^2 & 2q_1q_2 + 2q_0q_3 & 2q_1q_3 - 2q_0q_2 \\ 2q_1q_2 - 2q_0q_3 & q_0^2 - q_1^2 + q_2^2 - q_3^2 & 2q_2q_3 + 2q_0q_1 \\ 2q_1q_3 + 2q_0q_2 & 2q_2q_3 - 2q_0q_1 & q_0^2 - q_1^2 - q_2^2 + q_3^2 \end{bmatrix} \qquad (3.57)$$

Therefore, the reverse mapping from a rotation matrix can be calculated by first forming the following relationships based on the above function:

$$4q_0^2 = 1 + r_{11} + r_{22} + r_{33}$$

$$4q_1^2 = 1 + r_{11} - r_{22} - r_{33}$$

$$4q_2^2 = 1 - r_{11} + r_{22} - r_{33}$$

$$4q_3^2 = 1 - r_{11} - r_{22} + r_{33} \tag{3.58}$$

$$4q_0q_1 = r_{23} - r_{32}$$

$$4q_0q_2 = r_{31} - r_{13}$$

$$4q_0q_3 = r_{12} - r_{21}$$

$$4q_1q_2 = r_{12} + r_{21}$$

$$4q_1q_3 = r_{31} + r_{13}$$

$$4q_2q_3 = r_{23} + r_{32} \tag{3.59}$$

Finally, the attitude quaternion of a rigid body which can be calculated either from the rotation matrix R, or directly from the orthonormal basis vectors $\hat{\imath}$, $\hat{\jmath}$ and $\hat{k}$ via:

$$q_0 = \frac{\sqrt{r_{11} + r_{22} + r_{33} + 1}}{2} = \frac{\sqrt{i_x + j_y + k_z + 1}}{2}$$

$$q_1 = \frac{r_{23} - r_{32}}{4q_0} = \frac{j_z - k_y}{4q_0}$$

$$q_2 = \frac{r_{31} - r_{13}}{4q_0} = \frac{k_x - i_z}{4q_0}$$

$$q_3 = \frac{r_{12} - r_{21}}{4q_0} = \frac{i_y - j_x}{4q_0} \tag{3.60}$$

Depending on the values in the rotation matrix R, equation 3.60 can produce singularities or complex numbers, however, equations 3.58 and 3.59 permit the calculation of the attitude quaternion by three further means. Each permutation of the attitude quaternion may result in a slightly different quaternion, however, it will still represent the same rotation in R^3 space, as the rotation β about the axis $\boldsymbol{u}$ described in equations 3.52 and 3.53 may also be described in four ways, such as:

$$\begin{bmatrix} \beta \\ \boldsymbol{u} \end{bmatrix} = \begin{bmatrix} \beta - 2\pi \\ \boldsymbol{u} \end{bmatrix} = \begin{bmatrix} -\beta \\ -\boldsymbol{u} \end{bmatrix} = \begin{bmatrix} 2\pi - \beta \\ -\boldsymbol{u} \end{bmatrix}$$

(3.61)

The quaternion described by equation 3.60 will result in a scalar component in the range of 0 to 1; consequently, the angle β resulting from this will be in the range of 0 to π. However, this quaternion will still be able to define any rotation in R^3 space due to a change in the axis vector $\boldsymbol{u}$, described by the vector component. Essentially, this allows the quaternion calculated via equation 3.60 to describe rotations in a range of $-\pi$ to π, causing discontinuities when crossing $\pm\pi$. Using the other permutations of the attitude quaternion will result in a scalar component in the range of -1 to 1, but will constrict one of the vector components to a range of 0 to 1, such as:

$$q_0 = \frac{r_{23} - r_{32}}{4q_1} = \frac{j_z - k_y}{4q_1}$$

$$q_1 = \frac{\sqrt{r_{11} - r_{22} - r_{33} + 1}}{2} = \frac{\sqrt{i_x - j_y - k_z + 1}}{2}$$

$$q_2 = \frac{r_{12} + r_{21}}{4q_1} = \frac{i_y + j_x}{4q_1}$$

$$q_2 = \frac{r_{31} + r_{13}}{4q_1} = \frac{k_x + i_z}{4q_1}$$

(3.62)
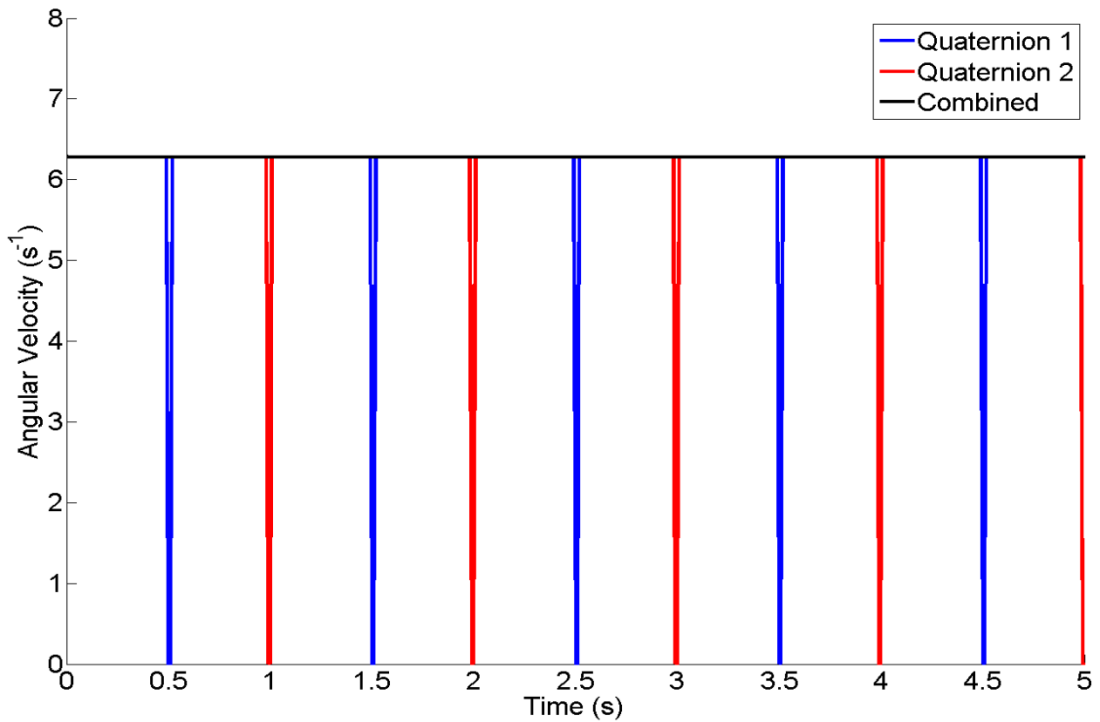
Figure 3.6: The angular velocity about the global x-axis resulting from continuous rotations about the x-axis at an angular velocity of $2\pi\ s^{-1}$, calculated by the quaternions from equation 3.60 (blue) and 3.62 (red); with the combination of these quaternions in black.
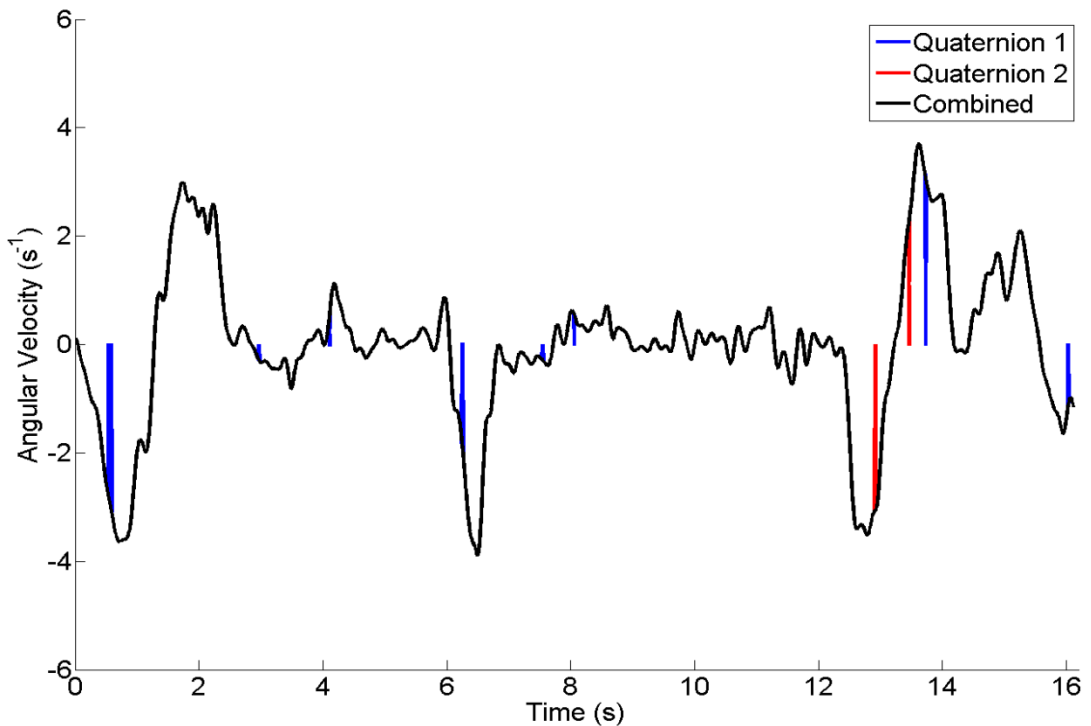
Figure 3.7: The angular velocity about the global x-axis of the right hand during various shoulder and elbow movements, calculated by the quaternions from equation 3.60 (blue) and 3.62 (red); with the combination of these quaternions in black.

76

Essentially, this allows the quaternion calculated via equation 3.62 to describe rotations in a range of 0 to 2π, causing discontinuities when crossing 0 or 2π. Together, these quaternions can be used to overcome these discontinuities and allow angular velocities to be calculated through any angular range without singularities (Figures 3.6 and 3.7)

3.5.4. Kinematics Using Quaternion Algebra

The kinematic formulation used in the current research is based on the paper by Dumas et al. (2004) using quaternion algebra and was implemented in Matlab (Appendix 5). The segment position is given by the generalised coordinates:

$$\begin{bmatrix} p_i \\ q_i \end{bmatrix}$$

(3.63)

Where the 3×1 vector p_i is the position of the segment proximal end P_i expressed in the GCS, and the 4×1 quaternion q_i represents the attitude of the LCS with respect to the GCS. The quaternion q_i is constructed based on the formulae explained previously in sections 3.5.2 and 3.5.3, therefore, the lever arm c_i, representing the distance from the proximal joint centre to the segment COM, can be transformed from the LCS to the GCS via:

$$\begin{bmatrix} 0 \\ c_i \end{bmatrix} = q_i \begin{bmatrix} 0 \\ c_i^{LCS} \end{bmatrix} q_i^*$$

(3.64)

Similarly, the position vector r_i of the segment COM expressed in the GCS is:

$$\begin{bmatrix} 0 \\ r_i \end{bmatrix} = \begin{bmatrix} 0 \\ p_i \end{bmatrix} + q_i \begin{bmatrix} 0 \\ c_i^{LCS} \end{bmatrix} q_i^*$$

(3.65)

The linear velocity v_i and linear acceleration a_i of the COM can be expressed in the GCS by direct differentiation:

$$\begin{bmatrix} 0 \\ \boldsymbol{v}_i \end{bmatrix} = \begin{bmatrix} 0 \\ \dot{\boldsymbol{p}}_i \end{bmatrix} + \dot{q}_i \begin{bmatrix} 0 \\ \boldsymbol{c}_i^{LCS} \end{bmatrix} q_i^* + q_i \begin{bmatrix} 0 \\ \boldsymbol{c}_i^{LCS} \end{bmatrix} \dot{q}_i^* \tag{3.66}$$

$$\begin{bmatrix} 0 \\ \boldsymbol{a}_i \end{bmatrix} = \begin{bmatrix} 0 \\ \ddot{\boldsymbol{p}}_i \end{bmatrix} + \ddot{q}_i \begin{bmatrix} 0 \\ \boldsymbol{c}_i^{LCS} \end{bmatrix} q_i^* + 2 \left(\dot{q}_i \begin{bmatrix} 0 \\ \boldsymbol{c}_i^{LCS} \end{bmatrix} \dot{q}_i^* \right) + q_i \begin{bmatrix} 0 \\ \boldsymbol{c}_i^{LCS} \end{bmatrix} \ddot{q}_i^* \tag{3.67}$$

Additionally, the angular velocity $\boldsymbol{\omega}_i$ and angular acceleration $\boldsymbol{\alpha}_i$ can be expressed in the GCS by:

$$\begin{bmatrix} 0 \\ \boldsymbol{\omega}_i \end{bmatrix} = 2\dot{q}_i q_i^* \tag{3.68}$$

$$\begin{bmatrix} 0 \\ \boldsymbol{\alpha}_i \end{bmatrix} = 2(\ddot{q}_i q_i^* + \dot{q}_i \dot{q}_i^*) \tag{3.69}$$

3.5.5. Conventional 3D Inverse Dynamics

Conventional 3D inverse dynamics is an expansion of 2D inverse dynamics, where net joint forces and moments are computed separately based on the following Newton-Euler equations of motion:

$$\left. \begin{array}{l} \Sigma F_x = ma_x \\ \Sigma F_y = ma_y \\ \Sigma F_z = ma_z \end{array} \right\} \Sigma \boldsymbol{F} = m\boldsymbol{a} \tag{3.70}$$

$$\left. \begin{array}{l} \Sigma M_x = I_x \alpha_x + (I_z - I_y)\omega_y \omega_z \\ \Sigma M_y = I_y \alpha_y + (I_x - I_z)\omega_z \omega_x \\ \Sigma M_z = I_z \alpha_z + (I_y - I_x)\omega_x \omega_y \end{array} \right\} \Sigma \boldsymbol{M} = \boldsymbol{I} \cdot \boldsymbol{\alpha} + \boldsymbol{\omega} \times (\boldsymbol{I} \cdot \boldsymbol{\omega}) \tag{3.71}$$

Where $\boldsymbol{a}$ is the linear acceleration of the segment COM, $\boldsymbol{\omega}$ is the angular velocity of the segment and $\boldsymbol{\alpha}$ is the angular acceleration of the segment. With known forces and moments to the distal joint, firstly the proximal joint forces are calculated in the GCS via:

$$\boldsymbol{F}_{ip}^{GCS} = m_i \boldsymbol{a}_i^{GCS} - m_i \boldsymbol{g}^{GCS} - \boldsymbol{F}_{id}^{GCS} \tag{3.72}$$

Where $\boldsymbol{F}_{ip}^{GCS}$ is the proximal joint force; $\boldsymbol{F}_{id}^{GCS}$ is the distal joint force; $m_i \boldsymbol{a}_i^{GCS}$ is the mass and acceleration of the segment COM; and $\boldsymbol{g}^{GCS}$ is the gravitational vector. The proximal joint moments are calculated in the LCS, therefore the distal and proximal joint forces need to be transferred from the GCS to the LCS, and the distal joint moments need to be transferred from the LCS of the preceding segment to the LCS for that particular segment, to give:

$$\boldsymbol{M}_{ip}^{LCS} = \dot{\boldsymbol{H}}_i^{LCS} - \boldsymbol{M}_{id}^{LCS} - \left(\boldsymbol{p}_i^{LCS} \times \boldsymbol{f}_{ip}^{LCS}\right) - \left(\boldsymbol{d}_i^{LCS} \times \boldsymbol{f}_{id}^{LCS}\right) \tag{3.73}$$

Where:

$$\dot{\boldsymbol{H}}^{LCS} = \begin{bmatrix} I_x \alpha_x + (I_z - I_y)\omega_y\omega_z \\ I_y \alpha_y + (I_x - I_z)\omega_z\omega_x \\ I_z \alpha_z + (I_y - I_x)\omega_x\omega_y \end{bmatrix} \tag{3.74}$$

$$\boldsymbol{p}_i^{LCS} = lever\ arm\ from\ mass\ centre\ to\ proximal\ joint$$

$$\boldsymbol{d}_i^{LCS} = lever\ arm\ from\ mass\ centre\ to\ distal\ joint$$

These numerous rotational transformations of force and moment vectors increase the likelihood of calculation errors (Dumas et al., 2004), leading some authors to turn to other methods for applying the Newton-Euler equations of motion, such as using wrenches (Dumas et al., 2004; Dumas and Cheze, 2007).

3.5.6. Inverse Dynamics with Wrench Notation

The inverse dynamics formulation used in the current research is based on the paper by Dumas et al. (2004) using wrench notation and was implemented in Matlab (Appendix 6). The wrench is a mechanical notation that represents both force and moment vectors, and is expressed at a defined point location and in a defined coordinate system. The following examples are all expressed in the GCS, with the points:

$$P_i = proximal\ end\ of\ segment\ i$$

$$C_i = centre\ of\ mass\ of\ segment\ i$$

$$D_i = distal\ end\ of\ segment\ i$$

A wrench at a particular point can be derived directly from the force and moment from a previous segment or from the mass/motion of that particular segment, as follows:

$$W_i^{proximal}(P_i) = \begin{cases} \boldsymbol{F}_i \\ \boldsymbol{M}_i \end{cases} \tag{3.75}$$

$$W_i^{distal}(D_i) = -W_{i-1}^{proximal}(P_{i-1}) = \begin{cases} -\boldsymbol{F}_{i-1} \\ -\boldsymbol{M}_{i-1} \end{cases} \tag{3.76}$$

$$W_i^{weight}(C_i) = \begin{cases} m_i \boldsymbol{g} \\ \boldsymbol{0}_{3 \times 1} \end{cases} \tag{3.77}$$

$$W_i^{dynamic}(C_i) = \begin{cases} m_i \boldsymbol{a}_i \\ \dot{\boldsymbol{H}}_i \end{cases} \tag{3.78}$$

$$W_i^{proximal}(P_i) = W_i^{dynamic}(P_i) - W_i^{distal}(P_i) - W_i^{weight}(P_i) \tag{3.79}$$

Where the moment of inertia tensor in the GCS is calculated from the principle moments of inertia via:

$$I_i = [R_{G \to L}]I_i^{LCS}[R_{G \to L}]^{-1} \tag{3.80}$$

And the time derivative of angular momentum is calculated via:

$$\dot{\boldsymbol{H}}_i = I_i \boldsymbol{\alpha}_i + \boldsymbol{\omega}_i \times I_i \boldsymbol{\omega}_i \tag{3.81}$$

To transform a wrench from one point to another requires the cross product of the lever arm and force to be added to the moment part of the wrench, resulting in:

$$W_i^{weight}(P_i) = \begin{cases} m_i \boldsymbol{g} \\ \boldsymbol{0}_{3 \times 1} + \boldsymbol{c}_i \times m_i \boldsymbol{g} \end{cases} \tag{3.82}$$

$$W_i^{dynamic}(P_i) = \begin{cases} m_i \boldsymbol{a}_i \\ I_i \boldsymbol{\alpha}_i + \boldsymbol{\omega}_i \times I_i \boldsymbol{\omega}_i + \boldsymbol{c}_i \times m_i \boldsymbol{a}_i \end{cases} \tag{3.83}$$

$$W_i^{distal}(P_i) = -W_{i-1}^{proximal}(P_i) = \begin{cases} -F_{i-1} \\ -M_{i-1} - d_i \times F_{i-1} \end{cases} \qquad (3.84)$$

Where $c_i = (\overrightarrow{P_i C_i})$ is the lever arm vector from the proximal end to the COM, and $d_i = (\overrightarrow{P_i D_i}) = (\overrightarrow{P_i P_{i-1}})$ is the lever arm vector from the proximal end to the distal end, both expressed in the GCS. Leading to:

$$\begin{cases} F_i \\ M_i \end{cases} = \begin{cases} m_i a_i \\ I_i \alpha_i + \omega_i \times I_i \omega_i + c_i \times m_i a_i \end{cases} - \begin{cases} m_i g \\ 0_{3\times1} + c_i \times m_i g \end{cases} - \begin{cases} -F_{i-1} \\ -M_{i-1} - d_i \times F_{i-1} \end{cases} \quad (3.85)$$

Representing the proximal and distal wrenches as 6D vectors, the above equation can be written in matrix form as follows:

$$\begin{bmatrix} F_i \\ M_i \end{bmatrix} = \begin{bmatrix} m_i E_{3\times3} & 0_{3\times3} \\ m_i \tilde{c}_i & I_i \end{bmatrix} \begin{bmatrix} a_i - g \\ \alpha_i \end{bmatrix} + \begin{bmatrix} 0_{3\times1} \\ \omega_i \times I_i \omega_i \end{bmatrix} + \begin{bmatrix} E_{3\times3} & 0_{3\times3} \\ \tilde{d}_i & E_{3\times3} \end{bmatrix} \begin{bmatrix} F_{i-1} \\ M_{i-1} \end{bmatrix} \qquad (3.86)$$

Where $E_{3\times3}$ is the identity matrix, $0_{3\times3}$ and $0_{3\times1}$ are a matrix and vector of zeros, and $\tilde{c}_i$ and $\tilde{d}_i$ are the skew symmetric matrix of lever arms c_i and d_i, such as:

$$\tilde{c} = \begin{bmatrix} 0 & -c_3 & c_2 \\ c_3 & 0 & -c_1 \\ -c_2 & c_1 & 0 \end{bmatrix}$$

$$(3.87)$$

Three dimensional joint moments from right and left joints were combined to obtain two dimensional joint moments about the global x-axis for the ankles, hips, shoulders, and wrist joints.

3.5.7. Adjustments for a Moving Platform

During platform movements the orientation and the position of each force plate relative to the GCS will move, therefore the force vector and COP coordinates calculated from each force plate will differ from their true values due to this movement, requiring a correction before joint moments can be calculated. One option would be to consider the GCS as a moving reference system aligned with the moving force plate coordinate system. However, this would result in a moving non-inertial reference frame, requiring the computation of fictional forces, such as centrifugal and Coriolis forces, adding increased complexity to

the calculations (Chaffin et al., 1999). The alternative method would be to recalculate the force and moment vectors, and the COP position in the static GCS.

The actual COP in the GCS will be related to the position calculated from the force plates, the displacement of the force plate origin relative to the GCS origin, and the angle of the force plate relative to the GCS (equation 3.88). In addition, the acceleration of the force plates will result in extra forces that are applied to the four tri-axial force sensors, resulting in a systematic error between the actual force and that calculated from the force plate. The ground reaction force vector, which is at the point of force application and is applied to the subject at this point, will be related to the reaction force calculated from the force plate, the product of the acceleration of the force plate and the mass of the force plate's top plate, and the angle of the force plate relative to the GCS (equation 3.89).

$$\begin{bmatrix} 0 \\ \boldsymbol{p_a} \end{bmatrix} = \begin{bmatrix} 0 \\ \boldsymbol{d} \end{bmatrix} + q \begin{bmatrix} 0 \\ \boldsymbol{p_c} \end{bmatrix} q^*$$

(3.88)

$$\begin{bmatrix} 0 \\ \boldsymbol{GRF_a} \end{bmatrix} = q \begin{bmatrix} 0 \\ \boldsymbol{GRF_c} - m\boldsymbol{a} \end{bmatrix} q^*$$

(3.89)

Where $\boldsymbol{p_c}$ and $\boldsymbol{GRF_c}$ are the position and vector of the COP and ground reaction force calculated from the force plate; $\boldsymbol{p_a}$ and $\boldsymbol{GRF_a}$ are the actual position and vector of the COP and ground reaction force; $\boldsymbol{d}$ is the displacement of the force plate origin relative to the GCS origin; m is the mass of the top plate; $\boldsymbol{a}$ is the acceleration of the force plate centre; and q is the attitude quaternion for the orientation of the platform. The mass of the top plate was determined by administering several discrete and continuous translations, in each of the three directions, with varying speeds and amplitudes. These translations showed that the mass of each force plate's top plate was approximately 29 kg. These corrections resulted in typical force errors of 0.6 N for small perturbations and 1.1 N for larger platform perturbations. Although these errors are slightly larger than those reported in Table 3.2 for a static

platform, this is still acceptable. Figure 3.8 shows an example of the corrected force obtained by this method during a large platform translation of 0.1 m at target velocity of 0.2 ms^{-1}.
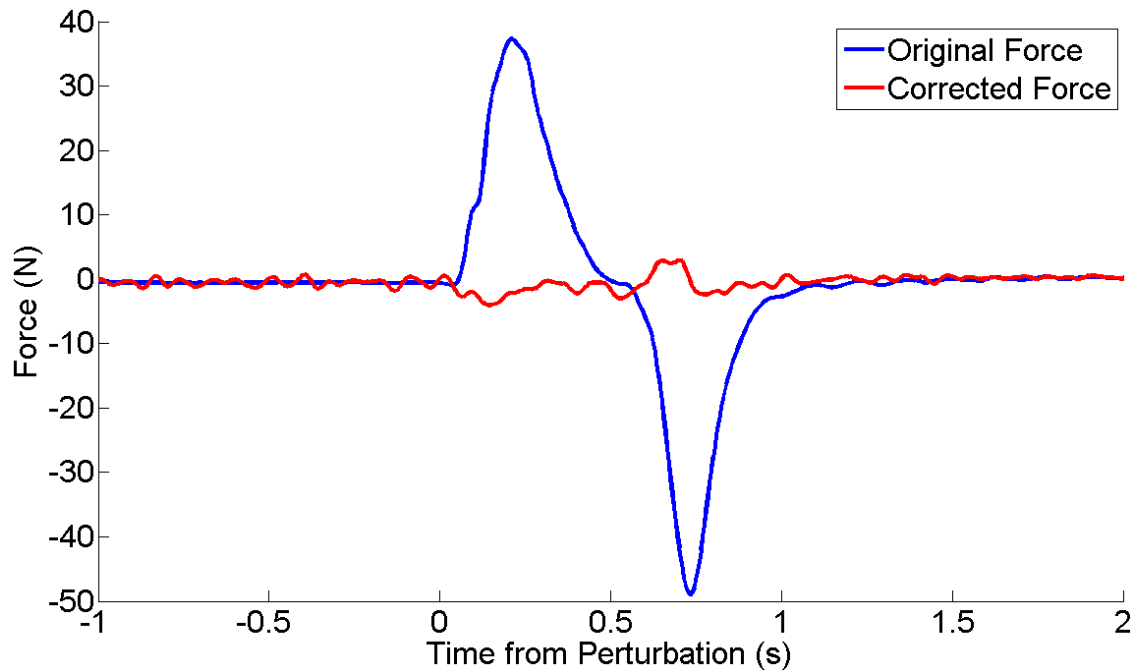
Figure 3.8: Force plate response to a platform translation of 0.1 m at a target velocity of 0.2 ms-1, with the horizontal force recorded by the force plates (blue) and the corrected force from equation 3.89 (red)

CHAPTER 4

DATA ANALYSIS AND ASSESSMENT OF BALANCE

This chapter examines the assumptions used by various data analysis methods to assess balance, with specific reference to the calculation and implementation of different balance metrics used within the literature. The chapter relates specifically to question one, and aims to determine which balance metrics best express the underlying control of posture, for balance with and without vision whilst in each of three postures.

4.1. Assessment of Balance

Twelve experienced handstanders completed the first part of study two. Subjects were required to perform five trials for a maximum of 30 seconds in each of the six conditions, including: standing, single leg stance, and handstand, each with eyes open and eyes closed. The data collection protocol and experimental procedures were as described previously in Chapter 3.

4.1.1. Traditional Balance Measures

Traditionally balance has been assessed by the relatively simple analysis of the trajectory of the COP to calculate quantities such as: range, standard deviation (SD), sway area, sway length, and mean frequency (Jiang et al., 2013; Kim et al., 2009; Wollseifen, 2011). Although sway area and sway length are commonly used to assess balance, these measures are calculated in two-dimensions. In the current research only one-dimensional signals will be analysed to allow for the comparison between traditional and nonlinear balance metrics. The traditional measures of balance that have been used within the current research include: range, SD, and mean sway velocity.

Traditional linear methods interpret all regular structure in a data set, such as a dominant frequency, this means that the presumed intrinsic dynamics of the system are governed by the linear paradigm that small causes lead to small

effects (Kantz and Schreiber, 2004). Since linear equations can only lead to solutions that oscillate periodically, either damped or undamped, or have exponential growth or decay, all irregular behaviour in the system has to be attributed to some random external input. Consequently, a growing number of studies have examined the data obtained from research into balance using other paradigms from dynamical systems theory, such as nonlinear, nonstationary, or stochastic dynamics.

4.1.2. Nonlinear and Nonstationary Measures of Balance

A dynamical system is one that evolves in time, that can be stochastic, and evolve according to some random process such as the toss of a coin, or they can be deterministic, in which case the future is uniquely determined by the past according to some rule or mathematical formula (Sprott, 2003). These formulae represent linear dynamic systems or nonlinear dynamic systems, where simple equations can lead to complicated behaviours, commonly known as deterministic chaos. Simple examples of dynamical systems include regular motions such as mass on a spring, pendulums, which in more complex forms can become nonlinear, leading into more complex dynamics such as the Rössler attractor, the Lorenz attractor, neural networks and eventually correlated noise and random noise. However, physical systems often exhibit a combination of behaviours, and experimental data commonly includes the addition of measurement error, making it extremely difficult to determine the underlying dynamics of the system based on a single sequence of measurements, the time series.

4.1.2.1. Time Series Analysis

A time series is a collection of observations indexed by the date or time of each observation. We often imagine that we could have obtained earlier or later observations had the process been observed for more time; in this way the observed sample could be viewed as a finite segment of a doubly infinite sequence (Hamilton, 1994). A time series is usually not a very compact representation of a time evolving phenomenon, therefore it is necessary to condense the information and find a parameterisation that contains the features

that are most relevant to the underlying system (Schreiber, 1999). Most ways to quantitatively describe a time series are derived from the methods to describe an assumed underlying process (Schreiber, 1999). The measures of dynamics in a time series are usually derived from measures of the assumed dynamics in the system, whether this is based on a stochastic, linear, or nonlinear dynamical system. The rationale is that a certain class of processes are assumed to have generated the time series and then the measure quantifying the process is estimated from the data. Since the underlying process is only observed through some measurement procedure, it is most useful to attempt to estimate quantities that are invariant under reasonable changes in the measurement procedure. The finite resolution and duration of time series recordings damage the invariance properties of quantities which are formally invariant for infinite data. Furthermore, if the value of an observable depends on the observation procedure it loses its value as an absolute characteristic (Schreiber, 1999). While in some cases we can still make approximate statements, the interpretation of results has to be undertaken with great care.

Time series analysis requires that the data should provide enough information to determine the quantity of interest unambiguously; this results in there being minimal requirements for how long and how precise the time series must be, and how frequently the measurements are observed. The time series should cover a stretch of time which is much longer than the longest characteristic time scale that is relevant for the evolution of the system. Most conventional time series analysis methods implicitly assume the data to have come from the stationary process of a linear dynamical system, perhaps with many degrees of freedom and some added noise (Sprott, 2003). Since time series analysis methods ultimately give rise to algorithms which just compress time series data into a set of a few numbers, they can be applied to any sequence of data, including stochastic, linear, and nonlinear data. The results however cannot be assumed to characterise the underlying system if these assumptions are not met (Kantz and Schreiber, 2004). Many nonlinear analysis methods assume data to be from a deterministic nonstationary process and to be described in

their state space. The state space is an N-dimensional vector space where the dynamical system can be defined at any point (Stergiou et al., 2004).

4.1.2.2. State Space Reconstruction

Mathematical models of dynamical systems are described in their state space, whose integer dimension is given by the number of the dependent variables of the model (Parlitz, 1998). The vast majority of time series measurements are single valued, and even if multiple simultaneous measurements are available, they will not typically cover all the degrees of freedom of the system (Schreiber, 1999). Fortunately, two methods for reconstructing the state space from scalar time series are available (Parlitz, 1998).

Derivative coordinates reconstruction involves using higher order derivatives of the measured time series, however such derivatives are susceptible to noise and are usually not appropriate for experimental data. Delay coordinates reconstruction is based on Takens' theorem (Takens, 1981 in Marwan et al., 2007), and is generated by constructing a delayed coordinates map that maps the state x from the original state space M to a point y in a reconstructed state space R^d. The reconstruction from delay coordinates is based on two parameters: the embedding dimension (m) and the delay time (τ), both of which are crucial for any successful analysis. These parameters may be estimated by several methods, such as using false nearest neighbours for estimating the embedding dimension, or using linear autocorrelation functions for determining the delay time (Figure 4.1).

Although a naive interpretation of Takens' theorem might suggest that any coordinate system that forms an embedding is equivalent to any other, in practice the choice of parameters used to reconstruct the coordinates dramatically affects the ability to make predications (Hasson et al., 2008). It is always important to remember that a poor reconstruction amplifies noise and increases estimation error (Casdagli, 1991), and no parameter determination methods are considered to be the right one for all systems. For real data, which is contaminated by noise, the optimal delay is typically around one-tenth to one-

half the mean orbital period around the attractor (Strogatz, 1994), however this can be difficult to determine when reconstructing the higher dimensional attractor from a one dimensional signal.
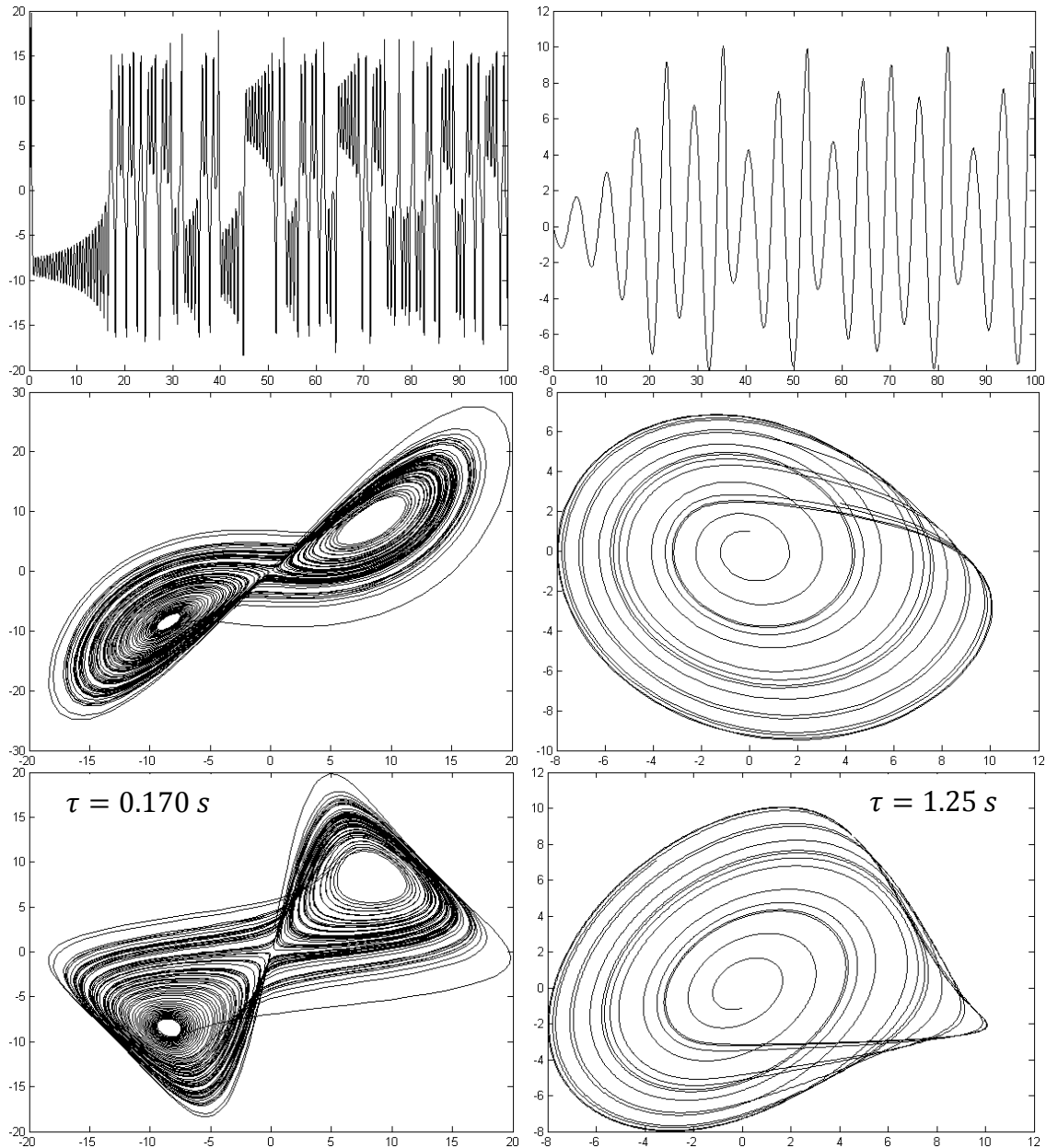
Figure 4.1: The Lorenz (left) and Rossler (right) systems expressed in one (top) and two (middle) dimensions, and reconstructed via delay coordinates (bottom), with τ determined by mutual information.

In the current research, the one dimensional signals of anteroposterior COP trajectories were reconstructed into the higher dimensional state space via

delay coordinates reconstruction. τ was determined using the principle of mutual information described by Fraser and Swinney (1986). Mutual information describes the general dependence between two variables, providing a better estimate of τ than autocorrelation which only measures linear dependence (Fraser and Swinney, 1986). Mutual information was calculated for a range of time steps, with the time corresponding to the first local minima providing the appropriate τ. Once τ was determined m was ascertained by employing the false nearest neighbour principle. The original signal was reconstructed into higher dimensional states in one dimensional increments and the number of nearest neighbours in the newly constructed higher dimensional signal was calculated. The number of nearest neighbours will initially be high due to the attractor overlapping onto itself when it is expressed in a low dimensional state space, therefore some of these nearest neighbours can be considered as 'false'. As the dimensions of the state space increase, the number of these false nearest neighbours will decrease until at the appropriate dimension there are none left. The total number of nearest neighbours will remain relatively unchanged when the reconstructed dimension is at or above the appropriate value for m.

Reconstruction parameters τ and m were determined for a random selection of trials from different subjects and experimental conditions. τ ranged from 0.2 to 0.45 seconds, and m ranged from 4 to 5. Hasson et al. (2008) applied a similar principle to the reconstruction of multiple balance trials, with and without added noise, and found average parameters of $\tau = 0.3$ and $m = 5$ provided the most stable outcome. Following their advice, and the close match to their parameters and those from a sample of data collected in this study, the same parameters of $\tau = 0.3$ and $m = 5$ were used for all subsequent reconstructions.

4.1.2.3. Nonlinear Dynamical Systems

The hall mark of deterministic chaos is the sensitive dependence of future states on the initial conditions, where an initial infinitesimal perturbation will typically grow exponentially (Eckmann et al., 1986). The growth rate can be determined by the Lyapunov exponent (LyE), where a positive value describes

an exponential divergence of nearby trajectories and defines chaos (Wolf et al., 1985). Lyapunov spectra can be defined that take into account the different growth rates in different local directions of state space, however only the maximum LyE is usually used, as the non-leading exponents are notoriously difficult to estimate from time series data (Schreiber, 1999). While the average stretching, folding, and volume contraction rate is quantified by the LyE, the loss of information due to the folding is reflected by the entropy of the process (Schreiber, 1999).

Entropy is a measure of the unpredictability of information content, and relates to Shannon's information theory. Approximate Entropy (ApEn) is an estimate of the entropy in a signal, and has been used within time series analysis to give an estimate of the complexity, or regularity, within physiological data (Pincus, 1991; Pincus et al., 1991; Pincus and Goldberger, 1994; Pincus, 1995). This has been used in a variety of postural control studies, and has shown that as infants develop towards an independent sitting posture the complexity in the signal first decreases as the infant hones in on a successful strategy, then increases slightly as they begin to explore the stability region (Harbourne and Stergiou, 2003). Although ApEn has been recommended as an appropriate tool for assessing balance, it has nevertheless come under criticism for being heavily dependent on the length of the signal, giving lower values for short data sets; a problem that is overcome somewhat by Sample Entropy (Richman and Moorman, 2000).

ApEn inherently includes a bias towards regularity, caused by the inclusion of self-matches of vectors within the data set, leading to lower ApEn values for shorter data sets (Yentes et al., 2013). Sample Entropy (SampEn) provides an improved evaluation of time series regularity for short data sets by removing this bias (Richman and Moorman, 2000). SampEn has been suggested as a useful tool for analysing physiological signals with lengths as low as 200 samples (Yentes, et al., 2013). Due to the challenging nature of the balance tasks employed here, and the assessment of novice handstanders as they learn to balance, SampEn was preferred over ApEn as an assessment of signal

complexity, and LyE was used to assess the divergence of trajectories in the embedded dimension. SampEn and LyE will result in larger values for chaotic signals compared to periodic signals, however both will also present larger values for stochastic data, making it difficult to determine the true characteristic of the signal without further inquiry. It is important to evaluate results against a surrogate data set to determine if a signal comes from a deterministic or stochastic process (Theiler et al., 1992).

Surrogation is a technique that compares the original time series against a random data set with the same mean, standard deviation, and power spectra to determine if the source of the signal is deterministic or stochastic (Stergiou et al., 2004). In the current research surrogate data sets were constructed in Matlab using the method described by Theiler et al. (1992). A fast Fourier transform (FFT) was computed for each COP time series and a normally distributed random data set of equal length. The inverse FFT was then computed on the magnitudes from the original data set and the phase angles of the random data set to produce a shuffled version of the original time series (Figure 4.2).
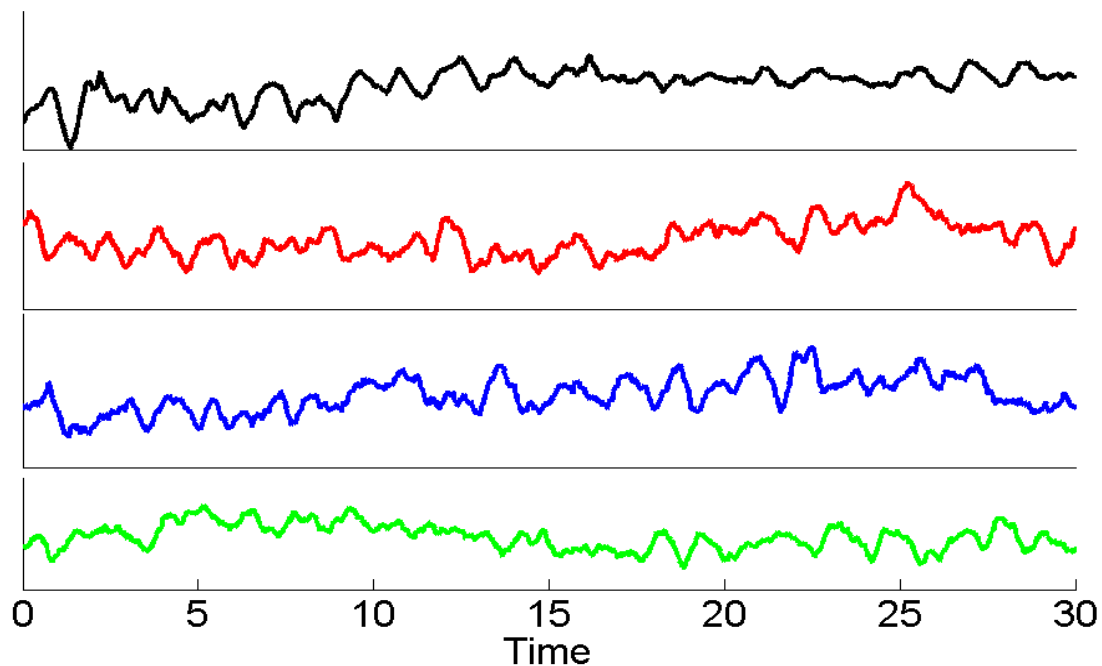
Figure 4.2: Three different surrogate data sets (coloured) computed from an original COP time series (black).

4.1.2.4. Stationarity

A signal is called stationary if all joint probabilities of finding the system at some time in one state and at some time in another state are independent of time within the observation period when calculated from the data (Hamilton, 1994). An evident consequence of this is that, if there exists a mathematical model of the process, it has to be autonomous, therefore there is no explicit time dependence in the equations and that in a physical realisation all system parameters, including the influences from the environment, must be strictly fixed (Kantz and Schreiber, 2004). Non-stationarity is a property of the underlying process, not the data, and arises when mechanisms producing the data change over time, however, a time-series that is too short to capture the slowest variations of the measured quantity produces the same effect (Sprott, 2003). A time series whose first two moments (mean and variance) are constant is said to exhibit weak stationarity. This is sufficient for linear time series analysis, but insufficient for analysing a chaotic system (Sprott, 2003; Kantz and Schreiber, 2004).

The most evident form of stationarity requires that all parameters that are relevant for a system's dynamics have to be fixed and constant during the measuring period. Unfortunately, in most cases we do not have direct access to the system which produces a signal and we cannot establish evidence that its parameters are indeed constant. Furthermore, there are many processes which are formally stationary when the limit of infinitely long observations can be taken, but which behave effectively like non-stationary processes when studied over finite times; human balance is an example of this. COP trajectories show what is called bounded nonstationarity, bounded within the base of support, suggesting from a purely biomechanical perspective that postural control is under-constrained (Riley et al., 1999). This provides a particular problem when comparing balance trials of different durations, as will undoubtedly occur when assessing novices learning to balance, or when balance is stressed to the limits of the postural control system.

Many statistical analysis methods typically require stationarity, and even slight non-stationarity can sometimes lead to severe misinterpretations (Kantz and Schreiber, 2004). Variables such as mean, standard deviation, variance, average deviation, skewness, and kurtosis should be similar for the first and second half of the time series for a nonlinear analysis to be used. Small differences in these variables are normal, but a significant difference between different portions of the signal can be determined via the standard error; if the difference is more than a few standard errors then the data is non-stationary.

If a signal is found to be non-stationary, then any further analysis of the time series using linear or nonlinear processing tools which assume stationarity are invalid. A nonstationary signal may be de-trended by removing the deterministic trend if it is a trend stationary process, or by differencing the signal once if it is a unit root process. In this study the augmented Dickey-Fuller test of stationarity was used to first test for nonstationarity within the data. If a balance metric required data to be stationary, any nonstationarity data sets were subsequently de-trended using a Butterworth high pass filter at the dominant frequency.

The nonstationarities within the COP time series may be a fundamental characteristic of postural control, and may reflect motions about a moving, rather than static, set-point (Riley et al., 1999; Zatsiorsky and Duarte, 1999). The dynamics of a moving reference point, usually exhibited as a slow drift in the mean COP displacement, may be described as stochastic, where the motion is a consequence of an inadequate deterministic stabilisation about the set point via closed loop control (Riley et al., 1999). The nonstationarity of this moving reference may provide insight into the underlying process of postural control. Indiscriminately removing the nonstationarity from COP signals may result in spurious results, and alternative methods of assessing balance without removing any nonstationarities are required. One alternative is to assess the COP time series from the paradigm of stochastic dynamics, such as a modelling COP as a random walk process (Collins and DeLuca, 1993).

4.1.2.5. Stochastic Dynamical Systems

A stochastic process can be defined as a family of random variables used to represent the evolution of some random value over time; this can be a discrete time process or a continuous time process (Astrom, 2006). The simplest case of a discrete time stochastic process is known as a Markov chain, where the system undergoes transitions from one state to another and the evolution of the system is based only on the current state and not any preceding states. A continuous time stochastic process is described by the Wiener process, a stochastic process with stationary independent increments, and occurs frequently in pure and applied mathematics, economics, and physics. A simple one dimensional random walk may be considered as a discrete time stochastic process, with either a uniform or Gaussian step size. As the step size decreases, and approaches zero, you get an approximation of a Wiener process, and less accurately Brownian motion. A Wiener process is the scaling limit of a random walk in one dimension.

Postural control has been modelled as one and two dimensional random walks with two distinct phases (Collins and DeLuca, 1993), and as a simple linear random walk (Newell et al., 1997). In nonlinear dynamics, randomness emerges out of deterministic dynamics, whereas in random walk dynamics, noise is not directly linked to deterministic dynamics (Yamada, 1995). It can be argued that in order to analyse COP signals, which consists of irregular and unpredictable components, the presence of nonlinear dynamics can be assumed. Even if a fluctuating signal apparently seems to be stochastic, it frequently includes a determinist aspect (Sasaki et al., 2001). Nonstationarities and apparent stochastic elements within deterministic COP dynamics become apparent when one considers that the postural fluctuations are primarily produced by the postural system, and yet must also be resolved and possibly countered by the postural system (Riley et al., 1999). Nonstationarities are a fundamental part of the COP signal, however simplifying this into a stochastic process seems unwise when the signal is produced from the deterministic process that is postural control.

4.1.2.6. Recurrence Plots and Recurrence Quantification Analysis

Recurrence is a fundamental property of dynamical systems, which can be exploited to characterise the system's behaviour in state space (Marwan *et al.*, 2007). The formal concept of recurrences was introduced by Henri Poincaré (1890) when addressing the restricted three body problem where, although unable to calculate the exact dynamics of the system, he described how the system would recur many times to a similar state (in Marwan *et al.*, 2007). Recurrences can be identified by calculating the distances between the trajectory of the system at one time to the trajectory of the system at every other point in time, thus creating a matrix of distances. The distance matrix can be converted into a recurrence matrix by allocating the number 1 to any distances that fall within a particular distance, described by:

$$\boldsymbol{R}_{i,j} = \begin{cases} 1 : \vec{x}_i \approx \vec{x}_j \\ 0 : \vec{x}_i \not\approx \vec{x}_j \end{cases} \qquad i,j = 1, \dots, N, \tag{4.1}$$

$$\boldsymbol{R}_{i,j}(\varepsilon) = \Theta\big(\varepsilon - \|\vec{x}_i - \vec{x}_j\|\big), \qquad i,j = 1, \dots, N, \tag{4.2}$$

Where ε is the distance threshold, $\vec{x}_i$ and $\vec{x}_j$ represent the time series with N data points, and $\Theta(\cdot)$ represents the Heaviside function (i.e. $\Theta(x) = 0$, if $x < 0$, and $\Theta(x) = 1$ otherwise).

Eckmann *et al.* (1987) introduced the method of recurrence plots to visualise the recurrences of dynamical systems in N dimensional space; created by plotting the recurrence matrix, with each 1 as a black square and each 0 as a white square. Additionally, the distance matrix may be plotted as a colour plot or a surface plot to visualise the dynamics of the system outside of the recurrence threshold (Figure 4.3). Originally these plots were used diagnostically as a qualitative assessment of system dynamics, but didn't offer any quantitative measures until Zbilut and Webber (1992), and later Marwan *et al.* (2002), developed what is now known as Recurrence Quantification Analysis (RQA).
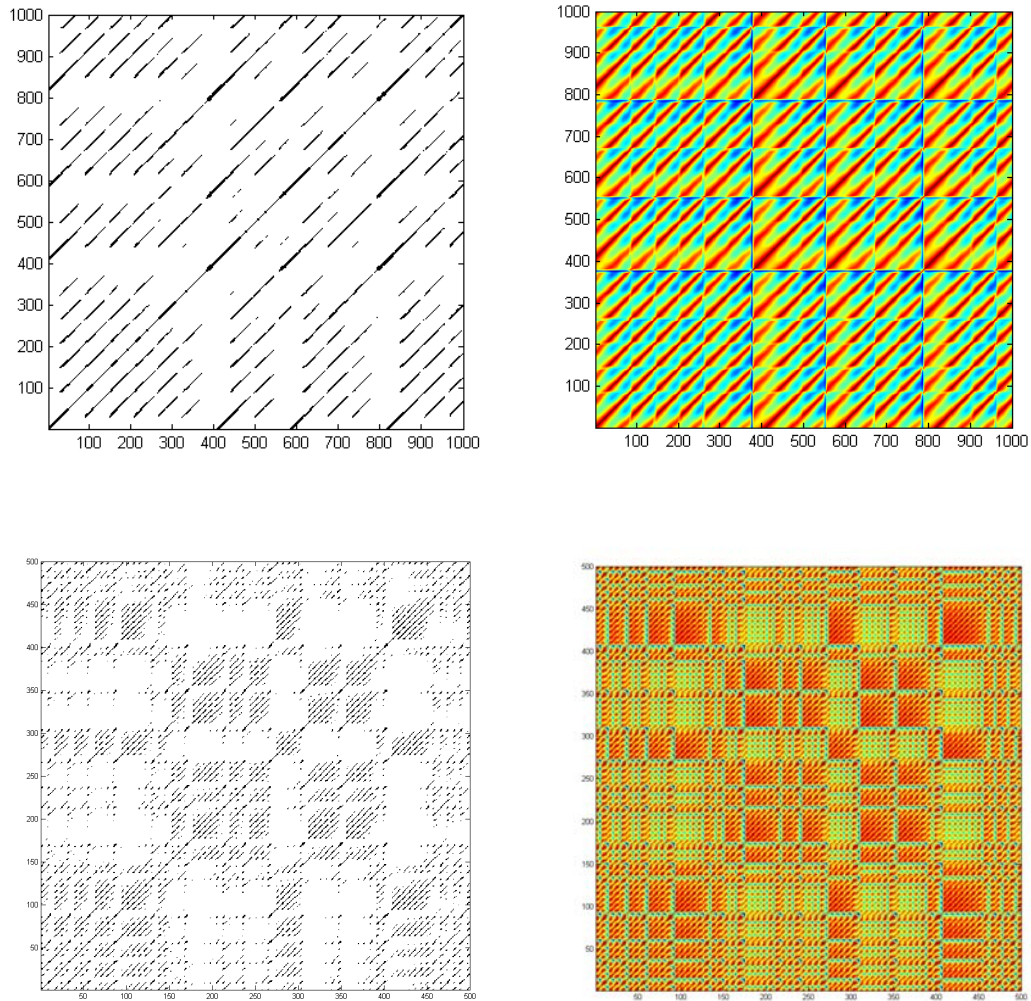
Figure 4.3: Recurrence plots (left) and distance plots (right) of two non-linear systems; from the Rossler equations (top) and the Lorenz equations (bottom).

Zbilut and Webber (1992) used the patterns in recurrence plots to quantify different characteristics of the underlying dynamics, such as measuring the lengths of all diagonal lines parallel to the main diagonal. The main diagonal line in the recurrence plot is called the line of identity, which represents each point in time compared to itself. Each diagonal line parallel to the line of identity represents continuous points in time that recur, thus the trajectory evolves in a similar way to the trajectory of the main diagonal. Further quantitative measures of recurrence plots include recurrence rate, determinism, laminarity, divergence, entropy, and trend (Webber and Zbilut, 2005; Marwan et al., 2007).The

Recurrence Rate (RR) is the percentage of recurrence points that fall within the specified radius, this is related to the correlation sum, and is calculated via:

$$RR = \frac{1}{N^2} \sum_{i,j=1}^{N} R_{i,j}$$

(4.3)

Determinism (DET) represents the percentage of recurrence points which form diagonal line structures, and describes trajectories that evolve in a similar way to past trajectories:

$$DET = \frac{\sum_{l=l_{min}}^{N} lP(l)}{\sum_{i,j}^{N} R_{i,j}}$$

(4.4)

Where $lP(l)$ is the histogram of the lengths of diagonal lines that are larger than the line threshold, which is usually set to two points. Laminarity (LAM) is the percentage of recurrence points which form vertical lines, and represents times when the system is evolving slowly or changing to a new state:

$$LAM = \frac{\sum_{v=v_{min}}^{N} vP(v)}{\sum_{v=1}^{N} vP(v)}$$

(4.5)

The longest diagonal line (L_{max}), excluding those close to the line of identity, represents the longest time when two trajectories evolve in a similar manner:

$$L_{max} = \max(\{l_i; i = 1 \dots N_l\})$$

(4.6)

L_{max} is an important recurrence variable because it will scale inversely with the largest Lyapunov exponent and is related to the rate at which nearby trajectories diverge (DIV):

$$DIV = \frac{1}{L_{max}}$$

(4.7)

Entropy is an estimate of Shannon information entropy, calculated from the inverse of the probability distribution of the diagonal line lengths:

$$ENTROPY = -\sum_{l=l_{min}}^{N} p(l)\, In\, p(l)$$

(4.8)

Trend (TND) is a measure of the stationarity within the system, where a nonstationarity will be exhibited as a paling of the recurrence plot towards the edges due to a drift in the signal. TND is calculated as the slope of the percentage of local recurrences against the displacements from the main diagonal, expressed in units of percentage recurrence per 1000 data points. If recurrence points are homogenously distributed across the recurrence plot then TND will be close to zero, indicating stationarity.

Since all nonlinear tools are calculated within the embedded space, it is logical that stationarity should be examined at this level (Stergiou et al., 2004). A major advantage of RQA is that it assesses all aspects of the system embedded in its state space, including estimates of divergence, entropy and stationarity. RQA is suitable for short non-stationary signals, quantifies dynamical structure and non-stationarity, making it a promising tool for assessing the short nonstationary signals that are expected to be found in the COP trajectories of novices learning to balance. RQA has been employed to assess the effect of visual information on standing balance (Riley et al., 1999), the dynamics of sitting balance (Hermann, 2005), and the noise within the COP signal whilst standing (Hasson et al., 2008). Nevertheless, it is important to note that no one measure of overall system complexity has emerged as sufficient (Riley et al., 1999).

4.1.3. Estimates of Feedback Time Delay

Cross correlations have shown there to be zero delay between COM and COP trajectories, with some authors suggesting this is evidence of a passive control system (Winter et al., 1998; Winter et al., 2001; Winter et al., 2003), while others suggest it is evidence of an active anticipatory feedforward control

process (Gatev et al., 1999). These assumptions neglect the possibility of a reactive control strategy that relies on proportional and derivative gains from COM motion. Assuming a reactive control strategy is employed (Figures 4.4 and 4.5) such a control process may be described as:

t_0 – An imbalance in force leads to a small acceleration with a small amount of motion that goes undetected by the sensory system.

t_1 – A sensory threshold is reached and a neurological signal is sent from the sensors to the CNS whilst sway continues.

t_2 – Signals are received at the muscle to produce an intended response.

t_3 – After a short electromechanical delay the muscle begins to produce force, but the resulting joint torque is initially too low.

t_4 – The joint torque rises to be larger than the torque due to COM position; sway velocity is at its peak and begins to fall, but sway continues and joint torque will continue to rise.

t_5 – Sway velocity reaches zero and sway angle is at its maximum before it is reversed; joint torque may continue to rise, or it could have begun to reduce before this point.
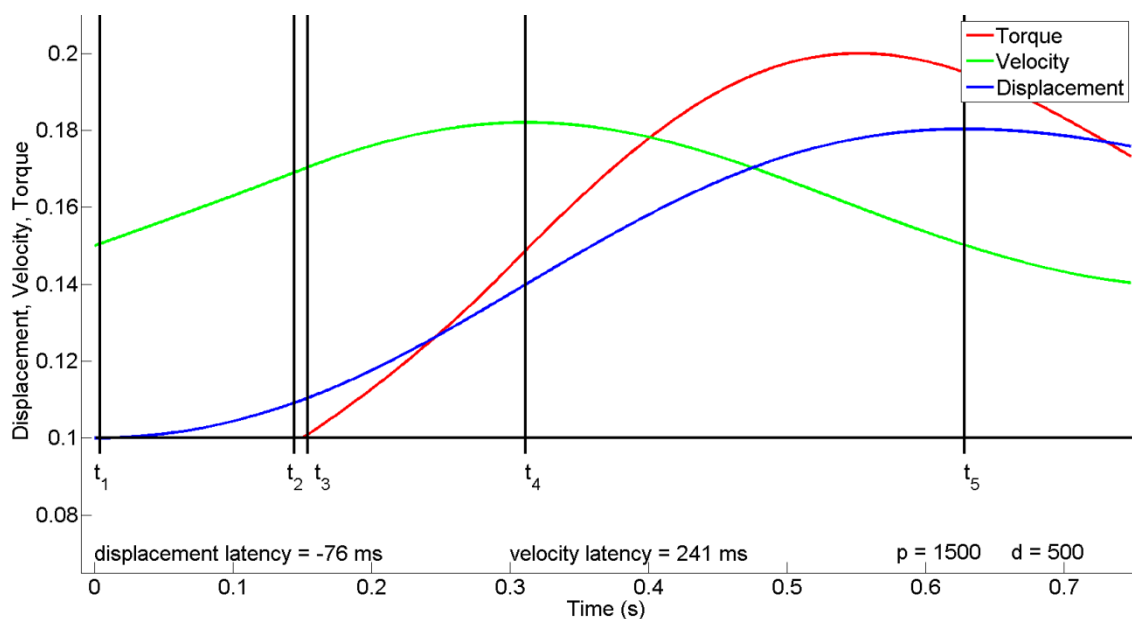
Figure 4.4: An example of the relationship between COM displacement, COM velocity, and joint torque from a simple inverted pendulum with PD control and a delay of 150 ms.

99
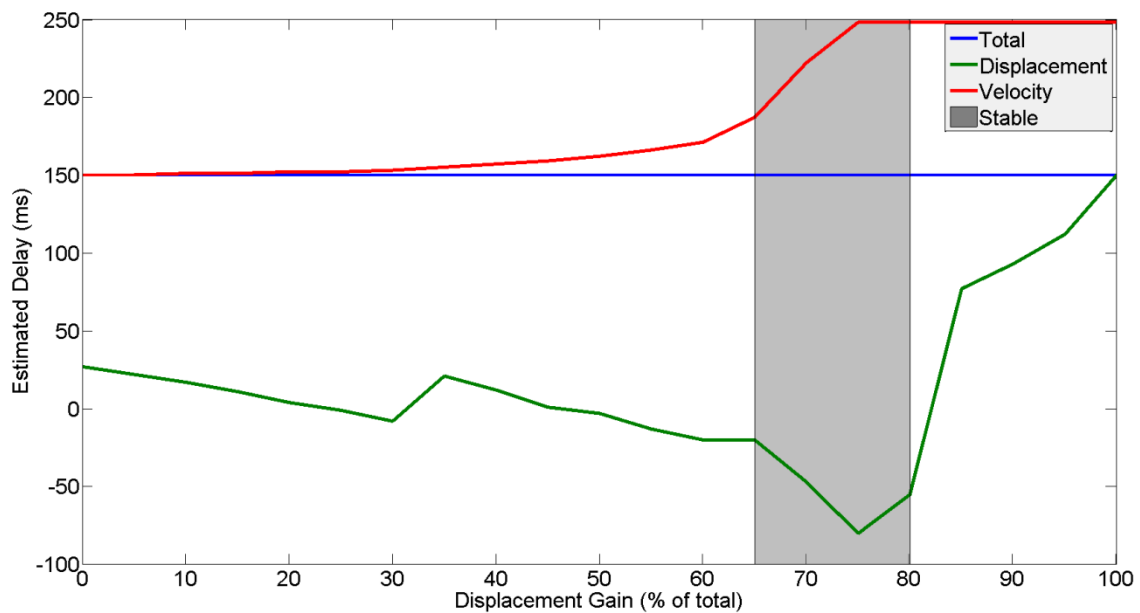
Figure 4.5: An example of how the estimated feedback time delay can be affected by adjusting the proportional and derivative gains in a simple inverted pendulum with PD control.

Research examining the latency between an external perturbation and the onset of muscle EMG, such as Nashner (1976), will determine the time between t_0 and t_2, with the time from t_0 to t_1 minimised during larger perturbations. Research employing cross correlations to examine delays between COP and COM, such as Gatev et al. (1999), will determine the time between peak COP (ankle torque) and peak COM. A simple inverted pendulum model of balance that is controlled with a PD controller based on COM motion from earlier times, due to a feedback delay, can produce stable postural control. If the proportional and derivative gains are adjusted and the delay in the system kept constant, cross correlation between the controlling joint torque and COM displacement can produce large underestimates of the actual delay (Figures 4.2 and 4.3). Stable control in a simple model as this is usually achieved with a combination of proportional and derivative inputs, indicating the importance of both COM displacement and velocity in the control of posture.

Yeadon and Trewartha (2003) examined the feedback time delay during static balance via examination of the relationship between joint torques and COM motion whilst in handstand. Wrist joint torques were regressed against COM displacement and velocity at earlier times, with peak R^2 values occurring at 160

to 240 ms. It is important to note that this method will only provide a rough estimate of the average delay over the full duration of the trial, incorporating several delays within it, such as: electromechanical delay (EMD), joint torque rise times, and the time for any sensory thresholds to be reached. Based on literature values, Yeadon and Trewartha subtracted an estimated value of 40 ms from all trials to account for these delays, resulting in estimated delays of 120 to 200 ms. No passive elements are included in this model, which have been estimated to account for 64% to 90% of critical torque (Casadio et al., 2005; and Loram and Lakie, 2002a respectively).

Joint torques may be modelled as a composite of active torque, passive stiffness, and a bias torque representing the tonic activity within the muscles (Jacono et al., 2004). Jacono et al. (2004) used literature values in the range of 70% to 90% as estimates of passive stiffness, and calculated the remaining active torque required to maintain balance during standing. In the current research this principle was combined with the method used by Yeadon and Trewartha (2003) to estimate the percentage of torque from passive stiffness and that from delayed COM motion. A third parameter was added to the original regression model used by Yeadon and Trewartha (equation 4.9) representing a passive stiffness element based on the COM displacement with zero delay (equation 4.10):

$$T_{(t)} = p x_{(t-t_0)} + d \dot{x}_{(t-t_0)}$$
(4.9)

$$T_{(t)} = p_1 x_{(t)} + p_2 x_{(t-t_0)} + d \dot{x}_{(t-t_0)}$$
(4.10)

Both regression models were employed to examine the delay between ankle joint torque and COM motion in normal standing and single leg stance, and between wrist joint torque and COM motion in handstand. The coefficients from each model were combined with their respective COM variable to calculate the relative contributions to overall joint torque.

4.1.4. Movement Corrections

Roncesvalles et al. (2001) examined the number and magnitude of joint torque corrections during perturbed standing in children ranging from 9 months to 10 years of age. Movement units were defined as one cycle of positive and negative acceleration of the respective segment, for example the foot accelerations were used to determine movement units relating to ankle torque. Mean joint torque was calculated for each movement unit and the total number of movement units were counted from the start of the perturbation until balance had been recovered. An increased number of movement units were evident in younger children, with larger mean joint torques occurring with a decreased number of movement units.

During static stance it would be impractical to count movement units for the ankle based on accelerations of the foot, and one could argue the same for all balance in standing. Therefore, the method of determining the start and end of each movement unit was altered and determined based on a change in joint torque; this will be referred to as movement corrections. Joint torque signals were differentiated and zero crossings detected to determine when minima and maxima turning points occurred. Thresholds of 1, 2, and 3 SD were used to classify the change in joint torques from one minimum to the subsequent maximum as either small, medium, or large corrections respectively. The time from one minimum to the subsequent minimum was used to determine the duration of the correction, and mean joint torque and torque impulse were calculated for this period. Filtered EMG data were assessed in the same manner, with root mean square (RMS) values calculated during the duration of the movement correction.

4.1.5. Statistical Analysis

Determinism and SampEn values of the surrogate data were compared to those obtained from the original data using a repeated measures t-test with a significance level of 0.05 in accordance with the suggestions of Harbourne and Stergiou (2003) and Stergiou et al. (2004).

A two-way repeated measures ANOVA (posture vs. vision) was used to compare mean values for all dependent variables (Table 4.1), and significant differences were examined further using multiple t-tests with a Bonferroni correction. Further comparisons were only made within each independent factor, either based on posture or vision. Prior to statistical testing, all data were assessed for normality and sphericity by the one-sample Kolmogorov-Smirnov test and Mauchly's test of sphericity respectively. A Greenhouse-Geisser correction was used to adapt the degrees of freedom of statistical tests for any data that was found to violate the assumption of sphericity.

Table 4.1: All variables used to assess balance

Group	Variables	Number
Traditional	duration, standard deviation (SD), range, mean sway velocity (SV)	4
Nonlinear	sample entropy (SampEn), lyapunov exponent (LyE)	2
Recurrence Quantification Analysis	recurrence rate (RR), determinism (DET), entropy (ENT), divergence (DIV), trend (TND)	5
Estimated Delays	delay, R^2, proportional and derivative coefficients, torque percentages, cross correlations	17
Movement Corrections (Torque)	corrections per second, mean torque, torque impulse, burst duration [small, medium, large (S,M,L)]	12
Movement Corrections (EMG)	corrections per second, root mean square (RMS), burst duration [small, medium, large (S,M,L)]	9

Note: Movement corrections for EMG were only used in handstand as no sensors were placed on the lower leg; estimated delays were calculated by two different methods and will be prefixed with M1 or M2 (M1 = Yeadon and Trewartha method)

4.2. Findings and Discussion

The results of this study were examined from several perspectives, including: linear, nonlinear, recurrence, feedback time delays, and movement corrections. Interpretation of the analysis from each perspective follows, with comparison of these results to past literature where appropriate.
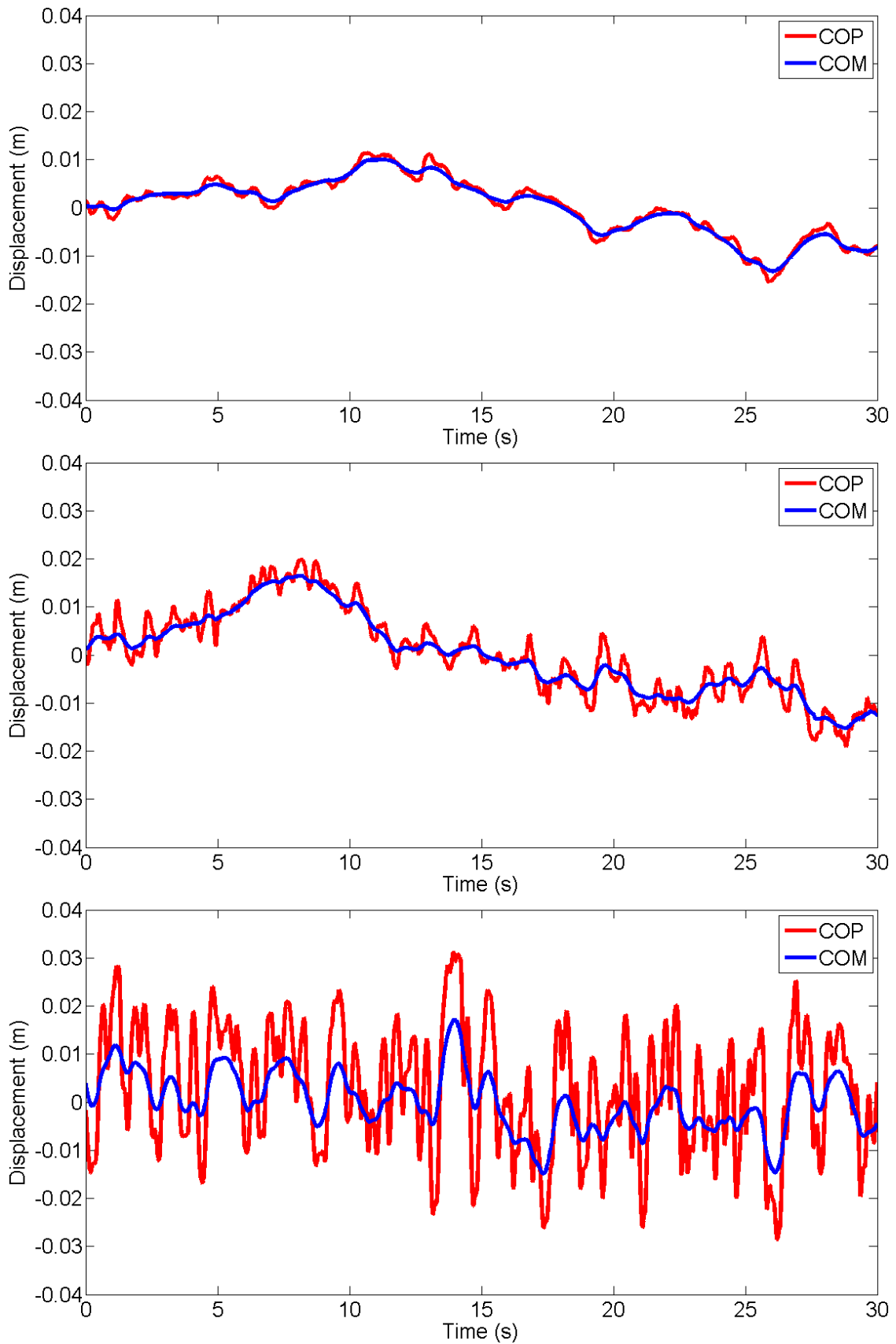
Figure 4.6: An example trial from each posture showing the COM (blue) and COP (red) trajectories in standing (top), single leg stance (middle) and handstand (bottom).

Significant differences were found between the original data sets and the surrogate data sets for both SampEn (t = -10.9; p = 0.00) and DET (t = 15.4; p = 0.00), indicating the fluctuations observed were distinguishable from linearly correlated Gaussian noise. The original data most likely have a deterministic nature and the use of nonlinear techniques are supported. All data were found to be normally distributed by the one-sample Kolmogorov-Smirnov test. Most data was found to violate the assumption of sphericity, therefore the Greenhouse-Geisser correction was employed. Examples of each posture are shown in Figure 4.6 with COM and COP trajectories plotted.

4.2.1. Traditional Measures of Balance

A statistically significant interaction between the effects of posture and vision was found for all traditional variables. Further comparisons and group means are given in table 4.2. Significant differences were found for most traditional balance measures, with all traditional measures, except for trial duration, presenting with larger values as the complexity of the task increased. The duration of trials in handstand with eyes closed was significantly shorter compared to all other trials, in agreement with the findings of Asseman and Gahery (2005) and highlighting the high difficulty level of this task.

Table 4.2: Mean values for traditional measures of balance

| Variable | Normal Standing | | Single Leg Stance | | Handstand | |
	$EO_{(a)}$	$EC_{(b)}$	$EO_{(c)}$	$EC_{(d)}$	$EO_{(e)}$	$EC_{(f)}$
Trial Duration (s)	30.0	30.0	30.0	27.9	27.7	$18.6^{b,d,e}$
SD (cm)	$0.5^{c,e}$	$0.5^{d,f}$	$0.7^{a,d,e}$	$1.2^{b,c,f}$	$1.3^{a,c,f}$	$1.6^{b,d,e}$
Range (cm)	$2.1^{c,e}$	$2.2^{d,f}$	$3.7^{a,d,e}$	$7.0^{b,c}$	$5.9^{a,c}$	6.6^{b}
SV (cm s^{-1})	$0.7^{b,c,e}$	$0.9^{a,d,f}$	$2.5^{a,d,e}$	$5.2^{b,c,f}$	$6.8^{a,c}$	$7.7^{b,d}$

Note: superscripts indicate significant differences between conditions at the Bonferroni adjusted significance level of 0.0056

Significant differences between eyes open and eyes closed conditions in standing balance were observed for mean sway velocity, however, no significant difference was found for standard deviation or range, confirming

numerous past findings (Le Clair and Riach, 1996; Blaszczyk, 2008; Salavati et al., 2009). Similar to past literature, significant differences were found for standard deviation between eyes open and eyes closed conditions for handstand (Gautier et al., 2007) and single leg stance (Asseman et al., 2005), but not in the normal standing. All traditional balance metrics successfully distinguished between each posture, with noticeably large changes in sway velocity between each posture in the eyes open condition, similar to the findings of Asseman et al. (2005).

4.2.2. Nonlinear Measures of Balance

There was a statistically significant interaction between the effects of posture and vision for TND and DET, and statistically significant differences for effects of posture on SampEn, RR, ENT, and DIV. Statistically significant differences from the effects of vision were also found for ENT. Further comparisons and group means are given in table 4.3, and example recurrence and distance plots for each posture are shown in figure 4.7.

Table 4.3: Mean values for nonlinear and recurrence measures of balance.

Variable	Normal Standing		Single Leg Stance		Handstand	
	$EO_{(a)}$	$EC_{(b)}$	$EO_{(c)}$	$EC_{(d)}$	$EO_{(e)}$	$EC_{(f)}$
SampEn	$0.07^{c,e}$	$0.09^{d,f}$	0.10^{a}	$0.11^{b,f}$	0.14^{a}	$0.15^{b,d}$
LyE	1.14	0.95	0.88	0.98^{f}	0.66	0.60^{d}
RR (%)	$9.32^{c,e}$	$6.94^{d,f}$	$3.25^{a,e}$	2.21^{b}	$1.04^{a,c}$	1.66^{b}
DET (%)	99.95^{e}	$99.94^{d,f}$	99.72^{a}	99.65^{b}	$99.31^{a,c}$	99.51^{b}
ENT (bits)	$4.83^{c,e}$	$4.56^{d,f}$	$3.65^{a,d,e}$	$3.37^{b,c,f}$	$2.88^{a,c}$	$2.81^{b,d}$
DIV	$0.13^{c,e}$	$0.26^{d,f}$	$1.26^{a,e}$	$2.24^{b,c}$	$3.67^{a,c}$	6.53^{d}
TND	$-3.28^{c,e}$	-2.28	-1.06^{a}	-0.81	-0.64^{a}	-4.18

Note: superscripts indicate significant differences between conditions at the Bonferroni adjusted significance level of 0.0056
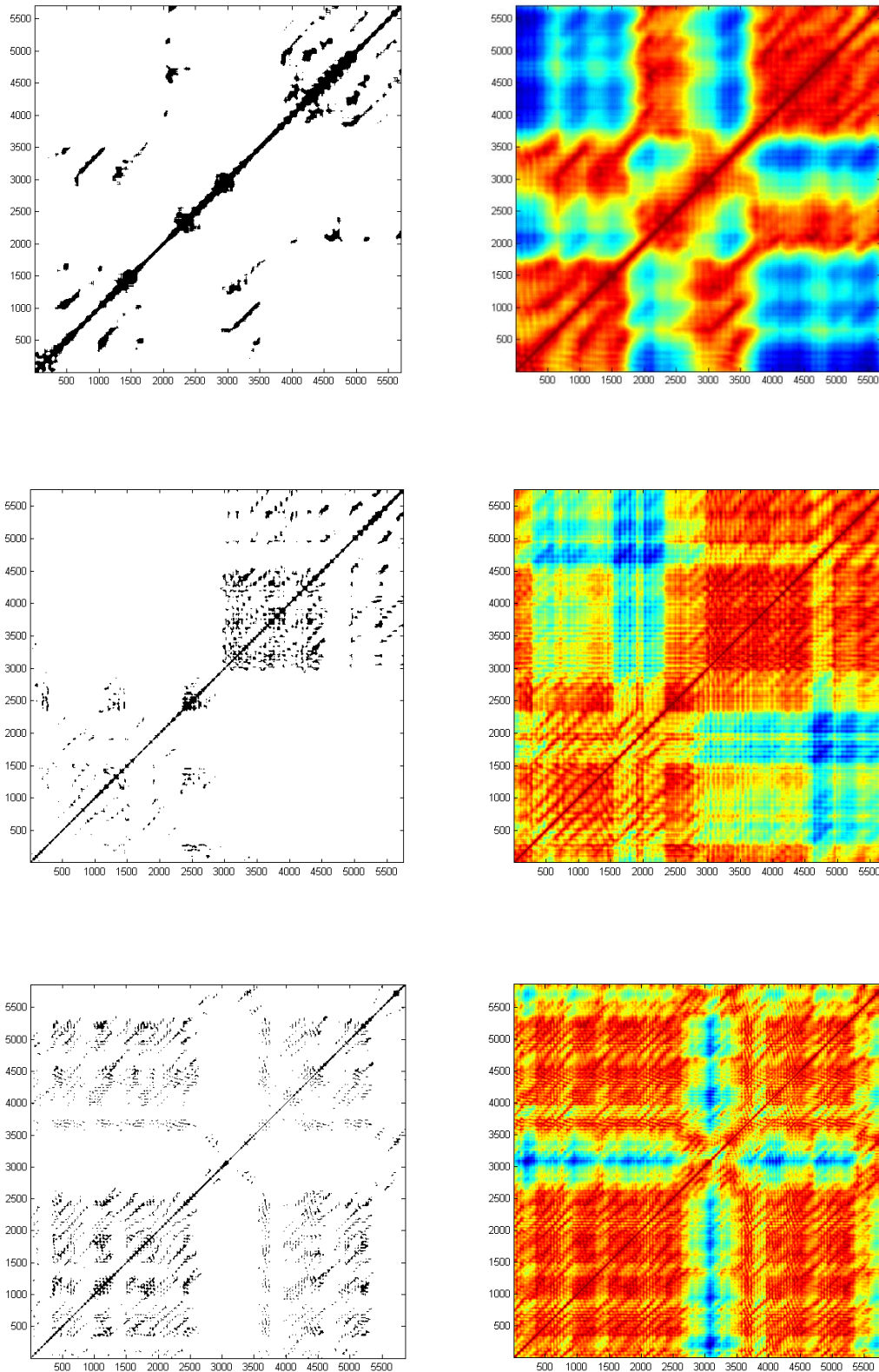
Figure 4.7: Recurrence plots (left) and distance plots (right) from example trials in: standing (top), single leg stance (middle), and handstand (bottom); input parameters: embedding dimension = 5, time lag = 0.3 s, and radius = 10% of maximum distance.

All recurrence plots contained isolated single recurrent points, indicating noise, and upwards diagonal line segments, indicating deterministic structure. Downward line segments along with vertical and horizontal line segments are also evident, suggesting the presence of short-term transient behaviour similar to past use of RQA in COP analysis (Riley et al., 1999). Plots show larger recurrences close to the line of identity for standing balance, with a more diffuse recurrence in the more challenging postures of single leg stance and handstand. This is supported by the general change in TND from the standing posture to single leg stance and handstand, with more negative values in standing indicating nonstationarity.

RQA values show a decrease in recurrences (RR) as the task difficulty increases from normal standing to single leg stance to handstand. RR is related to time correlation, quantifying the percentage of points which over time return to the same local neighbourhood in the reconstructed state space. Higher values of RR for standing trials would seem to suggest higher time correlation, however, examining typical plots will show that most of the recurrences occur close to the line of identity. This is likely caused by a decreased sway velocity in standing trials resulting in points remaining within the distance threshold for longer. This is a particular problem of slowly evolving systems and has been discussed at length in the dynamical systems literature (Marwan et al., 2007). One possible option would be to use a perpendicular recurrence plot, where recurrences are only recorded for points that fall into the local neighbourhood of the $(d-1)$ dimensional subspace that is perpendicular to the state space trajectory (Choi et al., 1999). This method has not been employed much within dynamical systems and will require further study before it can be employed within COP analysis.

As task difficulty increases the number of recurrences that form diagonal line structures decreases, indicating a slight decrease in system determinism (DET). Although the differences between several conditions are significant, all values remain above 99%, suggesting that the system can still be considered deterministic. Small reductions in DET percentages are likely related to

changes in short term transient behaviour, slightly increasing the number of single points within the recurrence plot (Marwan et al., 2007). This is further supported by the increase in sample entropy from standing to handstand postures, indicating an increase in system complexity. Similarly, divergence increases with task complexity, representing shorter diagonal line segments, and an increase or change in system dynamics. Similar to several traditional measures of balance, all nonlinear measures fail to discriminate between visual changes within a specific posture.

4.2.3. Estimated Feedback time Delay

There was a statistically significant interaction between the effects of posture and vision for the delay between joint torques and COM displacement as estimated by cross correlations, and for the calculated R^2 value and the estimated feedback time delay from the method employed by Yeadon and Trewartha (2003). There was a statistically significant interaction between the effects of posture and vision for the calculated R^2 value from the adapted method, but not for the estimated delay time. There was however significant main effects from posture and vision for the estimated delay from the adapted method. Further comparisons and group means are given in tables 4.4 to 4.6

Cross correlations between joint torques and COM show almost zero delay, in agreement with previous research (Jacono et al., 2004; Winter et al., 1998; Winter et al., 2001; Winter et al., 2003). Some cross correlations display negative delays, indicating joint torques are peaking before COM displacement, as was predicted in the example PD controller shown in Figures 4.4 and 4.5 previously. Cross correlations between EMG of wrist flexor/extensor muscles and COM displacement show delays of approximately 94 ms, with similar delay between EMG and wrist flexor torques. Combined, these results would seem to suggest the delay between EMG and COM displacement is due to an electromechanical delay (EMD) from the EMG signal to the rise in joint torque. An EMD of 94 ms is somewhat higher than the 13.5 ms to 55 ms reported in previous studies (Cavanagh and Komi, 1979; Muraoka et al., 2004; Tillin et al., 2010; Zhou et al., 1995). A higher estimated EMD found here is most likely due

to use of cross correlations with EMG signals, where slower components can dominate and hinder the detection of faster components (Nikolic et al., 2012). This issue will be addressed further in Chapter 6.

Table 4.4: Cross correlations between Torque and COM displacement in standing, single leg stance and handstand.

	Normal Standing		Single Leg Stance		Handstand	
Variable	$EO_{(a)}$	$EC_{(b)}$	$EO_{(c)}$	$EC_{(d)}$	$EO_{(e)}$	$EC_{(f)}$
Delay (ms)	1^c	-1^d	-4^a	$-17^{b,f}$	-3	9
R^2	$0.94^{b,c,e}$	$0.91^{a,d,f}$	$0.85^{a,d,e}$	$0.75^{b,c,f}$	$0.64^{a,c,f}$	$0.56^{b,d,e}$

Note: superscripts indicate significant differences between conditions at the Bonferroni adjusted significance level of 0.0056

Table 4.5: Cross correlations between EMG and COM, and between EMG and torque in handstand.

Variable	$EO_{(e)}$	$EC_{(f)}$
EMG – COM: Delay (ms)	95	93
EMG – COM: R^2	0.59	0.65
EMG – Torque: Delay (ms)	94	92
EMG – Torque: R^2	0.59	0.64

Cross correlations between joint torques and COM show almost zero delay, in agreement with previous research (Jacono et al., 2004; Winter et al., 1998; Winter et al., 2001; Winter et al., 2003). Some cross correlations display negative delays, indicating joint torques are peaking before COM displacement, as was predicted in the example PD controller shown in Figures 4.4 and 4.5 previously. Cross correlations between EMG of wrist flexor/extensor muscles and COM displacement show delays of approximately 94 ms, with similar delay between EMG and wrist flexor torques. Combined, these results would seem to suggest the delay between EMG and COM displacement is due to an electromechanical delay (EMD) from the EMG signal to the rise in joint torque. An EMD of 94 ms is somewhat higher than the 13.5 ms to 55 ms reported in

previous studies (Cavanagh and Komi, 1979; Muraoka et al., 2004; Tillin et al., 2010; Zhou et al., 1995). A higher estimated EMD found here is most likely due to use of cross correlations with EMG signals, where slower components can dominate and hinder the detection of faster components (Nikolic et al., 2012). This issue will be addressed further in Chapter 6.

Table 4.6: Mean values for estimated feedback time delay in each posture, from the Yeadon and Trewartha regression model (M1) and the adapted method (M2).

Variable	Normal Standing		Single Leg Stance		Handstand	
	$EO_{(a)}$	$EC_{(b)}$	$EO_{(c)}$	$EC_{(d)}$	$EO_{(e)}$	$EC_{(f)}$
M1 Delay (ms)	$234^{c,e}$	$244^{d,f}$	191^{a}	174^{b}	$176^{a,f}$	$200^{b,e}$
M1 R^2	$0.96^{b,c,e}$	$0.94^{a,d,f}$	$0.89^{a,d,e}$	$0.82^{b,c}$	$0.79^{a,c}$	0.80^{b}
M1 p coefficient	657	683^{d}	689^{d}	$776^{b,c,f}$	596	603^{d}
M1 d coefficient	236	252	246	191	237	237
M1 p torque (%)	-15.9	742.8	124.0	116.7	402.3	960.1
M1 d torque (%)	115.9	-642.8	-24.0	-16.7	-302.3	-860.1
M2 Delay (ms)	$262^{c,e}$	$278^{d,f}$	221^{a}	$235^{b,f}$	$212^{a,f}$	244^{e}
M2 R^2	$0.96^{b,c,e}$	$0.94^{a,d,f}$	$0.89^{a,d,e}$	$0.82^{b,c}$	$0.78^{a,c}$	0.79^{b}
M2 p_1 coefficient	25	23	37	267	51	67
M2 p_2 coefficient	628^{e}	650^{f}	644^{e}	491	$529^{a,c}$	511^{b}
M2 d coefficient	247^{b}	267^{a}	256	193	243	240
M2 p_1 torque (%)	2.21	2.61	7.28	27.75	7.29	10.83
M2 p_2 torque (%)	70.25	69.13	66.33	52.50	63.53	60.30
M2 d torque (%)	27.54	28.26	26.39	19.75	29.18	28.87

Note: superscripts indicate significant differences between conditions at the Bonferroni adjusted significance level of 0.0056

Both methods of calculating feedback time delay via regression models display high R^2 values, with individual mean values ranging from 0.72 to 0.99 for all trial

types. Standing trials typically displayed the highest R^2 values, with the lowest values found in either handstand with eyes closed or single leg stance with eyes closed. Estimated delays were generally higher for the adapted method compared to the Yeadon and Trewartha method, with individual mean times ranging from 173 to 340 ms and 72 to 317 ms respectively. Highest estimated delay times were typically found in standing trials with eyes closed, with trials in handstand with eyes open and in single leg stance with eyes closed exhibiting the lowest delay estimates.

Results for estimated delays and R^2 values in handstand trials are in accordance with those obtained from Yeadon and Trewartha (2003), who found R^2 values from 0.74 to 0.86 and delays ranging from 160 ms to 240 ms. Yeadon and Trewartha (2003) filtered joint torques and COM displacements and velocities above 2 Hz to remove high frequency vibrations due to muscle stiffness. When unfiltered data were used the authors obtained R^2 values of 0.50 to 0.73 with delays of 160 ms to 180 ms; explaining the 40 ms reduction in estimated delays to the inclusion of the muscle stiffness response which has a delay close to zero. The present study did not filter calculated joint torques and COM motion in the same way, however, the adapted method did provide estimated delays that were on average 38 ms higher than the Yeadon and Trewartha method, with larger differences found when estimates of passive stiffness were higher. The inclusion of the third term into the adapted method is to account for the effects of any passive stiffness in the control of COM motion. These results seem to support this assertion, and may provide an alternative to filtering calculated joint toques and COM motion to allow the full signal to be analysed in its entirety.

All proportional and derivative coefficients were positive and within a similar range to those reported for handstand trials by Yeadon and Trewartha (2003). In the present study, the Yeadon and Trewartha method often produced percentage torque estimates from derivative coefficients that were negative. In contrast, the adapted method always produced reasonable estimates of joint torque percentages, with the sum of the absolute values equal to 100% in all

cases. Individual mean estimates of passive torques from this method range from 1% to 87%, showing large individual variation. Smaller values are typically found for standing trials (<10%), with larger values usually found in single leg stance with eyes closed. Estimates of passive stiffness contributions to whole joint torque during normal stance are several times smaller than the 64% and 90% of critical torque reported by Casadio et al. (2005) and Loram and Lakie (2002a) respectively. Both past studies calculated passive stiffness as a percentage of the torque needed to maintain static stance, and not the actual torque that was produced by the individual. In addition, both assessed passive stiffness during small continuous oscillations at the ankle joint and not during static stance as was done here. It is unclear if these differences can account for the large discrepancies in estimated stiffness. Further study is required in this area to examine both the role and contribution of passive stiffness to static balance.

Extremely high R^2 values for standing trials are consistent with modelling human standing balance as a simple inverted pendulum about the ankle joint. Lower R^2 values in handstand are still promising, but may suggest that other factors need to be considered. Yeadon and Trewartha (2003) suggested that one cause for the lower R^2 values could be due to noise within the sensory system resulting in errors in the subsequent responses. This view may be supported by the high R^2 values found in standing trials, where sensory noise may be expected to be less.

Longer estimated delay times found in handstand compared to standing trials might suggest different sensory systems are at work (Nashner, 1976). It is important to remember that these delays are still estimates that will also include several other delays, such as: electromechanical delay, joint torque rise times, and the time for any sensory thresholds to be reached. Sensory thresholds have been shown to be dependent on both position and velocity, with an increased positional sense with faster movements (Clark et al., 1985; Fitzpatrick and McCloskey, 1994). General decreases in delay times with increases with mean sway velocity (Figure 4.8) would suggest that velocity

113

dependent sensory thresholds may need to be considered for further improvements in estimating feedback time delay. Further study in this area is required before a comprehensive mathematical relationship may be proposed.
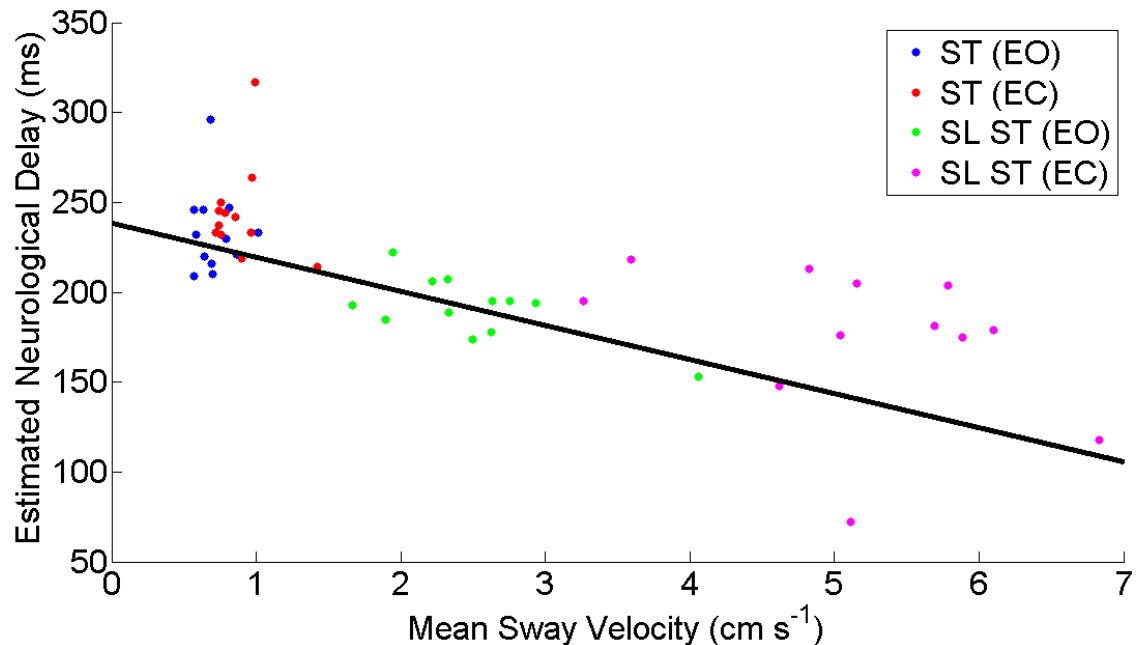
Figure 4.8: Relationship between estimated feedback time delay and mean sway velocity for standing (ST) and single leg stance (SL ST) trials.

4.2.4. Movement Corrections

There were statistically significant interactions between the effects of posture and vision for the number of small, medium, and large corrections per second based on joint torques from the wrist and ankle. There were statistically significant differences for the effects of posture on mean torque, torque impulse and burst duration from small, medium, and large movement corrections. Further comparisons and group means are given in table 4.5.

Data typically show that balance in standing exhibits bursts of torque activity that are longer and with a higher torque impulse compared to balance in handstand. Balance in single leg stance typically have a higher mean joint torque with moderate burst durations, leading to the highest joint torque impulses from the three postures. A lower number of movement corrections per second are evident in standing trials, with the largest number of corrections occurring in handstand with eyes open and single leg stance with eyes open.

114

The number of corrections per second in handstand with eyes closed was significantly lower than handstand with eyes open for all movement correction magnitudes. Reduced mean torque and torque impulse during all movement corrections in handstand are indicative of the reduced muscular strength of the muscles found in the forearm compared to the lower leg. It would appear this leads to the requirement for a larger number of corrections per second, but with reduced burst duration. It is unclear how these factors may be affected by trial duration and muscle fatigue in the handstand position.

Table 4.7: Movement corrections based on joint torques, with large, medium, and small (L, M, S) corrections based on torque above 1, 2, and 3 SD respectively.

Variable	Normal Standing		Single Leg Stance		Handstand	
	$EO_{(a)}$	$EC_{(b)}$	$EO_{(c)}$	$EC_{(d)}$	$EO_{(e)}$	$EC_{(f)}$
L - Corrections/s	0.09^c	0.11	0.17^a	0.13	0.19^f	0.08^e
M - Corrections/s	0.19^c	0.22	0.41^a	0.27	0.41^f	0.18^e
S - Corrections/s	0.41^c	0.44	0.85^a	0.53	0.75^f	0.32^e
L - Mean Torque	$0.57^{c,e}$	$0.59^{d,f}$	$0.83^{a,d,e}$	$0.92^{b,c,f}$	$0.46^{a,c}$	$0.54^{b,d}$
M - Mean Torque	$0.56^{c,e}$	$0.58^{d,f}$	$0.84^{a,d,e}$	$0.91^{b,c,f}$	$0.46^{a,c}$	$0.54^{b,d}$
S - Mean Torque	$0.57^{c,e}$	$0.59^{d,f}$	$0.84^{a,d,e}$	$0.91^{b,c,f}$	$0.46^{a,c}$	$0.54^{b,d}$
L – Impulse	127	124	186^e	210	50^c	76
M – Impulse	85^e	84	97^e	116^f	$25^{a,c}$	38^d
S – Impulse	45^e	43	46^e	55^f	$14^{a,c}$	21^d
L – Duration (s)	6.36^e	6.50	4.64	4.43	3.40^a	3.67
M – Duration (s)	$4.49^{c,e}$	$4.15^{d,f}$	$2.37^{a,e}$	2.48^b	$1.60^{a,c}$	1.77^b
S – Duration (s)	$2.42^{c,e}$	$2.18^{d,f}$	$1.11^{a,e}$	1.20^b	$0.85^{a,c}$	0.92^b

Note: superscripts indicate significant differences between conditions at the Bonferroni adjusted significance level of 0.0056; mean torque and impulse are normalised to mh^2 (m =mass and h =height of COM)

Group mean values for movement correction analysis biased on forearm EMG are presented in table 4.8. No significant differences were found for movement correction analyses based on EMG activity between handstand with eyes open and handstand with eyes closed, whereas there were significant differences between these conditions based on torque data. This may be due to poor signal to noise ratios within the EMG data during balance trials, or it may be due to increased individual variations. More study is required to clarify this matter.

Table 4.8: Movement corrections based on wrist flexor/extensor EMG, with large, medium, and small (L, M, S) corrections based on EMG above 1, 2, and 3 SD respectively.

Variable	$EO_{(e)}$	$EC_{(f)}$
L - Corrections/s	0.75	0.88
M - Corrections/s	1.75	1.67
S - Corrections/s	2.20	2.41
L - RMS	0.56	0.61
M - RMS	0.53	0.59
S – RMS	0.51	0.55
L – Duration (s)	1.31	1.24
M – Duration (s)	0.55	0.52
S – Duration (s)	0.28	0.28

4.3. Summary

Analysis shows that COP signals contain a degree of deterministic structure, reinforcing the view that postural sway is not purely a random process. Variability is inherent within all biological systems and can be characterised as the normal changes that occur in motor performance across multiple repetitions of a task (Stergiou et al., 2004). Some COP signals may be considered to contain subtle structure in the form of time correlation information which may be extracted through advanced techniques (Riley et al., 1999). Nevertheless the relevance of such analyses within human balance remains questionable. Riley

et al. (1999) describe human balance as an under-constrained task, and suggest the use of advanced nonlinear analysis tools to unravel the mysteries within this complex system. It is unclear if these techniques are suitable for investigating balance tasks that, instead of being under-constrained, are in fact extremely challenging, such as handstand and single leg stance with eyes closed. A summary of each of the groups of balance measures used within the current research is presented in tables 4.9 to 4.12.

Data from this study suggests that the best balance metrics for distinguishing between each of the six conditions was the traditional balance measure of sway velocity. Sway velocity was able to distinguish between each posture, and between eyes open and eyes closed conditions in each posture. However, this measure cannoot provide any further information on the underlying process of balance.

Nonlinear measures of balance appear to offer insight into the underlying deterministic processes that control balance, offering measures of system determinism, complexity, and predictability. Unfortunately, using multiple measures can sometimes produce conflicting results, leaving much to the interpretation of the reader. Assessments of feedback time delay and movement corrections appear to provide both an insight into the control of posture and help distinguish one condition from another. In addition, both feedback time delay and movement corrections and magnitudes may be used simultaneously to delve further into the control of posture. Yeadon and Trewartha (2003) examined two-dimensional wrist, shoulder, and hip joint torques using the estimated delay method, and it should be an unproblematic process to transfer this to other joints or to three-dimensional analysis. Roncesvalles et al. (2001) examined movement units (corrections) across multiple joints during perturbed stance, and it would be a simple procedure to convert the method used here to examine unperturbed stance across multiple joints.

A disadvantage of both the assessment of feedback time delays and movement corrections is the increased complexity of data collection and data processing required in comparison to simple force plate measures. Nevertheless, several methods exist to calculate COM and ankle joint torque estimates from a single force plate recording (Benda et al., 1994; Kingma et al., 1995; Shimba, 1984). Such methods could be employed, with caution, to calculate both feedback time delay and movement units during single or double leg stance from a single force plate assessment.

The aim of this chapter was to examine how different balance metrics are expressed in different postures with and without vision, and to provide some insight into which balance metric is best for assessing balance within or between the different postures. The answer to this is not straightforward and will depend to some extent on the scope of the research. If the aim of a study is to assess balance performance, with no interest in the underlying postural control process, such as in an intervention study, then the traditional measure of sway velocity appears to be sufficient. If a researcher aims to delve further into the processes of postural control, more advanced analyses will be required. Although there is a growing number of studies within this area that are employing sophisticated nonlinear analysis methods, researchers must be clear in how these techniques inform on the underlying postural control process. Assessment of feedback time delay and movement corrections may offer more insight into this process. Further study may wish to combine these two tools and aim to provide insight into the nature of individual corrections, both with respect to incorporating estimates of feedback time delay and in attempting to classify these corrections into general or specific strategies used to maintain or regain balance.

CHAPTER 5

LEARNING TO BALANCE

The emergence of postural control has often been examined from the perspective of an infant learning to balance in standing (Roncesvalles et al., 2001). It is generally agreed that the development of postural control during the first decade of life is associated with the development of other motor competencies (Woollacott and Sveistrup, 1992; Roncesvalles et al., 2001; Sundermier et al., 2001). Young children learning to balance will be experiencing multiple developmental changes, such as: enhanced muscular strength, sensory calibration and exploration, and myelination of neurological pathways. It is unclear how these developmental changes may influence the emergence of postural control. Examining how individuals with a mature neurological system learn to balance in a novel task might provide some insight. This would require assessing neurologically sound adults in a balance task that is unfamiliar to them, and therefore could not be assessed in normal upright stance. One possible approach would be to assess how individuals learn to balance in inverted stance. The purpose of this chapter is to examine which balance metrics best characterise improvements in balance performance when a novice learns to balance in handstand.

5.1. Assessment of Balance

Thirteen subjects completed all parts of study one, where they were required to practice handstands three times a week for 10-15 minutes each session over a period of eight months. Subjects were tested once a month to examine performance in handstand along with various kinematic and kinetic variables. The inclusion criteria and data collection procedures were as described previously in Chapter 3.

If balance is viewed as a continuous skill, the amount of time an individual can maintain balance may be the best method for assessing balance in a novel task,

however, this will become less sensitive as balance improves. The previous chapter introduced a variety of balance metrics that have been employed by researchers to examine the postural control system in a variety of areas. The balance metrics described can be effective at differentiating between clinical and healthy populations, but it is unknown how sensitive these measures are to the subtle changes that occur while learning to balance.

The main criterion for assessing handstand performance was the duration that participants could maintain independent balance in the handstand position. All participants were unable to maintain independent balance in handstand for more than five seconds when attending the first assessment session. Short trials can result in spurious results from the various balance metrics previously described (Table 5.1), therefore only those trials that lasted longer than three seconds were used in the subsequent analysis. Movement corrections based on joint torques resulted in zero large, medium, and small corrections for more than half of the trials recorded above the three second threshold. Consequently, mean and maximum joint torques were calculated in its place for all subjects.

Table 5.1: All variables used to assess balance

Group	Variables	Number
Traditional	duration, standard deviation (SD), range, mean sway velocity (SV)	4
Nonlinear	sample entropy (SampEn), lyapunov exponent (LyE)	2
Recurrence Quantification Analysis	recurrence rate (RR), determinism (DET), entropy (ENT), divergence (DIV), trend (TND)	5
Estimated Delays	delay, R^2, proportional and derivative coefficients, torque percentages	12
Joint Torques	Mean and maximum joint torques [wrist, shoulder, hip]	6
Movement Corrections (EMG)	corrections per second, root mean square (RMS), burst duration [small, medium, large (S,M,L)]	9

Note: Estimated delays were calculated by two different methods and will be prefixed with M1 or M2 (M1 = Yeadon and Trewartha method)

5.1.1. Statistical Analysis

The relationship between each balance metric and the duration of the handstand trial was examined via linear and quadratic regressions, with a significance level of 0.05. All regressions were performed with each balance metric scaled to a range of ± 1, based on the maximum value from each metric, to assist in comparison of regression coefficients.

5.2. Findings and Discussion

Improvements in handstand performance were variable across the group, with some subjects making very little improvement over the eight month period (Table 5.2).

Table 5.2: Maximum duration in handstand for each assessment session.

Subject	Maximum Duration of Handstand Trial (seconds)								
	Test 0	Test 1	Test 2	Test 3	Test 4	Test 5	Test 6	Test 7	Test 8
1	1.2	1.7	1.5	3.4	5.8	8.9	5.1	7.6	9.7
2	2.3	8.6	5.6	12.0	11.8	13.1	5.7	7.5	10.3
3	1.0	2.1	2.2	3.0	3.8	3.6	4.8	2.1	3.2
4	2.6	N/A	11.5	N/A	10.0	6.0	N/A	12.4	11.3
5	1.4	1.8	8.2	9.1	3.3	5.4	11.2	11.2	7.7
6	1.1	9.3	30.7	13.4	10.9	21.1	23.7	13.8	15.2
7	2.1	2.2	3.3	3.4	3.4	4.7	4.6	5.0	4.2
8	1.6	3.1	3.5	3.9	5.9	9.3	N/A	13.2	None
9	2.7	8.1	12.1	16.7	23.4	25.6	27.5	28.5	36.0
10	4.4	4.4	5.9	11.9	20.2	34.7	28.7	44.5	28.2
11	None	1.0	1.1	1.8	1.7	N/A	2.3	N/A	3.2
12	None	2.6	7.3	10.9	9.9	13.1	11.5	14.5	9.7
13	None	1.2	1.5	2.7	2.7	2.5	3.2	1.9	2.2

Note: N/A = subject not available for the testing session on that occasion, but still continued to practice; None = subject started testing late, or left early, due to limited time.

Novice handstanders showed a large variation in balance performance based on all balance metrics, with practice and a longer duration in handstand this variability reduces. Large amounts of variation for handstand trials of short

duration make it extremely difficult to compare residual plots to determine if a linear or quadratic regression is more appropriate. In addition, these large variations result in poor R^2 values, indicating all variables will be poor predictors of handstand performance. Nevertheless, regressions were used to discover general trends within the data, not predictions, and they may be interpreted with caution for this purpose. Subjects 11 and 13 were only able to perform one handstand trial that lasted longer than the three second threshold, resulting in 11 subjects that were used for further analysis. Only subjects six, nine, and ten managed to maintain balance in handstand for more than 30 seconds. All subsequent scatter plots displaying the relationship between handstand duration and each balance metric will highlight subjects six, nine, and ten to help determine if these subjects have skewed the relationships presented.

5.2.1. Traditional Measures of Balance

Linear and quadratic regressions between the duration of handstand trials and each traditional balance measure show significant p values for sway range (Tables 5.3 to 5.5). Comparing p values and R^2 values from linear and quadratic regressions indicates that a quadratic regression model may be an appropriate fit for sway range.

Table 5.3: Linear and quadratic regressions for the relationships between handstand duration and each traditional measure of balance (scaled to ± 1).

Variable	Linear Regression		Quadratic Regression	
	Adjusted R^2	p value	Adjusted R^2	p value
SD	0.0000	0.7582	0.0314	0.0034
Range	0.0429	0.0002	0.0969	0.0000
SV	0.0018	0.2165	0.0068	0.1363

Table 5.4: Linear regression coefficients for the relationships between handstand duration and each traditional measure of balance (scaled to ± 1).

Variable	C_1	C_2	Adjusted R^2	p value
SD	0.5517	0.0004	0.0000	0.7582
Range	0.5510	0.0044	0.0429	0.0002
SV	0.5624	0.0016	0.0018	0.2165

Note: C_1 = intercept coefficient; C_2 = slope coefficient

Table 5.5: Quadratic regression coefficients for the relationships between handstand duration and each traditional measure of balance (scaled to ± 1).

Variable	C_1	C_2	C_3	Adjusted R^2	p value
SD	0.4907	0.0125	-0.0004	0.0314	0.0034
Range	0.4825	0.0180	-0.0004	0.0969	0.0000
SV	0.5334	0.0074	-0.0002	0.0068	0.1363

Note: C_1 = intercept coefficient; C_2 = slope coefficient; C_3 = squared coefficient

Quadratic regression coefficients show negative squared terms and positive linear terms for sway range, suggesting an initial increase for trials of short duration before reducing again for trials of longer durations (Figure 5.1).

All scatter plots show large variation in the values from each traditional balance measure for handstand trials of short duration. It seems likely that all regressions are effected by subjects six, nine, and ten, however, these subjects have a similar range of variance to other subjects for trials of short duration.
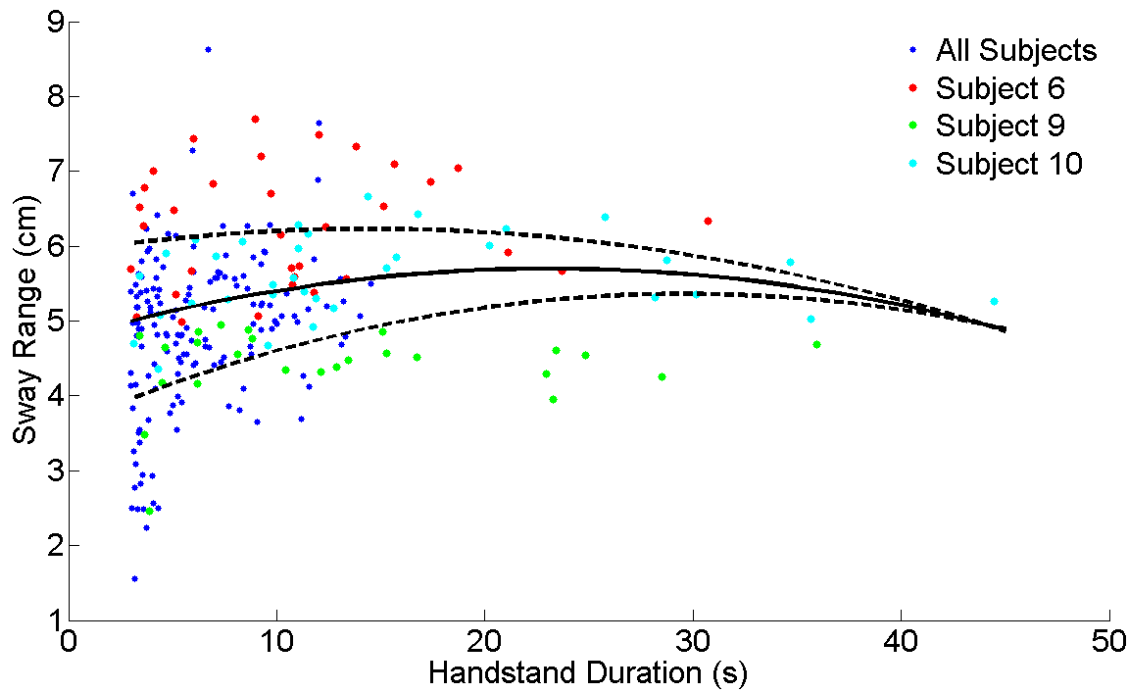
Figure 5.1: Scatter plot of handstand duration to sway range, with a quadratic regression fit (bold line) ± 1 SD for each five second time bin (dotted lines); the three best subjects are indicated by the red, green, and cyan coloured markers.

When first learning to balance in handstand it appears as though subjects display large variations in handstand performance based on either trial duration or traditional measures of balance. With increased competence in handstand balance, as described by longer trial durations, sway range decrease after an initial increase. However, changes in sway range are subtle and generally remain within the variance from multiple trials. These large variations make it difficult to use any of the traditional measures of balance to characterise improvements in balance performance in handstand.

5.2.2. Nonlinear Measures of Balance

Linear and quadratic regressions between the duration of handstand trials and each nonlinear measure of balance show significant p values for: sample entropy (SampEn), recurrence rate (RR), determinism (DET), entropy (ENT), divergence (DIV), and trend (TND) (Tables 5.6 to 5.8). Comparing p values and R^2 values from linear and quadratic regressions indicates that a linear regression model is an appropriate fit for SampEn, but a quadratic regression model may be a more appropriate fit for RR, DET, ENT, DIV and TND.

Table 5.6: Linear and Quadratic regressions for the relationships between handstand duration and each nonlinear measure of balance (scaled to ± 1).

	Linear Regression		Quadratic Regression	
Variable	Adjusted R^2	p value	Adjusted R^2	p value
SampEn	0.0533	0.0000	0.0505	0.0002
LyE	0.0000	0.6409	0.0000	0.8654
RR	0.2648	0.0000	0.3467	0.0000
DET	0.0620	0.0000	0.0939	0.0000
ENT	0.1021	0.0000	0.2195	0.0000
DIV	0.1493	0.0000	0.2251	0.0000
TND	0.2986	0.0000	0.5259	0.0000

Table 5.7: Linear regressions coefficients for the relationships between handstand duration and each nonlinear measure of balance (scaled to ± 1).

Variable	C_1	C_2	Adjusted R^2	p value
SampEn	0.2440	0.0050	0.0533	0.0000
LyE	0.0420	0.0005	0.0000	0.6409
RR	0.2895	-0.0109	0.2648	0.0000
DET	0.9978	-0.0001	0.0620	0.0000
ENT	0.3595	0.0114	0.1021	0.0000
DIV	0.3376	-0.0133	0.1493	0.0000
TND	-0.3307	0.0176	0.2986	0.0000

Note: C_1 = intercept coefficient; C_2 = slope coefficient

Table 5.8: Quadratic regressions coefficients for the relationships between handstand duration and each nonlinear measure of balance (scaled to ± 1).

Variable	C_1	C_2	C_3	Adjusted R^2	p value
SampEn	0.2380	0.0061	0.0000	0.0505	0.0002
LyE	0.0383	0.0012	0.0000	0.0000	0.8654
RR	0.3749	-0.0277	0.0005	0.3467	0.0000
DET	0.9969	0.0001	0.0000	0.0939	0.0000
ENT	0.1910	0.0448	-0.0010	0.2195	0.0000
DIV	0.4812	-0.0402	0.0008	0.2251	0.0000
TND	-0.5458	0.0599	-0.0013	0.5259	0.0000

Note: C_1 = intercept coefficient; C_2 = slope coefficient; C_3 = squared coefficient

Similar to the findings from the traditional measures of balance, there is a large amount of variation in the values from each nonlinear measure of balance for handstand trials of short duration. In addition, subjects six, nine, and ten have a similar range of variance to other subjects for trials of short duration.

Linear regression coefficients show SampEn generally increases as time in handstand increases (Figure 5.2). Quadratic regression coefficients show negative squared terms and positive linear terms for ENT and TND, but positive squared terms and negative linear terms for RR and DIV. Further inspection of scatter plots (Figures 5.3 and 5.5) show that the cause for a possible quadratic relationship is likely due to a ceiling effect with TND and a floor effect with DIV. A quadratic model is unlikely to be an appropriate fit for TND and DIV, so data were re-analysed using an exponential fit, giving an adjusted R^2 of 0.77 for TND (Figure 5.4) and an adjusted R^2 of 0.26 for DIV (Figure 5.6).
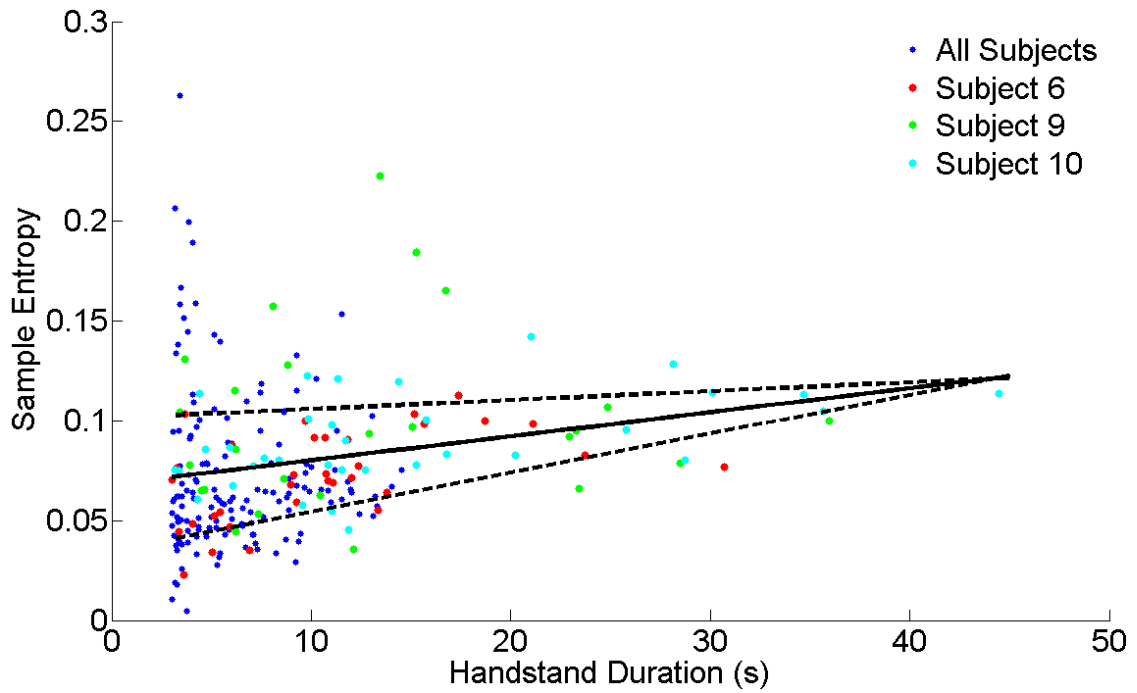
Figure 5.2: Scatter plot of handstand duration to sample entropy, with a linear regression fit (bold line) ± 1 SD for each five second time bin (dotted lines); the three best subjects are indicated by the red, green, and cyan coloured markers.
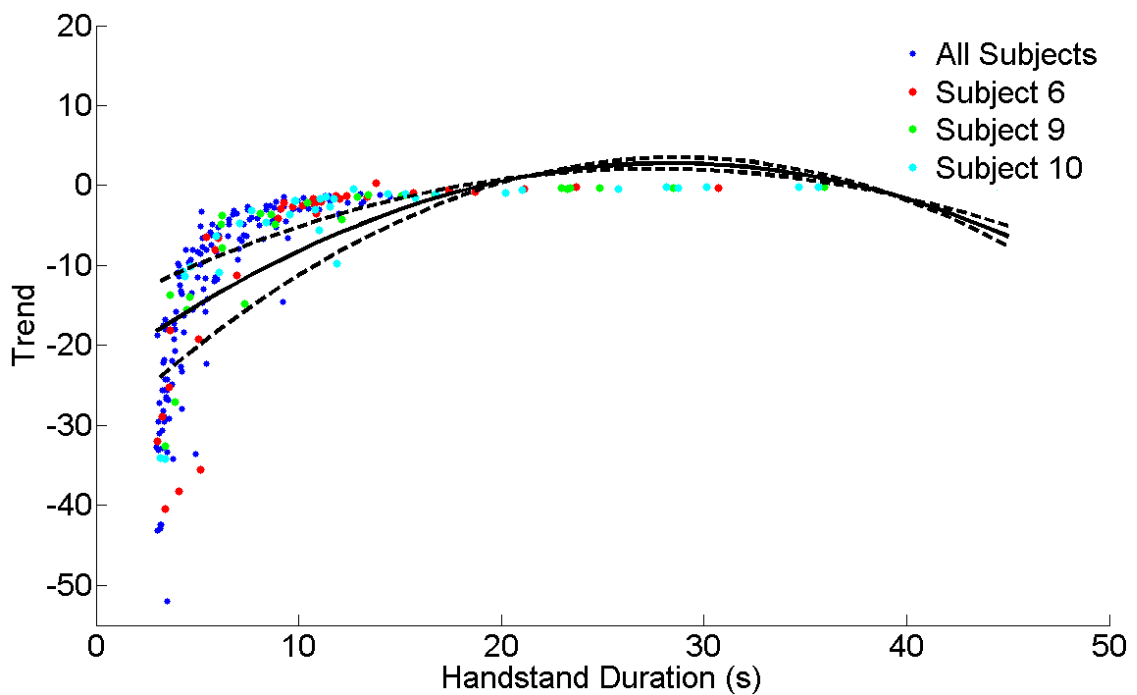
Figure 5.3: Scatter plot of handstand duration to trend, with a quadratic regression fit (bold line) ± 1 SD for each five second time bin (dotted lines); the three best subjects are indicated by the red, green, and cyan coloured markers.

127
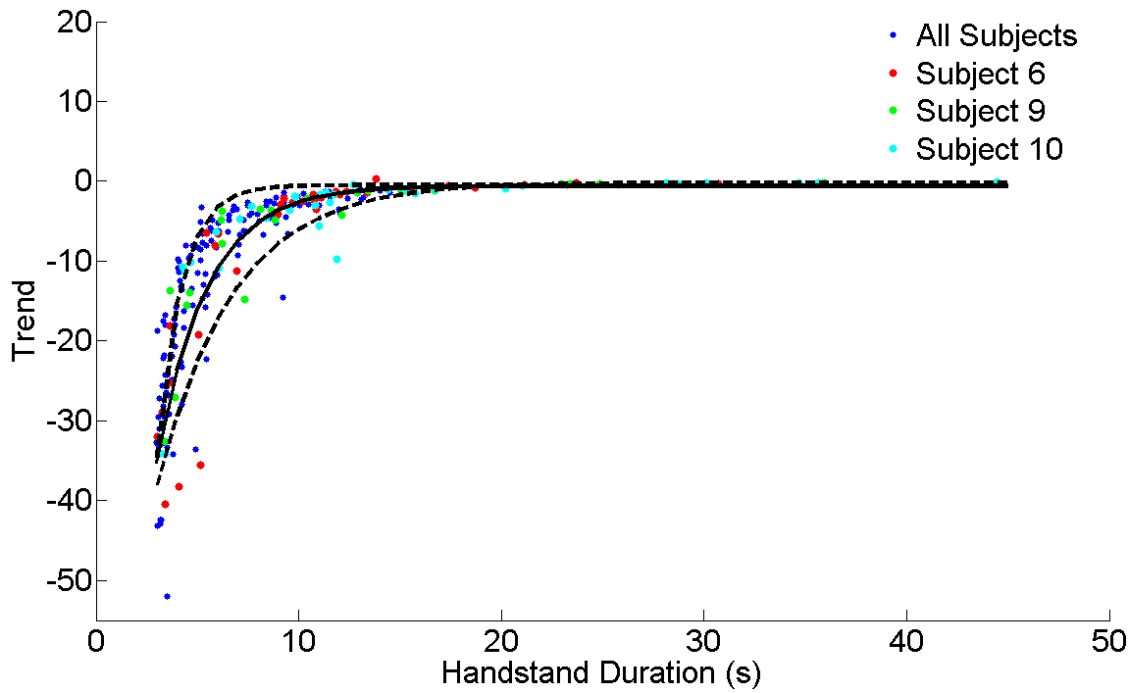
Figure 5.4: Scatter plot of handstand duration to trend, with an exponential curve fit (bold line) ± 1 SD for each five second time bin (dotted lines); the three best subjects are indicated by the red, green, and cyan coloured markers.

Figure 5.5: Scatter plot of handstand duration to divergence, with a quadratic regression fit (bold line) ± 1 SD for each five second time bin (dotted lines); the three best subjects are indicated by the red, green, and cyan coloured markers.
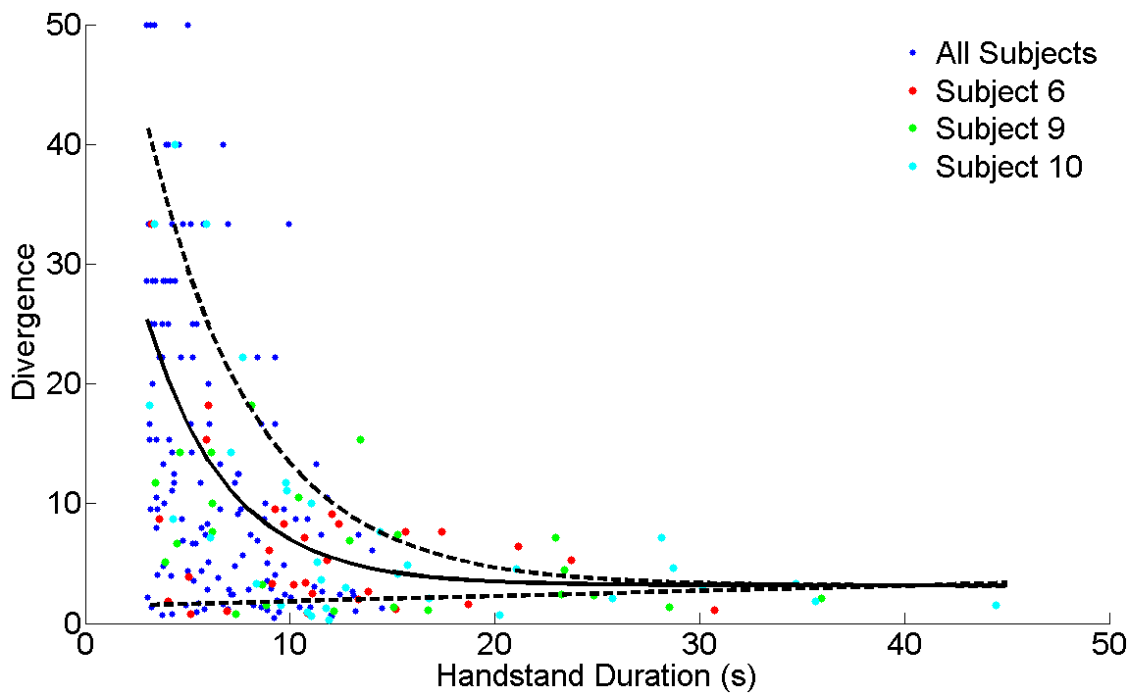
Figure 5.6: Scatter plot of handstand duration to divergence, with an exponential curve fit (bold line) ± 1 SD for each five second time bin (dotted lines); the three best subjects are indicated by the red, green, and cyan coloured markers.

Generally lower values for TND in handstand trials of short duration suggest large amounts of nonstationarity in postural control, which reduces to levels comparable to experienced handstanders with trial durations of more than 15 seconds (Figures 5.3 and 5.4). Likewise, larger values for DIV in handstand trials of short duration suggest large amounts of local divergence in COP trajectories (Figures 5.5 and 5.6). DIV appears to remain above experienced handstanders values until trials of more than 20 to 30 seconds duration. When learning to balance in handstand nonlinear measures of balance display large amounts of variation, similar to those seen in traditional measures of balance. With increased competence in handstand balance, as described by longer trial durations, this variance appears to reduce quicker in some nonlinear measures of balance than in the traditional measures. It may be that more pronounced changes in nonlinear measures represent changes in the subjects' underlying process of postural control, whereas less pronounced changes in traditional measures relate more to their general ability or performance in the balance task.

5.2.3. Estimated Feedback time Delay

Linear and quadratic regressions between the duration of handstand trials and estimates of feedback time delay show significant p values for: estimates of feedback time delay, R^2 value, and the proportional coefficient from the Yeadon and Trewartha method; and the passive stiffness coefficient, the derivative coefficient, and the percentage of joint torque estimated by each of the three coefficients from the adapted model (Tables 5.9 to 5.11).

Table 5.9: Linear and Quadratic regressions for the relationships between handstand duration and estimates of feedback time delay (scaled to ± 1), from the Yeadon and Trewartha method (M1) and the adapted method (M2).

	Linear Regression		Quadratic Regression	
Variable	Adjusted R^2	p value	Adjusted R^2	p value
M1 Delay (ms)	0.0210	0.0087	0.0407	0.0012
M1 R^2	0.0067	0.0900	0.0162	0.0387
M1 p coefficient	0.0530	0.0001	0.0862	0.0000
M1 d coefficient	0.0000	0.7453	0.0000	0.9479
M1 p torque (%)	0.0000	0.3186	0.0139	0.0531
M1 d torque (%)	0.0000	0.3186	0.0139	0.0531
M2 Delay (ms)	0.0044	0.1377	0.0059	0.1647
M2 R^2	0.0000	0.9828	0.0000	0.8944
M2 p_1 coefficient	0.0936	0.0000	0.1346	0.0000
M2 p_2 coefficient	0.0000	0.9115	0.0000	0.7208
M2 d coefficient	0.0126	0.0344	0.0169	0.0354
M2 p_1 torque (%)	0.0648	0.0000	0.0966	0.0000
M2 p_2 torque (%)	0.0626	0.0000	0.0935	0.0000
M2 d torque (%)	0.0177	0.0152	0.0234	0.0145

Table 5.10: Linear regression coefficients for the relationships between handstand duration and estimates of feedback time delay (scaled to ± 1), from the Yeadon and Trewartha method (M1) and the adapted method (M2).

Variable	C_1	C_2	Adjusted R^2	p value
M1 Delay (ms)	0.3892	0.0035	0.0210	0.0087
M1 R^2	0.7917	0.0016	0.0067	0.0900
M1 p coefficient	0.4193	-0.0063	0.0530	0.0001
M1 d coefficient	0.3861	-0.0004	0.0000	0.7453
M1 p torque (%)	0.0330	-0.0013	0.0000	0.3186
M1 d torque (%)	0.0021	0.0012	0.0000	0.3186
M2 Delay (ms)	0.2836	-0.0019	0.0044	0.1377
M2 R^2	0.7995	0.0000	0.0000	0.9828
M2 p_1 coefficient	0.1814	-0.0080	0.0936	0.0000
M2 p_2 coefficient	0.2856	-0.0002	0.0000	0.9115
M2 d coefficient	0.4081	0.0035	0.0126	0.0344
M2 p_1 torque (%)	0.1527	-0.0069	0.0648	0.0000
M2 p_2 torque (%)	0.2134	0.0087	0.0626	0.0000
M2 d torque (%)	0.1818	0.0028	0.0177	0.0152

Table 5.11: Quadratic regression coefficients for the relationships between handstand duration and estimates of feedback time delay (scaled to ± 1), from the Yeadon and Trewartha method (M1) and the adapted method (M2).

Variable	C_1	C_2	C_3	Adjusted R^2	p value
M1 Delay (ms)	0.3406	0.0132	-0.0003	0.0407	0.0012
M1 R^2	0.7665	0.0066	-0.0002	0.0162	0.0387
M1 p coefficient	0.4903	-0.0205	0.0004	0.0862	0.0000
M1 d coefficient	0.3853	-0.0003	0.0000	0.0000	0.9479
M1 p torque (%)	0.0729	-0.0092	0.0002	0.0139	0.0531
M1 d torque (%)	-0.0364	0.0089	-0.0002	0.0139	0.0531
M2 Delay (ms)	0.3053	-0.0062	0.0001	0.0059	0.1647
M2 R^2	0.7939	0.0011	0.0000	0.0000	0.8944
M2 p_1 coefficient	0.2587	-0.0232	0.0005	0.1346	0.0000
M2 p_2 coefficient	0.3060	-0.0042	0.0001	0.0000	0.7208
M2 d coefficient	0.3728	0.0105	-0.0002	0.0169	0.0354
M2 p_1 torque (%)	0.2227	-0.0208	0.0004	0.0966	0.0000
M2 p_2 torque (%)	0.1246	0.0263	-0.0005	0.0935	0.0000
M2 d torque (%)	0.1559	0.0079	-0.0002	0.0234	0.0145

A comparison of p values and R^2 values from linear and quadratic regressions indicate that a quadratic regression model may be the most appropriate fit for all significant variables.

Quadratic regression coefficients show negative squared terms and positive linear terms for estimates of feedback time delay and the R^2 values from the Yeadon and Trewartha method. Similarly, quadratic regression coefficients show negative squared terms and positive linear terms for estimates of joint torques based on proportional and derivative coefficients of delayed COM motion from the adapted method (Figures 5.9 and 5.11). Quadratic regression coefficients show positive squared terms and negative linear terms for

estimates of joint torques based on a passive stiffness component from the adapted method, estimated from COM motion with zero delay (Figure 5.7). Further inspection of scatter plots of the percentage of torque from a passive stiffness component (Figure 5.7) and the percentage of torque from delayed COM displacement (Figure 5.9) show data begins to plateau for handstands of more than 15 seconds duration. A quadratic model is unlikely to be an appropriate fit, so data were re-analysed using an exponential fit, giving an adjusted R^2 of 0.12 for the percentage of torque from a passive stiffness component (Figure 5.8) and an adjusted R^2 of 0.13 for the percentage of torque from delayed COM displacement (Figure 5.10).
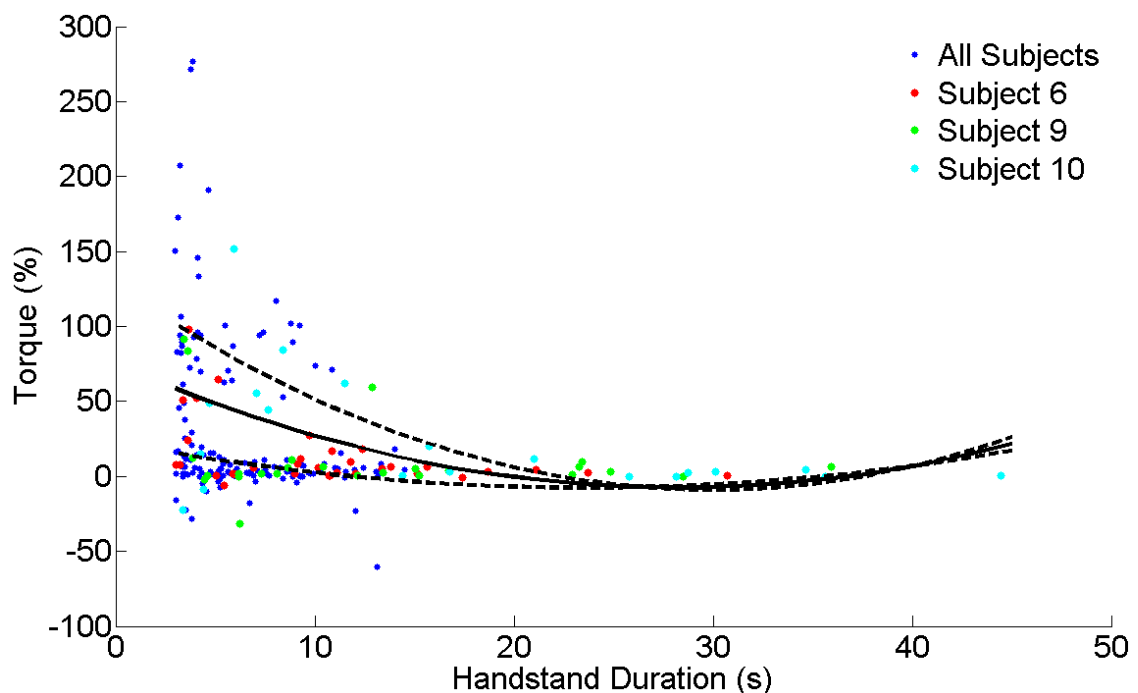
Figure 5.7: Scatter plot of handstand duration to the torque estimated from passive stiffness (p_1) from the adapted method, with a quadratic regression fit (bold line) ± 1 SD for each five second time bin (dotted lines); the three best subjects are indicated by the red, green, and cyan coloured markers.
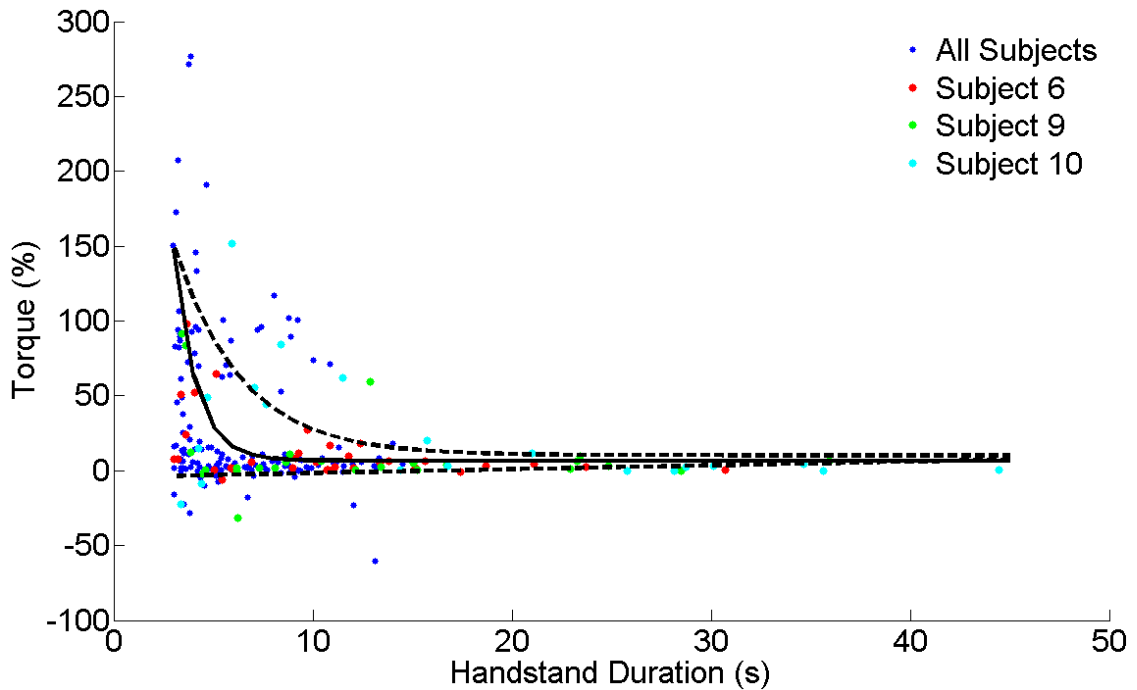
Figure 5.8: Scatter plot of handstand duration to the torque estimated from passive stiffness (p_1) from the adapted method, with an exponential curve fit (bold line) ± 1 SD for each five second time bin (dotted lines); the three best subjects are indicated by the red, green, and cyan coloured markers.
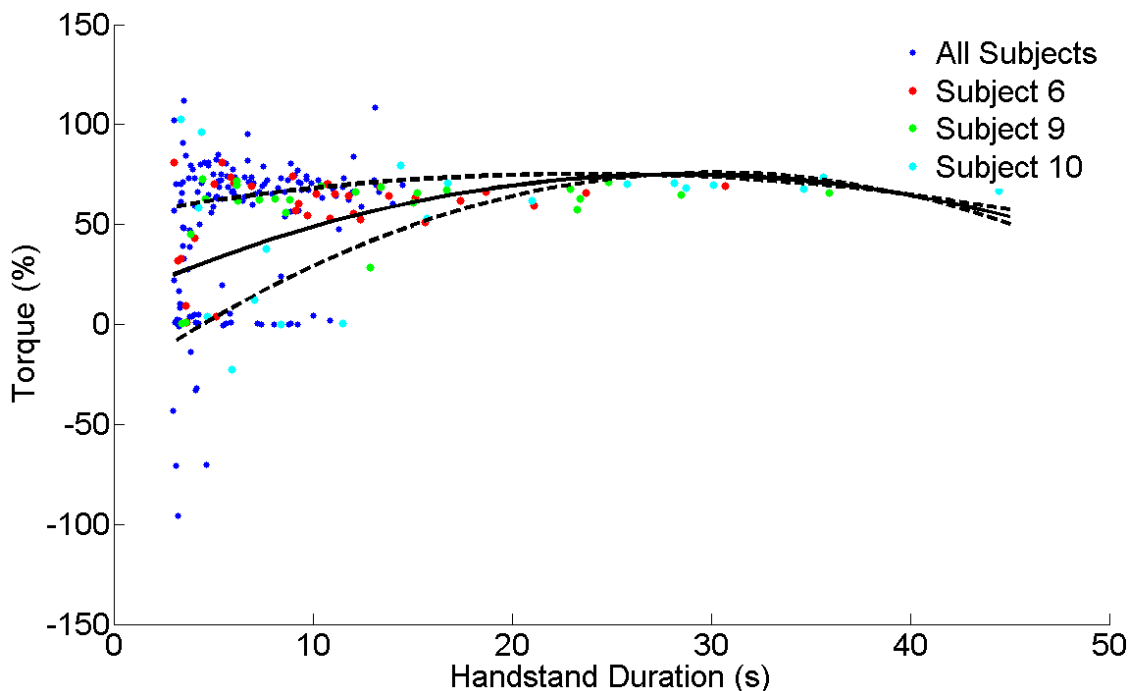
Figure 5.9: Scatter plot of handstand duration to the torque estimated from delayed COM displacement (p_2) from the adapted method, with a quadratic regression fit (bold line) ± 1 SD for each five second time bin (dotted lines); the three best subjects are indicated by the red, green, and cyan coloured markers.
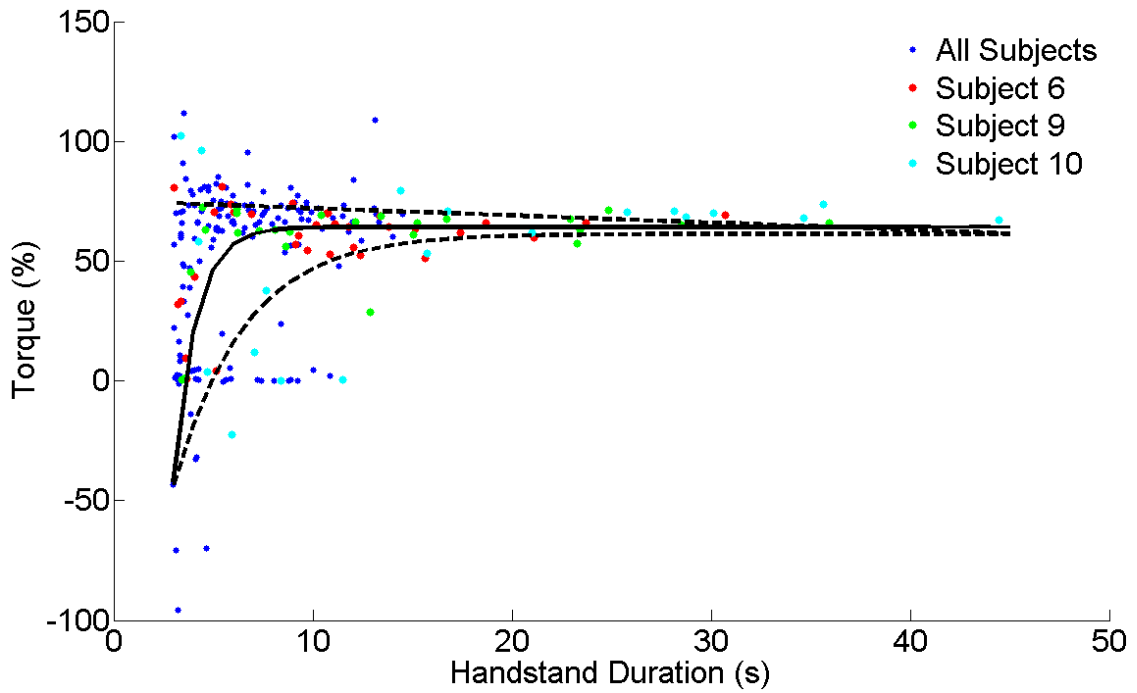
Figure 5.10: Scatter plot of handstand duration to the torque estimated from delayed COM displacement (p_2) from the adapted method, with an exponential curve fit (bold line) ± 1 SD for each five second time bin (dotted lines); the three best subjects are indicated by the red, green, and cyan coloured markers.
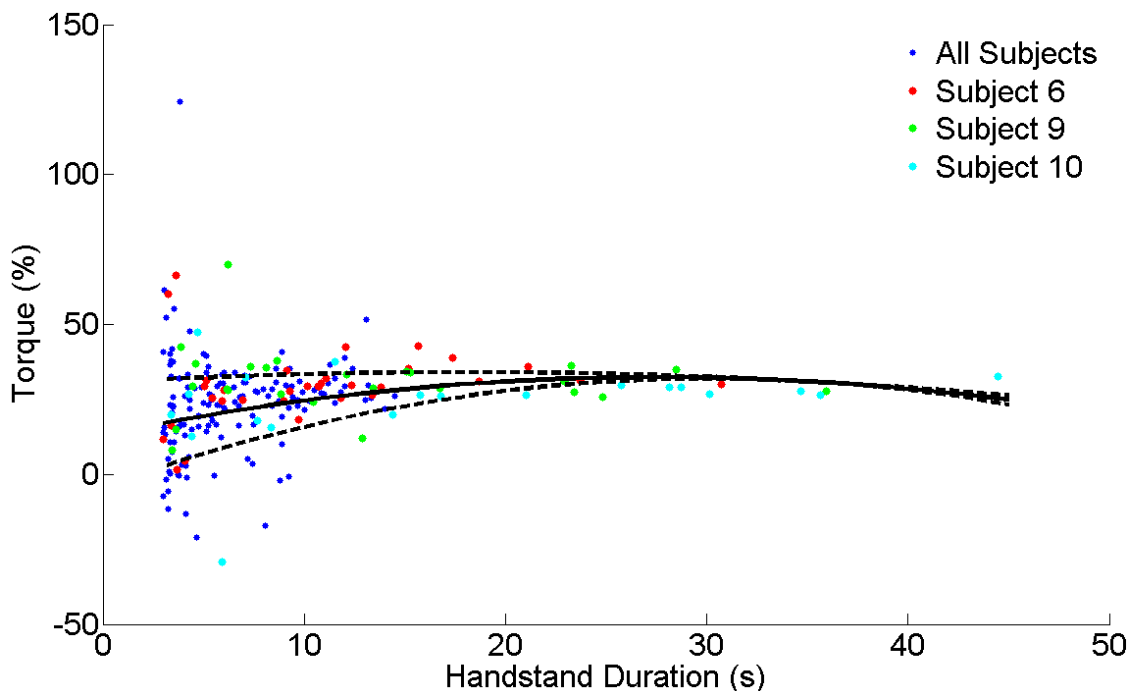
Figure 5.11: Scatter plot of handstand duration to the torque estimated from delayed COM velocity (d) from the adapted method, with a quadratic regression fit (bold line) ± 1 SD for each five second time bin (dotted lines); the three best subjects are indicated by the red, green, and cyan coloured markers.

Once again, data shows there is a large amount of variation in the estimates of feedback time delay for handstand trials of short duration. In addition, subjects six, nine, and ten have a similar range of variance to other subjects for trials of short duration. Data suggests that the regression models of balance may be a poor estimate of the postural control strategies employed when novices first learn to balance. With increased competence in handstand balance, as described by longer trial durations, regression models appear to become more applicable, suggesting subjects begin to adapt a strategy that is close to the one suggested by the regression model. With increased competence in handstand the amount of torque estimated from a passive stiffness mechanism generally decreases (Figures 5.7 and 5.8), whereas the amount of torque from delayed COM displacements and velocities generally increase (Figures 5.9 to 5.11). Estimates of torque contributions begin to plateau and resemble experienced handstanders for handstand trials above 15 to 20 seconds duration. Changes in torque contribution estimates may suggest that subjects are beginning to rely more on sensory feedback for postural control.

5.2.4. Movement Corrections

Linear and quadratic regressions between the duration of handstand trials and mean and maximum joint torques show significant p values for: mean wrist torque, mean hip torque, and maximum wrist torque (Tables 5.12 to 5.14). A comparison of p values and R^2 values from linear and quadratic regressions indicate that a linear regression model may be an appropriate fit for maximum wrist torque, but a quadratic regression model may be the most appropriate fit for mean wrist torque and mean hip torque. Linear regression coefficients show maximum wrist torques generally increase as time in handstand increases (Figure 5.13). Quadratic regression coefficients show positive squared terms and negative linear terms for mean wrist torque (Figure 5.12), but negative squared terms and positive linear terms for mean hip torque.

Table 5.12: Linear and Quadratic regressions for the relationships between handstand duration and mean/maximum joint torques (scaled to ± 1).

	Linear Regression		Quadratic Regression	
Variable	R^2	p value	Adjusted R^2	p value
Mean Wrist	0.0088	0.0632	0.0176	0.0314
Mean Shoulder	0.0034	0.1640	0.0143	0.0502
Mean Hip	0.0003	0.2978	0.0243	0.0121
Max Wrist	0.0436	0.0003	0.0436	0.0007
Max Shoulder	0.0000	0.8975	0.0009	0.3238
Max Hip	0.0000	0.9216	0.0000	0.7076

Table 5.13: Linear regression coefficients for the relationships between handstand duration and mean/maximum joint torques (scaled to ± 1).

Variable	C_1	C_2	Adjusted R^2	p value
Mean Wrist	0.4632	0.0028	0.0088	0.0632
Mean Shoulder	0.2315	0.0043	0.0034	0.1640
Mean Hip	-0.3784	0.0026	0.0003	0.2978
Max Wrist	0.6176	0.0049	0.0436	0.0003
Max Shoulder	0.0767	0.0002	0.0000	0.8975
Max Hip	0.0990	-0.0001	0.0000	0.9216

Table 5.14: Quadratic regression coefficients for the relationships between handstand duration and mean/maximum joint torques (scaled to ± 1).

Variable	C_1	C_2	C_3	Adjusted R^2	p value
Mean Wrist	0.5029	-0.0051	0.0002	0.0176	0.0314
Mean Shoulder	0.1446	0.0217	-0.0005	0.0143	0.0502
Mean Hip	-0.4743	0.0217	-0.0006	0.0243	0.0121
Max Wrist	0.5987	0.0087	-0.0001	0.0436	0.0007
Max Shoulder	0.0504	0.0054	-0.0002	0.0009	0.3238
Max Hip	0.0847	0.0027	-0.0001	0.0000	0.7076
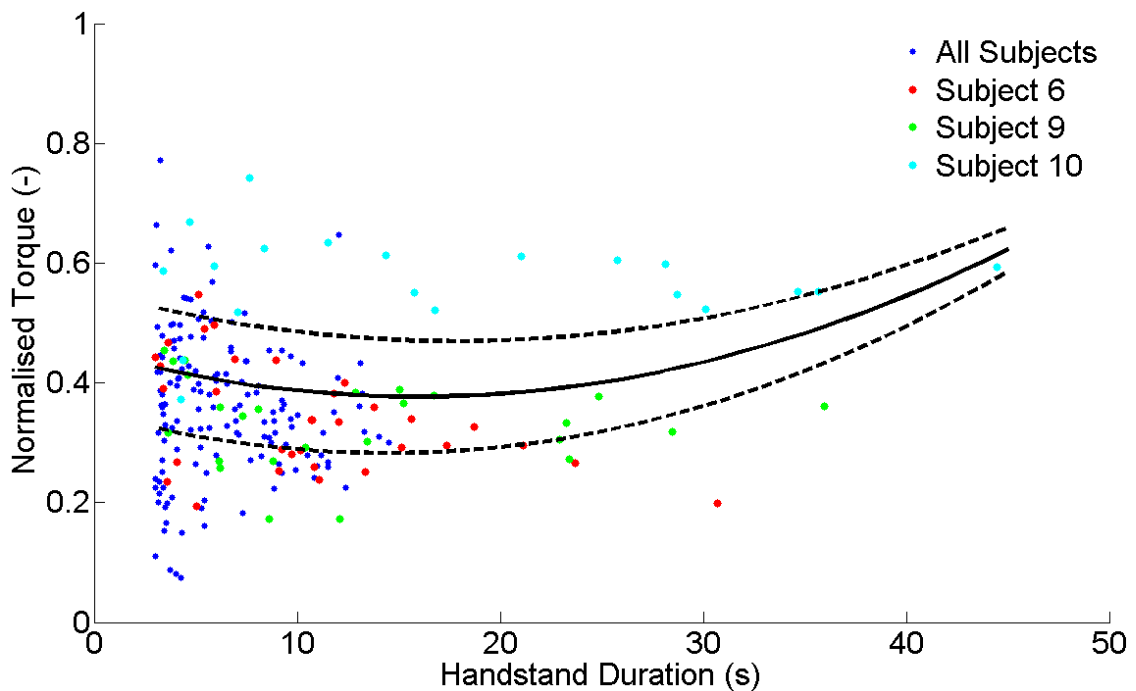
Figure 5.12: Scatter plot of handstand duration to mean wrist torque, with a quadratic regression fit (bold line) ± 1 SD for each five second time bin (dotted lines); the three best subjects are indicated by the red, green, and cyan coloured markers.
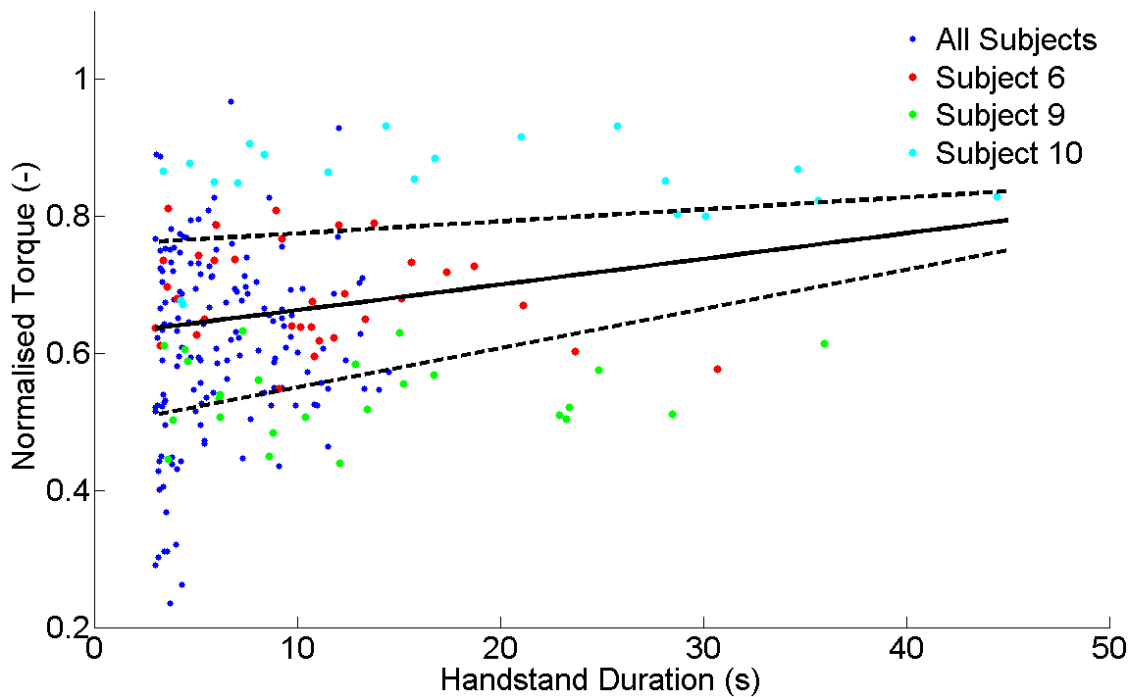
Figure 5.13: Scatter plot of handstand duration to maximum wrist torque, with a linear regression fit (bold line) ± 1 SD for each five second time bin (dotted lines); the three best subjects are indicated by the red, green, and cyan coloured markers.

Regression coefficients suggest subjects generally increase the wrist torque, and therefore the position of the COP relative to the wrist joint, as time in handstand increases. This may indicate that with increased handstand performance subjects gradually become more reliant on a wrist mechanism for postural control, with reducing hip torques suggesting less reliance on a hip mechanism. However, scatter plots show that subject ten has generally larger mean and maximum wrist torques than other subjects. Additional regressions with subject ten removed show both mean and maximum wrist torques are no longer significant at the 0.05 level (Figures 5.14 and 5.15).
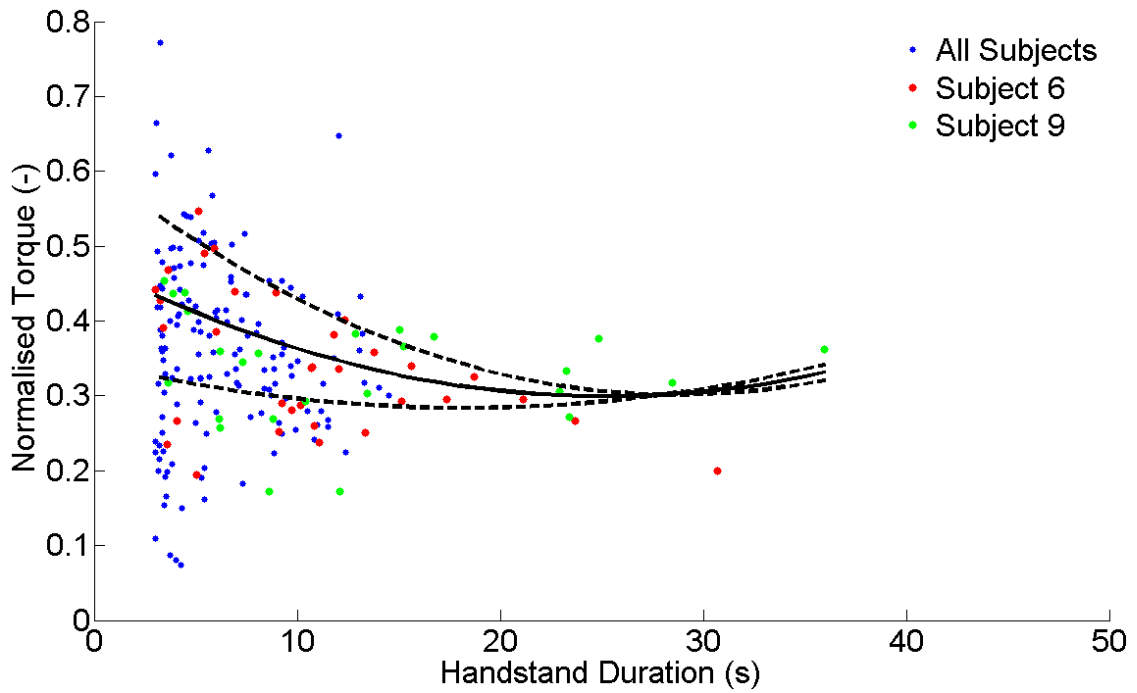
Figure 5.14: Scatter plot of handstand duration to mean wrist torque, with a quadratic regression fit (bold line) ± 1 SD for each five second time bin (dotted lines); the subjects six and nine are indicated by the red and green coloured markers, subject ten has been removed.
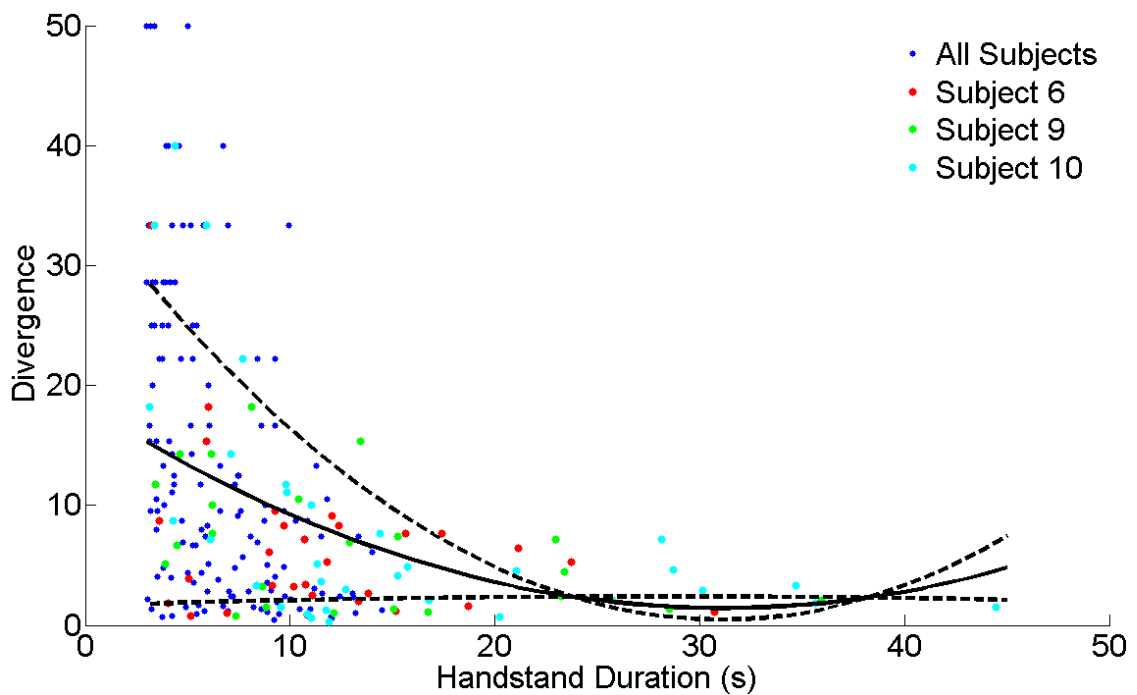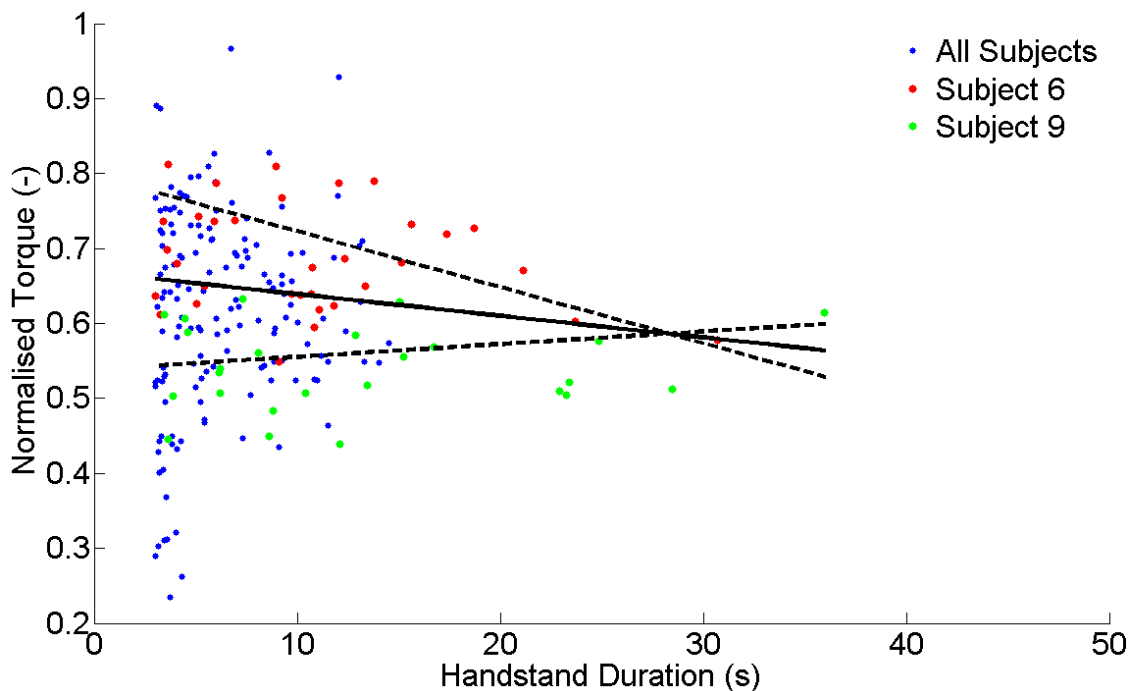

Figure 5.15: Scatter plot of handstand duration to maximum wrist torque, with a linear regression fit (bold line) ± 1 SD for each five second time bin (dotted lines); the subjects six and nine are indicated by the red and green coloured markers, subject ten has been removed.

Linear and quadratic regressions between the duration of handstand trials and movement correction values based on wrist EMG show significant p values for: the number of corrections per second and the duration of EMG bursts for large, medium, and small movement corrections (Tables 5.15 to 5.17). A comparison of p values and R^2 values from linear and quadratic regressions indicate that a quadratic regression model may be the most appropriate fit for all significant variables. Quadratic regression coefficients show positive squared terms and negative linear terms for the number of corrections per second (Figures 5.16 and 5.17), but negative squared terms and positive linear terms for the duration of EMG bursts (Figure 5.18). Regression coefficients suggest subjects generally decrease the number of corrections per second as time in handstand increases, while also increasing the duration of each EMG burst of activity. The number of corrections per second generally approaches that of experienced handstanders with handstand durations above 15 to 20 seconds.

Table 5.15: Linear and Quadratic regressions for the relationships between handstand duration and wrist EMG based movement correction values (scaled to ± 1), for large, medium, and small (L, M, S) corrections based on EMG above 1, 2, and 3 SD respectively.

	Linear Regression		Quadratic Regression	
Variable	Adjusted R^2	p value	Adjusted R^2	p value
L - Corrections/s	0.2531	0.0000	0.3636	0.0000
M - Corrections/s	0.1974	0.0000	0.3111	0.0000
S - Corrections/s	0.1416	0.0000	0.2503	0.0000
L - RMS	0.0000	0.8827	0.0000	0.9567
M - RMS	0.0001	0.3140	0.0000	0.4330
S – RMS	0.0000	0.6095	0.0000	0.5465
L – Duration (s)	0.4848	0.0000	0.5270	0.0000
M – Duration (s)	0.3211	0.0000	0.4592	0.0000
S – Duration (s)	0.1906	0.0000	0.3071	0.0000

Table 5.16: Linear regression coefficients for the relationships between handstand duration and wrist EMG based movement correction values (scaled to ± 1), for large, medium, and small (L, M, S) corrections based on EMG above 1, 2, and 3 SD respectively.

Variable	C_1	C_2	Adjusted R^2	p value
L - Corrections/s	0.4905	-0.0187	0.2531	0.0000
M - Corrections/s	0.5078	-0.0117	0.1974	0.0000
S - Corrections/s	0.6280	-0.0100	0.1416	0.0000
L - RMS	0.4422	0.0002	0.0000	0.8827
M - RMS	0.4665	-0.0014	0.0001	0.3140
S – RMS	0.4102	0.0009	0.0000	0.6095
L – Duration (s)	0.0754	0.0182	0.4848	0.0000
M – Duration (s)	0.2259	0.0128	0.3211	0.0000
S – Duration (s)	0.4411	0.0098	0.1906	0.0000

Table 5.17: Quadratic regression coefficients for the relationships between handstand duration and wrist EMG based movement correction values (scaled to ± 1), for large, medium, and small (L, M, S) corrections based on EMG above 1, 2, and 3 SD respectively.

Variable	C_1	C_2	C_3	Adjusted R^2	p value
L - Corrections/s	0.6752	-0.0559	0.0012	0.3636	0.0000
M - Corrections/s	0.6398	-0.0375	0.0008	0.3111	0.0000
S - Corrections/s	0.7474	-0.0333	0.0007	0.2503	0.0000
L - RMS	0.4358	0.0015	0.0000	0.0000	0.9567
M - RMS	0.4839	-0.0048	0.0001	0.0000	0.4330
S – RMS	0.3862	0.0056	-0.0001	0.0000	0.5465
L – Duration (s)	-0.0057	0.0345	-0.0005	0.5270	0.0000
M – Duration (s)	0.1011	0.0372	-0.0007	0.4592	0.0000
S – Duration (s)	0.3369	0.0301	-0.0006	0.3071	0.0000
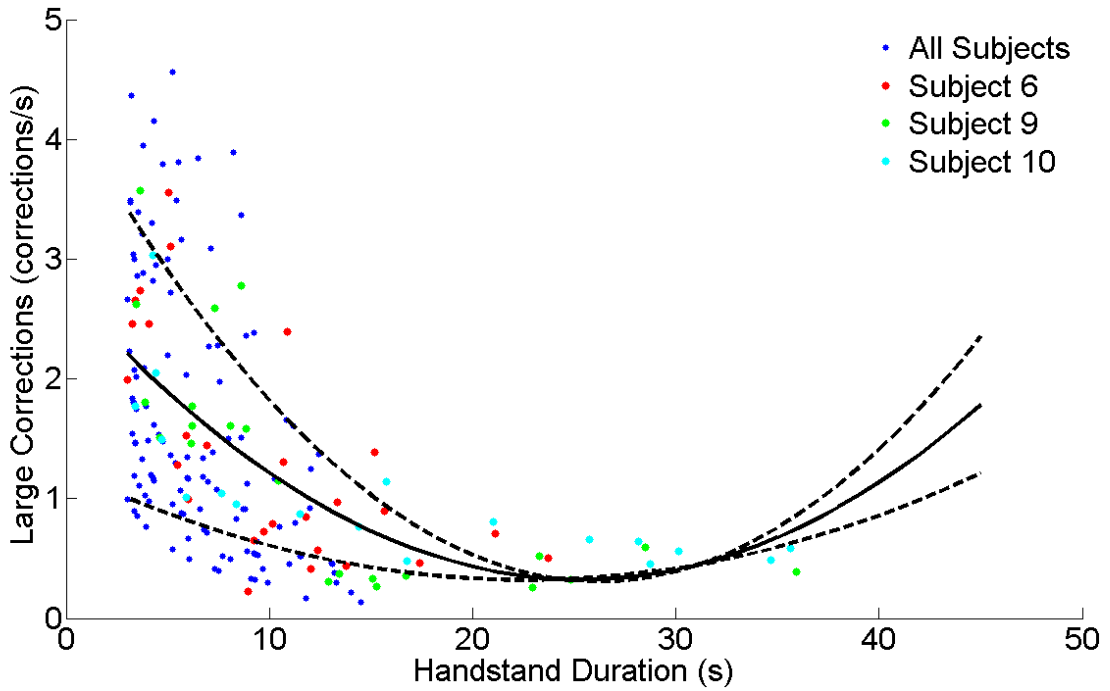
Figure 5.16: Scatter plot of handstand duration to the number of large corrections per second based on wrist EMG activity, with a quadratic regression fit (bold line) ± 1 SD for each five second time bin (dotted lines); the three best subjects are indicated by the red, green, and cyan coloured markers.
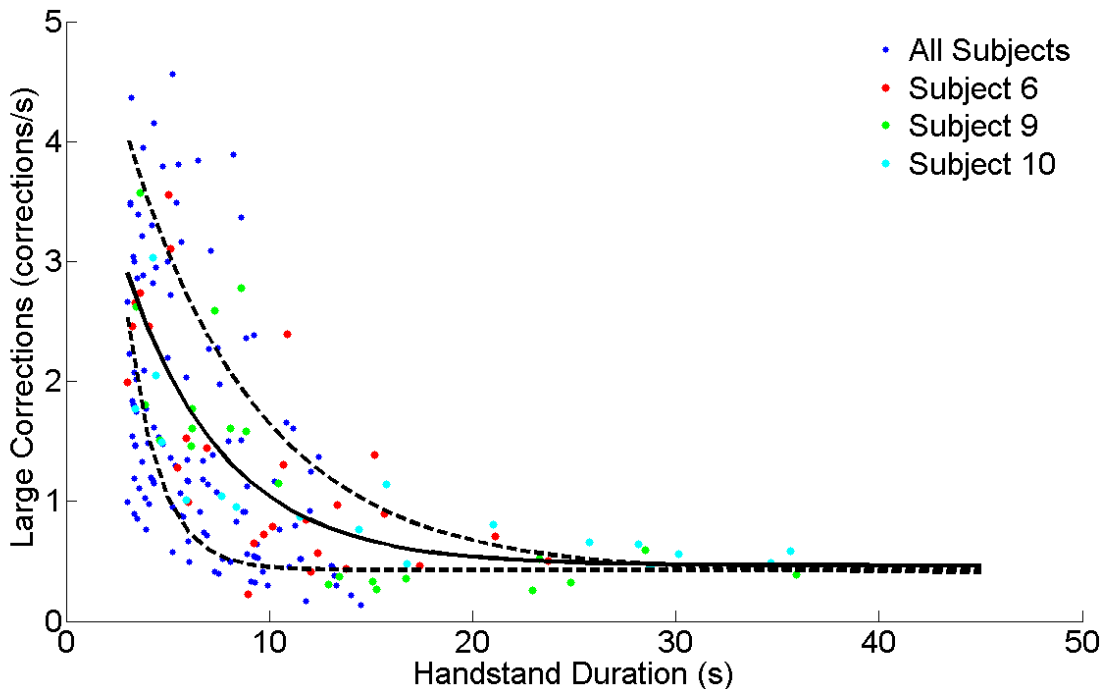
Figure 5.17: Scatter plot of handstand duration to the number of large corrections per second based on wrist EMG activity, with an exponential curve fit (bold line) ± 1 SD for each five second time bin (dotted lines); the three best subjects are indicated by the red, green, and cyan coloured markers.
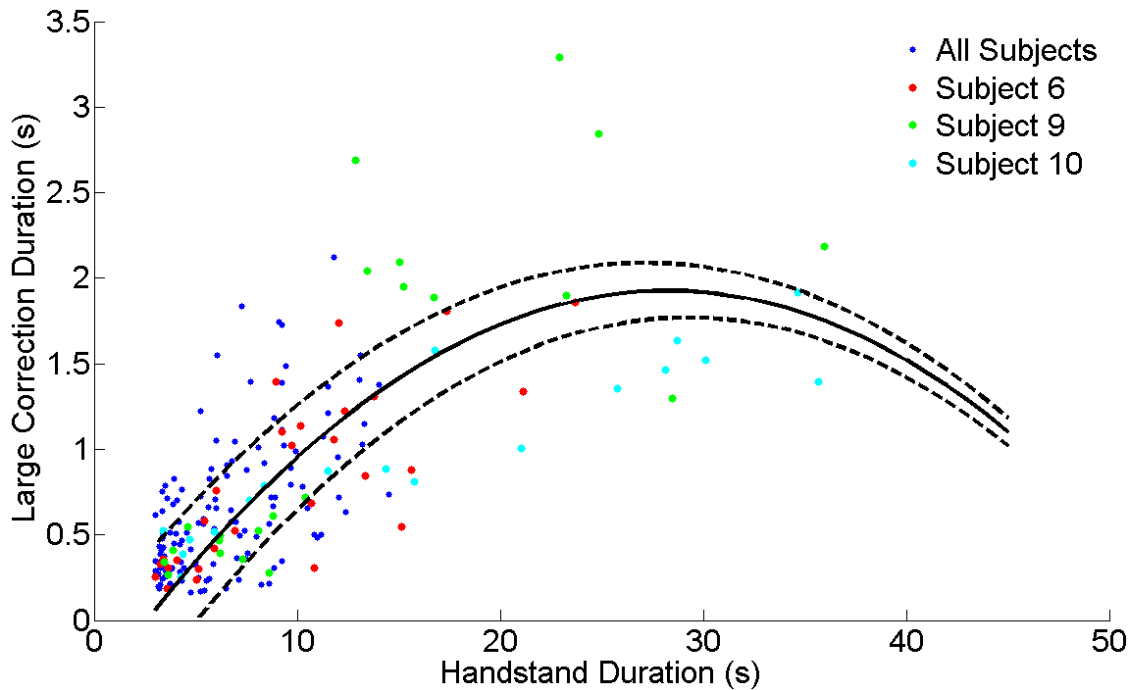
Figure 5.18: Scatter plot of handstand duration to the duration of large corrections based on wrist EMG activity, with a quadratic regression fit (bold line) ± 1 SD for each five second time bin (dotted lines); the three best subjects are indicated by the red, green, and cyan coloured markers.

Further inspection of the scatter plot of the number of large corrections per second (Figure 5.16) show data begins to plateau for handstands of more than 20 seconds duration. A quadratic model is unlikely to be an appropriate fit for the number of corrections per second, so data were re-analysed using an exponential fit, giving an adjusted R^2 of 0.37 (Figure 5.17).

Scatter plots show large variation in the number of corrections per second for trials of short duration, but relatively less variation in the duration of EMG burst. This is likley due to the limited time within a handstand trial of short duration and the expected inverse relationship between the number of corrections per second and the mean duration of those corrections. With increasing competence in handstand, and increasing handstand duration, subjects typically produce fewer corrections per second, however, the variation of the mean duration of those corrections typically increase. Changes in the variation of EMG burst duration are likely due to the subjects having more time to elicit a correction and may be related to exploration of different response strategies.

The duration of EMG bursts during handstand trials of longer durations are typically higher than those of experinced handstanders, suggesting novice handstanders that can maintain handstands for more than 20 seconds may still be adapting their postural control strategies.

5.3. Summary

Novice handstanders showed a large variation in handstand balance performance based on all balance metrics, with practice and a longer duration in handstand this variability generally reduces. Large amounts of variation for handstand trials of short duration make it extremely difficult to compare data to determine if a linear or quadratic relationship is present. At the end of eight months of practising handstands most subjects could not perform handstands for longer than 15 seconds duration, with only three subjects able to perform handstands for more than 20 seconds. Generally, with increased duration in handstand subjects displayed reduced sway as measured by traditional measures of balance. A more marked change in nonlinear measures of balance can be seen, with quicker reductions in variance for some nonlinear measures of balance than in the traditional measures. It may be that more pronounced changes in nonlinear measures represent changes in the subjects' underlying process of postural control, whereas less pronounced changes in traditional measures relate more to their general ability or performance in the balance task.

Data suggests that the regression models of balance used to estimate feedback time delay may be a poor estimate of the postural control strategies employed when novices first learn to balance. With increased competence in handstand balance, as described by longer trial durations, regression models appear to become more applicable, suggesting subjects begin to adapt a strategy that is close to the one suggested by the regression model. Estimates of torque contributions from these regression models begin to plateau and resemble experienced handstanders for handstand trials above 15 seconds duration. Changes in torque contribution estimates may suggest that subjects are beginning to rely more on sensory feedback for postural control.

Le Clair and Riach (1996) suggest the best test-retest reliability in standing balance is achieved by trials of 20 to 30 seconds. Although this relates to assessing standing trials were the subjects would have been capable of performing trials of longer durations if required, a time of 20 to 30 seconds appears to be a suitable criterion for handstand balance. In general, most measures of handstand balance began to plateau or approach that of experienced handstanders for handstand trials above 20 seconds duration. Handstand trials below 20 seconds duration appear to display large amounts of variation for all balance measures, making it difficult to examine the relationships between each balance metric and handstand performance. However, it must be stated that only three subjects managed to perform handstand trials for more than 20 seconds duration, and reductions in variability for trials longer than 20 seconds may be as a consequence of this.

The purpose of this chapter was to examine which balance metrics best characterise improvements in balance performance when a novice learns to balance in handstand. No balance metric can be considered to be appropriate for assessing handstand performance when a novice first learns to balance in handstand, as all measures show large amounts of variation for trials of short duration. Some nonlinear measures of balance, such as divergence and trend, appear to be sensitive to improvements in handstand performance based on handstand durations of more than ten seconds. As handstand balance improves and independent balance can be maintained for longer than 20 seconds, regression models, and their estimates of feedback time delay and the percentage torque from passive stiffness and delayed COM motion, appear to become appropriate approximations of the underlying postural control strategies employed by the subjects. Postural control strategies appear to resemble those of experienced handstanders when the novice was able to maintain independent handstand balance for more than 20 seconds duration. Future research may wish to examine this further by assessing novice, intermediate, and experienced handstanders to see if similar relationships are evident.

5.3.1. Conceptual Model of Learning to Balance

In the current research the relationships between an improvement in balance performance and changes in different balance metrics were examined. Some metrics, such as trend and divergence, appear to change quickly in the early stages of learning, with only small changes as performance improves further. Conversely, other metrics, such as sample entropy and sway range, appear to change relatively slowly throughout the learning process, with either linear or quadratic relationships with improvements in performance. When learning to balance, numerous control strategies are likely to be attempted by an individual in a trial and error approach to discovering how balance may be achieved and maintained. The success or failure of these attempts will depend on the suitability of the strategy chosen and any limitations in sensory acuity and muscular strength and control which may impair the execution of the strategy.

During the early stages of learning to balance it is expected that individuals will experiment with a relatively large number of control strategies, but with more experience these will be focused toward those few strategies that are most effective. It is possible that the exponential relationship between balance performance and trend and divergence are a representation of this search for a suitable control strategy. In this view large changes in, and variance in, trend and divergence during the early stages of learning could be explained by attempts to balance via different control strategies that may cause local trajectories in COM and COP to diverge quickly resulting in large drift and ultimately a failure to maintain balance. Further refinement of those few successful strategies would be achieved by improvements in sensory acuity, muscular strength and endurance, and neuromuscular control and coordination. This refinement would be expected to result in a more gradual change in balance performance, steadily improving the finer control of posture and the execution of the strategy. In this view, the slowly changing linear and quadratic relationships of sway range and sample entropy may represent the gradual improvement in the execution of the balance strategy. Together, this describes a process of learning that has two stages operating in parallel and which helps to explain the different relationships between balance performance and each

balance metric. This process of searching for a suitable strategy and gradually improving the execution of that strategy would also explain the large amounts of variation in all balance metrics during trials of short duration, and why some individuals struggled to balance at all. An illustration of the two aspects of this process can be seen in Figure 5.19.
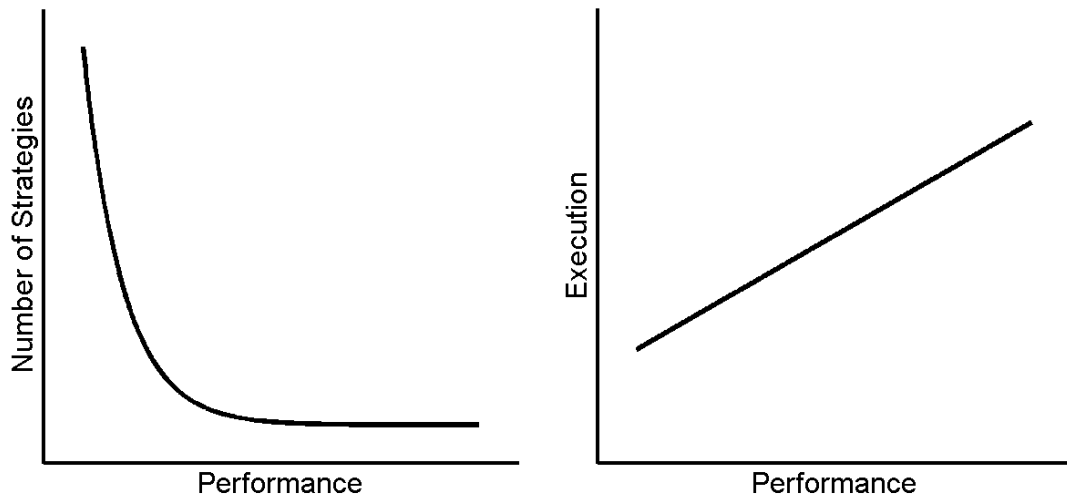
Figure 5.19: A conceptual model of learning to balance showing the two stages of strategy search and execution refinement operating in parallel.

This two stage process is analogous to the constraints led approach proposed by Newell (1986), where motor learning is defined as an ongoing dynamic process involving a search for and stabilisation of specific functional movement patterns across the perceptual motor landscape (Davids et al., 2008). Practice in the task results in a continual exploration of the perceptual-motor landscape, eventually leading to the emergence of an approximate solution to the task (Thelen, 1995). Further practice results in increased awareness of perceptual information and enhanced proficiency of motor outputs, strengthening connections within the coordinative structure to gain a tighter fit to the solution (Newell, 1991). Over time this process can expand to allow the individual to achieve a skilled optimisation of control for the task, exploiting environmental and task information to enhance the efficiency and control of the coordinative structure. Although the current research does not continue as far into the task of learning to balance in handstand, the final stage of Newell's constraints

theory would suggest enhanced postural control and further changes in the balance metrics examined here are expected. It is likely that with enhanced perceptual-motor coupling, postural control in handstand would become more akin to standing balance, with a stable and functional movement solution. This level on control is likely to result in a further increase in sample entropy, with a possible increase in trend and divergence, as postural sway becomes more nonlinear and possibly more nonstationary once again.

CHAPTER 6

RESPONSES TO MECHANICAL PERTURBATIONS

Research examining feedback time delays between sensory input and motor output has primarily focused on assessing EMG latencies from responses to discrete perturbations in standing (Nashner, 1976; Nashner et al., 1979; Horak et al., 1989). Delays between the initiation of platform translations and a noticeable rise in EMG activity are approximately 65 to 130 ms, with corresponding joint torques occurring approximately 30 ms later (Nashner et al., 1979; Horak et al., 1989). However, these feedback time delays to a platform perturbation have been shown to be affected by the velocity and amplitude of the perturbation, making it difficult to compare the results from multiple studies.

In general feedback time delays to platform perturbations are believed to be as a result of medium and long latency reflexes in the ankle muscles. Longer delays of approximately 200 to 300 ms have been found during perturbations with reduced ankle motion, and are believed to be due to responses associated with visual or vestibular inputs (Nashner, 1976). Although these dynamic posturography techniques have received a great deal of attention in the literature, it is important to note that static and dynamic posturography techniques address different aspects of the postural control system (Baratto et al., 2002). Baratto et al. (2002) explain how during dynamic posturography testing all sensory channels employed to provide information regarding postural control are activated above threshold levels and feed into strong reflex actions. In comparison, when balancing in quiet stance most of the sensory channels are activated near or below their physiological threshold. It is unclear whether feedback time delays calculated during dynamic posturography tests should be assumed to apply to quiet stance. It seems reasonable to assume that these values represent a lower limit, and that during quiet stance higher values may be expected. An assessment of feedback time delay in quiet standing is required.

Estimates of feedback time delay in quiet stance have been provided by cross correlations between COM and COP trajectories, with some authors suggesting the apparent zero delay between these two signals is evidence of a passive control system (Winter et al., 1998; Winter et al., 2001; Winter et al., 2003), while others suggest it is evidence of an active anticipatory feedforward control process (Gatev et al., 1999). Baratto et al. (2002) conclude that the main source of disturbance during static posturography testing is internal and predictable, and therefore the control system can rely on some kind of internal anticipatory model. These assumptions disregard the possibility of a reactive control strategy that relies on proportional and derivative gains from COM motion.

Yeadon and Trewartha (2003) examined the feedback time delay during static balance via examination of the relationship between joint torques and COM motion whilst in handstand. Wrist joint torques were regressed against COM displacement and velocity at earlier times, with peak R^2 values occurring at 160 to 240 ms. It is important to note that this method will only provide a rough estimate of the average delay over the full duration of the trial, incorporating several delays within it, such as: electromechanical delay (EMD), joint torque rise times, and the time for any sensory thresholds to be reached. Based on literature values, Yeadon and Trewartha subtracted an estimated value of 40 ms from all trials to account for these delays, resulting in estimated delays of 120 to 200 ms.

Horak and Nashner (1986) explain how an ankle strategy will result in activation of ankle extensors, knee flexors and hip extensors, and a hip strategy will result in activation of the knee extensors and hip flexors. Consequently, cross correlations between ankle and hip torques will result in a positive correlation coefficient if an ankle strategy is employed and a negative correlation coefficient if a hip strategy is employed. Yeadon and Trewartha (2003) followed this principle for handstand balance, where positive coefficients between wrist and shoulder/hip torques would suggest a wrist strategy and negative coefficients would suggest a shoulder or hip strategy. This principle can be

combined with an assessment of feedback time delay in either perturbed balance or quiet stance, providing information for the strategies used to maintain balance and the respective delays between joints in a coordinated response.

At present, feedback time delay has been examined either via EMG latencies to discrete perturbations or via estimates from cross correlations or delayed regression models in static balance. The aim of this chapter is to combine these methods during discrete perturbations in standing and handstand balance and evaluate the estimates of feedback time delay provided by cross correlations and delayed regression models. Further analysis of response strategies will be provided by cross correlations between ankle and hip joint torques in standing and wrist, shoulder, and hip joint torques in handstand.

6.1. Assessment of Feedback time Delay

Eleven experienced handstanders completed the second part of study two. The data collection protocol and experimental procedures were as described previously in Chapter 3. Subjects experienced a total of twelve platform perturbations in each posture, with three trials of each of the four platform perturbations, including: forwards and backwards translations of 0.1 m at 0.2 m·s^{-1}, and forwards and backwards translations of 0.05 m at 0.1 m·s^{-1}.

EMG latencies in standing trials were calculated from the start of the platform translation to the time of the first major EMG burst via visual inspection (Tillin et al., 2010). Large amounts of EMG activity were present throughout the duration of handstand trials, making it extremely difficult to determine the onset of a single muscular response to the platform movements. Consequently, only those trials where a clear response to the platform perturbation was evident were used for analysis, resulting in a mean of 9.1 ± 1.9 trials remaining for analysis, with no fewer than seven trials for any subject.

Feedback time delay estimates from cross correlations were calculated between: COM and ankle/wrist joint torque, COM and ankle/wrist EMG, and

ankle/wrist joint torques and ankle/wrist EMG signals. Further cross correlations were calculated between ankle and hip, and between wrist, shoulder, and hip joint torques to calculate the delay between the major segments involved and to provide insight into the balance strategies to discrete perturbations in each posture.

Estimates of feedback time delay via delayed regression models were provided by the Yeadon and Trewartha method (equation 6.1) and the adapted method (equation 6.2) previously described in Chapter 4.

$$T_{(t)} = p x_{(t-t_0)} + d \dot{x}_{(t-t_0)}$$

(6.1)

$$T_{(t)} = p_1 x_{(t)} + p_2 x_{(t-t_0)} + d \dot{x}_{(t-t_0)}$$

(6.2)

6.2. Findings and Discussion

Discrete platform perturbations during standing trials typically resulted in a characteristic rise in both ankle EMG and ankle joint torque (Figure 6.1).
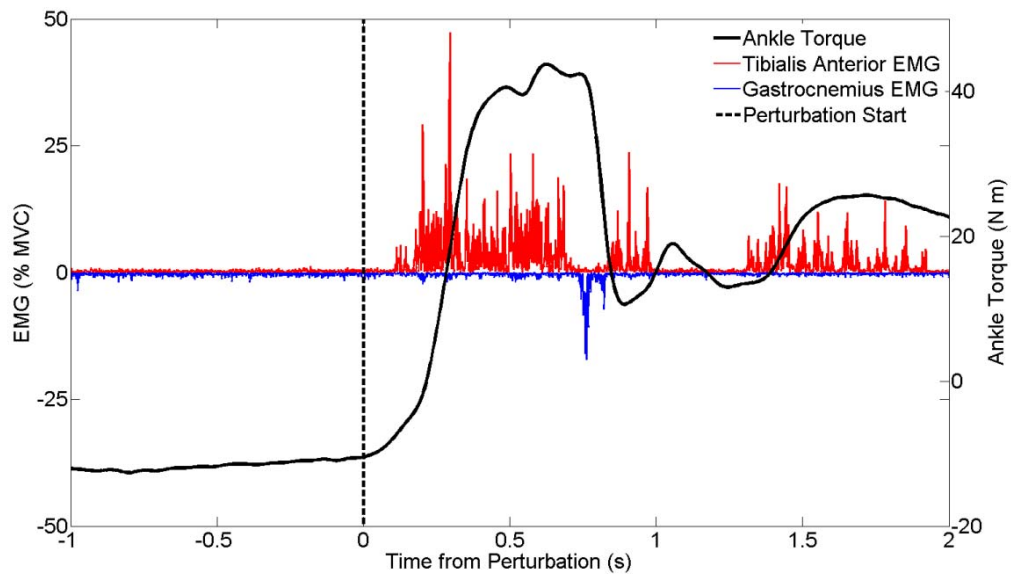
Figure 6.1: Example of the ankle EMG and torque response to a discrete perturbation in standing

Due to the demanding nature of the handstand posture discrete platform perturbations may have occurred during a corrective action, or may have resulted in a loss of balance before any noticeable correction was evident. Consequently, only those trials where an appropriate response was evident were used for further analysis (Figure 6.2).
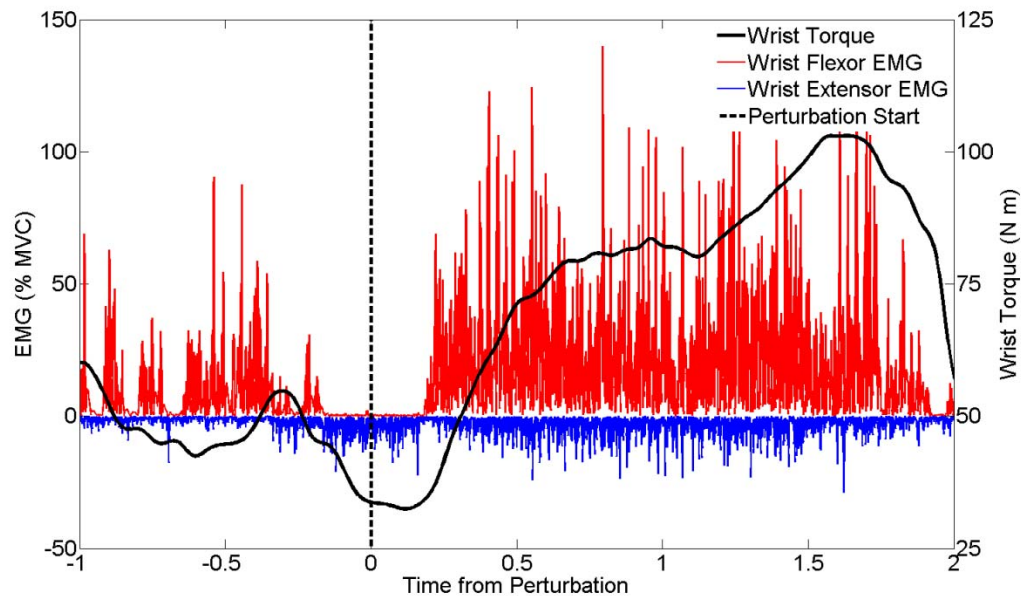
Figure 6.2: Example of the wrist EMG and torque response to a discrete perturbation in handstand.

6.2.1. Standing: Feedback time Delay

Individual mean EMG latencies during platform translations in standing were approximately 96 to 126 ms (Table 6.1), in agreement with previous research employing similar magnitude perturbations (Horak et al., 1989; Nashner et al., 1979). All responses began before 150 ms, suggesting they were most likely due to long latency reflexes from ankle plantar flexors and dorsi flexors (Nashner, 1976). Estimates of feedback time delay from delayed regression models were always longer than those calculated from EMG latencies, ranging from 2 to 39 ms longer for the Yeadon and Trewartha method and 11 to 60 ms longer for the adapted method (Table 6.1). Estimates of feedback time delays in perturbed stance were approximately 100 ms lower than those from static stance reported previously in Chapter 4.

154

Table 6.1: Subject mean values for feedback time delay during standing, calculated from the start of platform perturbation to first major EMG response and the two regression models.

		Yeadon & Trewartha Method			Adapted Method		
Subject	EMG$_{(a)}$	Delay$_{(b)}$	R^2	Diff $_{(a-b)}$	Delay$_{(c)}$	R^2	Diff $_{(a-c)}$
1	125.5	127.5	0.90	**-2.0**	162.8	0.90	**-37.3**
2	122.9	140.8	0.96	**-17.9**	178.8	0.96	**-55.8**
3	102.7	141.3	0.96	**-38.5**	162.9	0.96	**-60.2**
4	109.6	115.5	0.92	**-5.9**	121.0	0.92	**-11.4**
5	96.4	118.6	0.89	**-22.2**	129.3	0.89	**-32.9**
6	114.1	143.3	0.94	**-29.2**	158.8	0.94	**-44.7**
7	93.8	127.8	0.92	**-34.0**	151.3	0.92	**-57.5**
8	121.5	149.2	0.91	**-27.7**	174.2	0.92	**-52.7**
9	104.5	138.8	0.94	**-34.3**	160.5	0.94	**-56.0**
10	113.9	128.6	0.84	**-14.7**	158.8	0.86	**-44.9**
11	117.2	152.9	0.97	**-35.7**	172.9	0.97	**-55.7**
Mean	**111.1**	**134.9**	**0.92**	**-23.8**	**157.4**	**0.93**	**-46.3**
SD	**10.7**	**12.2**	**0.04**	**12.4**	**17.9**	**0.03**	**14.5**

Research examining the electromechanical delay (EMD) from the onset of EMG to the onset of force production has shown force production can lag behind the EMG signal by approximately 13 to 55 ms (Cavanagh and Komi, 1979; Muraoka et al., 2004; Tillin et al., 2010; Zhou et al., 1995). The difference between feedback time delays from EMG latencies and those estimated from both delayed regression models fall mostly within this range, suggesting EMD may account for a large part of this difference. Previous research has shown EMD values can vary within or between individuals, and that the slack length and tension in the tendon may be important factors in this variation (Muraoka et al., 2004). It is possible that the large variation in the differences between EMG latencies and estimated feedback time delays from regression models may also

be explained by variations in the slack length and tension in the Achilles tendon. The purpose of the current research was not to examine EMD, but further inquiry into EMD during standing balance would be informative.

Table 6.2: Subject mean values for cross correlations in standing trials between EMG and COM, ankle torque and COM, and EMG and ankle torque.

	EMG - COM		Torque - COM		EMG - Torque		
Subject	Delay$_{(a)}$	R^2	Delay$_{(b)}$	R^2	Delay	R^2	**Diff $_{(a-b)}$**
1	185.8	0.21	60.0	0.83	101.3	0.29	**125.8**
2	276.7	0.30	42.5	0.86	186.7	0.45	**234.2**
3	217.9	0.22	60.4	0.79	187.1	0.44	**157.5**
4	193.8	0.13	89.2	0.64	151.3	0.29	**104.6**
5	212.5	0.36	35.8	0.77	156.3	0.58	**176.7**
6	234.2	0.19	63.3	0.76	145.4	0.35	**170.8**
7	180.8	0.44	22.9	0.85	157.1	0.61	**157.9**
8	208.8	0.35	53.8	0.71	156.3	0.53	**155.0**
9	218.3	0.26	61.3	0.72	152.5	0.45	**157.1**
10	145.4	0.22	12.5	0.71	126.7	0.35	**132.9**
11	207.5	0.28	42.1	0.85	129.2	0.41	**165.4**
Mean	**207.4**	**0.27**	**49.4**	**0.77**	**150.0**	**0.43**	**158.0**
SD	**33.1**	**0.09**	**21.3**	**0.07**	**25.0**	**0.11**	**33.0**

Cross correlations show a delay between ankle EMG and COM displacement, with the anteroposterior motion of the COM lagging behind ankle EMG by approximately 145 to 277 ms (Table 6.2). These results are similar to previous research in quiet stance, which has shown ankle EMG can precede COM displacement by approximately 260 – 350 ms (Gatev et al., 1999). Gatev et al. (1999) concluded that these large delays between ankle EMG and COM motion provide evidence for a feedforward anticipatory mechanism for postural control. Similar values reported in the current research for perturbed stance, where

anticipatory control should not be possible, would indicate that further analysis of cross correlations between EMG and COM motion is required.

Gatev et al (1999) found the COP trajectory lagged behind ankle EMG by 240 to 270 ms. In static stance the COP signal may be considered as proportional to ankle joint torque (Baratto et al., 2002). In the current research cross correlations show ankle joint torques can lag behind ankle EMG by approximately 105 to 235 ms. Delays between ankle EMG and ankle joint torques, or COP in static stance, will represent the EMD between ankle EMG and the production of muscular force, however, an EMD of 105 to 235 ms is not representative of literature values. A higher estimated EMD found here is most likely due to the use of cross correlations with EMG signals, where slower components can dominate and hinder the detection of faster components (Nikolic et al., 2012).

Cross correlations show COM displacements lag behind ankle joint torques by approximately 12 to 90 ms, all of which are below the values calculated from EMG latencies. Comparing the delays from cross correlations of ankle EMG and COM displacements to the delays form cross correlations of ankle joint torques and COM displacements suggests approximately 158 ms remains unaccounted for. This value is close to the group average delay for cross correlations between ankle EMG and ankle joint torques, which would be expected to explain the remainder. However, large variations within the group suggest this is not always the case. Low R^2 values may suggest that poor correlations between EMG and COM displacement, or between EMG and joint torques, are resulting in poor estimates of signal delays. Alternatively, these differences may highlight the problems with using cross correlations to assess signals with vastly different frequency contents (Nikolic et al., 2012).

6.2.2. Handstand: Feedback time Delay

Individual mean EMG latencies during platform translations in handstand were approximately 102 to 192 ms (Table 6.3), which is on average 47 ms higher than that obtained from standing trials. Most responses began before 200 ms,

suggesting they are unlikely to be from visual or vestibular processes (Nashner, 1976). EMG latencies below 150 ms may be from long latency reflexes from wrist flexor muscles, however, longer latencies my represent other control systems are involved. Estimates of feedback time delay from delayed regression models were not always longer than those calculated from EMG latencies, ranging from 39 ms shorter than to 72 ms longer than EMG latencies for the Yeadon and Trewartha method and 1.5 ms shorter than to 101 ms longer than EMG latencies for the adapted method (Table 6.3).

Table 6.3: Subject mean values for feedback time delay during handstand, calculated from the start of platform perturbation to first major EMG response and the two regression models.

		Yeadon & Trewartha Method			Adapted Method		
Subject	$EMG_{(a)}$	$Delay_{(b)}$	R^2	**Diff $_{(a-b)}$**	$Delay_{(c)}$	R^2	**Diff $_{(a-c)}$**
1	137.1	161.8	0.74	**-24.7**	182.2	0.74	**-45.1**
2	101.7	173.8	0.71	**-72.1**	202.5	0.71	**-100.8**
3	152.3	154.6	0.83	**-2.3**	177.5	0.82	**-25.2**
4	151.8	155.0	0.72	**-3.2**	161.9	0.72	**-10.1**
5	161.1	161.4	0.65	**-0.3**	193.9	0.68	**-32.8**
6	165.0	163.5	0.78	**1.5**	206.9	0.85	**-41.9**
7	161.5	163.2	0.78	**-1.7**	197.2	0.80	**-35.7**
8	173.6	167.7	0.80	**5.8**	190.0	0.80	**-16.4**
9	171.7	169.6	0.74	**2.1**	207.3	0.74	**-35.6**
10	191.7	152.7	0.67	**38.9**	196.3	0.75	**-4.6**
11	171.0	147.5	0.80	**23.5**	169.5	0.80	**1.5**
Mean	**158.0**	**161.0**	**0.75**	**-2.9**	**189.6**	**0.76**	**-31.5**
SD	**23.4**	**7.9**	**0.06**	**28.0**	**15.1**	**0.05**	**27.7**

A purely reactive control strategy should result in EMG latencies that are always lower than feedback time delays based on joint torques. Trials that

show the opposite likely reflect experimental error or a non-reactive strategy has been employed. In standing trials, EMG latencies showed similar variance to estimates of feedback time delays from both regression models. EMG latencies during handstand trials displayed a standard deviation of approximately 2 to 3 times that of the regression models. It seems likely that the increased variation in EMG latencies during handstands is related to the difficulties in determining EMG onset during these trials. Although changes in passive stiffness may still account for earlier torque relationships, individual estimates of the contribution of passive stiffness to the total torque show no clear relationship, with stiffness usually higher in standing trials (Table 6.4).

Table 6.4: Subject mean values for the difference between EMG latencies and feedback time delay estimated by the adapted method, and the percentage of joint torques from the three coefficients for standing and handstand trials.

	Standing Trials				Handstand Trials			
Subject	Diff $_{(a-c)}$	p_1 (%)	p_2 (%)	d (%)	Diff $_{(a-c)}$	p_1 (%)	p_2 (%)	d (%)
1	-37.3	64.0	19.6	16.4	-45.1	33.5	44.9	21.6
2	-55.8	53.0	27.3	19.8	-100.8	29.5	42.7	27.8
3	-60.2	45.7	29.9	24.4	-25.2	19.3	59.4	21.3
4	-11.4	29.3	39.7	31.0	-10.1	40.9	34.2	24.9
5	-32.9	47.8	35.7	16.4	-32.8	39.0	40.0	21.0
6	-44.7	39.1	29.7	31.1	-41.9	37.1	49.8	13.1
7	-57.5	35.4	46.9	17.7	-35.7	22.6	57.4	20.0
8	-52.7	45.2	28.0	26.7	-16.4	34.0	45.6	20.3
9	-56.0	42.8	31.8	25.4	-35.6	17.7	62.4	19.9
10	-44.9	59.2	23.6	17.2	-4.6	50.1	29.2	20.8
11	-55.7	42.7	32.8	24.5	1.5	36.0	40.0	24.0
Mean	**-46.3**	**45.8**	**31.4**	**22.8**	**-31.5**	**32.7**	**46.0**	**21.3**
SD	**14.5**	**10.0**	**7.5**	**5.6**	**27.7**	**9.8**	**10.5**	**3.7**

Note: p_1 represents the percentage of torque estimated by a passive stiffness mechanism

Similar to standing trials, estimates of feedback time delays in perturbed handstands were on average lower than those from the static handstand trials reported previously in Chapter 4. However, the difference between static and perturbed handstand trials was much lower than that of standing, with a mean difference of 15 ms for the Yeadon and Trewartha method and 23 ms for the adapted method. It would be reasonable to suggest that balancing in handstand is a challenging task, with the postural control system operating close to the limits of its capability even during static balance conditions. If EMG latencies during perturbed balance tasks provide a lower limit for the response time of the postural control system, then these smaller differences between static and perturbed trials further highlights the challenging nature of this task.

Table 6.5: Subject mean values for cross correlations in handstand trials between EMG and COM, wrist torque and COM, and EMG and wrist torque.

	EMG - COM		Torque - COM		EMG - Torque		
Subject	Delay$_{(a)}$	R^2	Delay$_{(b)}$	R^2	Delay	R^2	**Diff $_{(a-b)}$**
1	302.1	0.26	147.9	0.40	94.2	0.56	**154.2**
2	194.6	0.33	39.2	0.54	99.6	0.66	**155.4**
3	165.4	0.32	57.9	0.59	100.0	0.62	**107.5**
4	132.1	0.31	75.8	0.52	76.7	0.70	**56.2**
5	93.8	0.38	70.0	0.49	77.5	0.57	**23.8**
6	272.9	0.12	57.1	0.32	77.1	0.46	**215.8**
7	93.8	0.47	10.4	0.62	97.5	0.80	**83.3**
8	105.0	0.36	2.9	0.68	93.8	0.60	**102.1**
9	84.2	0.45	-13.8	0.66	100.0	0.70	**97.9**
10	200.4	0.21	78.3	0.44	80.0	0.59	**122.1**
11	276.3	0.26	55.0	0.70	88.3	0.54	**221.3**
Mean	**174.6**	**0.32**	**52.8**	**0.54**	**89.5**	**0.62**	121.8
SD	**80.8**	**0.10**	**44.1**	**0.12**	**9.9**	**0.09**	61.2

Cross correlations show a delay between wrist EMG and COM displacement, with the anteroposterior motion of the COM lagging behind wrist EMG by approximately 84 to 302 ms (Table 6.5). These results are somewhat larger than the 95 ms delay reported during static handstand trials in Chapter 4, but are comparable to the 145 to 277 ms delay between ankle EMG and COM displacements found in perturbed standing. Cross correlations between wrist joint torques and wrist EMG show torques lag behind EMG by approximately 77 to 100 ms, similar to the mean of 94 ms for the static handstand trials reported in Chapter 4. These values are a little lower than the 105 to 235 ms delay between ankle EMG and ankle joint torque reported for standing trials. Smaller delays between EMG and joint torque for handstand trials may be due to an increased tension in the tendons of the wrist flexor muscles during handstand compared to that of the Achilles tendon during standing. This would suggest a shorter EMD between wrist EMG and wrist joint torque than between ankle EMG and ankle joint torques, and is further supported by the smaller difference between EMG latencies and estimates of feedback time delay in handstand trials. Alternatively, these smaller values may be due to higher R^2 values from the cross correlations, showing a value of 0.62 for handstand trials compared to a value of 0.43 for standing trials. Higher R^2 values in handstand trials are likely due to an increased activity in wrist flexor and extensor muscles compared to that of ankle plantar flexors and dorsi flexors in standing trials.

Cross correlations show delays between COM displacements and wrist joint torques range from -14 to +148 ms, with negative values indicating wrist joint torques lag behind COM displacements. Similar to standing trials, large variations in delays from these cross correlations may highlight that cross correlations are an unsuitable tool for assessing signal delays. Alternatively, poor R^2 values in handstand trials may indicate that subjects were not employing a wrist strategy, suggesting further analysis is required.

6.2.3. Control Strategies

Similar delays were found between ankle and hip joint torques in standing and between wrist and shoulder joint torques and wrist and hip joint torques in

handstand (Table 6.6). No significant differences were found for the delays between ankle and hip joint torques compared to wrist and shoulder joint torques ($t = 1.29$; $p > 0.05$) or for the delays between ankle and hip joint torques compared to wrist and hip joint torques ($t = 1.84$; $p > 0.05$). Large variations were found for the delays calculated between segments in both handstand and standing trials.

Table 6.6: Cross correlations between ankle and hip joint torques in standing, and between wrist and hip joint torques, and wrist and shoulder joint torques in handstand.

Subject	Ankle - Hip		Wrist - Shoulder		Wrist - Hip	
	Delay	R^2	Delay	R^2	Delay	R^2
1	295.8	0.48	292.5	0.36	317.9	0.36
2	37.5	0.41	253.3	0.51	250.4	0.48
3	57.1	0.40	101.7	0.41	120.4	0.37
4	59.2	0.29	274.6	0.36	162.5	0.35
5	145.0	0.44	438.8	0.33	440.0	0.34
6	-11.3	0.31	245.4	0.28	215.4	0.23
7	143.8	0.35	234.2	0.47	244.6	0.50
8	195.0	0.32	174.6	0.45	203.3	0.42
9	342.5	0.32	85.8	0.51	167.1	0.50
10	166.7	0.59	175.0	0.43	170.4	0.45
11	50.0	0.30	-67.5	0.48	9.6	0.49
Mean	**134.7**	**0.38**	**200.8**	**0.42**	**209.2**	**0.41**
SD	**111.2**	**0.09**	**131.4**	**0.08**	**110.1**	**0.08**

Most associated correlation coefficients were positive for handstand trials, with 97% of trials providing a positive correlation coefficient for delays between wrist and shoulder joint torques and between wrist and hip joint torques. Slightly fewer trials in standing displayed correlation coefficients that were positive, with

85% of trials providing a positive correlation coefficient for delays between ankle and hip joint torques. Cross correlations between shoulder and hip joint torques in handstand trials show all trials have positive correlation coefficients with approximately zero delay. In response to a discrete platform perturbation subjects frequently attempted to use a wrist strategy to prevent falling in handstand and an ankle strategy to prevent falling in standing. The wrist strategy was accompanied by synergistic shoulder and hip joint torques to maintain the inverted posture, and the ankle strategy was accompanied by synergistic hip joint torques to maintain a vertical posture.

Yeadon and Trewartha reported estimates of wrist and shoulder joint torques with approximately zero delay and wrist and hip joint torques with approximately 50 ms delay in static handstands. In the current research delays between wrist and shoulder joint torques, and between wrist and hip joint torques, were on average 200 ms for handstands during platform perturbations. Delays from wrist joint torques to shoulder and hip joint torques of approximately 200 ms were similar to the delay of 161 to 190 ms for wrist joint torques to COM displacement and velocity predicted by the two regression models. Similarly, delays from ankle to hip joint torques of approximately 135 ms are similar to the delay of 135 to 158 ms for ankle joint torques to COM displacement and velocity predicted by the two regression models. These results may indicate that, during perturbations, the torque produced at distal joints, such as the ankle or wrist, is not well coordinated with that from proximal joints, such as the hip or shoulder respectively. An extra 200 ms delay between distal and proximal joints would suggest proximal joints are responding to the perturbation imposed on them from the torque produced at the distal joints. Previous research has found intersegmental delays of 4 to 100 ms between the EMG onset of ankle muscles and that of hip or trunk muscles to a discreet platform perturbation (Diener et al., 1988; Horak and Nashner, 1986; Woolacott and Sveistrup, 1992). Although the intersegmental delays of 135 ms in standing and 200 ms in handstand reported here are somewhat large compared to past literature, there was also a large amount of subject variability in these values, possibly related to the use of cross correlations.

6.3. Summary

The purpose of this chapter was to evaluate the estimates of feedback time delay provided by cross correlations and delayed regression models by comparison to the values provided by EMG latencies to a discrete perturbation. Estimates of feedback time delays provided by cross correlations of ankle joint torque and COM displacement produced values that were on average 62 ms lower than that of EMG latencies in standing. Similarly, estimates of feedback time delays provided by cross correlations of wrist joint torque and COM displacement produced values that were on average 105 ms lower than that of EMG latencies in handstand. Results suggest that cross correlations between joint torques and COM displacements can severely underestimate feedback time delay to a discrete perturbation. Using cross correlations to estimate feedback time delays during balance are not recommended.

Ankle EMG latencies to a discrete perturbation in standing were 96 to 126 ms, with estimates of feedback time delays provided by delayed regression models that were on average 24 ms longer for the Yeadon and Trewartha method and 46 ms longer for the adapted method. Similarly, wrist EMG latencies to a discrete perturbation in handstand were 102 to 192 ms, with estimates of feedback time delays provided by delayed regression models that were on average 3 ms longer for the Yeadon and Trewartha method and 32 ms longer for the adapted method. These differences are most likely due to an electromechanical delay between the start of the EMG response to the start of a change in ankle and wrist joint torques. Shorter delays for the Yeadon and Trewartha method were expected, as passive stiffness within the musculotendinous unit is likely to produce extra torque when forced into an eccentric action. The extra torque produced by this passive stiffness will have approximately zero delay and will cause the estimated feedback time delay based on delayed regressions between joint torque and COM motion to be slightly underestimated. The adapted method addressed this issue by including a third term into the regression model based on COM displacement with zero delay. These results appear to support the use of this third term as a means of estimating the effect of passive stiffness on feedback time delay. Delayed

regression models seem to be an appropriate and useful tool for estimating feedback time delays during balance. There were differences in feedback time delay between static balance and perturbed balance of approximately 100 ms for standing and up to 25 ms for handstand. These differences are likely to be due to the extra time required to reach sensory thresholds in static balance conditions, with the lower difference in handstand trials indicating the difficult nature of balance in handstand. Future studies may want to examine this further with different magnitudes of perturbations or with other estimates of passive stiffness.

Most trials in standing appear to use an ankle strategy with synergistic torques at the hip to maintain balance in response to a discrete perturbation. Similarly, most trials in handstand appear to use a wrist strategy with synergistic torques at the shoulder and hip to maintain balance in response to a discrete perturbation. Intersegmental delays of 135 ms for standing and 200 ms for handstand are somewhat large compared to previous research. Although there was a large amount of variability in these intersegmental delays between subjects, both the high variability and the elevated intersegmental delay times are likely due to the use of cross correlations. Cross correlations appear to result in poor estimates of time lags between signals that have different frequency components, such as comparing EMG to joint torque or comparing wrist joint torque to hip joint torque. Further study is required to provide an estimate of the overestimation or underestimation of signal delay caused by the differences in frequency components within two signals.

CHAPTER 7

SENSORY PERTURBATIONS AND RESTRICTIONS

The sensory organisation test (SOT) was developed by Nashner (1972) and is a computerised system that consists of a movable dual force plate support surface within a moveable surround. The SOT is an integral part of computerised dynamic posturography, and is commercially available in the NeuroCom BalanceMaster and EquiTest systems used for clinical testing in a variety of conditions that can affect balance. One of the components of the SOT is that the support surface can rotate about an axis level with a patient's ankle and track their forwards and backwards sway during quiet stance. This is termed as a sway referenced platform and is intended to reduce the amount of ankle motion in an attempt to reduce sensory feedback from the surrounding somatosensory proprioceptors. The SOT has been used to examine recovery in patients with uni- and bi-lateral vestibular deficits (Nashner et al., 1982; Nashner et al., 1983; Perietti-Winkler et al., 2006), and the role of visual cues in vestibular loss patients (Mergner et al., 2005). It has also been used to estimate the contributions of visual, vestibular, and somatosensory cues to the maintenance of balance in normal stance, suggesting an approximate weighting of 10%, 20%, and 70% respectively (Horak, 2006, Peterka, 2002; Peterka and Benolken, 1995). Lastly, McCollum et al. (1996) have suggested that performance in the different tests within the SOT may be affected by the order of the testing, suggesting a link to how the CNS re-weighs different sensory cues due to environmental changes and recent events.

Vision has been found to affect balance in handstand as well as standing (Asseman et al., 2005; Gautier et al., 2007). Similar to standing, foam supports have been used to assess the role of somatosensory information whilst balancing in handstand (Croix et al., 2010a). Although control of handstand is adversely affected by balancing on a foam support, it is unclear if this is purely due to altered sensory feedback or a mechanical by-product of trying to

generate joint torques on a compliant surface. The purpose of this chapter is to examine how balance in standing and handstand may be affected by altered sensory feedback and to provide insight into the importance of ankle and wrist somatosensory feedback during balance.

7.1. Assessment of Balance

Ten experienced handstanders completed the final stage of study two. The data collection protocol and experimental procedures were as described previously in Chapter 3. Using the algorithms of Barton et al. (2006) the Stewart platform within the CAREN system was controlled so that horizontal and vertical translations of the platform were combined with rotations about the mediolateral axis so the platform could rotate about a virtual point. The virtual point was determined by markers placed on the subject's ankle or wrist joints while in standing or handstand respectively. Body sway was tracked by markers at the next proximal joint, the knee for standing and the elbow for handstand, so that the rotation of the platform would track sway about the ankle or wrist. This procedure simulated the sway referenced platform motion of the SOT in both a standing and a handstand posture in an attempt to reduce ankle and wrist joint movement whilst allowing unrestricted body sway.

Subjects completed three trials in each of the eight conditions, including: standing on a static and sway referenced platform with eyes open and eyes closed, and handstand on a static and sway referenced platform with eyes open and eyes closed. All balance measures described in Chapter 4 were calculated and analysed for each posture.

7.1.1. Statistical Analysis

Determinism and SampEn values of the surrogate data were compared to the SampEn values of the original data using a repeated measures t-test with a significance level of 0.05 in accordance with the suggestions of Harbourne and Stergiou (2003) and Stergiou et al. (2004).

Table 7.1: All variables used to assess balance.

Group	Variables	Number
Traditional	duration, standard deviation (SD), range, mean sway velocity (SV)	4
Nonlinear	sample entropy (SampEn), lyapunov exponent (LyE)	2
Recurrence Quantification Analysis	recurrence rate (RR), determinism (DET), entropy (ENT), divergence (DIV), trend (TND)	5
Estimated Delays	delay, R^2, proportional and derivative coefficients, torque percentages, cross correlations	17
Movement Corrections (Torque)	corrections per second, mean torque, torque impulse, burst duration [small, medium, large (S,M,L)]	12
Movement Corrections (EMG)	corrections per second, root mean square (RMS), burst duration [small, medium, large (S,M,L)]	9

Note: Movement corrections for EMG were only used in handstand as no sensors were placed on the lower leg; Estimated delays were calculated by two different methods and will be prefixed with M1 or M2 (M1 = Yeadon and Trewartha method)

Two separate two-way repeated measures ANOVAs (platform vs. vision) were used to compare mean values for all dependent variables (Table 7.1) in the standing position and the handstand position. Significant differences were examined further using multiple *t*-tests with a Bonferroni correction. Further comparisons were also made between trials of the same type from the data in the static session, presented previously in Chapter 4. Prior to statistical testing, all data were assessed for normality and sphericity by the one-sample Kolmogorov-Smirnov test and Mauchly's test of sphericity respectively. A Greenhouse-Geisser correction was used to adapt the degrees of freedom of statistical tests for any data that was found to violate the assumption of sphericity.

7.2. Findings and Discussion

Significant differences were found between the original data sets and the surrogate data sets for both SampEn (t = - 4.6; p < 0.001) and DET (t = 3.8; p <

0.001), indicating the fluctuations observed were distinguishable from linearly correlated Gaussian noise. The original data most likely have a deterministic nature and the use of nonlinear techniques are supported. All data were found to be normally distributed by the one-sample Kolmogorov-Smirnov test. Most data were found to violate the assumption of sphericity, therefore the Greenhouse-Geisser correction was employed.

7.2.1. Traditional Measures of Balance

A statistically significant interaction between the effects of platform motion and vision, and statistically significant main effects for platform motion and vision were found for SD, range, and mean SV variables. Further comparisons and group means are given in table 7.2. All measures except trial duration presented with significantly larger values of sway in eyes closed and sway referenced conditions. Similar to previous research, results suggest that a sway reference platform increases AP sway in standing, with an increased effect during trials when no visual cues are available (Peterka and Benolken, 1995).

Table 7.2: Mean values for traditional measures of balance in standing trials.

Variable	Static Platform		Sway Referenced Platform	
	$EO_{(a)}$	$EC_{(b)}$	$EO_{(c)}$	$EC_{(d)}$
Trial Duration (s)	30.0	30.0	29.2	27.6
SD (cm)	$0.5^{c,d}$	0.6^{d}	$1.0^{a,d}$	$1.9^{a,b,c}$
Range (cm)	$2.2^{c,d}$	$2.8^{c,d}$	$5.5^{a,b,d}$	$10.2^{a,b,c}$
SV (cm s^{-1})	$0.9^{b,c,d}$	$1.3^{a,d}$	$1.8^{a,d}$	$4.2^{a,b,c}$

Note: superscripts indicate significant differences between conditions at the Bonferroni adjusted significance level of 0.0083

A statistically significant interaction between the effects of platform motion and vision, and statistically significant main effects for platform motion and vision was found for the duration in handstand. No other significant interactions were found for the traditional measures in the handstand trials, however, statistically significant main effects were found in vision for SD and in platform motion for

mean SV. Further comparisons and group means are given in table 7.3. Duration in handstand was specifically affected by the sway referenced platform, resulting in no subject being able to hold a handstand with eyes open for longer than eight seconds. Handstand on a sway referenced platform appears to be extremely difficult, individuals who had previously managed to perform five handstand trials for the full duration of 30 seconds, both with eyes open and eyes closed, regressed to a novice stage where balance could only be maintained for a few seconds. Surprisingly, few significant differences were found between experimental conditions, most likely due to the short trial durations and the presence of large individual variation between trials, similar to the novice subjects in Chapter 5.

Table 7.3: Mean values for traditional measures of balance in handstand trials.

	Static Platform		Sway Referenced Platform	
Variable	$EO_{(a)}$	$EC_{(b)}$	$EO_{(c)}$	$EC_{(d)}$
Trial Duration (s)	$24.9^{b,c,d}$	$12.8^{a,c,d}$	$4.6^{a,b}$	$3.6^{a,b}$
SD (cm)	$1.2^{c,d}$	1.6	1.5^{a}	1.6^{a}
Range (cm)	5.4	6.0	6.4	6.6
SV (cm s^{-1})	6.7	7.2	8.0	8.2

Note: superscripts indicate significant differences between conditions at the Bonferroni adjusted significance level of 0.0083

Comparisons between static trials in standing from the first testing session (Chapter 4) and the static platform in the SOT show a significant increase in SD, range, and mean SV during stance with eyes closed (Table 7.4). This is in agreement with previous research that has suggested a link between how visual and somatosensory information is processed (Peterka and Benolken, 1995), and specifically that recent environmental changes may alter how the CNS weighs the relative information from each system (McCollum et al., 1996). A significant reduction in the duration of handstand trials with eyes closed was observed when comparing the static trials from the first testing session to those in the static platform condition in the SOT (Table 7.4). It would appear that the relationship between somatosensory and visual cue utilisation, and how this is

affected by recent environment experiences, is similar in both standing and handstand postures. Unfortunately, no other balance measures presented with a significant difference between the two sessions for the handstand posture, making it difficult to draw further conclusions regarding this matter.

Table 7.4: Mean values for traditional measures of balance for comparison to the static session (reported in Chapter 4).

| | Standing | | | | Handstand | | | |
| | Static | | SOT | | Static | | SOT | |
Variable	$EO_{(a)}$	$EC_{(b)}$	$EO_{(c)}$	$EC_{(d)}$	$EO_{(e)}$	$EC_{(f)}$	$EO_{(g)}$	$EC_{(h)}$
Trial Duration (s)	30.0	30.0	30.0	30.0	27.7	18.6^h	24.9	12.8^f
SD (cm)	0.5	0.5^d	0.5	0.6^b	1.3	1.6	1.2	1.6
Range (cm)	2.1	2.2^d	2.2	2.8^b	5.9	6.6	5.4	6.0
SV (cm s^{-1})	0.7^c	0.9^d	0.9^a	1.3^b	6.8	7.7	6.7	7.2

Note: superscripts indicate significant differences between conditions at the significance level of 0.05

7.2.2. Nonlinear Measures of Balance

There were no statistically significant interactions between the effects of platform motion and vision for any of the nonlinear measures of balance during standing trials. There were statistically significant main effects for both platform motion and vision for LyE. Further comparisons revealed that these differences were between standing on a static platform with eyes open and on a sway reference platform with eyes closed or eyes open; group means are given in table 7.5. Reduced LyE values for sway referenced platform conditions suggest that COP trajectories become more organised with lower localised divergence.

Table 7.5: Mean values for nonlinear and recurrence measures for balance in standing.

Variable	Static Platform		Sway Referenced Platform	
	EO(a)	EC(b)	EO(c)	EC(d)
SampEn	0.05	0.06	0.04	0.05
LyE	0.94[c,d]	0.78	0.57[a,d]	0.33[a,c]
RR (%)	6.01	3.81	7.44	4.42
DET (%)	99.91	99.91	99.95	99.95
ENT (bits)	4.44	4.29	4.78	4.55
DIV	0.38	0.55	0.25	0.34
TND	-1.32	-1.33	-2.51	-1.88

Note: superscripts indicate significant differences between conditions at the Bonferroni adjusted significance level of 0.0083

There were no statistically significant interactions between the effects of platform motion and vision for any of the nonlinear measures of balance during handstand trials. There were statistically significant main effects in both platform motion and vision for ENT, in vision for DET, and in platform motion for DIV and LyE. Further comparisons and group means are given in table 7.6. Significant differences were found between handstands on a static platform with eyes open and on sway referenced platform with eyes closed for RR, ENT, DIV, and TND. Although there was a significant increase in RR between handstands on a static platform with eyes open compared to on a sway referenced platform with eyes closed, this is most likely due to a large decrease in the trial duration reported previously. Increases in DIV and TND with a decrease in ENT indicate a drift in COP throughout the trial when performing a handstand in the sway referenced condition. Collectively, these results suggest that when performing a handstand on a sway referenced platform, subjects tended to drift, or fall, with few corrections, leading to nonstationary signals with large divergence in local trajectories.

Table 7.6: Mean values for nonlinear and recurrence measures for balance in handstand.

Variable	Static Platform		Sway Referenced Platform	
	EO$_{(a)}$	EC$_{(b)}$	EO$_{(c)}$	EC$_{(d)}$
SampEn	0.14	0.09	0.09	0.09
LyE	0.76	0.61	1.05	0.96
RR (%)	1.13[d]	3.01	4.98	5.09[a]
DET (%)	99.27	99.58	99.44	99.66
ENT (bits)	2.60[d]	2.22[d]	1.56	1.07[a,b]
DIV	4.84[c,d]	10.14	20.23[a]	19.92[a]
TND	-4.20[d]	-31.10	-37.93	-41.02[a]

Note: superscripts indicate significant differences between conditions at the Bonferroni adjusted significance level of 0.0083

Further comparisons between static trials in standing from the first testing session (Chapter 4) and the static platform in the SOT show a significant increase in SampEn, DIV, and TND during stance with eyes open and stance with eyes closed (Table 7.7). Results suggest that the possible re-weighing of sensory inputs during sway referenced platform motion results in a residual effect that increases stationarity, but also increases localised divergence. Such a manifestation would likely be caused by fewer small adjustments and larger amplitudes of sway, possibly indicating a change in sensory thresholds.

The only significant difference between static handstand from the first session and those during the SOT was for ENT, with a decreased value for trials during the SOT for both eyes open and eyes closed conditions. Lower ENT values would represent a decrease in Shannon entropy, meaning the spread of recurrence lines has reduced, increasing the probability of any line length. These results may be interpreted as providing further evidence of the sway referenced platform altering how sensory information is weighed during subsequent static balance in handstand.

Table 7.7: Mean values for nonlinear and recurrence measures of balance for comparison to the static session (reported in Chapter 4).

| | Standing | | | | Handstand | | | |
| | Static | | SOT | | Static | | SOT | |
Variable	$EO_{(a)}$	$EC_{(b)}$	$EO_{(c)}$	$EC_{(d)}$	$EO_{(e)}$	$EC_{(f)}$	$EO_{(g)}$	$EC_{(h)}$
SampEn	0.03^c	0.04^d	0.05^a	0.06^b	0.11	0.11	0.14	0.09
LyE	1.14	0.95	0.94	0.78	0.66	0.60	0.76	0.61
RR (%)	9.32	6.94	6.01	3.81	1.04	1.66	1.13	3.01
DET (%)	99.95	99.94	99.91	99.91	99.31	99.51	99.27	99.58
ENT (bits)	4.83	4.56	4.44	4.29	2.88^g	2.8^h	2.60^e	2.22^f
DIV	0.13^c	0.26^d	0.38^a	0.55^b	3.67	6.53	4.84	10.14
TND	-3.28^c	-2.28^d	-1.32^a	-1.33^b	-0.64	-4.18	-4.20	-31.10

Note: superscripts indicate significant differences between conditions at the significance level of 0.05

7.2.3. Estimated Feedback time Delay

There were no statistically significant interactions or main effects for the cross correlations between ankle torque and COM displacements in standing trials; mean values are given in Table 7.8.

Table 7.8: Cross correlations between ankle torque and COM displacement in standing.

| | Static Platform | | Sway Referenced Platform | |
Variable	$EO_{(a)}$	$EC_{(b)}$	$EO_{(c)}$	$EC_{(d)}$
Delay (ms)	-4	-6	3	-6
R^2	0.77	0.75	0.69	0.75

Note: A negative delay indicates the COM peak occurs after the ankle torque peak

There were no statistically significant interactions between the effects of platform motion and vision for cross correlations between wrist torque and COM displacements, wrist flexor/extensor EMG and COM displacements, or

wrist flexor/extensor EMG and wrist torques in handstand trials. There were significant main effects in platform motion for the delay from cross correlations between EMG and COM displacements, and between wrist torque and COM displacements, but not for cross correlations between wrist flexor/extensor EMG and wrist torques in handstand trials. There was also a significant main effect in platform motion for the R^2 value calculated from cross correlations between wrist torque and COM displacements in handstand trials. Significant differences and group mean values are given in Table 7.9.

A large increase in the delay from cross correlations between wrist joint torque and COM displacement from the static platform to the sway referenced platform conditions may suggest a change in the corrective strategy used to maintain balance in handstand. On the other hand, decreases in the R^2 value calculated from these cross correlations make it apparent that a simple linear relationship between wrist joint torque and COM displacement is inappropriate in this case.

Table 7.9: Cross correlations between wrist torque and COM, EMG and COM, and between EMG and wrist torque in handstand.

	Static Platform		Sway Referenced Platform	
Variable	$EO_{(a)}$	$EC_{(b)}$	$EO_{(c)}$	$EC_{(d)}$
Torque – COM: Delay (ms)	$5^{c,d}$	25	164^a	128^a
Torque – COM: R^2	0.54^d	0.55^d	0.36	$0.26^{a,b}$
EMG – COM: Delay (ms)	117^c	125	240^c	194
EMG – COM: R^2	0.20	0.29	0.29	0.17
EMG – Torque: Delay (ms)	89	63	40	53
EMG – Torque: R^2	0.49	0.62	0.55	0.45

Note: superscripts indicate significant differences between conditions at the Bonferroni adjusted significance level of 0.0083

Table 7.10: Mean values for estimated feedback time delay for balance in standing, from the Yeadon and Trewartha regression model (M1) and the adapted method (M2).

Variable	Static Platform		Sway Referenced Platform	
	EO$_{(a)}$	EC$_{(b)}$	EO$_{(c)}$	EC$_{(d)}$
M1 Delay (ms)	243	249	234	228
M1 R^2	0.83	0.83	0.85	0.89
M1 p coefficient	666[c]	676[c]	548[a,b]	584
M1 d coefficient	260	274	308	284
M1 p torque (%)	90.1	105.4	11.6	87.8
M1 d torque (%)	9.9	-5.4	88.4	12.2
M2 Delay (ms)	283	288	276	269
M2 R^2	0.82	0.83	0.84	0.88
M2 p_1 coefficient	55	63	75	56
M2 p_2 coefficient	601[c]	597[c]	466[a,b]	515
M2 d coefficient	267	279	303	291
M2 p_1 torque (%)	5.8	7.5	11.2	7.9
M2 p_2 torque (%)	65.4[a]	61.9	54.7[a]	59.3
M2 d torque (%)	28.8	30.6	34.1	32.8

Note: superscripts indicate significant differences between conditions at the Bonferroni adjusted significance level of 0.0083

There were no statistically significant interactions between the effects of platform motion and vision for the estimated delay, R^2 values, or percentage of joint torques calculated from either the Yeadon and Trewartha method or the adapted method in standing trials. There were statistically significant main effects for platform motion for the coefficients based on delayed displacement from both methods. Further analysis via multiple *t*-tests show these differences are between static platform trials with eyes open or eyes closed and sway

referenced platform trials with eyes open; group mean values and comparisons are given in table 7.10.

Table 7.11: Mean values for estimated feedback time delay for balance in handstand, from the Yeadon and Trewartha regression model (M1) and the adapted method (M2).

Variable	Static Platform		Sway Referenced Platform	
	$EO_{(a)}$	$EC_{(b)}$	$EO_{(c)}$	$EC_{(d)}$
M1 Delay (ms)	177[b]	210[a]	202	205
M1 R^2	0.76	0.78	0.75	0.75
M1 p coefficient	689	683	581	824
M1 d coefficient	243	233	270	265
M1 p torque (%)	51.0	92.6	71.5	67.0
M1 d torque (%)	49.0	7.4	28.5	33.0
M2 Delay (ms)	219[b]	291[a]	263	301
M2 R^2	0.75	0.78	0.73	0.75
M2 p_1 coefficient	37[d]	162	179	290[a]
M2 p_2 coefficient	615[c]	489	351[a]	521
M2 d coefficient	262	224	266	241
M2 p_1 torque (%)	4.0[d]	19.0	21.6	27.4[a]
M2 p_2 torque (%)	66.9[c,d]	54.6	41.2[a]	45.3[a]
M2 d torque (%)	29.0	26.4	37.2	27.3

Note: superscripts indicate significant differences between conditions at the Bonferroni adjusted significance level of 0.0083

There were no statistically significant interactions between the effects of platform motion and vision for the estimated delay, R^2 values, or percentage of joint torques calculated from either the Yeadon and Trewartha method or the adapted method in handstand trials. There was a statistically significant main effect for vision for the estimated delay calculated from the adapted method,

and a statistically significant main effect for platform motion for the percentage of joint torque based on delayed displacement from the adapted method. Further analysis via multiple *t*-tests (Table 7.11) show there was a significant increase in the estimated delay calculated from both methods between static handstand trials with eyes open and eyes closed conditions. A significant decrease in the percentage torque from delayed displacement, with a corresponding increase in the percentage torque estimated from a passive stiffness mechanism, were found when comparing static handstand trials with eyes open to sway referenced handstand trials with eyes open or eyes closed.

Increased feedback time delay between handstands with eyes open and handstands with eyes closed replicates the finding from the static session previously reported in Chapter 4. It would be expected that a sway referenced platform that successfully reduced somatosensory feedback during handstands would also result in an increased feedback time delay. Although there was a small increase in feedback time delay during the sway referenced platform condition, this difference is not statistically significant. A reason for this may be the apparent increase in passive stiffness of the wrist. In standing trials on a sway referenced platform with amplified platform rotation, previous research has shown an increase in ankle stiffness by as much as 60%, with further increased stiffness in vestibular loss patients (Peterka, 2002). Peterka (2002) suggested that the increased stiffness may help to provide additional sensory feedback during times of sensory insufficiency.

Table 7.12: Cross correlations between ankle torque and COM displacement in standing trials from the static session (reported in Chapter 4) and the static platform condition of the SOT.

	Static		SOT	
Variable	EO$_{(a)}$	EC$_{(b)}$	EO$_{(c)}$	EC$_{(d)}$
Delay (ms)	1	-1	-4	-6
R^2	0.94[c]	0.91[d]	0.77[a]	0.75[b]

Note: superscripts indicate significant differences between conditions at the significance level of 0.05; a negative delay indicates the COM peak occurs after the ankle torque peak

Further comparisons between static trials in standing from the first testing session (Chapter 4) and the static platform in the SOT show there was not a significant difference in delay from cross correlations between ankle torque and COM displacement, but there was a significant decrease in the calculated R^2 value from these cross correlations (Table 7.12). Similar comparisons in handstand trials show there were no significant differences in the calculated delay or R^2 values from cross correlations between: wrist joint torque and COM displacements, wrist flexor/extensor EMG and COM displacements, or flexor/extensor EMG and wrist joint torque (Table 7.13).

Table 7.13: Cross correlations between wrist torque and COM, EMG and COM, and between EMG and wrist torque in handstand trials from the static session (reported in Chapter 4) and the static platform condition of the SOT.

	Static		SOT	
Variable	EO$_{(a)}$	EC$_{(b)}$	EO$_{(c)}$	EC$_{(d)}$
Torque – COM: Delay (ms)	-3	9	5	25
Torque – COM: R^2	0.64	0.56	0.54	0.55
EMG – COM: Delay (ms)	107	118	117	125
EMG – COM: R^2	0.27	0.30	0.20	0.29
EMG – Torque: Delay (ms)	95	93	89	63
EMG – Torque: R^2	0.59	0.65	0.49	0.62

Note: superscripts indicate significant differences between conditions at the Bonferroni adjusted significance level of 0.0083; a negative delay indicates the COM peak occurs after the wrist torque peak

Comparisons between static trials in standing or handstand from the first testing session and those from the static platform condition in the SOT show there were no significant differences in the estimated feedback time delay from either the Yeadon and Trewartha method or the adapted method (Table 7.14). There was a significant reduction in R^2 values from both methods for standing trials, suggesting a slight change in the balance strategies used by the subjects that is not represented by the regression models employed here.

Table 7.14: Mean values for estimated feedback time delay for balance in comparison to the static session (reported in Chapter 4), from the Yeadon and Trewartha regression model (M1) and the adapted method (M2).

| | Standing | | | | Handstand | | | |
| | Static | | SOT | | Static | | SOT | |
Variable	$EO_{(a)}$	$EC_{(b)}$	$EO_{(c)}$	$EC_{(d)}$	$EO_{(e)}$	$EC_{(f)}$	$EO_{(g)}$	$EC_{(h)}$
M1 Delay (ms)	234	244	243	249	176	200	177	210
M1 R^2	0.96^c	0.94^d	0.83^a	0.83^b	0.79	0.80	0.76	0.78
M1 p coefficient	657	683	666	676	596	603	689	683
M1 d coefficient	236	252	260	274	237	237	243	233
M1 p torque (%)	-15.9	742.8	90.1	105.4	402.3	960.1	51.0	92.6
M1 d torque (%)	115.9	-642.8	9.9	-5.4	-302.3	-860.1	49.0	7.4
M2 Delay (ms)	262	278	283	288	212	244	219	291
M2 R^2	0.96^c	0.94^d	0.82^a	0.83^b	0.78^g	0.79	0.75^e	0.78
M2 p_1 coefficient	25	23	55	63	51	67	37	162
M2 p_2 coefficient	628	650	601	597	529	511	615	489
M2 d coefficient	247	267	267	279	243	240	262	224
M2 p_1 torque (%)	2.8	2.4	5.8	7.5	6.4	9.3	4.0	19.0
M2 p_2 torque (%)	69.8	69.2	65.4	61.9	64.1	60.7	66.9	54.6
M2 d torque (%)	27.4	28.3	28.8	30.6	29.5	30.0	29.0	26.4

Note: superscripts indicate significant differences between conditions at the significance level of 0.05

7.2.4. Movement Corrections

There were statistically significant interactions between the effects of platform motion and vision in standing trials for the mean ankle torques during small and large movement corrections. Statistically significant main effects for platform motion were found for mean ankle torques and the duration of torque activity for small, medium, and large movement corrections, and for the number of medium and small corrections per second. Further comparisons and group means for standing trials are given in table 7.15.

Table 7.15: Movement corrections based on joint torques for balance in standing, with large, medium, and small (L, M, S) corrections based on torque above 1, 2, and 3 SD respectively.

	Static Platform		Sway Referenced Platform	
Variable	$EO_{(a)}$	$EC_{(b)}$	$EO_{(c)}$	$EC_{(d)}$
L - Corrections/s	0.08	0.11	0.06	0.08
M - Corrections/s	$0.20^{c,d}$	$0.23^{c,d}$	$0.10^{a,b}$	$0.09^{a,b}$
S - Corrections/s	$0.45^{c,d}$	$0.44^{c,d}$	$0.19^{a,b}$	$0.20^{a,b}$
L - Mean Torque	$0.65^{c,d}$	$0.76^{c,d}$	$1.18^{a,b}$	$1.10^{a,b}$
M - Mean Torque	$0.66^{c,d}$	$0.76^{c,d}$	$1.19^{a,b}$	$1.10^{a,b}$
S - Mean Torque	$0.65^{c,d}$	$0.75^{c,d}$	$1.20^{a,b}$	$1.15^{a,b}$
L – Impulse	161	171	186	147
M – Impulse	97^{c}	112	137^{a}	121
S – Impulse	$54^{b,c}$	63^{a}	79^{a}	73
L – Duration (s)	$6.41^{c,d}$	5.48^{d}	3.65^{a}	$3.19^{a,b}$
M – Duration (s)	$3.92^{c,d}$	3.56^{d}	2.79^{a}	$2.35^{a,b}$
S – Duration (s)	$2.09^{c,d}$	1.98^{d}	1.58^{a}	$1.52^{a,b}$

Note: superscripts indicate significant differences between conditions at the Bonferroni adjusted significance level of 0.0083; mean torque and impulse are normalised to mh^2 (m =mass and h =height of COM)

Data typically show that balance in standing on a sway referenced platform has a lower number of corrections per second, with decreased burst duration and an increase in mean ankle torque. These results may provide evidence that the sway referenced platform successfully reduces somatosensory feedback, resulting in fewer corrections per second when controlling balance. Larger mean joint torques during stance on a sway referenced platform likely represents an increase in postural lean with the COM positioned further forwards. The reasons for this are unclear, but one possibility is that this may be to increase tension in the ankle plantar flexors in an attempt to either gain more sensory information from force sensitive proprioceptors or to rely more on

a passive stiffness control mechanism. Both hypotheses have been suggested by Peterka (2002), who found an increase in ankle stiffness by as much as 60% with increased support surface amplitudes, with further increased stiffness in vestibular loss patients.

It was not possible to calculate any movement corrections for handstand trials on a sway referenced platform (Table 7.16). Similar to the novice data from Chapter 5, this is likely due to short trial durations and a lack of any coordinated mechanism to maintain balance in this challenging task.

Table 7.16: Movement corrections based on joint torques for balance in handstand, with large, medium, and small (L, M, S) corrections based on torque above 1, 2, and 3 SD respectively.

	Static Platform		Sway Referenced Platform	
Variable	$EO_{(a)}$	$EC_{(b)}$	$EO_{(c)}$	$EC_{(d)}$
L - Corrections/s	$0.12^{c,d}$	0.03	0^a	0^a
M - Corrections/s	$0.32^{c,d}$	0.10	0^a	0^a
S - Corrections/s	$0.58^{c,d}$	0.21	0^a	0^a
L - Mean Torque	0.38	0.38	N/A	N/A
M - Mean Torque	0.38	0.38	N/A	N/A
S - Mean Torque	0.37	0.37	N/A	N/A
L – Impulse	51	54	N/A	N/A
M – Impulse	23	20	N/A	N/A
S – Impulse	11	11	N/A	N/A
L – Duration (s)	3.60	5.52	N/A	N/A
M – Duration (s)	1.76	1.74	N/A	N/A
S – Duration (s)	0.91	0.86	N/A	N/A

Note: superscripts indicate significant differences between conditions at the significance level of 0.05; mean torque and impulse are normalised to mh^2 (m =mass and h =height of COM)

There were statistically significant interactions between the effects of platform motion and vision in handstand trials for the RMS EMG activity of wrist flexor/extensor muscles for all movement correction magnitudes. Statistically significant main effects for platform motion were found for EMG burst duration in large and medium movement corrections, and the number of large and small movement corrections per second. Further comparisons and group means are given in table 7.17. Data typically show an increase in the number of corrections per second, with a reduced EMG burst duration, for handstands on a sway referenced platform. These results may indicate the attempt by subjects to correct a possible detection of falling, but it is unclear if this data supports a coordinated or uncoordinated response to this threat.

Table 7.17: Movement corrections based on wrist flexor/extensor EMG for balance in handstand, with large, medium, and small (L, M, S) corrections based on EMG above 1, 2, and 3 SD respectively.

	Static Platform		Sway Referenced Platform	
Variable	$EO_{(a)}$	$EC_{(b)}$	$EO_{(c)}$	$EC_{(d)}$
L - Corrections/s	$0.89^{c,d}$	1.26	1.62^{a}	2.04^{a}
M - Corrections/s	1.74^{c}	2.06	2.42^{a}	2.37
S - Corrections/s	2.23^{c}	3.13	3.68^{a}	3.39
L – RMS	0.45^{c}	0.54	0.58^{a}	0.51
M – RMS	0.43^{c}	0.51	0.57^{a}	0.52
S – RMS	0.41	0.50	0.55	0.50
L – Duration (s)	$1.24^{c,d}$	0.97	0.58^{a}	0.46^{a}
M – Duration (s)	$0.53^{c,d}$	0.45^{d}	0.34^{a}	$0.29^{a,b}$
S – Duration (s)	$0.28^{b,c,d}$	0.25^{a}	$0.23^{a,d}$	$0.19^{a,c}$

Note: superscripts indicate significant differences between conditions at the Bonferroni adjusted significance level of 0.0083

Comparisons between static trials in standing from the first testing session (Chapter 4) and the static platform in the SOT show a significant increase in mean ankle torque during the SOT, and an increase in torque impulse during

the SOT with eyes closed (Table 7.18). Larger mean joint torques during stance on a static platform in the SOT would suggest that recent experiences of the sway referenced platform encourages subjects to position their COM further forward for subsequent trials. This further supports the assertion that the sway referenced platform has residual effects on an individual's balance strategy. This may also suggest that, instead of altering of the way the CNS weighs different sensory inputs, changes in balance performance after experiencing the sway referenced platform may be due to increased postural lean to increase tension in the ankle plantar flexors. Further study in this regard is required to understand the full implications of the sway referenced platform and the influence it has on an individual's balance strategies.

Table 7.18: Mean values for movement corrections based on joint torques for balance in the static session (reported in Chapter 4) and the static platform condition of the SOT.

	Standing				Handstand			
	Static		SOT		Static		SOT	
Variable	$EO_{(a)}$	$EC_{(b)}$	$EO_{(c)}$	$EC_{(d)}$	$EO_{(e)}$	$EC_{(f)}$	$EO_{(g)}$	$EC_{(h)}$
L - Corrections/s	0.09	0.11	0.08	0.11	0.19^g	0.08	0.12^e	0.03
M - Corrections/s	0.19	0.22	0.20	0.23	0.41^g	0.18	0.32^e	0.10
S - Corrections/s	0.41	0.44	0.45	0.44	0.75	0.32	0.58	0.21
L - Mean Torque	0.57	0.59^d	0.65	0.76^b	0.46	0.54^h	0.38	0.38^f
M - Mean Torque	0.56^c	0.58^d	0.66^a	0.76^b	0.46	0.54^h	0.38	0.38^f
S - Mean Torque	0.57	0.59^d	0.65	0.75^b	0.46	0.54^h	0.37	0.37^f
L – Impulse	127	124^d	161	171^b	50	75	51	54
M – Impulse	85	84	97	112	25	38	23	20
S – Impulse	45	43^d	54	63^b	14	21^h	11	11^f
L – Duration (s)	6.36	6.50	6.41	5.48	3.40	3.67	3.60	5.52
M – Duration (s)	4.49	4.15	3.92	3.56	1.60	1.77	1.76	1.74
S – Duration (s)	2.42	2.18	2.09	1.98	0.85	0.92	0.91	0.86

Note: superscripts indicate significant differences between conditions at the significance level of 0.05; mean torque and impulse are normalised to mh^2 (m =mass and h =height of COM)

Comparisons between static trials in handstand from the first testing session and the static platform in the SOT show a significant decrease in the number of large and medium corrections per second in trials with eyes open (Table 7.18). In contrast to standing trials, handstand with eyes closed showed a significant decrease in mean wrist torque for all correction magnitudes, and a decrease in torque impulse for small corrections. Collectively these results may suggest that recent experience of balancing in handstand on a sway referenced platform reduces the effectiveness of the balance strategy usually employed. This may represent a change to how the CNS weighs the different sensory inputs during balance, as was previously suggested.

Table 7.19: Movement corrections based on wrist flexor/extensor EMG for balance in handstand in the static session (reported in Chapter 4) and the static platform condition of the SOT.

	Static		SOT	
Variable	$EO_{(a)}$	$EC_{(b)}$	$EO_{(c)}$	$EC_{(d)}$
L - Corrections/s	0.75	0.88	0.89	1.26
M - Corrections/s	1.75	1.67	1.74	2.06
S - Corrections/s	2.20	2.41	2.23	3.13
L – RMS	0.56	0.61	0.45	0.54
M – RMS	0.53	0.59	0.43	0.51
S – RMS	0.51	0.55	0.41	0.50
L – Duration (s)	1.31	1.24	1.24	0.97
M – Duration (s)	0.55	0.52	0.53	0.45
S – Duration (s)	0.28	0.28	0.28^{d}	0.25^{c}

Note: superscripts indicate significant differences between conditions at a significance level of 0.05

Few significant differences were found regarding the analysis of movement corrections based on wrist flexor/extensor EMG between static trials in handstand from the first testing session and the static platform in the SOT (Table 7.19).

7.3. Summary

The sway referenced platform resulted in increased sway in standing as measured by the traditional balance metrics. While past literature using the SOT has been mainly concerned with clinical populations with vestibular loss or feedback time deficits, these results are in agreement with this literature, which has shown a degradation of postural stability caused by the decreased accuracy of somatosensory cues during sway referenced conditions (Nashner et al., 1982; Nashner et al., 1983; Peterka, 2002; Peterka and Benolken, 1995). Further increases in postural sway were observed for subjects balancing on a sway referenced platform with eyes closed. This may support the suggestion of a link between how visual and somatosensory information are processed (Peterka and Benolken, 1995), or may simply be a result of increased sway due to a further decrease in sensory information. A residual effect from the sway referenced platform appears to result in increased sway during static stance compared to a previous session, supporting the view that recent environmental changes may alter how the CNS weighs the relative information from each sensory system (McCollum et al., 1996).

Although inaccurate somatosensory information is harder to supress than inaccurate visual or vestibular information (Nashner et al., 1982), adults will typically respond to the sensory conflicts imposed by a sway referenced platform by ignoring irrelevant sensory cues and focusing on those pertinent to a vertical orientation (Nashner et al., 1983). Children of 6 to 9 years of age will respond to sensory cues that are perceptually correct, and possibly orientationally incorrect, usually resulting in a loss of balance (Nashner et al., 1983). In the current research experienced handstanders balancing on a sway referenced platform in the handstand position found it particularly difficult to balance with reduced sensory information from wrist somatosensory proprioceptors, usually resulting in a loss of balance within five seconds. Similar to standing, a reduced performance during handstand balance on static platform within the SOT was observed when compared to a previous session involving only static balance. This would appear to indicate the relationship between somatosensory and visual cue utilisation, and how this is affected by

recent environment experiences, is similar in both standing and handstand postures.

Further analysis of COP trajectories during balance in handstand and standing in each of the SOT conditions revealed little insight into the causes for increased sway during sway referenced conditions. Similarly, little change to the estimated feedback time delays during static platform and sway referenced platform conditions were evident. It would be expected that a sway referenced platform that successfully reduced somatosensory feedback during balance would also result in an increased feedback time delay. Although there was a small increase in feedback time delay during the sway referenced platform condition, this difference is not statistically significant. A reason for this may be the apparent increase in passive stiffness at the controlling joint.

Peterka (2002) found that sway referenced platform motion with amplified rotation could increase active and passive muscle stiffness by as much as 60%, and suggested that the increased stiffness may help to provide additional sensory feedback during times of sensory insufficiency. This view may be supported further by the results of the current research, which found a significant increase in mean joint torques for all movement correction magnitudes during standing trials on a sway referenced platform. One possibility is that increased joint torques, and increased tension in the ankle plantar flexors, will increase sensory information from force sensitive proprioceptors in the musculotendinous complex. Alternatively, this may simply be an attempt to rely on a passive stiffness mechanism to either control balance or to reduce sway velocity to allow more time for an appropriate response to be initiated. The latter interpretation seems to be the most likely, as subjects typically displayed fewer corrections per second when controlling balance on the sway referenced platform. In addition, standing trials during the static platform condition of the SOT compared to the static session displayed a significant reduction in R^2 values calculated from both cross correlations and regression models, suggesting a slight change in the balance strategies used by subjects that is not represented by the analyses employed here.

The aim of this chapter was to examine how balance in standing and handstand may be affected by altered sensory feedback and to provide insight into the importance of ankle and wrist somatosensory feedback in human balance. Peterka (2002) concluded that the simple act of standing quietly relies on a remarkably complex sensorimotor control system. It seems likely that during handstand balance the process is essentially the same. With reduced muscular strength in the wrist compared to the ankle, and an increased moment of inertia about the supporting joint in handstand, the demands on the CNS system increases. One consequence may be the requirement for more finely tuned somatosensory feedback to affect an appropriate response in a timely fashion. In the current research experienced handstanders experiencing the sway referenced platform appear to have found the subsequent reduction in somatosensory feedback impossible to manage. Results suggest that adequate wrist and hand somatosensory feedback is essential for successful balance in the handstand position.

CHAPTER 8

SUMMARY AND CONCLUSION

The purpose of the current research was to examine how a novel balance task is learnt by individuals with a mature neurological system, and to investigate the responses of experienced hand balancers to mechanical and sensory perturbations. Within this chapter the extent to which this aim has been achieved is considered. The methods used within the study are summarised and limitations and potential improvements are identified. The research questions posed are addressed and future applications are discussed.

8.1. Thesis Summary

Chapter 2 reviewed the literature surrounding balance and postural control. The relevance of both the neurological and the mechanical implications for postural control were highlighted, and a means through which these may be assessed were provided. The development of postural control as a child ages was discussed, and balance in the handstand position was suggested as a possible alternative to assessing how postural control is learnt.

8.1.1. Data Collection and Processing

Chapter 3 detailed the collection of the experimental data in the current research, and described the experimental protocol that was used for both studies. The methods used to process the data were explained, highlighting areas where specific care was taken to minimise and reduce any systematic and random errors within the data.

Kinematic, kinetic, EMG, and anthropometric data were collected on novice and experienced handstanders during balance in three postures, including: double leg stance, single leg stance, and handstand.

8.1.1.1. Kinematic Data

Kinematic data were collected via a Vicon system with nine T20 cameras using a sample frequency of 200 Hz, employing a set of 53 markers to divide the body into 18 segments. Marker displacements were filtered with a fourth order, zero lag, low-pass Butterworth filter with a cut-off frequency of 10 Hz. Segment local coordinate systems were constructed and quaternion algebra was used to calculate: segment COM linear displacements, velocities, and accelerations; and segment angular velocities and accelerations relative to the global coordinate system.

8.1.1.2. Kinetic Data

Kinetic data were collected via two Bertec strain gauge force plates with a sample frequency of 2000 Hz, before being resampled to 200 Hz. Data were resampled using the Matlab decimate function, where the signal was first filtered with a low-pass anti-aliasing filter before being resampled at the lower rate. Raw COP data were saved for further analysis using nonlinear analysis tools that require data to be unfiltered. Force, COP, and moment data were filtered using a fourth order, zero lag, low-pass Butterworth filter with a cut-off frequency of 10 Hz.

8.1.1.3. Anthropometric Data

Subject segmental inertia parameters were determined via the geometric inertia model of Yeadon (1990). Adjustments were made to alter the geometric segmental definitions of the trunk to match those defined from the kinematic data.

8.1.1.4. Inverse Dynamics

Kinetic, kinematic, and anthropometric data were used to calculate three dimensional joint moments and forces via wrench notation, based on the work of Dumas et al. (2004). Great care was taken to correct for systematic errors during trials with a moving platform by adjusting both the COP location and the force vector calculated from the force plate software. Three dimensional joint moments from right and left joints were combined to obtain two dimensional

joint moments about the global x-axis for the ankles, hips, shoulders, and wrist joints.

8.1.1.5. EMG Data

Muscle activity data were collected on 16 locations via the Delsys Trigno wireless EMG system, using a sample frequency of 2000 Hz. Raw EMG data were filtered with a fourth order, zero lag, band-pass Butterworth filter with cut-off frequencies of 20 Hz and 450 Hz. EMG data were analysed unfiltered for perturbation trials and filtered using a fourth order, zero lag, low-pass Butterworth filter with a cut-off frequency of 10 Hz for static balance trials.

8.1.1.6. Centre of Mass Calculations

The horizontal displacement and velocity of the COM was determined via a combination of the segmental method from kinematic and anthropometric data, and the double integration of ground reaction force divided by body mass, following the equations from Yeadon and Trewartha (2003). Additional modifications were made to the COM displacement provided by the segmental method, by adjusting the COM positions of the segments that form the torso, similar to procedure of Kingma et al. (1995).

8.1.2. Assessing Balance

Chapter 4 examined the assumptions used by various data analysis methods to assess balance, with specific reference to the calculation and implementation of different balance metrics used within the literature. Twelve experienced handstanders completed the first part of study two. Subjects were required to perform five trials for a maximum of 30 seconds in each of the six conditions, including: double leg stance, single leg stance, and handstand, each with eyes open and eyes closed conditions. Traditional balance measures based on COP trajectories were compared with more sophisticated nonlinear time series analysis techniques. Analysis showed that COP signals contained a degree of deterministic structure, reinforcing the view that postural sway is not purely a random process. A summary of each of the groups of balance measures used within the current research is presented in tables 8.1 to 8.4.

Table 8.1: Summary of the traditional balance measures used in the current research

Variable	Description
Range, SD, mean SV	Standard deviation, range, and mean sway velocity of the COP signal, indicating how well the individual is controlling and minimising the displacement of their COP trajectory

Table 8.2: Summary of the nonlinear and recurrence balance measures used in the current research

Variable	Description
Determinism	Assesses whether the underlying process of the signal is deterministic or stochastic; a higher value indicates balance is controlled by a deterministic process
Lyapunov exponent/ Divergence	The exponential divergence of local trajectories, relating to the stretching, folding, and contraction rate of the signal when reconstructed in the higher dimensional state space. Higher values suggest balance is controlled by a nonlinear process with quickly changing dynamics
Entropy/ Sample Entropy	The complexity and regularity within the signal, relating to the loss of information as the system evolves. Higher values suggest a complex nonlinear process is controlling balance
Trend	The amount of drift in the signal, with zero describing a stationary process. Non-zero values suggest drift within balance

Table 8.3: Summary of the feedback time delay balance measures used in the current research

Variable	Description
Delay	An estimate of the feedback time delay based on delayed regressions, incorporating: time to reach sensory thresholds, neurological delay, and electromechanical delay
R^2	The R^2 value for the regression model of torque against COM motion that was used to determine the feedback time delay
Torque percentages	The torque from proportional and derivative gains from the regression model, providing an estimate of passive stiffness control and the importance of COM displacement and velocity for determining the total torque generated to maintain balance

Table 8.4: Summary of the movement correction balance measures used in the current research

Variable	Description
Corrections per second	The number of small, medium, and large corrections per second used to maintain balance, based on joint torques or EMG activity
Mean Torque/ Torque Impulse/ RMS	The average amount of torque or muscle activity during small, medium, and large movement corrections
Burst duration	The average duration of small, medium, and large movement corrections

Data suggests that the best balance metrics for distinguishing between each of the six conditions was the traditional balance measure of sway velocity. Sway velocity was able to distinguish between each posture, and between eyes open and eyes closed conditions in each posture. In contrast, nonlinear measures successfully differentiated between each posture, but not between eyes open and eyes closed conditions within each posture. Traditional measures of balance appear to be more sensitive to changes in balance performance, but cannot provide any further information on the underlying process of balance. Nonlinear measures of balance appear to offer insight into the underlying deterministic processes that control balance, offering measures of system determinism, complexity, and predictability.

Further assessments of balance performance and the underlying process of postural control were provided by estimates of feedback time delay and movement corrections. Balance was modelled as a simple proportional and derivative controlled process, where joint torques about the ankle or wrist were regressed against COM displacements and velocities at earlier times based on the method of Yeadon and Trewartha (2003). The time that provided the largest R^2 value was used as an estimate of the feedback time delay for postural control. An adapted model was also used, where a third term was entered into the regression model based on the COM displacement with zero delay, representing the torque due to a passive stiffness mechanism.

Feedback time delay estimates from the adapted method were typically larger than those from the Yeadon and Trewartha method, supporting the view that contributions of a passive stiffness mechanism may cause underestimations of feedback time delay from the Yeadon and Trewartha method (Yeadon and Trewartha, 2003). Typical estimates for feedback time delay from the adapted method were approximately: 265 ms for double leg standing trials, 225 ms for single leg standing trials, and 220 ms for handstand trials. Feedback time delay estimates were typically higher for trials with eyes closed compared to trials with eyes open for all postures.

Extremely high R^2 values for standing trials are consistent with modelling human standing balance as a simple inverted pendulum about the ankle joint. Lower R^2 values in handstand are still promising, but may suggest that other factors need to be considered. Yeadon and Trewartha (2003) suggested that one cause for the lower R^2 values could be due to noise within the sensory system resulting in errors in the subsequent responses. This view may be supported by the high R^2 values found in standing trials, where sensory noise may be expected to be less. Additionally, a general decrease in feedback time delay estimates with increased mean sway velocity may suggest that velocity dependent sensory thresholds are of importance.

Movement correlations were calculated based on changes in wrist and ankle joint torques. Data typically show that balance in standing exhibits bursts of torque activity that are longer and with a higher torque impulse compared to balance in handstand. Lower numbers of movement corrections per second are evident in standing trials, with the largest number of corrections occurring in handstand with eyes open and single leg stance with eyes open.

Reduced mean torque and torque impulse during all movement corrections in handstand are indicative of the reduced muscular strength of the muscles found in the forearm compared to the lower leg. It would appear this leads to the requirement for a larger number of corrections per second, but with reduced burst duration, while balancing in handstand.

Assessments of feedback time delay and movement corrections appear to provide both an insight into the control of posture and help distinguish one condition from another. Future research may wish to employ both feedback time delay and movement corrections and magnitudes simultaneously to delve further into the postural control process.

8.1.3. Learning to Balance

Chapter 5 assessed which balance metrics best characterise improvements in balance performance when a novice learns to balance in handstand. Thirteen subjects completed all parts of study one, where they were required to practice handstands three times a week for 10-15 minutes each session over a period of eight months. Subjects were tested once a month to examine performance in handstand along with various kinematic and kinetic variables. The main criterion for assessing handstand performance was the duration that participants could maintain independent balance in the handstand position. All participants were unable to maintain independent balance in handstand for more than five seconds when attending the first assessment session.

Novice handstanders showed a large variation in handstand balance performance based on all balance metrics. With practice and a longer duration in handstand this variability generally reduces. Large amounts of variation for handstand trials of short duration make it extremely difficult to compare data to determine if a linear or quadratic relationship is present. At the end of eight months of practicing handstands most subjects could not perform handstands for longer than 15 seconds duration, with only three subjects able to perform handstands for more than 20 seconds. Generally, with increased duration in handstand subjects displayed reduced sway as measured by traditional measures of balance. A more marked change in nonlinear measures of balance can be seen, with quicker reductions in variance for some nonlinear measures of balance than in the traditional measures. It may be that more pronounced changes in nonlinear measures represent changes in the subjects' underlying process of postural control, whereas less pronounced changes in traditional measures relate more to their general ability or performance in the balance task.

Data suggests that the regression models of balance used to estimate feedback time delay may be a poor estimate of the postural control strategies employed when novices first learn to balance. With increased competence in handstand balance, as described by longer trial durations, regression models appear to become more applicable, suggesting subjects begin to adapt a strategy that is close to the one suggested by the regression model. Estimates of torque contributions from these regression models begin to plateau and resemble experienced handstanders for handstand trials above 15 seconds duration. Changes in torque contribution estimates may suggest that subjects are beginning to rely more on sensory feedback for postural control.

Using a constraints led approach Newell (1986) redefined motor learning as an ongoing dynamic process involving a search for and stabilisation of specific functional movement patterns across the perceptual-motor landscape (Davids et al., 2008). In this way the exponential relationship between balance performance and trend and divergence may be described by the searching for a suitable pattern, or strategy, suggested by the first stage of Newell's constraints theory. Practice in the task results in a continual exploration of the perceptual-motor landscape, eventually leading to the emergence of an approximate solution to the task (Thelen, 1995). The slower changes to sway range and sample entropy would relate to refinement of this approximate solution, linked to improved fine control within the balance task.

8.1.4. Responses to Mechanical Perturbations

Chapter 6 evaluated estimates of feedback time delay provided by cross correlations and delayed regression models by comparison to the values provided by EMG latencies to a discrete perturbation. Eleven experienced handstanders completed the second part of study two. Subjects experienced a total of twelve platform perturbations in each posture, with three trials of each of the four platform perturbations, including: forwards and backwards translations of 0.1 m at 0.2 m·s^{-1}, and forwards and backwards translations of 0.05 m at 0.1 m·s^{-1}.

EMG latencies in standing trials were calculated from the start of the platform translation to the time of the first major EMG burst via visual inspection (Tillin et al., 2010). Feedback time delay estimates from cross correlations were calculated between: COM and ankle/wrist joint torque, COM and ankle/wrist EMG, and ankle/wrist joint torques and ankle/wrist EMG signals. Further estimates of feedback time delay were provided by delayed regression models via the Yeadon and Trewartha method and the adapted method.

Ankle EMG latencies to a discrete perturbation in standing were 96 to 126 ms, with estimates of feedback time delays provided by delayed regression models that were on average 24 ms longer for the Yeadon and Trewartha method and 46 ms longer for the adapted method. Whereas, estimates of feedback time delays provided by cross correlations of ankle joint torque and COM displacement produced values that were on average 62 ms lower than that of EMG latencies in standing.

Wrist EMG latencies to a discrete perturbation in handstand were 102 to 192 ms, with estimates of feedback time delays provided by delayed regression models that were on average 3 ms longer for the Yeadon and Trewartha method and 32 ms longer for the adapted method. Estimates of feedback time delays provided by cross correlations of wrist joint torque and COM displacement produced values that were on average 105 ms lower than that of EMG latencies in handstand.

Results suggest that cross correlations between joint torques and COM displacements can severely underestimate feedback time delay to a discrete perturbation. Using cross correlations to estimate feedback time delays during balance is not recommended. Delayed regression models seem to be an appropriate and useful tool for estimating feedback time delays during balance.

Shorter delays for the Yeadon and Trewartha method were expected, as passive stiffness within the musculotendinous unit is likely to produce extra torque when forced into an eccentric action. The extra torque produced by this

passive stiffness will have approximately zero delay and will cause the estimated feedback time delay based on delayed regressions between joint torque and COM motion to be slightly underestimated. The adapted method addressed this issue by including a third term into the regression model based on COM displacement with zero delay. These results appear to support the use of this third term as a means of estimating the effect of passive stiffness on feedback time delay.

Differences between EMG latencies and estimates of feedback time delay from regression models are most likely due to an electromechanical delay between the start of the EMG response to the start of a change in ankle or wrist joint torque. Comparisons between feedback time delay estimates in static balance and perturbed balance show differences of approximately 100 ms for standing trials and up to 25 ms for handstand trials. These differences are likely due to the extra time required to reach sensory thresholds in static balance conditions, with the lower difference in handstand trials indicating the difficult nature of balance in handstand.

8.1.5. Sensory Perturbations and Restrictions

Chapter 7 assessed how balance in standing and handstand may be affected by altered sensory feedback. Ten experienced handstanders completed the final stage of study two. Using the algorithms of Barton et al. (2006) the Stewart platform within the CAREN system was controlled so that horizontal and vertical translations of the platform were combined with rotations about the mediolateral axis so the platform could rotate about a virtual point. The virtual point was determined by markers placed on the subject's ankle or wrist joints while in standing or handstand respectively. Body sway was tracked by markers at the next proximal joint, the knee for standing and the elbow for handstand, so that the rotation of the platform would track sway about the ankle or wrist. This procedure simulated the sway referenced platform motion of the sensory organisation test in both a standing and a handstand posture in an attempt to reduce ankle and wrist joint movement whilst allowing unrestricted body sway.

Subjects completed three trials in each of the eight conditions, including: standing on a static and sway referenced platform with eyes open and eyes closed, and handstand on a static and sway referenced platform with eyes open and eyes closed.

The sway referenced platform resulted in increased sway in standing as measured by the traditional balance metrics. Further increases in postural sway were observed for subjects balancing on a sway referenced platform with eyes closed. A residual effect from the sway referenced platform appears to result in increased sway during static stance compared to a previous session, supporting the view that recent environmental changes may alter how the CNS weighs the relative information from each sensory system (McCollum et al., 1996).

Experienced handstanders balancing on a sway referenced platform in the handstand position found it particularly difficult to balance with reduced sensory information from wrist somatosensory proprioceptors, usually resulting in a loss of balance within five seconds. Similar to standing, a reduced performance during handstand balance on static platform within the sensory organisation test was observed when compared to a previous session involving only static balance. This would appear to indicate the relationship between somatosensory and visual cue utilisation, and how this is affected by recent environment experiences, is similar in both standing and handstand postures.

Further analysis of COP trajectories during balance in handstand and standing in each of the conditions revealed little insight into the causes for increased sway during sway referenced conditions. Similarly, little change to the estimated feedback time delays during static platform and sway referenced platform conditions were evident. It would be expected that a sway referenced platform that successfully reduced somatosensory feedback during balance would also result in an increased feedback time delay. Although there was a small increase in feedback time delay during the sway referenced platform

condition, this difference is not statistically significant. A reason for this may be the apparent increase in passive stiffness at the controlling joint.

Peterka (2002) found that sway referenced platform motion with amplified rotation could increase active and passive muscle stiffness by as much as 60%, and suggested that the increased stiffness may help to provide additional sensory feedback during times of sensory insufficiency. This view may be supported further by the results of the current research, which found a significant increase in mean joint torques for all movement correction magnitudes during standing trials on a sway referenced platform. One possibility is that increased joint torques, and increased tension in the ankle plantar flexors, will increase sensory information from force sensitive proprioceptors in the musculotendinous complex. Alternatively, this may simply be an attempt to rely on a passive stiffness mechanism to either control balance or to reduce sway velocity to allow more time for an appropriate response to be initiated. The latter interpretation seems to be the most likely, as subjects typically displayed fewer corrections per second when controlling balance on the sway referenced platform.

8.2. Limitations and Future Directions

The assumption of planar motion may be reasonable for balance in double leg stance, however, this may not be true for single leg stance or handstands. Several subjects were observed producing out of plane movements during attempts to remain balanced, such as flexing the elbows or abducting the hips during handstands. Although three dimensional joint moments were calculated in an attempt to address this issue, data were only analysed from a two dimensional perspective. Future research may wish to pursue additional methods of assessing balance that incorporates three dimensional motions. This would be particularly useful for assessing balance in single leg stance, where muscles crossing the ankle joint are likely to result in alterations to both mediolateral and anteroposterior sway.

Several methods of assessing balance have been designed to examine the trajectory of the COP. There is a growing number of sophisticated time series analysis tools employed in this area, but they remain focused on examining the trajectory of the COP, often in just one dimension. It may be possible to estimate the higher dimensional state space of a system via the delayed coordinates of a one dimensional signal, as discussed in Chapter 4. However, it is unwise to assume this method can accurately reconstruct the system in its entirety from just the COP trajectory. One alternative would be to reconstruct the state space from multiple signals, such as joint angles, joint torques, EMG, COM motion, and COP trajectories. Such an approach may provide further insight into the role of each signal in the postural control system, and may provide more insight into this challenging area of research. Before such an approach can be attempted, three main issues will need to be addressed: redundancy, scaling, and delays.

Constructing the state space from multiple signals may result in a space that has higher dimensions than is required, and may lead to incorrect conclusions regarding which variables are of importance for the system to operate. In addition, signals with higher values, such as forces, may be given more importance than signals with lower values, such as displacements or EMG. A system incorporating such variables will likely use multiple gains to scale the signals in a meaningful way. Discovering these gains would be of enormous value in postural control research, however, this becomes increasingly difficult with a higher number of variables. The above difficulties are compounded if one or more of the variables required by the system to operate have a time delay relative to the other variables.

8.3. Research Questions

Four research questions were presented in Chapter 1, with each being addressed in Chapters 4, 5, 6, and 7 respectively. A summary of these are presented here.

Q1. How are balance metrics expressed differently when balancing in different postures; including handstand, single leg stance and normal standing?

If the aim of a study is to assess balance performance, with no interest in the underlying postural control process, such as in an intervention study, then the traditional measure of sway velocity appears to be sufficient. If a researcher aims to delve further into the processes of postural control, more advanced analyses will be required. Although there is a growing number of studies within this area that are employing sophisticated nonlinear analysis methods, researchers must be clear in how these techniques inform on the underlying process of postural control. Assessment of feedback time delay and movement corrections may offer more insight into this process.

Q2. Which balance metrics best characterise improvements in balance performance when a novice first learns to balance in handstand?

No balance metric can be considered to be appropriate for assessing handstand performance when a novice first learns to balance in handstand, as all measures show large amounts of variation for trials of short duration. Some nonlinear measures of balance, such as divergence and trend, appear to be sensitive to improvements in handstand performance based on handstand durations of more than ten seconds. As handstand balance improves and independent balance can be maintained for longer than 20 seconds, regression models, and their estimates of feedback time delay and the percentage torque from passive stiffness and delayed COM motion, appear to become appropriate approximations of the postural control strategies employed by the subjects. Postural control strategies appear to resemble those of experienced handstanders when the novice was able to maintain independent handstand balance for more than 20 seconds duration.

Q3. How are the responses to mechanical perturbations different when balancing in handstand and normal stance postures?

EMG latencies to a discrete platform perturbation were generally shorter for standing trials than for handstand trials, with a mean latency of 111 ms for

standing trials and 158 ms for handstand trials. Similarly, estimates of feedback time delay were shorter for standing trials than handstand trials, with a mean delay of 157 ms for standing trials and 190 for handstand trials. However, the difference between EMG latencies and estimates of feedback time delays were smaller for handstand trials, suggesting a smaller electromechanical delay. This is supported by the delays from cross correlations between EMG and torque, with a lower delay of 90 ms for handstand trials compared to 150 ms fom standing trials.

Cross correlations between ankle and hip torques in standing, and between wrist and shoulder torques, and wrist and hip torques in handstand show no significant differences between delay estimates in standing and handstand trials. Data suggests the main strategy employed to maintain balance after a platform perturbation in standing was an ankle strategy with compensatory hip torques. Similarly, the main strategy employed to maintain balance after a platform perturbation in handstand was a wrist strategy with compensatory shoulder and hip torques. Although there appears to be some large intersegmental delays within the current findings, results suggest little difference between response strategies to a perturbation in standing versus handstand.

Q4. In what way is balance affected by altered sensory inputs, and does this result in a change to the corrective strategies used to maintain balance?

The sway referenced platform resulted in increased sway in standing as measured by the traditional balance metrics. Further increases in postural sway were observed for subjects balancing on a sway referenced platform with eyes closed. A residual effect from the sway referenced platform appears to result in increased sway during static stance compared to a previous session. Experienced handstanders balancing on a sway referenced platform in the handstand position found it particularly difficult to balance with reduced sensory information from wrist somatosensory proprioceptors, usually resulting in a loss of balance within five seconds. Similar to standing, a reduced performance

during handstand balance on static platform within the sensory organisation test was observed when compared to a previous session involving only static balance. This would appear to indicate the relationship between somatosensory and visual cue utilisation, and how this is affected by recent environment experiences, is similar in both standing and handstand postures.

Further analysis of COP trajectories during balance in handstand and standing in each of the conditions revealed little insight into the causes for increased sway during sway referenced conditions. Similarly, little change to the estimated feedback time delays during static platform and sway referenced platform conditions were evident. It would be expected that a sway referenced platform that successfully reduced somatosensory feedback during balance would also result in an increased feedback time delay. Although there was a small increase in feedback time delay during the sway referenced platform condition, this difference is not statistically significant. A reason for this may be the apparent increase in passive stiffness at the controlling joint.

8.4. Conclusions

The purpose of the current research was to examine how a novel balance task is learnt by individuals with a mature neurological system, and to investigate the responses of experienced hand balancers to mechanical and sensory perturbations. Data from this study suggests that the best balance metrics for distinguishing between each of the balance conditions was the traditional balance measure of sway velocity. Nonlinear measures of balance appear to offer insight into the underlying deterministic processes that control balance, offering measures of system determinism, complexity, and predictability. Assessments of feedback time delay and movement corrections appear to provide both an insight into the postural control process and help distinguish one condition from another. In addition, both feedback time delay and movement corrections and magnitudes may be used simultaneously to delve further into the postural control process.

Generally, with increased duration in handstand novice subjects displayed reduced sway as measured by traditional measures of balance. A more marked change in nonlinear measures of balance can be seen, with quicker reductions in variance for some nonlinear measures of balance than in the traditional measures. It may be that more pronounced changes in nonlinear measures represent changes in the subjects' underlying process of postural control, whereas less pronounced changes in traditional measures relate more to their general ability or performance in the balance task.

Results suggest that cross correlations between joint torques and COM displacements can severely underestimate feedback time delay to a discrete perturbation. Using cross correlations to estimate feedback time delays during balance is not recommended. Delayed regression models seem to be an appropriate and useful tool for estimating feedback time delays during balance. Findings support the use of the third term in the adapted regression model as a means of estimating the effect of passive stiffness on feedback time delay. Differences between EMG latencies and estimates of feedback time delay from regression models are most likely due to an electromechanical delay between the start of the EMG response to the start of a change in ankle or wrist joint torque.

REFERENCES

Alderton, A. -K., Moritz, U., and Moe-Nilssen, R. (2003). Forceplate and accelerometer measures for evaluating the effect of muscle fatigue on postural control during one-legged stance. *Physiotherapy Research International.* **8**, 187-199.

Allum, J. H. J. and Honegger, F. (1998). Interactions between vestibular and proprioceptive inputs triggering and modulating human balance-correcting responses differ across muscles. *Experimental Brain Research.* **121**, 478-494.

Altmann , S. L. (2005). *Rotations, quaternions, and double groups.* Mineola, New York: Dover Publications.

Asseman, F. and Gahéry, Y. (2005). Effects of head position and visual condition on balance control in inverted stance. *Neuroscience Letters.* **375**, 134-137.

Asseman, F., Caron, O., and Cremiéux, J. (2004). Is there a transfer of postural ability from specific to unspecific postures in elite gymnasts. *Neuroscience Letters.* **358**, 83-86.

Asseman, F., Caron, O., and Cremiéux, J. (2005). Effects of the removal of vision on body sway during different postures in elite gymnasts. *International Journal of Sports Medicine.* **26**, 116-119.

Astrom, K. J. (2006). *Introduction to stochastic control theory.* Mineola, New York: Dover Publications.

Baratto, L., Morasso, P.G., Re, C., and Spada, G. (2002). A new look at posturographic analysis in the clinical context: Sway-density versus other parameterization techniques. *Motor Control.* **6**, 246-270.

Barton, G., Vanrenterghem, J., Lees, A., and Lake, M. (2006). A method for manipulating a movable platform's axes of rotation: A novel use of the CAREN system. *Gait and Posture.* **24**, 510-514.

Benda, B. J., Riley, P. O., and Krebs, D. E. (1994). Biomechanical relationship between center of gravity and center of pressure during standing. *IEEE Transactions on Rehabilitation Engineering.* **2**(1), 3-10.

Bernstein, N. (1967). *Coordination and regulation of movements.* New York: Pergamon Press.

Bisdorff, A. R., Wolsley, C. J., Anastasopoulos, D., Bronstein, A. M., and Gresty, M. A. (1996). The perception of body verticality (subjective postural vertical) in peripheral and central vestibular disorders. *Brain.* **119**, 1523-1534.

Blackburn, J. T., Riemann, B. L., Myers, J. B., and Lephart, S. M. (2003). Kinematic analysis of the hip and trunk during bilateral stance on firm, foam, and multiaxial support surfaces*. Clinical Biomechanics.* **18**, 655-661.

Blaszczyk, J. W. (2008). Sway ratio - a new measure for quantifying postural stability. *Acta Neurobiologiae Experimentalis.* **68**, 51-57.

Bloem, B. R., Visser, J. E. and Allum, J. H. (2003). Posturography. In: Hallett, M. (Ed), *Movement Disorders – Handbook of Clinical Neurophysiology.* Elsevier, Amsterdam, pp. 295-336.

Bonnet, C. T., Kinsella-Shaw, J. M., Frank, T. D., Bubela, D. J., Harrison, S. J., and Turvey, M. T. (2010). Deterministic and stochastic postural processes: Effects of task, environment, and age. *Journal of Motor Behavior.* **42**(1), 85-97.

Bothner, K. E. and Jensen, J. L. (2001). How do non-muscular torques contribute to the kinetics of postural recovery following a support surface translation? *Journal of Biomechanics.* **34**, 245-250.

Bottaro, A., Casadio, M., Morasso, P. G., and Sanguineti, V. (2005). Body sway during quiet standing: is it the residual chattering of an intermittent stabilization process? *Human Movement Science.* **24**, 588-615.

Bottaro, A., Yasutake, Y., Nomura, T., Casadio, M., and Morasso, P. (2008). Bounded stability of the quiet standing posture: an intermittent control model. *Human Movement Science.* **27**, 473-495.

Buckley, J. G., Heasley, K., Scally, A., and Elliott, D. B. (2005). The effects of blurring vision on medio-lateral balance during stepping up or down to a new level in the elderly. *Gait and Posture.* **22**, 146-153.

Camicioli, R., Panzer, V. P., and Kaye, J. (1997). Balance in the healthy elderly: Posturography and clinical assessment. *Archives of Neurology*, **54**(8), 976-981.

Cappa, P., Patanè, F., Rossi, S., Petrarca, M., Castelli, E., and Berthoz, A. (2008). Effect of changing visual condition and frequency of horizontal oscillations on postural balance of standing healthy subjects. *Gait and Posture.* **28**, 615-626.

Caron, O., Faure, B., and Brenière, Y. (1997). Estimating the centre of gravity of the body on the basis of the centre of pressure in standing posture. *Journal of Biomechanics.* **30**, 1169-1171.

Carroll, J. P. and Freedman, W. (1993). Nonstationary properties of postural sway. *Journal of Biomechanics.* **26**, 409-416.

Casadio, M., Morasso, P., and Sanguineti, V. (2005). Direct measurement of ankle stiffness during quiet standing: Implications for control modelling and clinical application. *Gait and Posture.* **21**, 410-424.

Casdagli, M., Eubank, S., Farmer, J. D., and Gibson, J. (1991). State space reconstruction in the presence of noise. *Physica D*, **51**, 52-98.

Casslebrant, M. L., Mandel, E. M., Sparto, P. J., Redfern, M. S., and Furman, J. M. (2007). Contribution of vision to balance in children four to eight years of age. *Annals of Otology, Rhinology and Laryngology*. **116**, 653-657.

Cavanagh, P. R. and Komi, P. V. (1979). Electromechanical delay in human skeletal muscle under concentric and eccentric contractions. *European Journal of Applied Physiology*. **42**, 159-163.

Chaffin, D. B., Andersson, G. B. J., and Martin, B. J. (1999). *Occupational Biomechanics*. New York: John Wiley and Sons.

Chandler, R. F., Clauser, C. E., McConville, J. T., Reynolds, H. M., and Young, J. W. (1974). *Investigation of inertial properties of the human body* (AMRL TR 74-137), Wright-Patterson Air Force Base Ohio (NTIS No. AD-A016 485).

Choi, J.M., Bae, B.H. and Kim, S.Y. (1999). Divergence in perpendicular recurrence plot; quantification of dynamical divergence from short chaotic time series. *Physical Letters A*. **263**, 299-306.

Clark, F. J., Burgess, R. C., Chapin, J. W., and Lipscomb, W. T. (1985). Role of intramuscular receptors in the awareness of limb position. *Journal of Neurophysiology*. **54**, 1529-1540.

Clément, G. and Rézette, D. (1985). Motor behavior underlying the control of an upside-down vertical posture. *Experimental Brain Research*. **59**, 478-484.

Clement, G. and Rezette, D. (1985). Motor behaviour underlying the control of an upside-down vertical posture. *Experimental Brain Research*. **59**, 478-484.

Clément, G., Pozzo, T. and Berthoz, A. (1988). Contribution of eye positioning to control of the upside-down standing posture. *Experimental Brain Research*. **73**, 569-576.

Clement, G., Pozzo, T., and Berthoz, A. (1988). Contribution of eye positioning to control of the upside-down standing posture. *Experimental Brain Research.* **73**, 569-576.

Collins, J. J. and De Luca, C. J. (1993). Open-loop and closed-loop control of posture: A random-walk analysis of centre-of-pressure trajectories. *Experimental Brain Research.* **95**, 308-318.

Collins, J. J. and De Luca, C. J. (1995). The effects of visual input on open-loop and closed-loop postural control mechanisms. *Experimental Brain Research.* **103**, 151-163.

Collins, J. J. and De, C. J. L. (1994). Random walking during quiet standing. *Physical Review Letters.* **73**, 764-767.

Colobert, B., Crétual, A., Allard, P., and Delamarche, P. (2006). Force-plate based computation of the ankle and hip strategies from a double-inverted pendulum model. *Clinical Biomechanics.* **21**, 427-434.

Croix, G., Chollet, D., and Thouvarecq, R. (2010a). Effects of Expertise level on the perceptual characteristics of gymnasts. *Journal of Strength and Conditioning Research.* **24**, 1458-1463.

Croix, G., Lejeune, L., Anderson, D. I., and Thouvarecq, R. (2010b). Light finger contact on thigh facilitates handstand balance in gymnasts. *Psychology of Sport and Exercise.* **11**, 330-333.

Davids, K., Button, C., and Bennett, S. (2008). *Dynamics of skill acquisition: a constraints-led approach.* Champaign, IL: Human Kinetics.

Davis, R. B., Ounpuu, S., Tyburski, D., and Gage, J. R. (1991). A gait analysis data collection and reduction technique. *Human Movement Science.* **10**, 575-587.

De Luca, C.J., Gilmore, L.D., Kuznetsov, M., and Roy, S.H. (2010). Filtering surface EMG signal: Movement artefact and baseline noise contamination. *Journal of Biomechanics.* **43**, 1573-1579.

Delsys (2009). *Trigno^{TM} Wireless System: User's Guide.* Boston, MA: Delsys Inc.

Derrick, T. R. (2004). Signal processing. In: Robertson, D. G. E., Caldwell, G. E., Hamill, J., Kamen, G., and Whittlesey, S. N. (Eds). *Research Methods in Biomechanics*. Champaign, IL: Human Kinetics.

Diebel, J. (2006). *Representing Attitude: Euler Angles, Unit Quaternions, and Rotation Vectors*. Retrieved June 1 2013: https://moodle.swarthmore.edu/pluginfile.php/14933/mod_resource/content/0/diebel2006attitude.pdf

Diener, H. C., Horak, F. B., and Nashner, L. M. (1988). Influences of stimulus parameters on human postural responses. *Journal of Neurophysiology*. **59**, 1888-1905.

Duarte, M. and Zatsiorsky, V. M. (1999). Patterns of centre of pressure migration during prolonged unconstrained standing. *Motor Control*. **3**, 12-27.

Dumas, R. and Cheze, L. (2007). 3D inverse dynamics in non-orthonormal segment coordinate system. *Medical and Biological Engineering and Computing*. **45**, 315-322.

Dumas, R., Aissaoui, R., and De Guise, J. A. (2004). A 3D generic inverse dynamic method using wrench notation and quaternion algebra. *Computer Methods in Biomechanics and Biomedical Engineering*. **7**(3), 159-166.

Eckmann, J.-P., Ollifson Kamphorst, S. and Ruelle, D. (1987). Recurrence plots of dynamical systems. *Europhysics Letters*. **4**(9), 973-977.

Eckmann, J.-P., Ollifson Kamphorst, S., Ruelle, D., and Ciliberto, S. (1986). Liapunov exponents from time series. *Physical Review A*. **4**(9), 973-977.

Delsys (2009). *Trigno[TM] Wireless System: User's Guide.* Boston, MA: Delsys Inc.

Fitzpatrick, R. and McCloskey, D. I. (1994). Proprioceptive, visual and vestibular thresholds for the perception of sway during standing in humans. *Journal of Physiology.* **478.1**, 173-186.

Foster, E. C., Sveistrup, H., and Woollacott, M. (1996). Transactions in visual proprioception: A cross-sectional developmental study of the effects of visual flow on postural control. *Journal of Motor Behaviour.* **28**, 101-112.

Fraser, A. M. and Swinney, H. L. (1986). Independent coordinates for strange attractors from mutual information. *Physical Review A.* **33**(2), 1134-1140.

Gage, W. H., Winter, D. A., Frank, J. S., and Adkin, A. L. (2004). Kinematic and kinetic validity of the inverted pendulum model in quiet standing. *Gait and Posture.* **19**, 124-132.

Gatev, P., Thomas, S., Kepple, T., and Hallett, M. (1999). Feedforward ankle strategy of balance during quiet stance in adults. *Journal of Physiology.* **514.3**, 915-928.

Gautier, G., Marin, L., Leroy, D., and Thouvarecq, R. (2009). Dynamics of expertise level: Coordination in handstand. *Human Movement Science.* **28**, 129-140.

Gautier, G., Thouvarecq, R., and Chollet, D. (2007). Visual and postural control of an arbitrary posture: The handstand. *Journal of Sports Sciences.* **25**, 1271-1278.

Goodworth, A. D. and Peterka, R. J. (2009). Contribution of sensorimotor integration to spinal stabilization in humans. *Journal of Neurophysiology.* **102**, 496-512.

Gottlieb, G. L. and Agarwal, G. C. (1979). Response to sudden torques about ankle in man: Myotatic reflex. *Journal of Neurophysiology.* **42**, 91-106.

Gurfinkel, V. S., Kots, Y. M., and Shick, M. L. (1965). *Regulation of human posture.* Moscow: Nauka.

Hamill, J. and Selbie, W. S. (2004). Three-dimensional kinetics. In: Robertson, D. G. E., Caldwell, G. E., Hamill, J., Kamen, G., and Whittlesey, S. N. (Eds). *Research Methods in Biomechanics.* Champaign, IL: Human Kinetics.

Hamilton, J. D. (1994). *Time series analysis.* Princeton, New Jersey: Princeton University Press.

Harbourne, R. T. and Stergiou, N. (2003). Nonlinear analysis of the development of sitting postural control. *Developmental Psychobiology.* **42**, 368-377.

Hasson, C. J., Caldwell, G. E., and Van Emmerik, R. E. A. (2009). Scaling platerflexor muscle activity and postural time-to-contact in response to upper-body perturbations in young and older adults. *Experimental Brain Research.* **196**, 413-427.

Hasson, C. J., Van Emmerik, R. E. A., Caldwell, G. E., Haddad, J. M., Gagnon, J. L., and Hamill, J. (2008). Influence of embedding parameters and noise in center of pressure recurrence quantification analysis. *Gait and Posture.* **27**, 416-422.

Hayes, K. C. (1982). Biomechanics of postural control. *Exercise and Sport Sciences Reviews.* **10**, 363-391.

Helbostad, J. L., Vereijken, B., Hesseberg, K., and Sletvold, O. (2009). Altered vision destabilizes gait in older persons. *Gait and Posture.* **30**, 233-238.

Hermann, S. (2005). Exploring sitting posture and discomfort using nonlinear analysis methods. *IEEE Transactions on Information Technology in Biomedicine.* **9**(3), 392-401.

Horak, F. B. (2006). Postural orientation and equilibrium: What do we need to know about neural control of balance to prevent falls? *Age and Ageing.* **35**, ii7-ii11.

Horak, F. B., and Nashner, L. M. (1986). Central programming of postural movements: adaptation to altered support-surface configurations. *Journal of Neurophysiology*. **6**, 1369-1381.

Horak, F. B., Diener, H. C., and Nashner, L. M. (1989). Influence of central set on human postural responses. *Journal of Neurophysiology*. **62**, 841-853.

Horak, F. B., Nashner, L. M., and Diener, H. C. (1990). Postural strategies associated with somatosensory and vestibular loss. *Experimental Brain Research*. **82**, 167-177.

Hrysomallis, C. (2007). Relationship between balance ability, training and sports injury risk. *Sports Medicine*. **37**, 547-556.

Hrysomallis, C., McLaughlin, P., and Goodman, C. (2006). Relationship between static and dynamic balance tests among elite Australian footballers. *Journal of Science and Medicine in Sport*. **9**, 288-291.

Hug, F. (2011). Can muscle coordination be precisely studied by surface electromyography? *Journal of Electromyography and Kinesiology*. **21**, 1-12.

Jacono, M., Casadio, M., Morasso, P. G., and Sanguineti, V. (2004). The sway-density curve and the underlying postural stabilisation process. *Motor Control*. **8**, 292-311.

Jeka, J. J. and Lackner, J. R. (1994). Fingertip contact influences human postural control. *Experimental Brain Research*. **100**, 495-502.

Jeka, J. J. and Lackner, J. R. (1995). The role of haptic cues from rough and slippery surfaces in human postural control. *Experimental Brain Research*. **103**, 267-276.

Jeka, J. J., Ribeiro, P., Oie, K., and Lackner, J. R. (1998). The structure of somatosensory information for human postural control. *Motor Control*. **2**, 13-33.

Jiang, B. C., Yang, W. -H., Shieh, J. -S., Fan, J. S. -Z., and Peng, C. -K. (2013). Entropy-based method for COP data analysis. *Theoretical Issues in Ergonomics Science.* **14**(3), 227-246.

Kantz, H. and Schreiber, T. (2004). *Nonlinear time series analysis* (2nd ed), Cambridge: Cambridge University Press.

Karnath, H. -O., Ferber, S., and Dichgans, J. (2000). The origin of contraversive pushing: Evidence for a second graviceptive system in humans. *Neurology.* **55**(9), 1298-1304.

Kerwin, D. G. and Trewartha, G. (2001). Strategies for maintaining a handstand in the anterior-posterior direction. *Medicine and Science in Sports and Exercise.* **33**, 1182-1188.

Kim, G. T., Ferdjallah, M., and Harris, G. F. (2009). Fast computational analysis of sway area using centre of pressure data in normal children and children with cerebral palsy. *American Journal of Biomedical Sciences.* **1**(4), 364-372.

King, D. L. and Zatsiorsky, V. M. (1997). Extracting gravity line displacement from stabilographic recordings. *Gait and Posture.* **6**, 27-38.

Kingma, I., Toussaint, H. M., Commissaries, D. A. C. M., Hoozemans, M. J. M., and Ober, M. J. (1995). Optimizing the determination of the body center of mass. *Journal of Biomechanics.* **28**(9), 1137-1142.

Kirby, R. L., Price, N. A., and MacLeod, D. A. (1987). The influence of foot position on standing balance. *Journal of Biomechanics.* **20**, 423-427.

Konrad, P. (2005). The ABC of EMG. Retrieved June 2011: https://hermanwallace.com/download/The_ABC_of_EMG_by_Peter_Konrad.pdf

Kuipers, J. B. (1999). *Quaternions and rotation sequences.* Princeton, New Jersey: Princeton University Press.

Lafond, D., Duarte, M., and Prince, F. (2004). Comparison of three methods to estimate the center of mass during balance assessment. *Journal of Biomechanics.* **37**, 1421-1426.

Lakie, M., Caplan, N., and Loram, I. (2003). Human balancing of an inverted pendulum with a compliant linkage: Neural control by anticipatory intermittent bias. *Journal of Physiology.* **551**, 357-370.

Le Clair, K. and Riach, C. (1996). Postural stability measures: what to measure and for how long. *Clinical Biomechanics.* **11**, 176-178.

Lee, D. and Lishman, J. R. (1975). Visual proprioceptive control of stance. *Journal of Human Movement Studies.* **1**, X7-95.

Lin, D., Seol, H., Nussbaum, M. A., and Madigan, M. L. (2008). Reliability of COP-based postural sway measures and age-related differences. *Gait and Posture.* **28**, 337-342.

Loram, I. and Lakie, M. (2002a). Direct measurement of human ankle stiffness during quiet standing: The intrinsic mechanical stiffness is insufficient for stability. *Journal of Physiology.* **545**, 1041-1053.

Loram, I. and Lakie, M. (2002b). Human balancing of an inverted pendulum: position control by small, ballistic-like, throw and catch movements. *Journal of Physiology.* **240**, 1111-1124.

Magnusson, M., Enbom, H., Johansson, R., and Pyykko, I. (1990a). Significance of pressor input from the human feet in anterior-posterior postural control: The effect of hypothermia on vibration-induced body-sway. *Acta Otolaryngol (Stockh).* **110**, 182-188.

Magnusson, M., Enbom, H., Johansson, R., and Wiklund, J. (1990b). Significance of pressor input from the human feet in lateral postural control: The effect of hypothermia on galvanically induced body-sway. *Acta Otolaryngol (Stockh).* **110**, 321-327.

Marchetti, M. T. and Whitney, S. L. (2006). Postural control in older adults with cognitive dysfunction. *Physical Therapy Reviews*. **11**, 161-168.

Marwan, N., Romano, M. C., Thiel, M., and Kurths, J. (2007). Recurrence plots for the analysis of complex systems. *Physics Reports*. **438**, 237-329.

Marwan, N., Wessel, N., Meyerfeldt, U., Schirdewan, A., and Kurths, J. (2002). Recurrence-plot based measures of complexity and their application to heart rate variability data. *Physical Review E.* **66**, 026702-1 -026702-8.

Masani, K., Vette, A. H., and Popovic, M. R. (2006). Controlling balance during quiet standing: Proportional and derivative controller generates preceding motor command to body sway position observed in experiments. *Gait and Posture*. **23**, 164-172.

Massion, J. and Woolacott, M. H. (2004). Posture and Equilibrium. In: Bronstein, A. M., Brandt, T., Woollacott, M. H. and Nutt, J. G. (Eds). *Clinical Disorders of Balance, Posture and Gait* (2nd ed).London: Arnold.

Mauerberg-deCastro, E. (2004). Developing an anchor system to enhance postural control. *Motor Control*. **8**, 339-358.

Maurer, C., Mergner, T., and Peterka, R. J. (2006). Multisensory control of human upright stance. *Experimental Brain Research*. **171**, 231-250.

McClenaghan, B. A., Williams, H. G., Dickerson, J., Dowda, M., Thombs, L., and Eleazer, P. (1995). Spectral characteristics of aging postural control. *Gait and Posture*. **4**, 112-121.

McCollum, G., Shupert, C. L., and Nashner, L. M. (1996). Organizing sensory information for postural control in altered sensory environments. *Journal of Theoretical Biology*. **180**, 257-270.

McInnes, M. D. F., Kirby, R. L., and MacLeod, D. A. (2000). The contribution of vision to wheelie balance. *Archives of Physical Medicine and Rehabilitation*. **81**, 1081-1084.

Means, K. M., Rodell, D. E., O'Sullivan, P. S., and Winger, R. M. (1998). Comparison of a functional obstacle course with an index of clinical gait and balance and postural sway. *The Journals of Gerontology.* **53A**, M331-M335.

Mergner, T., Schweigart, G., Maurer, C., and Blüme, A. (2005). Human postural responses to motion of real and virtual visual environments under different support base conditions. *Experimental Brain Research.* **167**, 535-556.

Moe-Nilssen, R. and Helbostad, J. L. (2002). Trunk accelerometry as a measure of balance control during quiet standing. *Gait & Posture.* **16**, 60-68.

Moe-Nilssen, R., Helbostad, J. L., Åkra, T., Birkedal, L., and Nygaard, H. A. (2006). Modulation of gait during visual adaptation to dark. Journal of *Motor Behavior.* **38**, 118-125.

Moore, S. P., Rushmer, D. S., Windus, S. L., and Nashner, L. M. (1988). Human automatic postural responses: Responses to horizontal perturbations of stance in multiple directions. *Experimental Brain Research.* **73**, 648-658.

Morasso, P. G. and Sanguineti, V. (2002). Ankle stiffness alone cannot stabilize balance during quiet standing. *Journal of Neurophysiology.* **88**, 2157-2162.

Morrison, S., Hong, S. L., and Newell, K. M. (2007). Inverse relations in the patterns of muscle and center of pressure dynamics during standing still and movement postures. *Experimental Brain Research.* **181**, 347-358.

Muraoka, T., Muramatsu, T., Fukunaga, T., and Kanehisa, H. (2004). Influence of tendon slack on electromechanical delay in the human medial gastrocnemius in vivo. *Journal of Applied Physiology.* **96**, 540-544.

Nagano, A., Yoshioka, S., Hay, D. C., and Fukashiro, S. (2006). Light finger touch on the upper legs reduces postural sway during quasi-static standing. *Motor Control.* **10**, 348-358.

Nakagawa, H., Ohashi, N., Watanabe, Y., and Mizukoshi, K. (1993). The contribution of proprioception to postural control in normal subjects. *Acta Otolaryngol (Stockh).* **Suppl. 504**, 112-116.

Nashner, L. M. (1972). Vestibular postural control model. *Biological Cybernetics.* **10**, 106-110.

Nashner, L. M. (1976). Adapting reflexes controlling the human posture. *Experimental Brain Research.* **26**, 59-72.

Nashner, L. M., Black, F. O., and Wall, C. (1982). Adaptation to altered support and visual conditions during stand: Patients with vestibular deficits. *Journal of Neuroscience.* **2**, 536-544.

Nashner, L. M., Woollacott, M., and Tuma, G. (1979). Organization of rapid responses to postural and locomotor-like pertubrations of standing man. *Experimental Brain Research.* **36**, 463-476.

Nashner, L.M. and McCollum, G. (1985). The organization of human postural movements: A formal basis and experimental synthesis. *The Behavioral and Brain Sciences.* **8**, 135-172.

Newell, K. M. (1991). Motor skill acquisition. *Annual Review of Psychology*, **42**, 213-237.

Newell, K. M., Slobounov, S. M., Slobounova, B. S., and Molenaar, P. C. M. (1997). Short-term non-stationarity and the development of postural control. *Gait and Posture.* **6**, 56-62.

Nikolic, D., Muresan, R. C., Feng, W., and Singer, W. (2012). Scaled correlation analysis: a better way to compute a cross-correlogram. *European Journal of Neuroscience.* **35**(5), 742-762.

O'Connor, S. M. and Kuo, A. D. (2009). Direction-dependent control of balance during walking and standing. *Journal of Neurophysiology.* **102**, 1411-1419.

Parietti-Winkler, C., Gauchard, G. C., Simon, C., and Perrin, P. (2006). Sensorimotor postural rearrangement after unilateral vestibular deafferentation in patients with acoustic neuroma. *Neuroscience Research.* **55**, 171-181.

Parlitz, U. (1998). Nonlinear tine-series analysis. In: Suykens, J. A. K. and Vandewalle, J. (Eds). *Nonlinear Modeling: Advanced black-box techniques.* Boston: Kluwer Academic Publishers, pp. 209-239.

Pascolo, P. B., Barazza, F., and Carniel, R. (2006). Considerations on the application of the chaos paradigm. *Chaos, Solitons and Fractals.* **27**, 1339-1346.

Pascolo, P. B., Marini, A., Carniel, R., and Barazza, F. (2005). Posture as a chaotic system and an application to the Parkinson's disease. *Chaos, Solitons and Fractals.* **24**, 1343-1346.

Patla, A.E. (2004). Adaptive human locomotion: Influences of neural, biological and mechanical factors on control mechanisms. In: Bronstein, A.M., Brandt, T., Woollacott, M.H. and Nutt, J.G. (Eds). *Clinical Disorders of Balance, Posture and Gait* (2nd ed).London: Arnold.

Peterka, R. J. (2002). Sensorimotor integration in human postural control. *Journal of Neurophysiology.* **88**, 1097-1118.

Peterka, R. J., and Benolken, M. S. (1995). Role of somatosensory and vestibular cues in attenuating visually induced human postural sway. *Experimental Brain Research.* **105**, 101-110.

Peterson, M. L., Christou, E. and Rosengren, K. S. (2006). Children achieve adult-like sensory integration during stance at 12-years-old. *Gait and Posture.* **23**, 455-463.

Pincus S. M. (1991). Approximate entropy as a measure of system complexity. *Proceedings of the National Academy of Sciences.* **88**, 2297-2301.

Pincus S. M., Gladstone, I. M., and Ehrenkranz, R. A. (1991). A regularity statistic for medical data analysis. *Journal of Clinical Monitoring.* **7**(4), 335-345.

Pincus, S. M. (1995). Approximate entropy (ApEn) as a complexity measure. *Chaos.* **5**(1), 110-117.

Pincus, S. M. and Goldberger, A. L. (1994). Physiological time-series analysis: what does regularity quantify? *American Journal of Physiology: Heart and Circulatory Physiology.* **266**, H1643-H1656.

Pollock, A. S., Durward, B. R., Rowe, P. J., Paul, J. P. (2000). What is balance? *Clinical Rehabilitation.* **14**, 402-406.

Popovic, M. R., Pappas, P. I., Nakazawa, K., Keller, T., Morari, M., and Dietz, V. (2000). Stability criterion for controlling standing in able-bodied subjects. *Journal of Biomechanics.* **33**, 1359-1368.

Prince, F., Corriveau, H., Hebert, R. and Winter, D. A. (1997). Gait and the elderly. *Gait and Posture.* **5**, 128-135.

Richman , J. S. and Moorman, J. R. (2000). Physiological time-series analysis using approximate entropy and sample entropy. *American Journal of Physiology: Heart and Circulatory Physiology.* **278**, H2039-H2049.

Rietdyk, S., Palta, A. E., Winter, D. A., Ischac, M. G., and Little, C. E. (1999). Balance recovery from medio-lateral perturbations of the upper body during standing. *Journal of Biomechanics*, **32**, 1149-1158.

Riley, M. A., Balasubramaniam, R., and Turvey, M. T. (1999). Recurrence quantification analysis of postural fluctuations. *Gait and Posture.* **9**, 65-78.

Riley, M. A., Mitra, S., Stoffregen, A. T., and Turvey, M. T. (1997). Influences of body lean and vision on unperturbed postural sway. *Motor Control*. **1**, 229-246.

Rinaldi, N. M., Polastri, P. F., and Barela, J. A. (2009). Age-related changes in postural control sensory reweighting. *Neuroscience Letters*. **467**, 225-229.

Roncesvalles, M. N. C., Woollacott, M., and Jensen, J. L. (2001). Development of lower extremity kinetics for balance control in infants and young children. *Journal of Motor Behaviour*. **33**, 180-192.

Row, B. and Cavanagh, P. R. (2007). Reaching upwards is more challenging to dynamic balance than reaching forward. *Clinical Biomechanics*. **22**, 155-164.

Runge, C. F., Shupert, C. L., Horak, F. B., and Zajac, F. E. (1999). Ankle and hip postural strategies defined by joint torques. *Gait and Posture*. **10**, 161-170.

Saffer, M., Kiemel, T., and Jeka, J. (2008). Coherence analysis of muscle activity during quiet stance. *Experimental Brain Research*. **185**, 215-226.

Salavati, M., Hadian, M. R., Mazaheri, M., Negahban, H., Ebrahimi, I., Talebian, S., Jafari, A. H., Sanjari, M. A., Sohani, S. M., and Parnianpour, M. (2009). Test-retest reliability of center of pressure measures of postural stability during quiet standing in a group with musculoskeletal disorders consisting of low back pain, anterior cruciate ligament injury and functional ankle instability. *Gait and Posture*. **29**, 460-464.

Sasagawa, S., Ushiyama, J., Masani, K., Kouzaki, M., Kanehisa, H. (2009). Balance control under different passive contributions of the ankle extensors: Quiet standing on inclined surfaces. *Experimental Brain Research*. **196**, 537-544.

Sasaki, O., Gagey, P.-M., Ouaknine, A. M., Martinerie, J., Quyen, M. L. V., Toupet, M., and L'Heritier, A. (2001). Nonlinear analysis of orthostatic

posture in patients with vertigo or balance disorders. *Neuroscience Research*. **41**, 185-192.

Schrager, M. A., Kelly, V. E., Price, R., Ferrucci, L. and Shumway-Cook, A. (2008). The effects of age on medio-lateral stability during normal and narrow base walking. *Gait and Posture*. **28**, 466-471.

Schreiber, T. (1999). Interdisciplinary application of nonlinear time series methods. *Physics Reports*. **308**, 1-64.

Schumann, T., Redfern, M. S., Furman, J. M., El-Jaroudi, A., Chaparro, L. F., (1995). Time-frequency analysis of postural sway. *Journal of Biomechanics*. **28**, 603-607.

Seo, M. J. and Choi, H. (2005). The assessment of ankle joint forces during the postural balance control movement. In Proceedings of the 2005 IEEE Engineering in Medicine and Biology 27th Annual Conference, Shanghai, China.

Shimba, T. (1984). An estimation of center of gravity from force platform data, *Journal of Biomechanics*. **17**(1), 53-60.

Shkuratova, N. and Taylor, N. (2008). The influence of age on gait parameters during the transition from wide to a narrow pathway. *Physiotherapy Research International*. **13**(2), 75-83.

Shumway-Cook, A. and Woollacott, M. (2007). *Motor Control: Translating Research into Clinical Practice (3rd ed)*. Philadelphia: Lippincott Williams and Wilkins.

Shumway-Cook, A., Woollacott, M., (1985). The growth of stability: Postural control from a developmental perspective. *Journal of Motor Behaviour*. **17**, 131-147.

Slobounov, S. M. and Newell, K. M. (1994). Dynamics of posture in 3- and 5-year-old children as a function of task constraints. *Human Movement Science*. **13**, 861-875.

Slobounov, S. M. and Newell, K. M. (1996). Postural dynamics in upright and inverted stances. *Journal of Applied Biomechanics*. **12**, 185-196.

Slobounov, S. M., Hallett, M., Stanhope, S., and Shibasaki, H. (2005). Role of cerebral cortex in human postural control: An EEG study. *Clinical Neurophysiology*. **116**, 315-323.

Sobera, M., Siedlecka, B., Piestrak, P., Sojka-Krawiec, K., and Graczykowska, B. (2007). Maintaining body balance in extreme positions. *Biology of Sport*. **24**, 81-88.

Sprott, J. C. (2003). *Chaos and time-series analysis*. Oxford: Oxford University Press.

Stergiou, N., Buzzi, U. H., Kurz, M. J., and Heidel, J. (2004). Nonlinear tools in human movement. In: Stergiou, N. (Ed). *Innovative Analyses of Human Movement*. Champaign, IL: Human Kinetics, pp. 63-90.

Stoffregen, T. A. (1985). Flow Structure versus retinal location in the optical control of stance. *Journal of Experimental Psychology: Human Perception and Performance*. **11**, 554-565.

Strogatz, S. H. (1994). *Nonlinear Dynamics and Chaos*. Cambridge, MA: Westview Press.

Sundermier, L., Woollacott, M., Roncesvalles, M. N. C., and Jensen, J. L. (2001). The development of balance control in children: comparisons of EMG and kinetic variables and chronological and developmental groupings. *Experimental Brain Research*. **136**, 340-350.

Sveistrup, H. and Woollacott, M. (1997). Practice modifies the developing automatic postural response. *Experimental Brain Research*. **114**, 33-43.

Teasdale, N. and Simoneau, M. (2001). Attentional demands for postural control: the effects of aging and sensory reintegration. *Gait and Posture*. **14**, 203-210.

Theiler, J., Eubank, S., Longtin, A., Galdrikian, B., and Farmer, J. D. (1992). Testing for nonlinearity in time series: the method of surrogate data. *Physica D.* **58**, 77-94.

Thelen, E. (1995). Motor development: A new synthesis. *American Psychologist*, **50**(2), 79-95.

Tillin, N. A., Jimenez-Reyes, P., Pain, M. T. G., and Folland, J. P. (2010). Neuromuscular performance of explosive power athletes versus untrained individuals. *Medicine and Sciences in Sports and Exercise.* **42**, 781-790.

Tucker, M. G., Kavanagh, J. J., Barrett, R. S., and Morrison, S. (2008). Age-related differences in postural reaction time and coordination during voluntary sway movements. *Human Movement Science.* **27**(5), 728-737.

Visser, J. E., Carpenter, M. G., van der Kooij, H., and Bloem, B. R. (2008). The clinical utility of posturography. *Clinical Neurophysiology.* **119**, 2424-2436.

Wade, M. G. and Jones, G. (1997). The role of vision and spatial orientation in the maintenance of posture. *Physical Therapy.* **77**, 619-628.

Wade, M. G., Lindquist, R., Taylor, J. R., and Treat-Jacobson, D. (1995). Optical flow, spatial orientation, and the control of posture in the elderly. Gerontology. **50**(1), 51-58.

Webber, C. L. and Zbilut, J. P. (2005). Recurrence quantification analysis of nonlinear dynamical systems. In: Riley, M. A. and Van Orden, G. (Eds). *Tutorials in Contemporary Nonlinear Methods for the Behavioral Sciences*, Retrieved June 1, 2013 from http://www.nsf.gov/sbe/bcs/pac/nmbs/nmbs.jsp (Chapter 2, pp. 26-94).

Wilson, M. L., Rome, K., Hodgson, D., and Ball, P. (2008). Effect of textured foot orthotics on static and dynamic postural stability in middle-aged females. *Gait and Posture.* **27**, 36-42.

Winter D. A., Patla, A. E., Rietdyk, S., and Ishac, M. G. (2001). Ankle muscle stiffness in the control of balance during quiet standing. *Journal of Neurophysiology.* **85**, 2630-2633.

Winter, D. A. (1995). Human balance and posture control during standing and walking. *Gait and Posture.* **3**, 193-214.

Winter, D. A. (2009). *Biomechanics and motor control of human movement* (4th Ed). New Jersey: John Wiley and Sons.

Winter, D. A., Patla, A. E., Ischac, M. G., and Gage, W. H. (2003). Motor mechanisms of balance during quiet standing. *Journal of Electromyography and Kinesiology.* **13**, 49-56.

Winter, D. A., Patla, A. E., Prince, F., Ishac, M., and Gielo-Perczak, K. (1998). Stiffness control of balance in quiet standing. *Journal of Neurophysiology.* **80**, 1211-1221.

Wolf, A., Swift, J. B., Swinney, H. L., and Vastano, J. A. (1985). Determining Lyapunov exponents from a time series. *Physica D.* **16**, 285-317.

Wollseifen, T. (2011). Different methods of calculating body sway area. *Pharma Prog.* **4**, 91-96.

Woollacott, M. and Sveistrup, H. (1992). Changes in the sequencing and timing of muscle response coordination associated with developmental transitions in balance abilities. *Human Movement Science.* **11**, 23-36.

Woollacott, M., Debu, B., and Shumway-Cook, A. (1987). *Children's development of posture and balance control: Changes in motor coordination and sensory integration.* Human Kinetics, Champaign, IL, pp. 211-234.

Yamada, N. (1995). Chaotic swaying of the upright posture. *Human Movement Science.* **14**, 711-726.

Yeadon, M. R. (1990). The simulation of aerial movement – II. A mathematical inertia model of the human body. *Journal of Biomechanics.* **23**, 67-74.

Yeadon, M. R. and Trewartha, G. (2003). Control strategy for a hand balance. *Motor Control.* **7**, 411-430.

Yentes, J. M., Hunt, N., Schmid, K. K., Kaipust, J. P., McGrath, D., and Stergiou, N. (2013). The appropriate use of approximate entropy and sample entropy with short data sets. *Annals or Biomedical Engineering.* **41**(2), 349-365.

Zatsiorsky, V. M. and Duarte, M. (1999). Instant equilibrium point and its migration in standing tasks: Rambling and trembling components of the stabilogram. *Motor Control.* **3**, 28-38.

Zatsiorsky, V. M. and King, D. L. (1998). An algorithm for determining gravity line location from posturographic recordings. *Journal of Biomechanics.* **31**, 161-164.

Zbilut, J. P. and Webber, C. L. (1992). Embeddings and delays as derived from quantification of recurrence plots. *Physical Letters A.* **171**, 199-203.

Zhou, S., Lawson, D. L., Morrison, W. E., and Fairweather, I. (1995). Electromechanical delay in isometric muscle contractions evoked by voluntary, reflex and electrical stimulation. *European Journal of Applied Physiology.* **70**, 138-145.

APPENDIX 1

Informed Consent Forms

Loughborough University

Learning to balance, its control, and its response to visual and proprioceptive stimuli

Part 1 – Learning to balance in handstand

INFORMED CONSENT FORM
(to be completed after Participant Information Sheet has been read)

The purpose and details of this study have been explained to me. I understand that this study is designed to further scientific knowledge and that all procedures have been approved by the Loughborough University Ethical Advisory Committee.

I have read and understood the information sheet and this consent form.

I have had an opportunity to ask questions about my participation.

I understand that I am under no obligation to take part in the study.

I understand that I have the right to withdraw from this study at any stage for any reason, and that I will not be required to explain my reasons for withdrawing.

I understand that all the information I provide will be treated in strict confidence and will be kept anonymous and confidential to the researchers unless (under the statutory obligations of the agencies which the researchers are working with), it is judged that confidentiality will have to be breached for the safety of the participant or others.

I agree to participate in this study.

Your name

Your signature

Signature of investigator

Date

Loughborough University

Learning to balance, its control, and its response to visual and proprioceptive stimuli

Part 2 – Response to sensory perturbations in handstand balance

INFORMED CONSENT FORM
(to be completed after Participant Information Sheet has been read)

The purpose and details of this study have been explained to me. I understand that this study is designed to further scientific knowledge and that all procedures have been approved by the Loughborough University Ethical Advisory Committee.

I have read and understood the information sheet and this consent form.

I have had an opportunity to ask questions about my participation.

I understand that I am under no obligation to take part in the study.

I understand that I have the right to withdraw from this study at any stage for any reason, and that I will not be required to explain my reasons for withdrawing.

I understand that all the information I provide will be treated in strict confidence and will be kept anonymous and confidential to the researchers unless (under the statutory obligations of the agencies which the researchers are working with), it is judged that confidentiality will have to be breached for the safety of the participant or others.

I agree to participate in this study.

Your name _____

Your signature _____

Signature of investigator _____

Date _____

APPENDIX 2

Subject Information Sheets

Loughborough University

Learning to balance, its control, and its response to visual and proprioceptive stimuli
Part 1 – Learning to balance in handstand

Participant Information Sheet

Investigator Contact Details:
Glen Blenkinsop – UU.1.15 – G.Blenkinsop@lboro.ac.uk
Dr Michael Hiley – UU.1.14 – M.J.Hiley@lboro.ac.uk
Dr Matthew Pain – UU.1.07 – M.T.G.Pain@lboro.ac.uk
Dr Sam Allen – UU.1.02 – S.J.Allen@lboro.ac.uk

What is the purpose of the study?
The aim of this research is to examine how balance in handstand is learnt over a period of approximately 8 months, and to assess what changes may occur to how a performer uses the different sensory information available to them as handstand balance improves.

Who is doing this research and why?
This study is part of a PhD research project examining the roles of different sensory information to balance in both normal stance and in handstand; and is conducted by the sports biomechanics and motor control research group.

Are there any exclusion criteria?
The study will include regular practice and assessment in the handstand position; therefore anyone who is unable to place themselves into the handstand position, either in free standing or against a support, will be unable to take part. In addition, anyone that has a current injury to their upper limbs that would make performing a handstand uncomfortable or unsafe should not take part in this study. It is expected that prospective participants will be able to perform a handstand for no more than 5 seconds when starting from support against a wall.

Once I take part, can I change my mind?
Yes! After you have read this information and asked any questions you may have we will ask you to complete an Informed Consent Form, however if at any time, before, during or after the sessions you wish to withdraw from the study please just contact the main investigator. You can withdraw at any time, for any reason and you will not be asked to explain your reasons for withdrawing.

What will I be asked to do?
Participants are asked to practice handstands up to 3 to 5 times a weeks, for a total of approximately 1hour per week, for the duration of the study. During this time participants are asked to monitor handstand performance on a weekly basis; therefore, stop watches will be available in the gymnastics hall along with a simple tracking sheet. Detailed biomechanical testing will be completed on a monthly basis, with the testing sessions

increasing in difficulty throughout the learning period (see timetable below). Testing session towards the end of the learning period will involve some changes to the environment, such as a moving platform; with testing spread over three sessions of approximately 30 minutes each. However, these more advanced sessions will only begin once participants have sufficient balance in handstand.

Table 1: Provisional timetable for handstand testing

Stage	Month	Protocol	Expected Time
Initial	Oct	5 handstands for maximal length (all eyes open)	20 minutes
1	Nov	5 handstands for maximal length (all eyes open)	20 minutes
2	Dec	5 handstands for maximal length (all eyes open)	20 minutes
3	Jan	10 handstands for maximal length (5 eyes open/ 5 eyes closed)	30 minutes
4	Feb	10 handstands for maximal length (5 eyes open/ 5 eyes closed)	30 minutes
5	Mar	10 handstands for maximal length (5 eyes open/ 5 eyes closed)	30 minutes
6	Apr	10 handstands for maximal length (5 eyes open/ 5 eyes closed)	30 minutes
		Sensory Test – Slow moving platform and visual surround	40 minutes
		Moving platform – Quick movements, of small or medium range	30 minutes
7	May	10 handstands for maximal length (5 eyes open/ 5 eyes closed)	30 minutes
		Sensory Test – Slow moving platform and visual surround	40 minutes
		Moving platform – Quick movements, of small or medium range	30 minutes
Finial	Jun	10 handstands for maximal length (5 eyes open/ 5 eyes closed)	30 minutes
		Sensory Test – Slow moving platform and visual surround	40 minutes
		Moving platform – Quick movements, of small or medium range	30 minutes

What type of clothing should I wear?
EMG and reflective motion markers will be placed on the skin, therefore shorts will be required for all testing sessions to allow placement of markers on the hip and trunk area.

What personal information will be required from me?
Measurements of weight and height will be taken during each testing session, and a one-off anthropometric assessment will be required. The anthropometric assessment will include measurements of different parts of the body, such as leg length and circumference, and can be performed at anytime when it is convenient to the participant.

Are there any risks in participating?
The activities within this study should be familiar to any recreational gymnast, and only those subjects that are comfortable in performing a handstand will be involved in this study. Although some testing procedures may be demanding, such as using a moving platform, the testing area is surrounded by a matted area to prevent injury in the unlikely event that a participant will lose control to such a degree that they fall off the platform. Also, all

handstand trials begin against a stable support surface to replicate how gymnasts often learn to handstand against a wall, and this support will remain in place for the participant to use to help prevent a fall.

Will my taking part in this study be kept confidential?
All data collected in this study will remain confidential and secure. Participants will be allocated an identification number for recording and storage of data, and no participant will be referred to by name outside of data collection sessions, such as publication of the study.

What will happen to the results of the study?
All data collected conform to the university's guidelines on data collection and storage, and will therefore be stored securely in its original state for the duration of the collection, analysis and publication of the study.

What do I get for participating?
Participants will be allowed ongoing feedback on performance in the handstand task throughout the time of the study; however, a detailed biomechanical analysis of handstand performance will not be available until the research is completed.

I have some more questions who should I contact?
Any questions regarding the testing procedures or handstand practice should be first addressed to Glen Blenkinsop (G.Blenkinsop@lboro.ac.uk); alternatively, further queries may be addressed to Dr Michael Hiley, Dr Matthew Pain or Dr Sam Allen listed above.

If you have any concerns regarding your participation in this study, or the conduct of any of the investigators involved, please refer to the university's policy relating to research misconduct at the following link:

http://www.lboro.ac.uk/admin/committees/ethical/Whistleblowing(2).htm.

Loughborough
University

Learning to balance, its control, and its response to visual and proprioceptive stimuli
Part 2 – Response to sensory perturbations in handstand balance

Participant Information Sheet

Investigator Contact Details:
Glen Blenkinsop – UU.1.15 – G.Blenkinsop@lboro.ac.uk
Dr Michael Hiley – UU.1.14 – M.J.Hiley@lboro.ac.uk
Dr Matthew Pain – UU.1.07 – M.T.G.Pain@lboro.ac.uk
Dr Sam Allen – UU.1.02 – S.J.Allen@lboro.ac.uk

What is the purpose of the study?
The aim of this research is to examine how different sensory information contributes to balance in handstand, normal stance and single leg stance. This study will assess how participants' performance in handstand, normal stance, and single leg stance balance tasks change when exposed to a number of sensory disturbances, such as moving the support surface or visual surround.

Who is doing this research and why?
This study is part of a PhD research project examining the roles of different sensory information to balance in both normal stance and in handstand; and is conducted by the sports biomechanics and motor control research group.

Are there any exclusion criteria?
The study will include some demanding tasks in the handstand position; therefore participants with a strong background in handstand balance are required, and anyone who is unable to remain in the handstand position for at least 30 seconds will be unable to take part. In addition, anyone that has a current injury to their upper limbs that would make performing a handstand uncomfortable or unsafe should not take part in this study. It is expected that prospective participants will have a strong gymnastic background, with experience in performing a variety of skills in hand support, and may be able to perform a handstand for more than 60 seconds.

Once I take part, can I change my mind?
Yes! After you have read this information and asked any questions you may have we will ask you to complete an Informed Consent Form, however if at any time, before, during or after the sessions you wish to withdraw from the study please just contact the main investigator. You can withdraw at any time, for any reason and you will not be asked to explain your reasons for withdrawing.

What will I be asked to do?
Participants will be asked to attend 4 testing sessions, where a detail biomechanical assessment will be completed for the different postures during a variety of testing procedures. During these sessions reflective markers will be placed on the skin to

measure the movement of different body landmarks, EMG sensors will be placed on key muscles to measure underlying muscle activity, and balance tasks will be performed on two force platforms to measure the forces generated by the body. The four different balance assessments are as follows:

- **Static balance** – Balance in handstand/standing for up to 60 seconds, with eyes open and eyes closed conditions

- **Muscle Response** – Specific platform movements intending to unbalance the participant and assess the muscle activity and response delay

- **Sensory Assessment** – Balance during 4 conditions aimed to reduce sensory inputs, where the support surface moves as the participant sways in balance

- **Visual Response** – Specific movement of the visual surround, to assess the importance of different types of visual information during balance

During each of the testing sessions balance will be assessed in both standing and handstand positions, and each task will be expected to last no more 90 minutes, to be completed at the participant's convenience.

What type of clothing should I wear?
EMG and reflective motion markers will be placed on the skin, therefore shorts will be required for all testing sessions to allow placement of markers on the hip and trunk area. Female participants are asked to wear a crop top or sports bra so that markes can be placed on the lower back and shoulders.

What personal information will be required from me?
Measurements of weight and height will be taken during the first testing session, and a one-off anthropometric assessment will be required. The anthropometric assessment will include measurements of different parts of the body, such as leg length and circumference, and can be performed at anytime when it is convenient to the participant. This will usuallt take place in one of sessions, and will add an extra 15-20 minutes to the session.

Are there any risks in participating?
The activities within this study are familiar to prospective participants, and only those subjects that are skilled in the handstand will be involved in this study. Although some testing procedures may be demanding, such as using a moving platform, the testing area is surrounded by a matted area to prevent injury in the unlikely event that a participant will lose control to such a degree that they fall off the platform. Also, all handstand trials begin against a stable support surface to replicate how gymnasts often learn to handstand against a wall, and this support will remain in place for the participant to use to help prevent a fall.

Will my taking part in this study be kept confidential?
All data collected in this study will remain confidential and secure. Participants will be allocated an identification number for recording and storage of data, and no participant will be referred to by name outside of data collection sessions, such as publication of the study.

What will happen to the results of the study?
All data collected conform to the university's guidelines on data collection and storage, and will therefore be stored securely in its original state for the duration of the collection, analysis and publication of the study.

What do I get for participating?
Participants will be allowed ongoing feedback on performance in the handstand task throughout the time of the study; however, a detailed biomechanical analysis of handstand performance will not be available until the research is completed.

I have some more questions who should I contact?
Any questions regarding the testing procedures or handstand practice should be first addressed to Glen Blenkinsop (G.Blenkinsop@lboro.ac.uk); alternatively, further queries may be addressed to Dr Michael Hiley, Dr Matthew Pain or Dr Sam Allen listed above.

If you have any concerns regarding your participation in this study, or the conduct of any of the investigators involved, please refer to the university's policy relating to research misconduct at the following link:

http://www.lboro.ac.uk/admin/committees/ethical/Whistleblowing(2).htm

APPENDIX 3

Marker Placement

Marker Label	Marker Position	Description and Directions
Finger (R/L)	End of 3rd distal phalanx (finger)	Tip of middle finger
5MCP (R/L)	Dorsal aspect of the head of the 5th metacarpal	Medial and lateral projections of the MCP joint centre (mid-point of these two markers is the MCP joint centre)
2MCP (R/L)	Dorsal aspect of the head of the 2nd metacarpal	
US (R/L)	Lateral aspect of the styloid process of the ulna	Medial and lateral projections of the wrist joint centre (mid-point of these two markers is the wrist joint centre)
RS (R/L)	Lateral aspect of the styloid process of the radius	
LE (R/L)	Lateral aspect of the lateral humeral epicondyle	Medial and lateral projections of the elbow joint centre (mid-point of these two markers is the elbow joint centre) – elbow extended
ME (R/L)	Lateral aspect of the medial humeral epicondyle	
Acromion (R/L)	Superior tip of the Acromion process	
Shoulder (R/L)	Estimated lateral projection of the glenohumeral joint centre when the arm is elevated	Approximately the belly of the posterior Deltoid when the arm is elevated
Anterior Shoulder (R/L)	Estimated anterior projection of the glenohumeral joint centre when in the anatomical position	Mid-point of these two markers is the shoulder joint centre (only used for static trials)
Posterior Shoulder (R/L)	Estimated posterior projection of the glenohumeral joint centre when in the anatomical position	
R_Scapula	Middle of right scapula	Used only for identification of right side
Sternum	Superior tip of the manubrium of the sternum	Suprasternal notch at top of sternum
Xiphoid	Centre of the xiphoid process of the sternum	Inferior tip of sternum

C7	7th cervical vertebra	Prominence at base of neck when the neck is flexed
T10	10th thoracic vertebra	Count up from L1 (moving the skin over the spinous processes)
L1	1st Lumbar vertebra	Find L5 between right and left PSIS and count up
L_iliac	Superior border of left iliac crest	Used only for identification of left side
ASIS (R/L)	Anterior superior iliac spine, in line with hip joint centre	Bony landmark on the front of the pelvis (level with your belt)
PSIS (R/L)	Posterior superior iliac spine	Dimple in the skin at the back of the pelvis (a little lower than ASIS)
Hip (R/L)	Greater trochanter of the femur	Palpate the upper and lower aspects, and place in centre
MK (R/L)	Lateral aspect of the medial femoral epicondyle	Medial and lateral projections of the knee joint centre (mid-point of these two markers is the knee joint centre) – knee extended
LK (R/L)	Lateral aspect of the lateral femoral epicondyle	
LM (R/L)	Lateral aspect of the lateral malleolus of the fibula	Medial and lateral projections of the ankle joint centre (mid-point of these two markers is the ankle joint centre)
MM (R/L)	Inferior tip of the medial malleolus of the fibula	
1MTP (R/L)	Head of the 1st metatarsal	Medial and lateral projections of the MTP joint centre (mid-point of these two markers is the MTP joint centre)
5MTP (R/L)	Head of the 5th metatarsal	
Toe (R/L)	End of 1st distal phalanx	Tip of big toe
Head Band	Four markers placed at front right/left and back left/right of the head	
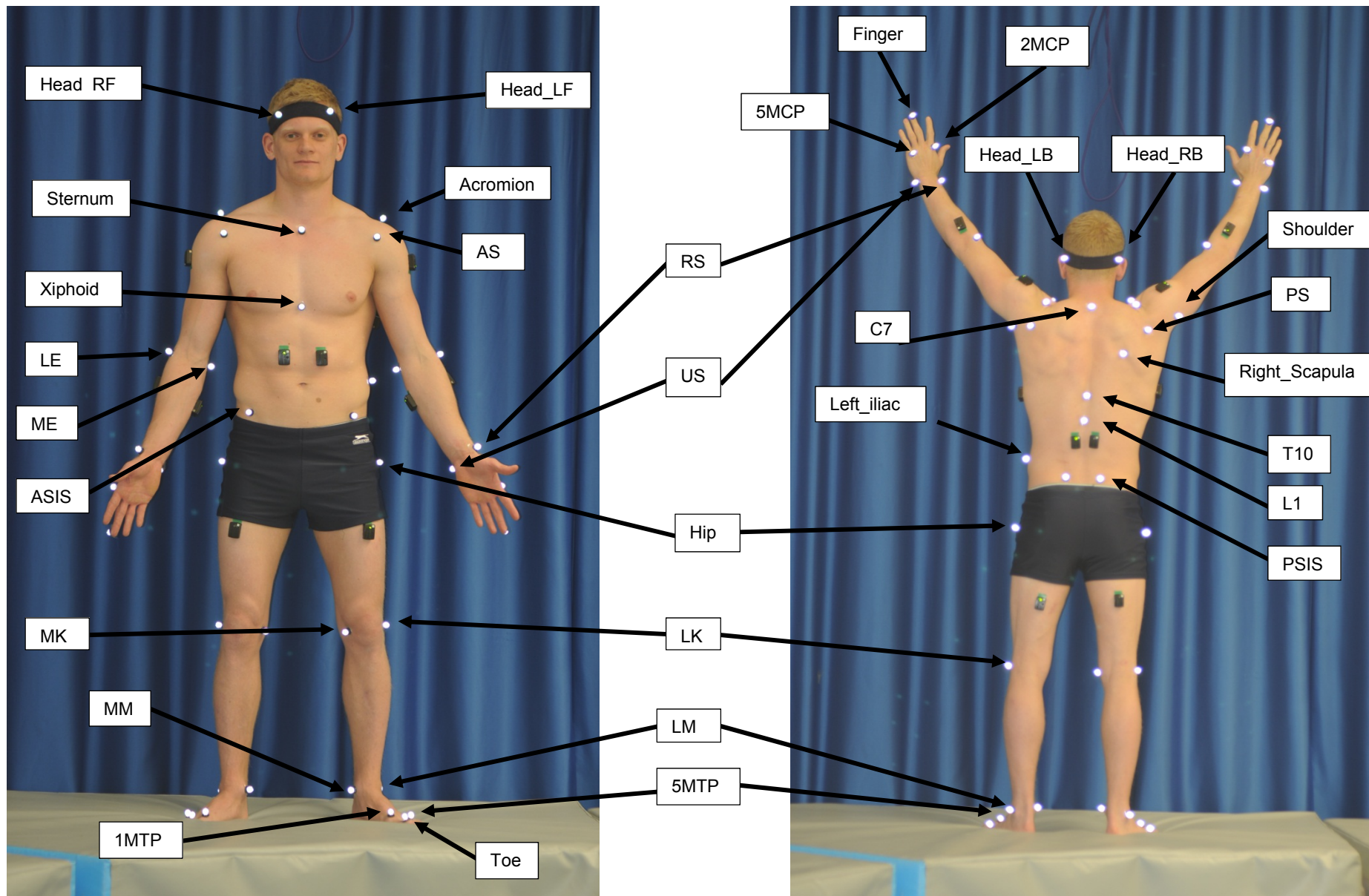
APPENDIX **4**

EMG Sensor Placement

EMG Label	Sensor Position	Description and Directions
1 + 2 = WF (wrist flexors)	Medial aspect of the forearm, approximately 6-7 cm distal to the medial epicondyle of the humerus and lying over the bellies of flexor carpi ulnaris and Palmaris longus muscles	With forearm in supination, palpate during resisted wrist flexion and position over largest and most tense bulk on line from medial epicondyle of the elbow to the styloid process of the ulna
3 + 4 = WE (wrist extensors)	Posterior lateral aspect of the forearm, approximately 6-7 cm distal to the lateral epicondyle of the humerus and lying over the bellies of extensor carpi radialis longus and brevis muscles	With forearm in pronation, palpate during resisted wrist extension and position over largest and most tense bulk on line from lateral epicondyle of the elbow to the styloid process of the ulna
5 + 6 = MD (shoulder flexors)	The belly of the middle fibres of the deltoid muscle (which is positioned posterior to the glenohumeral joint when the arm is elevated fully)	With arms fully elevated, position over the belly of the medial deltoid muscle, which will be approximately 5-10 cm above the acromion process (viewed as a depression)
7 + 8 = LD (shoulder extensors)	Middle of the latissimus dorsi muscle, which is approximately 5-10 cm inferior to the tip of the scapula when the arm is relaxed	With arms fully elevated, position over the middle portion of the lateral aspect of the latissimus dorsi muscle; this should be prominent as a band of muscle running down the lateral side of the trunk from behind the posterior deltoid muscle to mid-low ribs
9 + 10 = RA (trunk flexors)	Belly of rectus abdominis muscle, 3 cm superior and 2 cm lateral to the umbilicus	In standing, look for and palpate the muscle segment approximately 3 cm superior and 2 cm lateral to the umbilicus; place in the middle of muscle segment
11 + 12 = PS (trunk extensors)	Belly of the paraspinal muscles, 2 cm lateral and 5 cm inferior to the spinous process of the L1 vertebra (L2 – L3 region)	In standing, place 2 cm lateral and 5 cm inferior to the marker placed on the spinous process of the L1 vertebra
13 + 14 = RF (hip flexors)	Belly of rectus femoris muscle, approximately 1/3 of the way between the AIIS and the superior tip of the patella	In sitting with the leg extended fully and with thigh above the chair (straight leg raise), find the distal end of the rectus femoris muscle and place sensor 5-10 cm proximal to this.
15 + 16 = BF (hip extensors)	Belly of biceps femoris muscle on the middle of the posterior lateral aspect of the thigh	In standing, palpate the distal aspect of the biceps femoris muscle on the posterior lateral aspect of the thigh, and place the sensor 10-15 cm proximal to this

Odd = Right; Even = Left

EMG Label	Sensor Position	Description and Directions
1 + 2 = TA (tibialis anterior)	At 1/3 on the line between the head of the fibula and the tip of the medial malleolus.	With the subject standing, palpate the head of the fibula just below the lateral aspect of the knee, and trace a line to the medial malleolus of the ankle. The sensor should be positioned on the muscle belly, lateral to the anterior crest of the tibia.
3 + 4 = MG (medial gastrocnemius)	On the most prominent bulge of the gastrocnemius on the medial aspect of the lower leg.	With the subject standing, palpate the most prominent bulge on the medial aspect of the posterior lower leg (calf muscle). Position the sensor in the middle of the bulge.

Odd = Right; Even = Left

All EMG placements are in accordance with the SENIAM guidelines or from Konrad (2005).

Konrad, P. (2005). The ABC of EMG: a practical introduction to kinesiological electromyography. Retrieved June 2011:
https://hermanwallace.com/download/The_ABC_of_EMG_by_Peter_Konrad.pdf

APPENDIX 5

Matlab Function for Calculating Linear and Angular Kinematics Based on Quaternion Algebra

```matlab
function [AVQ,AAQ,LDQ,LVQ,LAQ,PQ] = QCAL(r,hz,p1,p2,warn)
%Quaternion calculations from the rotation matrices in r

%   The equations employed in this m-file are taken from the calculations
%   from:
%
%       Dumas, R., Aissaoui, R. and De Guise, J.A. (2004). A 3D generic
%       inverse dynamic method using wrench notation and quaternion
%       algebra, Computer Methods in Biomechanics and Biomedical
%       Engineering, 7(3), 159-166.
%
%   and
%
%       Kuipers, J.B. (1999). Quaternions and Rotation Sequences, Princeton
%       University Press: Oxford
%


%=========================================================================
% INPUTS:
%-------------------------------------------------------------------------
%
%    r = 3 by 3 by n matrix of n rotation matrices (n = number of frames)
%
%   hz = sample frequency (1/hz = time between frames)
%
%   p1 = COM local vector in a 3 by 1 or 3 by n matrix [optional]
%
%   p2 = segment end global vector in a 3 by n matrix [optional]
%
%
%-------------------------------------------------------------------------
% NOTES
%-------------------------------------------------------------------------
% 1. If p1 is in a 3 by 1 matrix, then it is assumed this is the local
%    vecor for all n frames, and it is copied n times into a 3 by n matrix
%
% 2. If p1 is not present then no linear calculations will be made, and
%    only angular outputs will be generated
%
% 3. If p2 is not present a matrix of zeros is used, therefore linear
%    motions of p1 will be relative to the segment end to which the vector
%    p1 relates
%
%=========================================================================
% OUTPUTS:
%-------------------------------------------------------------------------
%
%    PQ = 7 by n matrix with the displacement p2 (3 by n) and the
%         attitude quaternions from the rotation matrices (4 by n)
%
%   LDQ = 4 by n pure quaternion representing the displacement of p1
%
%   LVQ = 4 by n pure quaternion representing the linear velocity of p1
%
%   LAQ = 4 by n pure quaternion representing the linear acceleration of p1
%
%   AVQ = 4 by n pure quaternion representing the angular velocity of the
%         segment
%
%   AAQ = 4 by n pure quaternion representing the angular acceleration of
```

247

```matlab
%         the segment
%
%--------------------------------------------------------------------------
% NOTES
%--------------------------------------------------------------------------
% 1. All pure quaternions represent a vector, were the first element is
%    irrelevant (and should be close to zero) and the next three elements
%    represent the vector.
%
%==========================================================================

if nargin==3
    p2=zeros(size(r,3),3);
    warn=0;
elseif nargin==4
    warn=0;
end


n=size(r,3);

%Calculate quaternions (all versions):
[Q,QQ] = glen_dcm2quat2(r);
%q0=glen_dcm2quat(r);
%q0=dcm2quat(r);

q0=Q;
q1=QQ(:,:,1);
q2=QQ(:,:,2);
q3=QQ(:,:,3);
q4=QQ(:,:,4);

%check the size of p1 (COM)
if size(p1,1)<size(q1,1) && size(p1,1)==1
    p1=ones(size(q1,1),1)*p1;
end

%create the 7D vector of proximal end and quaternion (not needed?)
PQ=[p2,q1];

%differentiate ponits twice (segment proximal end)
dp2=glen_diff(p2);
ddp2=glen_diff(dp2);

%differentiate quaternions twice
dq1=glen_diff(q1);
dq2=glen_diff(q2);
dq3=glen_diff(q3);
dq4=glen_diff(q4);
dq0=glen_diff(q0);

ddq1=glen_diff(dq1);
ddq2=glen_diff(dq2);
ddq3=glen_diff(dq3);
ddq4=glen_diff(dq4);
ddq0=glen_diff(dq0);



%Calculate velocities and accelerations based on all sets of quaternions
% - LDQ = Linear Displacement
```

248

```matlab
% - LVQ = Linear Velocity
% - AVQ = Angular Velocity
% - LAQ = Linear Acceleration
% - AAQ = Angular Acceleration
AVQ0=2*(q_prod(dq0,[q0(:,1),-q0(:,2:4)]))*hz;
AVQ1=2*(q_prod(dq1,[q1(:,1),-q1(:,2:4)]))*hz;
AVQ2=2*(q_prod(dq2,[q2(:,1),-q2(:,2:4)]))*hz;
AVQ3=2*(q_prod(dq3,[q3(:,1),-q3(:,2:4)]))*hz;
AVQ4=2*(q_prod(dq4,[q4(:,1),-q4(:,2:4)]))*hz;


AAQ0=2*(q_prod(ddq0,[q0(:,1),-q0(:,2:4)])+q_prod(dq0,[dq0(:,1),...
    -dq0(:,2:4)]))*hz.^2;
AAQ1=2*(q_prod(ddq1,[q1(:,1),-q1(:,2:4)])+q_prod(dq1,[dq1(:,1),...
    -dq1(:,2:4)]))*hz.^2;
AAQ2=2*(q_prod(ddq2,[q2(:,1),-q2(:,2:4)])+q_prod(dq2,[dq2(:,1),...
    -dq2(:,2:4)]))*hz.^2;
AAQ3=2*(q_prod(ddq3,[q3(:,1),-q3(:,2:4)])+q_prod(dq3,[dq3(:,1),...
    -dq3(:,2:4)]))*hz.^2;
AAQ4=2*(q_prod(ddq4,[q4(:,1),-q4(:,2:4)])+q_prod(dq4,[dq4(:,1),...
    -dq4(:,2:4)]))*hz.^2;



%only run linear if p1 is present
if nargin>2
    %displacement
    LDQ=[zeros(n,1),p2]+q_prod(q_prod(q0,[zeros(n,1),p1]),...
        [q0(:,1),-q0(:,2:4)]);
    %velocities
    LVQ0=([zeros(n,1),dp2]+q_prod(q_prod(dq0,[zeros(n,1),p1]),...
        [q0(:,1),-q0(:,2:4)])+q_prod(q_prod(q0,[zeros(n,1),p1]),...
        [dq0(:,1),-dq0(:,2:4)]))*hz;
    LVQ1=([zeros(n,1),dp2]+q_prod(q_prod(dq1,[zeros(n,1),p1]),...
        [q1(:,1),-q1(:,2:4)])+q_prod(q_prod(q1,[zeros(n,1),p1]),...
        [dq1(:,1),-dq1(:,2:4)]))*hz;
    LVQ2=([zeros(n,1),dp2]+q_prod(q_prod(dq2,[zeros(n,1),p1]),...
        [q2(:,1),-q2(:,2:4)])+q_prod(q_prod(q2,[zeros(n,1),p1]),...
        [dq2(:,1),-dq2(:,2:4)]))*hz;
    LVQ3=([zeros(n,1),dp2]+q_prod(q_prod(dq3,[zeros(n,1),p1]),...
        [q3(:,1),-q3(:,2:4)])+q_prod(q_prod(q3,[zeros(n,1),p1]),...
        [dq3(:,1),-dq3(:,2:4)]))*hz;
    LVQ4=([zeros(n,1),dp2]+q_prod(q_prod(dq4,[zeros(n,1),p1]),...
        [q4(:,1),-q4(:,2:4)])+q_prod(q_prod(q4,[zeros(n,1),p1]),...
        [dq4(:,1),-dq4(:,2:4)]))*hz;
    %accelerations
    LAQ0=([zeros(n,1),ddp2]+q_prod(q_prod(ddq0,[zeros(n,1),p1]),...
        [q0(:,1),-q0(:,2:4)])+2*(q_prod(q_prod(dq0,[zeros(n,1),p1]),...
        [dq0(:,1),-dq0(:,2:4)]))+q_prod(q_prod(q0,[zeros(n,1),p1]),...
        [ddq0,-ddq0(:,2:4)]))*hz.^2;
    LAQ1=([zeros(n,1),ddp2]+q_prod(q_prod(ddq1,[zeros(n,1),p1]),...
        [q1(:,1),-q1(:,2:4)])+2*(q_prod(q_prod(dq1,[zeros(n,1),p1]),...
        [dq1(:,1),-dq1(:,2:4)]))+q_prod(q_prod(q1,[zeros(n,1),p1]),...
        [ddq1,-ddq1(:,2:4)]))*hz.^2;
    LAQ2=([zeros(n,1),ddp2]+q_prod(q_prod(ddq2,[zeros(n,1),p1]),...
        [q2(:,1),-q2(:,2:4)])+2*(q_prod(q_prod(dq2,[zeros(n,1),p1]),...
        [dq2(:,1),-dq2(:,2:4)]))+q_prod(q_prod(q2,[zeros(n,1),p1]),...
        [ddq2,-ddq2(:,2:4)]))*hz.^2;
    LAQ3=([zeros(n,1),ddp2]+q_prod(q_prod(ddq3,[zeros(n,1),p1]),...
        [q3(:,1),-q3(:,2:4)])+2*(q_prod(q_prod(dq3,[zeros(n,1),p1]),...
        [dq3(:,1),-dq3(:,2:4)]))+q_prod(q_prod(q3,[zeros(n,1),p1]),...
        [ddq3,-ddq3(:,2:4)]))*hz.^2;
    LAQ4=([zeros(n,1),ddp2]+q_prod(q_prod(ddq4,[zeros(n,1),p1]),...
```

```matlab
                    [q4(:,1),-q4(:,2:4)])+2*(q_prod(q_prod(dq4,[zeros(n,1),p1]),...
                    [dq4(:,1),-dq4(:,2:4)]))+q_prod(q_prod(q4,[zeros(n,1),p1]),...
                    [ddq4,-ddq4(:,2:4)]))*hz.^2;
end


% Remove singularities when crossing zero
limit=10;

AVQ=AVQ0;
AAQ=AAQ0;

AVQQ=AVQ1;
AVQQ(:,:,2)=AVQ2;
AVQQ(:,:,3)=AVQ3;
AVQQ(:,:,4)=AVQ4;

AAQQ=AAQ1;
AAQQ(:,:,2)=AAQ2;
AAQQ(:,:,3)=AAQ3;
AAQQ(:,:,4)=AAQ4;

for v=1:5
    if v==5
        %singularities from calculations
        if any(isnan(AVQ(:)))
            warning('Quaternion error: AVQ nan')
        end
        if any(isnan(AAQ(:)))
            warning('Quaternion error: AAQ nan')
        end

        % spikes in calculations
        AVQ_test=abs(AVQ(:,2:4))>ones(size(AVQ,1),1)...
                *(mean(abs(AVQ(:,2:4)))+std(abs(AVQ(:,2:4)))*limit);
        if any(AVQ_test(:))
            if warn==1
                warning('Possible AVQ error: spike')
            end
            %get lowest spike (could just be noisey
            [row,col]=find(abs(AVQ)>ones(size(AVQ,1),1)...
                    *(mean(abs(AVQ))+std(abs(AVQ))*limit));
            for v1=1:length(row)
                temp=permute(AVQQ(row(v1),:,:),[3,2,1]);    %collect all
                temp=sqrt(sum(temp.^2,2));                   %get norms
                f1=find(temp==min(temp),1);                  %use smallest
                AVQ(row(v1),:)=AVQQ(row(v1),:,f1);
            end
        end
        AAQ_test=abs(AAQ(:,2:4))>ones(size(AAQ,1),1)...
                *(mean(abs(AAQ(:,2:4)))+std(abs(AAQ(:,2:4)))*limit);
        if any(AAQ_test(:))
            if warn==1
                warning('Possible AAQ error: spike')
            end
            %get lowest spike (could just be noisey
            [row,col]=find(abs(AAQ)>ones(size(AAQ,1),1)...
                    *(mean(abs(AAQ))+std(abs(AAQ))*limit));
            for v1=1:length(row)
                temp=permute(AAQQ(row(v1),:,:),[3,2,1]);    %collect all
```

```matlab
                temp=sqrt(sum(temp.^2,2));                        %get norms
                f1=find(temp==min(temp),1);                       %use smallest
                AAQ(row(v1),:)=AAQQ(row(v1),:,f1);
            end
        end
    else
        %singularities from calculations
        if any(isnan(AVQ(:)))
            AVQ(isnan(AVQ(:,1)),:)=AVQQ(isnan(AVQ(:,1)),:,v);
        end
        if any(isnan(AAQ(:)))
            AAQ(isnan(AAQ(:,1)),:)=AAQQ(isnan(AAQ(:,1)),:,v);
        end

        % spikes in calculations
        AVQ_test=abs(AVQ(:,2:4))>ones(size(AVQ,1),1)...
                *(mean(abs(AVQ(:,2:4)))+std(abs(AVQ(:,2:4)))*limit);
        if any(AVQ_test(:))
            [row,col]=find(abs(AVQ)>ones(size(AVQ,1),1)...
                    *(mean(abs(AVQ))+std(abs(AVQ))*limit));
            AVQ(row,:)=AVQQ(row,:,v);
        end
        AAQ_test=abs(AAQ(:,2:4))>ones(size(AAQ,1),1)...
                *(mean(abs(AAQ(:,2:4)))+std(abs(AAQ(:,2:4)))*limit);
        if any(AAQ_test(:))
            [row,col]=find(abs(AAQ)>ones(size(AAQ,1),1)...
                    *(mean(abs(AAQ))+std(abs(AAQ))*limit));
            AAQ(row,:)=AAQQ(row,:,v);
        end
    end
end


if nargin>2
    % linear stuff
    LVQ=LVQ0;
    LAQ=LAQ0;

    LVQQ=LVQ1;
    LVQQ(:,:,2)=LVQ2;
    LVQQ(:,:,3)=LVQ3;
    LVQQ(:,:,4)=LVQ4;

    LAQQ=LAQ1;
    LAQQ(:,:,2)=LAQ2;
    LAQQ(:,:,3)=LAQ3;
    LAQQ(:,:,4)=LAQ4;

    for v=1:5
        if v==5
            %singularities from calculations
            if any(isnan(LVQ(:)))
                warning('Quaternion error: LVQ nan')
            end
            if any(isnan(LAQ(:)))
                warning('Quaternion error: LAQ nan')
            end

            % spikes in calculations
            LVQ_test=abs(LVQ(:,2:4))>ones(size(LVQ,1),1)...
```

251

```matlab
                    *(mean(abs(LVQ(:,2:4)))+std(abs(LVQ(:,2:4)))*limit);
            if any(LVQ_test(:))
                if warn==1
                    warning('Possible LVQ error: spike')
                end
                %get lowest spike (could just be noisey
                [row,col]=find(abs(LVQ)>ones(size(LVQ,1),1)...
                        *(mean(abs(LVQ))+std(abs(LVQ))*limit));
                for v1=1:length(row)
                    temp=permute(LVQQ(row(v1),:,:),[3,2,1]);%collect all
                    temp=sqrt(sum(temp.^2,2));                %get norms
                    f1=find(temp==min(temp),1);               %use smallest
                    LVQ(row(v1),:)=LVQQ(row(v1),:,f1);
                end
            end
            LAQ_test=abs(LAQ(:,2:4))>ones(size(LAQ,1),1)...
                    *(mean(abs(LAQ(:,2:4)))+std(abs(LAQ(:,2:4)))*limit);
            if any(LAQ_test(:))
                if warn==1
                    warning('Possible LAQ error: spike')
                end
                %get lowest spike (could just be noisey
                [row,col]=find(abs(LAQ)>ones(size(LAQ,1),1)...
                        *(mean(abs(LAQ))+std(abs(LAQ))*limit));
                for v1=1:length(row)
                    temp=permute(LAQQ(row(v1),:,:),[3,2,1]);%collect all
                    temp=sqrt(sum(temp.^2,2));                %get norm
                    f1=find(temp==min(temp),1);               %use smallest
                    LAQ(row(v1),:)=LAQQ(row(v1),:,f1);
                end
            end
        else
            %singularities from calculations
            if any(isnan(LVQ(:)))
                LVQ(isnan(LVQ(:,1)),:)=LVQQ(isnan(LVQ(:,1)),:,v);
            end
            if any(isnan(LAQ(:)))
                LAQ(isnan(LAQ(:,1)),:)=LAQQ(isnan(LAQ(:,1)),:,v);
            end

            % spikes in calculations
            LVQ_test=abs(LVQ(:,2:4))>ones(size(LVQ,1),1)...
                    *(mean(abs(LVQ(:,2:4)))+std(abs(LVQ(:,2:4)))*limit);
            if any(LVQ_test(:))
                [row,col]=find(abs(LVQ)>ones(size(LVQ,1),1)...
                        *(mean(abs(LVQ))+std(abs(LVQ))*limit));
                LVQ(row,:)=LVQQ(row,:,v);
            end
            LAQ_test=abs(LAQ(:,2:4))>ones(size(LAQ,1),1)...
                    *(mean(abs(LAQ(:,2:4)))+std(abs(LAQ(:,2:4)))*limit);
            if any(LAQ_test(:))
                [row,col]=find(abs(LAQ)>ones(size(LAQ,1),1)...
                        *(mean(abs(LAQ))+std(abs(LAQ))*limit));
                LAQ(row,:)=LAQQ(row,:,v);
            end
        end
    end

end


end
```

```matlab
%=========================================================================
% Quaternion Product Function
%-------------------------------------------------------------------------
function [Q] = q_prod(q1,q2)
    Q=nan(size(q1));
    Q(:,1)=(q1(:,1).*q2(:,1))-dot(q1(:,2:4),q2(:,2:4),2);
    Q(:,2:4)=q1(:,1)*[1,1,1].*q2(:,2:4)+q2(:,1)*[1,1,1].*q1(:,2:4)...
             +cross(q1(:,2:4),q2(:,2:4),2);
end
%=========================================================================
% DCM to Quaternion conversion - not used
%-------------------------------------------------------------------------
function [Q] = glen_dcm2quat(R)

    q=sqrt(R(1,1,:)+R(2,2,:)+R(3,3,:)+1)/2;
    Q=[q,(R(2,3,:)-R(3,2,:))./(4*q),(R(3,1,:)-R(1,3,:))./(4*q),...
      (R(1,2,:)-R(2,1,:))./(4*q)];
    Q=permute(Q,[3,2,1]);

    %find problems with rotations of 180 (divide by zero)
    f=find(isnan(sum(Q,2)));
    for n=1:length(f)
        Q(f(n),:)=[0,double(diag(R(:,:,f(n)))==1)'];
    end

end
%=========================================================================
% Differentiation with estimated terminal values
%-------------------------------------------------------------------------
function [out] = glen_diff(data)

    out=nan(size(data));
    out(2:end-1,:)=(data(3:end,:)-data(1:end-2,:))/2;

    %three point forward difference from Lagrange interpolating polynomial
    out(1,:)=(-3*data(1,:)+4*data(2,:)-data(3,:))/2;
    out(end,:)=(3*data(end,:)-4*data(end-1,:)+data(end-2,:))/2;

end
%=========================================================================
```

APPENDIX 6

Matlab Function for Calculating 3D Inverse Dynamics from Wrench Notation

```matlab
function [W1,W2,AVQ,AAQ,LDQ,LVQ,LAQ,PQ,dH,dH1] =
wrench(R,hz,I,COM,PROX,DIST,W0)
%Calculate joint moments and forces using wrenches


%   The equations employed in this m-file are taken from the calculations
%   from:
%
%       Dumas, R., Aissaoui, R. and De Guise, J.A. (2004). A 3D generic
%       inverse dynamic method using wrench notation and quaternion
%       algebra, Computer Methods in Biomechanics and Biomedical
%       Engineering, 7(3), 159-166.

%=========================================================================
% INPUTS:
%-------------------------------------------------------------------------
%
%     R = 3 by 3 by n matrix of n rotation matrices (n = number of frames)
%
%    hz = sample frequency (1/hz = time between frames)
%
%     I = inertial data of segment 1 by 4 array (mass, Ix,Iy,Iz)
%
%   COM = COM local vector in a 1 by 3 or n by 3 matrix
%
%  PROX = segment proximal end global vector in an n by 3 matrix
%
%  DIST = segment distal end(s) global vector(s) in an n by 3 by m matrix
%
%    W0 = distal wrench(es) from previous segment(s) in the GCS in an n by
%         6 by m matrix [optional]
%
%
%-------------------------------------------------------------------------
% NOTES
%-------------------------------------------------------------------------
% 1. If COM is in a 3 by 1 matrix, then it is assumed this is the local
%    vector for all n frames, and it is copied n times into a 3 by n matrix
%
% 2. If W0 or DIST is not present then a matrix of zeros is used as it
%    assumes it is the first segment
%
% 3. DIST and W0 can be more than one segment, denoted by m, and allows two
%    or more segments to come together, such as with the pelvis
%
%=========================================================================
% OUTPUTS:
%-------------------------------------------------------------------------
%
%    W1 = n by 6 matrix with the forces (columns 1:3) and the moments
%         columns (4:6) in the GCS
%
%    W2 = n by 6 matrix with the forces (columns 1:3) and the moments
%         columns (4:6) in the LCS of the present segment
%-------------------------------------------------------------------------
% NOTES
%-------------------------------------------------------------------------
% 1. This also outputs [AVQ,AAQ,LDQ,LVQ,LAQ,PQ] from the function QCAL
%=========================================================================
```

255

```matlab
if nargin == 6
    W0=zeros(size(R,3),6);
elseif nargin == 5
    W0=zeros(size(R,3),6);
    DIST=zeros(size(R,3),3);
end

s=size(R,3);

% Gravity vector
g=ones(s,1)*[0 0 -9.81];

% Call QCAL to calculate all quaternions
[AVQ,AAQ,LDQ,LVQ,LAQ,PQ] = QCAL(R,hz,COM,PROX);

 %Calculate segment inertial tensor and derivative of angular momentum
 I_GCS=nan(size(R));
 dH=nan(s,3);
 H=nan(s,3);
for n1=1:s %can only do this one frame at a time
    I_GCS(:,:,n1)=R(:,:,n1)*diag(I(2:4))*inv(R(:,:,n1));

    % Calculate derivative of angular momentum (dH/dt)
    dH(n1,:)=(I_GCS(:,:,n1)*AAQ(n1,2:4)'+cross(AVQ(n1,2:4)',...
             I_GCS(:,:,n1)*AVQ(n1,2:4)'))';

    % Alternative: Calculate angular momentum
    H(n1,:)=(I_GCS(:,:,n1)*AVQ(n1,2:4)')';
end

% Alternative: Calculate derivative of angular momentum (dH/dt)
dH1=glen_diff(H)*hz;

% weight wrench = mg & c x mg (at proximal joint)
Ww = [I(1)*g,cross(LDQ(:,2:4)-PROX,I(1)*g,2)];

% dynamic wrench = ma & c x ma (at proximal joint)
Wdyn = [I(1)*LAQ(:,2:4),cross(LDQ(:,2:4)-PROX,dH+I(1)*LAQ(:,2:4),2)];

% distal wrench
Wdis=zeros(s,6);
for m=1:size(DIST,3)
    Wdis = Wdis+[-W0(:,1:3,m),-W0(:,4:6,m)-cross(DIST(:,:,m)...
          -PROX,W0(:,1:3,m),2)];
end

% Combine all for the total wrench
W1 = Wdyn-Ww-Wdis;



%Matrix format? (need to do it in loop above

% Convert wrench into LCS of segment (is this needed?)
W2 = [q_prod(q_prod(PQ(:,4:7),[zeros(s,1),W1(:,1:3)]),...
     [PQ(:,4),-PQ(:,5:7)]),q_prod(q_prod(PQ(:,4:7),...
     [zeros(s,1),W1(:,4:6)]),[PQ(:,4),-PQ(:,5:7)])];

% Remove scalar parts
```

```matlab
W2(:,1)=[];
W2(:,5)=[];

end


%=========================================================================
% Quaternion Product Function
%-------------------------------------------------------------------------
function [Q] = q_prod(q1,q2)
    Q=nan(size(q1));
    Q(:,1)=(q1(:,1).*q2(:,1))-dot(q1(:,2:4),q2(:,2:4),2);
    Q(:,2:4)=q1(:,1)*[1,1,1].*q2(:,2:4)+q2(:,1)*[1,1,1]....
            *q1(:,2:4)+cross(q1(:,2:4),q2(:,2:4),2);
end


%=========================================================================
% Differentiation with estimated terminal values
%-------------------------------------------------------------------------
function [out] = glen_diff(data)

    out=nan(size(data));
    out(2:end-1,:)=(data(3:end,:)-data(1:end-2,:))/2;

    %three point forward difference from Lagrange interpolating polynomial
    out(1,:)=(-3*data(1,:)+4*data(2,:)-data(3,:))/2;
    out(end,:)=(3*data(end,:)-4*data(end-1,:)+data(end-2,:))/2;

end
%=========================================================================
```